# MATERIALS SCIENCE AND TECHNOLOGY

# 1997 ANNUAL REPORT

# MIDEG

TU Delft

Onderzoekschool
Materiaalkunde
Instituut
Delft
Eindhoven
Groningen

# RESEARCH IN MATERIALS SCIENCE AND TECHNOLOGY

## ANNUAL REPORT 1997

# RESEARCH IN MATERIALS SCIENCE AND TECHNOLOGY

# ANNUAL REPORT 1997

## MATERIALS INSTITUTE
Delft Eindhoven Groningen



Edited by Michael Janssen

Laboratory of Materials Science, Rotterdamseweg 137, 2628 AL Delft
+31 (15) 2785866, M.Janssen@stm.tudelft.nl

This Annual Report is published by:

Delft University Press
Mekelweg 4
2628 CD Delft
The Netherlands
Telephone +31 (15) 278 3254

by order of

Materials Institute Delft Eindhoven Groningen
Rotterdamseweg 137
2628 AL Delft
The Netherlands
Telephone +31 (15) 278 3976



CIP-DATA KONINKLIJKE BIBLIOTHEEK, DEN HAAG

Research

Research in Materials Science and Technology - Annual Report 1997 /
ed. Michael Janssen. - Delft : Delft University Press. - Ill. - With ref.
ISBN 90-407-1734-6
NUGI 831
Subject headings: Materials science / Materials technology / Annual report

## PREFACE

This 13th edition of the Annual Report on Materials Science and Technology provides an overview of the research performed by the groups that participate in the Materials Institute Delft Eindhoven Groningen (MIDEG).

In the first chapter some factual information is given about the graduate school MIDEG. Next, two leading articles are presented. In the first article Van der Wekken, Ament, Janssen and Zuidema compare experimental data for fatigue crack growth of steel in seawater with a model prediction. The second article, by Spoormaker, Skrypnyk and Vasyljkevych, deals with the way to incorporate time-dependent visco-elastic behaviour of plastics into finite element calculations.

The main part of the Annual Report is devoted to the reports of the 14 groups of MIDEG. Their personnel, research areas and available experimental facilities are described, together with a report of their research achievements and publications in 1997.

I hope this Annual Report on Materials Science and Technology serves as a useful source of information.

June 1998 Michael Janssen

## CONTENTS

**THE MATERIALS INSTITUTE Delft Eindhoven Groningen**
Secretariat: O. Wens, Laboratory of Materials Science
Rotterdamseweg 137, 2628 AL Delft
phone +31 (15) 2783976, fax +31 (15) 2786730
e-mail O.M.S.Wens-vanSwol@stm.tudelft.nl

# "Processing with Advanced Materials"

## INTRODUCTION

The 1997 issue of the Annual Report on Materials Science and Technology marks the third year of the graduate school for Materials Technology MIDEG. The aim of MIDEG is the strengthening of Dutch science-based technological research on the three major classes of materials: metals, polymers and inorganic materials as well as their combinations in the form of laminates and composites. The school aims to be fertile breeding ground for collaborative interdisciplinary materials research involving both junior and senior scientists.

Over the past year approximately 95 senior scientists, 140 junior scientists, 70 technicians and 100 research students contributed to the research of which this annual report is a summary. Together more than 170 publications were produced in scientific journals, not counting conference contributions and lectures. No less than 18 Ph.D. theses were successfully defended.

In short, 1997 has been a successful year for the graduate school MIDEG. However, we also witnessed the departure of prof.dr.ir. Eric J. Mittemeijer, who took up the honourable position of director of the Max Planck Institute in Stuttgart. Prof. Mittemeijer has made a large number of important contributions to materials science and has been one of the most outstanding materials scientist in the graduate school MIDEG. Eric Mittemeijer is also one of the founding fathers of the Annual Report on Materials Science and Technology of the Delft University of Technology, which forms the basis of the current series of MIDEG annual reports. It is with regret we say goodbye but we are certain that the fruits of his continued collaboration with MIDEG scientists can be witnessed in future issues of this Annual Report. We wish him well in his new career.

## Ph.D. THESES

1. J. Aué
   *Fractals and Fracture*
   University of Groningen
2. R. Benedictus
   *Solid state amorphisation: Thermodynamics and kinetics*
   Delft University of Technology
3. S.A. Fawaz
   *Fatigue crack growth in riveted joints*
   Delft University of Technology

4. M.A.J. van Gils
   *Quasi-Brittle Fracture of Ceramics*
   Eindhoven University of Technology
5. M.J.M. Hermans
   *A study of short circuiting arc welding*
   Delft University of Technology
6. H.D. Hoekstra
   *The mechanical behavior of UV-degraded HDPE: Consequences for Designers*
   Delft University of Technology
7. J.J. Horst
   *Influence of fibre orientation on fatigue of short glassfibre reinforced Polyamide*
   Delft University of Technology
8. J. Kerssemakers
   *Concepts of interactions in atomic force microscopy*
   University of Groningen
9. Lun-Zhi Liao
   *The application of in exchange membranes in choride related electro chemical technology*
   Delft University of Technology
10. T. Ma
    *Weldability of Al-Zn-Mg alloys*
    Delft University of Technology
11. A. Noordermeer
    *Wet Chemical Processing of MnZn-Ferrites*
    Eindhoven University of Technology
12. W.H.A. Peelen
    *Stability and reactivity of oxygen, nickel and cobalt species in molten carbonate*
    Delft University of Technology
13. P.W.C. Provó Kluit
    *The development of in-situ foamed sandwich panels*
    Delft University of Technology
14. A.C. Riemslag
    *Crack Growth in Polyethylene*
    Delft University of Technology
15. M. Schreiber
    *Hydrogen Mixed Conductors Properties and Applications*
    Delft University of Technology
16. D.H.J. Teeuw
    *Engineering ceramics and thermal stresses*
    University of Groningen
17. I.L. Tuinman
    *The Production of $Si_3N_4$ Powders in a Laser-Driven Aerosol Reactor*
    Delft University of Technology
18. A.P. Voskamp
    *Microstructural changes during rolling contact fatigue: Metal fatigue in the sub-surface region of deep groove ball bearing inner rings*
    Delft University of Technology

# PREDICTED AND EXPERIMENTAL CORROSION FATIGUE CRACK GROWTH RATES OF ANODICALLY POLARISED STEEL IN DEAERATED SEAWATER

C.J. van der Wekken [1], P.C.H. Ament [2], M. Janssen [1], J. Zuidema [1]

[1] Delft University of Technology, Laboratory for Materials Science
Rotterdamseweg 137, 2628 AL Delft, The Netherlands

[2] Hoogovens Research and Development, Product Application Centre
PO box 10000, 1970 CA IJmuiden, The Netherlands

A computer simulation model has been developed for predicting the corrosion fatigue behaviour of steel under anodic polarisation in deaerated seawater. Based on a distribution of sources of $H^+$ ions on the crack walls, the probability of $H^+$ ions reaching the crack tip could be calculated by modelling the solute transport. Assuming a critical hydrogen concentration in front of the crack tip the behaviour of $da/dN$ vs $\Delta K$ could be predicted. The results are compared with experimental data.

## 1 *Introduction*

The accelerated corrosion fatigue (CF) crack growth rates of steel in seawater are generally accepted to be due to hydrogen embrittlement of the crack tip material. During strong anodic polarisation the crack tip area is shielded from the applied potential by a potential drop in the crack solution arising from the high current densities at the crack walls, so that the crack tip is essentially at the local corrosion potential [1-3]. A cathodic overpotential for hydrogen reduction in an acidified crack tip solution has been measured and it could be concluded that this acidification originated from the dissolution reaction at the crack walls. A major role in the transport of $H^+$ ions can be ascribed to Flow Enhanced Diffusion (FED), a transport mechanism resulting from the interaction of diffusion and periodic flow [3, 4] which can be described in terms of an effective diffusion coefficient $D_{eff}$ and depends on the crack dimensions and the dimensionless parameter $G$:

$$G = d_{av}\sqrt{\frac{\omega}{D}} \qquad (1)$$

where $d_{av}$ = the average local distance between the crack walls, $\omega$ = the radial frequency and $D$ = the solute diffusion coefficient.

By means of computer simulation calculations it is possible to determine $D_{eff}$, which may be several orders of magnitude larger than $D$ [5]. Migration due to the electrical field can usually be neglected in the presence of FED [6]. The knowledge of $D_{eff}$ has been used as a basis for predicting the behaviour of the crack growth rate $da/dN$ [3, 7]. While in later studies [8,9] a single source of $H^+$ ions was placed near the crack mouth, the present modelling takes into account that acidification results from anodic dissolution along the whole length of the crack. The production rate of $H^+$ ions along the crack walls is assumed to be proportional to the anodic current density. Inside the crack the laminar flow during a small change $d\alpha$ in the crack tip angle $\alpha$ was as-

sumed to be parabolic, while in the bulk solution facing the crack mouth the velocity of the solution in the crack length direction was assumed to be equal to the average velocity at the crack mouth. Details of the model calculations of the path of a particle resulting from flow and diffusion inside the crack have been presented previously [7-9]. Solute particles were allowed random diffusion jumps $b$ in the crack length direction as well as perpendicular to the crack walls. The sinusoidal cycle was divided in $m$ steps, as illustrated in the Figures 1a and 1b, while $m$ and $b$ were chosen in correspondence with the Einstein relationship for random walk diffusion:

$$m \cdot b^2 = 2TD \tag{2}$$

where $T$ = the period of a cycle.

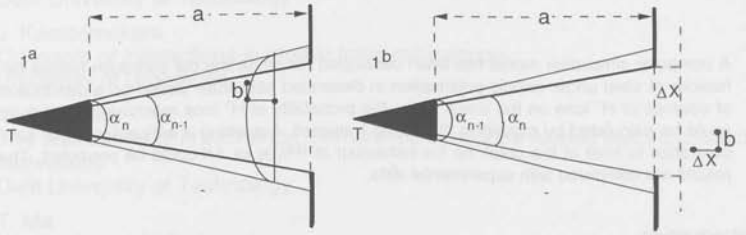


*Figure 1: Steps in the calculation of solute transport inside and outside of the crack*

The diffusion jump $b$ should be chosen much smaller than the distance between crack walls, which means that $m$ has to be sufficiently high. The flow calculations were checked to be sufficiently accurate to avoid systematic particle drift. As a result of the random diffusion jumps during fatigue cycling, the path of individual particles becomes unpredictable. Some particles will end up in the bulk solution and may again enter the crack. A particle was considered 'lost' in the bulk solution after having diffused up to a distance of the maximum CMOD from the centre plane of the crack. A fraction of the particles originating from the crack walls will eventually, after continued cycling, reach the crack tip. Using large numbers of particles, it was possible to determine the probability that $H^+$ ions, originating from the crack walls according to a given source distribution, would reach the crack tip.

The shape of the current density distributions along the crack walls was derived from data published by Edwards [1], who found, going from the crack tip, that the current density was increasing approximately quadratically with the distance along the crack length. A corresponding source distribution for $H^+$ ions was used in the present calculations. The electrical field is expected to penetrate deeper into the crack as the crack becomes wider. Under constant external anodic polarisation the source strength for $H^+$ ions at the crack mouth was therefore kept constant while the penetration depth of the source distribution in the crack was taken to be proportional to $CMOD_{av}$, the average CMOD. The number of $H^+$ ions produced per unit time at the crack walls will then also be proportional to $CMOD_{av}$.For given loading conditions a large number of $H^+$ ions was taken randomly from the statistical distribution along the crack walls to determine the probability $P$ that $H^+$ ions would reach the tip, where they were assumed to be reduced and absorbed into the material. As a result there is an effective line source for hydrogen diffusing into the material at the crack tip. The strength $S_{Htip}$ of this source is proportional to $CMOD_{av} \cdot P$:

$$S_{Htip} \div CMOD_{av} \cdot P \tag{3}$$

The H-concentration $C(r)$ at a distance $r$ in front of a moving line source moving with velocity $V$ has been calculated to be [10]:

$$C(r) \div \beta . K_0\left(\frac{Vr}{2D_H}\right) \exp\left(\frac{-Vr}{2D_H}\right) \tag{4}$$

where $K_0$ = a modified Bessel function of the second kind of order zero, $\beta$ is proportional to the source strength, and $D_H$ = the diffusion coefficient for hydrogen. It will be assumed that the crack will be extended during each cycle over a critical distance $r_{cr}$ through the embrittled zone, where the hydrogen concentration $C_H$ exceeds a critical value $(C_H)_{cr}$, which may depend on $\Delta K$. Since $V = da/dt$ and $r_{cr} = da/dN$, while $da/dt = f \cdot da/dN$ and $\beta \div S_{Htip}$, substitution in Eq. 4 yields:

$$S_{Htip} \cdot K_0\left(f \cdot \frac{(da/dN)^2}{2D_H}\right) \exp\left(-f \cdot \frac{(da/dN)^2}{2D_H}\right) = \text{constant} \tag{5}$$

According to Eq. 5, in loading situations where $S_{Htip}$ is independent of the frequency, which was found to apply for example at high $\Delta K$ values (see Figure 2), $f \cdot (da/dN)^2$ is expected to be constant. It follows that under these conditions

$$da/dN \div f^{-1/2} \tag{6}$$

This $f^{-1/2}$ dependence, differs significantly from the proportionality to $f^{-1}$ proposed earlier [3,7-9], when $da/dt$ was assumed to be proportional to the flux of $H^+$ ions to the crack tip. In the present work it will be assumed that the environmental contribution to the crack growth rate is proportional to $S_{Htip}$ as given by Eq. 3, but that the hydrogen diffusion mechanism in the material introduces a frequency dependence according to Eq. 6, so that

$$(da/dN)_{env} \div S_{Htip} \cdot f^{-1/2} \tag{7}$$

or

$$(da/dN)_{env} \div CMOD_{av} \cdot P \cdot f^{-1/2} \tag{8}$$

## 2 Experimental

Crack growth rates under sinusoidal constant load amplitude testing were measured using CT specimens of structural Steel FeE 355-KT, produced by Hoogovens, The Netherlands. The measurements were performed in air and under anodic polarisation at –500 mV vs Ag/AgCl in deaerated artificial ASTM seawater. The crack length was measured by means of a potential drop technique. The sides of the crack in the standard specimens of 12.5 × 12.5 × 2.5 cm were shielded, while a V-shaped precrack with a non standard tip angle of nearly 180° was used in order to obtain a approximately two dimensional flow pattern, in correspondence with the model calculations. The experimental data were obtained using a stress ratio $R = 0.7$ and a maxi-

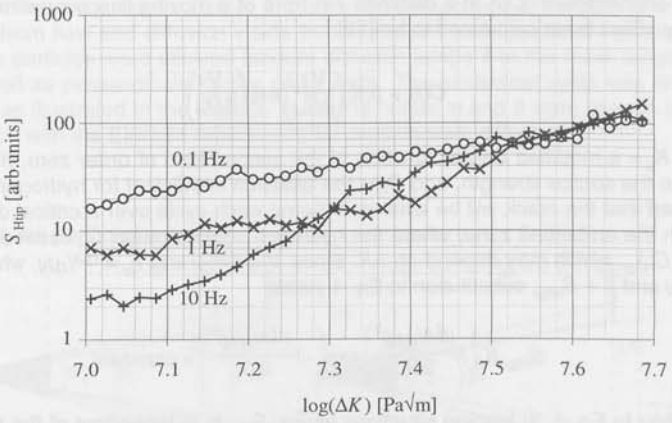


*Figure 2 The theoretically calculated behaviour of the source strength $S_{Htip}$.*

mum load $P_{max}$ = 35.4 kN. Similar values were used in the calculations of the crack geometry during fatigue cycling.

## 3 *Results and Discussion*

The predicted behaviour of the source strength $S_{Htip}$ is shown in Figure 2. Figure 3 shows experimental $da/dN$ data obtained in seawater at 0.1, 1 and 10 Hz and data obtained in air, as well as a representation of the corresponding theoretically predicted crack growth rates. The measurements on short cracks at 0.1 Hz were very time consuming. Data at this frequency were therefore obtained only for longer crack lengths. Theoretical and experimental results could be matched, regarding the experimental CF rate $(da/dN)_{CF}$ as a superposition of the rate in air $(da/dN)_{air}$ and the environmental contribution:

$$(da/dN)_{CF} = (da/dN)_{air} + (da/dN)_{env}$$

or, using Eq. 8:

$$(da/dN)_{CF} = (da/dN)_{air} + \varphi \cdot CMOD_{av} \cdot P \cdot f^{-1/2} \quad , \qquad (9)$$

where the fitting parameter $\varphi$ was chosen to obtain exact correspondence with the experimental data at 0.1Hz and log $\Delta K$ = 7.6. Experimental and theoretical curves for the various frequencies were then found to match quite well in the high $\Delta K$ range. At low $\Delta K$ and at 0.1 Hz the predicted crack growth rates are too high. The observed deviations especially occur in short and narrow cracks and at a low frequency. Under these conditions $G$ values are small (< 1) and FED is not significant, so that the role of ion migration in the electrical field in the crack solution may not be negligible [6]. Under anodic polarisation the positively charged $H^+$ ions will then be less likely to

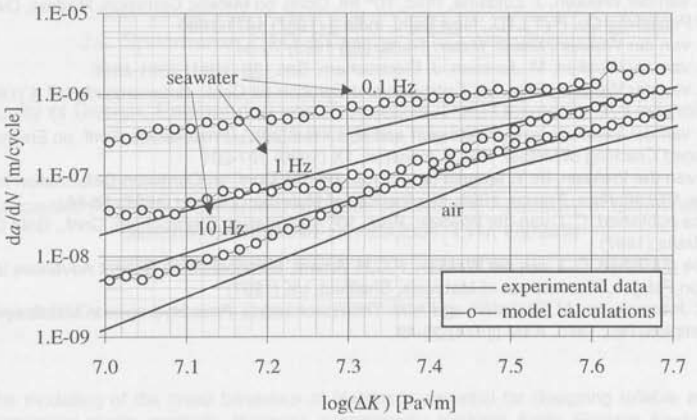


*Figure 3 Experimental and theoretical crack growth rates according to Eq. 9*

reach the crack tip. The incorporation of a migration term in the transport calculations should therefore be the next step in the development of the present model.

## 4 Conclusions

1. In the CF crack growth mechanism of anodically polarised steel in seawater, the transport of $H^+$ ions to the crack tip can be considered the rate determining step.
2. A major role in the $H^+$ ion transport in CF cracks is played by Flow Enhanced Diffusion, a mechanism arising from the interaction of diffusion and periodic flow.
3. The tip of the CF crack can be represented as a moving line source for H atoms.
4. Assuming that $da/dN$ is determined by a zone where the H-concentration exceeds a critical level, a frequency dependence of $da/dN$ can be predicted according to $f^{-1/2}$.
5. A simulation model for $H^+$ ion transport to the crack tip has been developed which predicts the behaviour of $da/dN$ as a function of the frequency and $\Delta K$.
6. Experimental data and theoretical predictions could be matched by superposition of a theoretical environmental contribution and the experimental crack growth rate in air.

## Acknowledgement

This research was supported by the Technology Foundation of the Netherlands (STW). The authors wish to thank STW for their financial assistance.
This article will be published in the Proc. of the 12th European Conference on Fracture (ECF 12), 14-18 September 1998, Sheffield, UK.

## *References*


1. R.A.H. Edwards, Corrosion 42 (1986) 245-247
2. C.J. van der Wekken, J. Zuidema, Proc. 10th Int. Cong. on Metallic Corrosion, Madras, Oxford & IBH Publishing Co. PVT LTD., New Delhi, India 3 (1987) 1871-1880
3. C.J. van der Wekken, Metall. Mater. Trans. 26A 1995) 75-84
4. C.J. van der Wekken, M. Janssen, J. Electrochem. Soc.138 (1991) 2891-2896
5. C.J. van der Wekken, Proc. UK Corrosion and Eurocorr 94 Conf., Bournemouth, UK 4 (1994) 29-40
6. C.J. van der Wekken, In: R.P. Gangloff and M.B. Ives (eds.), Proc. 1st Int. Conf. on Environment-Induced Cracking of Metals, NACE, Houston, TX (1990) 197-201
7. C.J.van der Wekken, In: T. Magnin (ed.), Proc. 2nd Int. Conf. on Corrosion-Deformation Interactions, CDI'96, Nice, France, 1996, The Institute of Materials, London (1997) 76-85
8. To be published: C.J. van der Wekken, Proc. 10th Australasian Electrochem. Conf., Gold Coast, Australia (1997)
9. To be published, C.J. van der Wekken, P.C.H. Ament, Symposium on Recent Advances in Corrosion Fatigue, The Institute of Materials, Sheffield, UK (1997)
10. H.H. Johnson, In: I.M. Bernstein and A.W. Thompson (eds.), Proc. Hydrogen in Metals conf., Champion, Pa., 1973, ASM (1974) 35-49

# SIMULATION OF THE NON-LINEAR VISCO-ELASTIC BEHAVIOUR OF PLASTIC PRODUCTS

J.L. Spoormaker [1], I.D. Skrypnyk [2], T.O. Vasyljkevych [2]

[1] Faculty of Design, Engineering and Production, Delft University of Technology, Jaffalaan 9, 2628 BX Delft, The Netherlands

[2] Karpenko Physico-Mechanical Institute of National Academy of Sciences of Ukraine, 5, Naukova St., 290601, Lviv, Ukraine

Keywords: Creep and recovery of plastics, FEM modelling

The modelling of the creep behaviour of plastics is essential for designing reliable and sustainable plastic products. However, commercially available Finite Element Analysis packages are lacking well-established models for characterising the non-linear time-dependent behaviour of plastics. Instead the traditional theory of elasticity or elasto-plasticity are used by designers to predict the long-term behaviour of plastic products. This paper describes the implementation of a model for non-linear visco-elastic behaviour in FEA package MARC.

For implementation, the Henriksen scheme of discretisation of the convolution integral is used. This scheme allows to build a fast procedure for modelling of the visco-elastic behaviour. As a result, the calculation time for visco-elasticity problems is not much larger than the calculation time required for modelling of elasto-plastic behaviour.

Some additional cases (a thick plate under distributed transversal loading and buckling of a U-profile under compressive loading) have been analysed in order to compare the existing models and newly proposed approach and to verify the model performance.

## Notations

| | |
|---|---|
| $\sigma$, $\sigma(t)$ | stress and stress history (one-dimensional formulation) |
| $\tilde{\sigma}$ | effective stress |
| $\varepsilon[\sigma,t]$ | strain as a function of stress and time (one-dimensional formulation) |
| $\varepsilon[\sigma_k,t]$ | experimental data from creep-recovery tests for stress level $\sigma_k$ |
| $t$ | time variable |
| $t_{k1}$ | time moments, when the stress level changes in multiple-steps-loading history |
| $\psi(t)$ | stress-reduced time |
| $a_\sigma(\sigma)$ | exponent of shifting factor for "time-stress" superposition principle |
| $\xi$ | dummy variable in the hereditary integral $\xi < t$ |
| $J_0[\sigma]$ | instantaneous (time-independent) strain as a function of the applied stresses |
| $J(t)$ | time-dependent creep compliance function |
| $F(t)$ | time-dependent part of creep function |
| $\phi(\sigma)$ | pre-integral stress function in Schapery type models |
| $g(\sigma)$ | non-linear stress function in hereditary integral in Schapery type models |
| $D_1$, $\lambda_1$, $\gamma_1$, $\alpha_1$ | constants in the functions $\phi(\sigma)$, $g(\sigma)$, $F(t)$ |
| $\nu_0$ | Poisson ratio (for elastic deformation of a visco-elastic body) |
| $\nu_t$ | Poisson ratio (for long-term deformation of a visco-elastic body) |

## 1 Introduction

Because of the improvement of many properties of plastic materials, they are becoming serious alternatives to metals in many load-bearing applications. While loaded, however, plastics feature the non-linear time-dependent behaviour (visco-elasticity, physical ageing, etc.) to a much bigger degree than metals. Although a number of non-linear models are available to describe these phenomena, they have not yet been implemented into commercially available FEA packages. Therefore, currently engineers rarely are using the modern constitutive models of visco-elasticity for design purposes.

In this paper the main elements of implementation of the non-linear visco-elasticity model into an FEA package are presented.

## 2 Generalised Form of the Schapery Model

The non-linear visco-elasticity model of a hereditary type proposed by Schapery [1]:

$$\varepsilon(t) = J_0 g_0(\sigma)\sigma + g_1(\sigma)\int_0^t F\left(\psi(t)-\psi(\xi)\right)\frac{\partial\left[g_2(\sigma)\sigma\right]}{\partial\xi}d\xi,$$

where

$$\psi(t) = \int_0^t \frac{d\xi}{a_\sigma\left[\sigma(\xi)\right]}, \tag{1}$$

is based on the assumption, that the principle of loading (stress) superposition is valid also for plastics, which display non-linear response to loading. In addition, this model incorporates the idea about the "time-stress" superposition principle (in the form of the stress-reduced time $\psi(t)$). The *physical meaning* of this principle is, that stress level $\sigma$ induces the same amount of creep effects during the time increment $\partial\psi$, as a certain reference stress level $\sigma_0$ (which usually should be chosen relatively small, so that $a_\sigma(\sigma_0)=1$) within the time period $\partial t$. The function $g_1(\sigma)$, multiplied by the hereditary integral, accounts for the difference between the creep and recovery behaviour.

The material functions in Equation (1) should be estimated, based on data from creep and recovery tests:

for creep

$$\hat{\varepsilon}\left[\sigma_k,t\right] = J_0[\sigma_k] + F\left(\frac{t}{a_\sigma(\sigma_k)}\right)g_1(\sigma_k)g_2(\sigma_k)\sigma_k\,. \tag{2}$$

for recovery

$$\hat{\varepsilon}\left[\sigma_k,t\right] = \left[F\left(\tilde{t}+t_1/a_\sigma(\sigma_k)\right)-F\left(\tilde{t}\right)\right]g_2(\sigma_k)\sigma_k \quad \tilde{t}=t-t_1\,. \tag{3}$$

Equation (3) implies, that functions $g_1(\sigma)$ and $a_\sigma(\sigma)$ are chosen in such a way, that $g_1(0)=1$ and $a_\sigma(0)=1$.

Often the "time-stress" superposition principle is referred to as the shifting rule. It means, that if experimental creep data correspond to the above principle, the creep compliance curves for different stress levels can be shifted over the logarithmic time scale to coincide and to form so-called "master curve". However, the creep curves

should be regular enough in order to coincide after shifting. The latter might be not a case, when the material undergoes the $\alpha$ or $\beta$ transition. For instance, at room temperature and within the stress range $\sigma = 22...28$ MPa, PMMA encounters the $\beta$ transition [2]. Therefore, it appears impossible to build a single "master-curve" for a whole loading range of PMMA: from low stresses till yield point [3,4].

Another representation, similar to the Equations (2) and (3) respectively, has been recently proposed by the authors [5,6]:

for creep $$\hat{\varepsilon}[\sigma_k,t] = J_0[\sigma_k] + \sum_i \phi(\sigma_k) F_i(t) g_i(\sigma_k) . \tag{4}$$

for recovery $$\hat{\varepsilon}[\sigma_k,t] = \sum_i \left[ F_i(\tilde{t} + t_1) - F_i(\tilde{t}) \right] g_i(\sigma_k)\sigma_k, \quad \tilde{t} = t - t_1 . \tag{5}$$

It shows a good ability to describe the experimental creep and recovery curves with different, even non-regular shapes. Similarly to Equations (2) and (3) this representation can be written in the hereditary integral form to account for a complex loading history:

$$\varepsilon[\sigma(t),t] = J_0[\sigma(t)] + \sum_i^n \phi_i[\sigma(t)] \int_0^t F_i(t-\xi) \frac{\partial g_i[\sigma(\xi)]}{\partial \xi} d\xi . \tag{6}$$

The conception of stress-reduced time is missing in the Equation (6), since the representation (4) - (5) enables proper fit to the creep and recovery data without any "shifting".

Although $J_0[\sigma(t)]$, $F_i(t)$, $\phi_i[\sigma(t)]$ and $g_i[\sigma(t)]$ might be chosen among the different function types (polynomial, exponential etc.), the following forms seem to be preferable [5,7] for the description of experimental data for many plastics:

$$J_0[\sigma] \quad - \quad A\sigma \quad \text{or} \quad A\left[\sigma + \sigma^{\beta}\right]; \tag{7}$$

$$g_i[\sigma] \quad - \quad D_i\sigma^{\alpha_i} \quad \text{or} \quad D_{i,1}\sigma^{\alpha_{i,1}} + D_{i,2}\sigma^{\alpha_{i,2}} ; \tag{8}$$

$$\phi_i[\sigma] \quad - \quad \exp(\gamma_i\sigma) \quad \text{or} \quad 1 + B_{i,1}\sigma^{\gamma_{i,1}} + B_{i,2}\sigma^{\gamma_{i,2}} ; \tag{9}$$

$$F_i(t) = \left(1 - \exp(-\lambda_i t)\right). \tag{10}$$

As always, the simpler form should be preferred. The more complex form is chosen, to better fit the experimental data, the longer calculation time is necessary for FE simulation and the more likely it is, that numerical instability might occur. Taking into account that creep tests on plastics can not be reproduced with less than 3...5% of deviation [5,8,9] and that the error of the FE analysis usually also is about 5...10%, there is no reason to aim for a fit better, than 3...5% of total deviation between data and model prediction.

There are convincing advantages in choosing the time functions $F_i(t)$ in the form of Prony series. First, it allows efficient numerical calculation [10] of hereditary integrals.

Secondly, together with the representation of the strain response $\varepsilon[\sigma_k, t]$ in the form of locally separated variables (Equations (4) and (5)) it gives better possibilities for establishing the parameter identification procedure. This procedure is based on the idea of minimisation of the relative deviation between experimental data and model prediction. The deviation can be considered as a function that depends on the model parameters $I(D_i, \alpha_i, \lambda_i, \gamma_i)$. From this point of view the parameter identification procedure involves a multi-dimensional minimisation. The algorithm used is based on the Powell's multi-dimensional minimisation procedure [11].

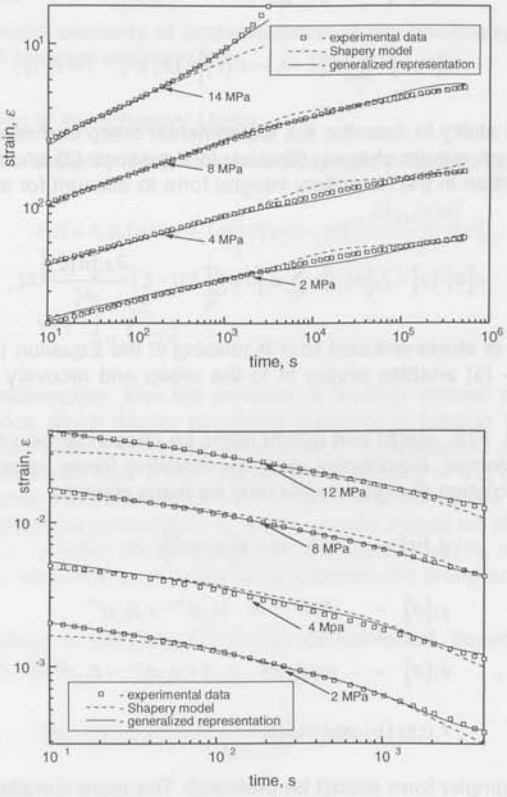


*Figure 1: Experimental data [12] and model prediction for the creep and recovery behaviour of HDPE*

The prediction of creep and recovery behaviour for HDPE is given in Fig. 1. The creep and recovery behaviour of HDPE can be modelled using the parameters given in Equations (7) - (10) and their numerical values are listed in Table 1. In order to evaluate the accuracy of the proposed generalised representation (6), the "curve fitting" has been performed also for the Schapery model (1).

The following material functions were used:

$$J_0 g_0[\sigma] = 1 \cdot 10^{-3}; \quad g_1[\sigma] = \exp(0.041 \cdot \sigma); \quad g_2[\sigma] = \sigma^{0.396}; \quad a[\sigma] = \exp[-0.15 \cdot \sigma];$$
$$F(t) = \sum_{n=1,6} D_n \left(1 - \exp\left(-t/10^n\right)\right); \tag{11}$$
$$D_n = \left\{0.281 \cdot 10^{-5}, \quad 0.224 \cdot 10^{-3}, \quad 0.283 \cdot 10^{-3}, \quad 0.720 \cdot 10^{-3}, \quad 0.161 \cdot 10^{-8}, \quad 0.824\text{E} \cdot 10^{-3}\right\}.$$

The total error reached for the Schapery model is less than 6.7%, while Equation (6) enabled to reach 2.2%. Both approaches model the creep behaviour well, but the generalised representation gives better fit for the recovery behaviour.

*Table 1: The set of model parameters for description of HDPE*

| Term, $i$ | A | | | $\beta$ | | |
|---|---|---|---|---|---|---|
| 0 | $7.852 \cdot 10^{-4}$ | | | 0.0 | | |
| | $D_{i,1}$ | $\alpha_{i,1}$ | $D_{i,2}$ | $\alpha_{i,2}$ | $\gamma_i$ | $\lambda_i$ |
| 1 | $.1278 \cdot 10^{-4}$ | 2.759 | $.2592 \cdot 10^{-3}$ | 1.059 | $-.2404 \cdot 10^{-1}$ | $10^{-1}$ |
| 2 | $.3364 \cdot 10^{-3}$ | 1.075 | $.5910 \cdot 10^{-5}$ | 2.872 | $-.1473 \cdot 10^{-3}$ | $10^{-2}$ |
| 3 | $.3729 \cdot 10^{-3}$ | 1.118 | $.9672 \cdot 10^{-5}$ | 2.740 | $.6727 \cdot 10^{-1}$ | $10^{-3}$ |
| 4 | $.5814 \cdot 10^{-4}$ | 2.193 | $.2842 \cdot 10^{-9}$ | 6.254 | $.4689 \cdot 10^{-1}$ | $10^{-4}$ |
| 5 | $.6187 \cdot 10^{-3}$ | 1.547 | $.6753 \cdot 10^{-11}$ | 9.779 | $.9244 \cdot 10^{-3}$ | $10^{-5}$ |
| 6 | $.4855 \cdot 10^{-1}$ | 1.637 | $.2791 \cdot 10^{-2}$ | 2.786 | -3.377 | $10^{-6}$ |

## 3 *Extension of the Model to 3-D Formulation*

One of the ways to develop the 3-D formulation is to assume, that the behaviour of visco-elastic materials is, to certain extent, similar to the elastic behaviour [8,9]. Since, this is a very general assumption, it leave place for some additional phenomenological hypotheses:

- the material is compressible and originally isotropic;
- strains are small enough to accept conventional definitions for stress and strain tensors;
- the rate of viscous flow is proportional to the effective stress $\hat{\sigma}$;
- the deviatoric and hydrostatic part of deformation process are completely uncoupled.

As a result, a three-dimensional formulation of the visco-elastic model has been proposed [5]:

$$\overline{\varepsilon} = \left[(1+\nu_0)\mathbf{M}_D + (1-2\nu_0)\mathbf{M}_H\right]\tilde{\varphi}(\hat{\sigma})\overline{\sigma} + \\ + \left[(1+\nu_1)\mathbf{M}_D + (1-2\nu_1)\mathbf{M}_H\right]\sum_{i=1}^{n}\phi_i(\hat{\sigma})\int_0^t F_i(t-\xi)\frac{\partial\left[\tilde{g}_i(\hat{\sigma})\overline{\sigma}\right]}{\partial\xi}d\xi. \tag{12}$$

Here, for the case of uniaxial loading:

$$J_0[\sigma] = \tilde{\varphi}(\sigma)\sigma; \quad g_1[\sigma] = \tilde{g}_1(\sigma)\sigma. \tag{13}$$

The following matrix and vector notations have been used above:

$$\overline{\sigma} = \left\{\sigma_{xx}\ \sigma_{yy}\ \sigma_{zz}\ \tau_{xy}\ \tau_{yz}\ \tau_{zx}\right\}^T; \quad \overline{\varepsilon} = \left\{\varepsilon_{xx}\ \varepsilon_{yy}\ \varepsilon_{zz}\ \gamma_{xy}\ \gamma_{yz}\ \gamma_{zx}\right\}^T. \tag{14}$$

$$\mathbf{M}_D = \begin{cases} \frac{2}{3}, & \text{if } i = j \text{ and } i, j \le 3; \\ -\frac{1}{3}, & \text{if } i \ne j \text{ and } i, j \le 3; \\ 2, & \text{if } i = j \text{ and } i, j > 3; \\ 0, & \text{if } i \ne j \text{ and } i, j \le 3. \end{cases} \quad \mathbf{M}_H^{i,j}\Big|_{i,j=1\ldots3} = \frac{1}{3}; \tag{15}$$

## 4 Main Elements of Numerical Algorithm

The MARC FEA package has been chosen for implementation of the visco-elasticity model (12), since it has an open structure, which enables easy access to the variables (stresses, strains, time increment) and extended facilities to handle the geometrically and physically non-linear problems. The non-linear problems can be solved by FEA software only incrementally. Since MARC is based on the displacement method, it requires the stress-strain relation to be given in terms of increments as follows:

$$\Delta\overline{\sigma} = \mathbf{L}(\Delta\overline{\varepsilon}, \Delta t \ldots). \tag{16}$$

Therefore, relation (12) has to be written in a finite form and inverted, in order to be implemented into a FEA package. For sufficiently regular functions $g_i(\sigma)$, such that $|\sigma \cdot [g_i(\sigma)]'_\sigma \cdot| << 1$, the hereditary integral with kernel function in the form of Prony series term can be discretised, following Henriksen [10] :

$$\int_0^t \left(1 - \exp\left(-\lambda_i (t-\xi)\right)\right) \frac{\partial\left[g_i(\sigma)\right]}{\partial \xi} d\xi = g_i(\sigma) + \theta_i(t). \tag{17}$$

The hereditary integral functions $\theta_i(t)$:

$$\theta_i(t) = -\int_0^t \exp\left(-\lambda_i (t-\xi)\right) \frac{\partial\left[g_i(\sigma)\right]}{\partial \xi} d\xi \tag{18}$$

can be calculated recurrently as follows:

$$\theta_i(t) = \exp(-\lambda_i \Delta t)\theta_i(t - \Delta t) - \Delta\left[g_i(\sigma)\right]\Gamma_i(\Delta t). \tag{19}$$

Here, for convenience the following notation has been introduced:

$$\Gamma_i(\Delta t) = \frac{1 - \exp(-\lambda_i \Delta t)}{\lambda_i \Delta t}. \tag{20}$$

The above transformations allow to rewrite relation (12) in the finite form. For this the total differential has to be derived and inverted to the form (16). Unfortunately, such a numerical scheme shows low convergence and often can become unstable [13]. In [9] similar derivations have been presented for the case of Schapery model (1). As a result, an expression has been obtained, which also shows low convergence.

Therefore, similarly to [8] it has been assumed that the pre-integral functions $\phi_i(\sigma)$ do

not vary during the time increment. In addition only partial factorisation has been used, while inverting the discretised stress-strain relation. As a result the following numerical scheme has been derived [13]:

$$\Delta\overline{\sigma} = \left\{\left[(1+\nu_0)\mathbf{M}_D + (1-2\nu_0)\mathbf{M}_H\right]\widetilde{\varphi}(\hat{\sigma})\right\}^{-1} \times \{\Delta\overline{\varepsilon} - \left[(1+\nu_1)\mathbf{M}_D + (1-2\nu_1)\mathbf{M}_H\right] \times$$
$$\times \sum_{i=1}^{n}\left[\left[\phi_i(\hat{\sigma})\widetilde{g}_i(\hat{\sigma})\left(1-\Gamma_i(\Delta t)\right)\right]\Delta\overline{\sigma}(t-\Delta t) + \phi_i(\hat{\sigma})\left(\exp\left(-\lambda_i\Delta t\right)-1\right)\widetilde{\theta}_i(t-\Delta t)\right]\}. \tag{21}$$

where:

$$\widetilde{\theta}_i(t) = \exp(-\lambda_i\Delta t)\widetilde{\theta}_i(t-\Delta t) - \Delta\left[\widetilde{g}_i(\hat{\sigma})\overline{\sigma}\right]\Gamma_i(\Delta t). \tag{22}$$

While deriving the above relations it has been implied, that the loading history begins always from zero $\sigma(0) = 0$.

The above scheme is recurrent. To estimate the viscous strains increment for the current time $t$, only the data for the stress field $\sigma$ and internal parameters $\widetilde{\theta}_i$ from the previous step are needed. Although for the models with a large number of elements this numerical scheme can require large amounts of computer memory, the advantage in decreasing computing time is obvious.

## 5 *Verification of the Schemes Proposed*

The tensile creep-recovery tests for several plastics have been simulated first. As mentioned above, due to strong non-linearity of the materials behaviour, numerical instabilities have been encountered, while testing the numerical scheme, based on complete total derivation and factorisation [6,13]. Unlike that, the scheme (21), which assumes pre-integral functions $\phi_i(\sigma)$ to be constant during the time increment and is derived using simplified factorisation, appears to be stable, has good convergence and, consequently, higher computational rate. However, it is obvious that because of accepted assumptions, the stiffness matrix becomes independent from the loading history. Therefore, this numerical scheme can not describe the strain recovery phenomenon properly, when material stiffness is changing significantly during the loading history [13].

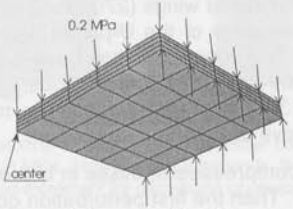


*Figure 2: One quarter of thick plate under transversal loading*

Further, to compare two approaches, namely: the Schapery model (1) and generalised representation (6), the behaviour of simply supported thick HDPE plate under transversal loading has been simulated (Fig. 2). The upper surface of the plane plate (60×60×3 mm) has been loaded by uniform pressure, applied gradually (in 20 loading steps). The edges of the plate were simply supported. The maximum level of

loading reached was 0.2 MPa. After that, the loading has been kept constant during 1200 s.

The results obtained using these two models (Fig. 3) are nearly similar. The plate features simultaneously the relaxation of stresses and creep (increasing in time deflection of the plate). The redistribution of stress fields during the sustained loading is qualitatively the same for both models. The transversal displacement (deflection) at the middle of the plate differs for two models by 3%, while the effective Von Mises stresses deviate by 5%. If to account for the accuracy of FE calculations (~5%) and for the deviation that is introduced by two different fittings to experimental data, this might be considered as a good agreement.

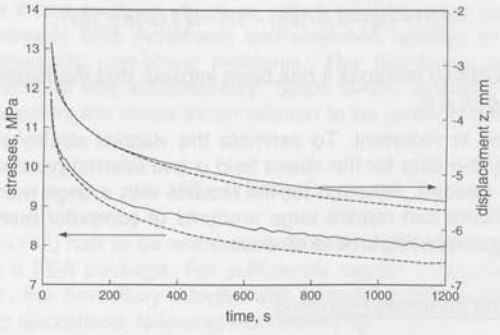


*Figure 3: Dependencies of the equivalent Von Mises stresses and deflection at the middle of HDPE plate vs. time, calculated using representation (6) – (straight line) and Schapery model (1) – (dashed line).*

Therefore, if both models are operational, the generalised representation (6) gives results, which correspond to those predicted by the Schapery model (1). On the other hand, representation (6) is also able to describe the behaviour of a polymer for the regions where experimental data are non-regular for some reason.

To demonstrate the ability of the developed model to simulate more sophisticated time dependent phenomena, the behaviour of an HDPE U-profile under compressive ramp loading has been calculated. The U-profile, consisted of a main plane (270×85×3 mm) and two symmetrical wings (270×35×3 mm), has been modelled by 256 shell elements. The lower edge of the U-profile has been clamped to prevent any displacement or rotation. The upper edge has been loaded by ramp compressive loading (the displacement rate was 0.24 mm/s). Thus, a single loading increment caused the displacement 0.135 mm of upper edge. The transversal deflections and rotations at the upper edge have also been restricted.

During the initial period, the compressive stresses in U-profile have been increasing, but remained uniform (Fig. 4). Then the first perturbation occurred, when the wings of U-profile have lost their plane shape. It is clearly seen that because of restriction from the stiffening ribs of the U-profiles the wings buckling is also delayed (3-rd buckling mode is realised). With further increase of compressive load the second perturbation, which relates to the buckling of stiffening ribs, has occurred. Here also the 3$^{rd}$ mode is realised, which was obviously initiated by the same mode of primary (wings) buckling. The loss of structure loadability has caused considerable redistri-

bution of stresses during a short period of time. The redistribution, which is presented on Fig. 4 (two lower frames) is happening within a period of time, when there is no change of applied load. Such an effect can not be modelled using constitutive models, which do not account for time variable.

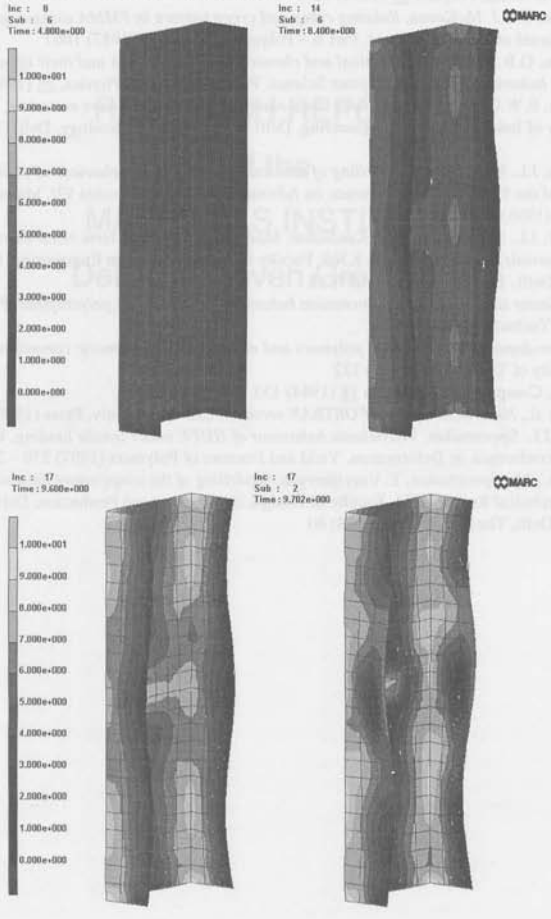


*Figure 4: Development of the buckling in time in U-profile under compressive loading. The stresses on the scale are given in MPa. Time is given in seconds. "Inc" denotes load increment, while "Sub" is a number of sub-increment for calculation of creep within an increment*

Therefore, in order to simulate the time-dependent phenomena in plastics properly, there is a need for further development on computer modelling of non-linear visco-elasticity. Having in mind practical applications, special attention should be paid, first of all, to realistic modelling of 3-D effects in non-linear visco-elasticity and to the development of more robust numerical schemes for implementation into FEM.

## References


1. R.A. Schapery, *On the Characterization of nonlinear viscoelastic materials*, Journal of Polymer Engineering Science 9 (1969) 295
2. B.E. Read, G.D. Dean, Polymer 25 (1984) 1679
3. J.M. Crissman, G.B.J. McKenna, *Relating creep and creep rupture in PMMA using a reduced variable approach*, Journal of Polymer Science, Part B – Polymers Physics 25 (1987) 1667
4. J.M. Crissman, G.B.J. McKenna, *Physical and chemical aging in PMMA and their affect on creep and creep rupture behavior*, Journal of Polymer Science, Part B – Polymers Physics, 28 (1990) 1463
5. I.D. Skrypnyk, E.W.G. Zweers, *Non-linear visco-elastic models for polymers materials*, Technical Report K345, Faculty of Industrial Design Engineering, Delft University of Technology, Delft, The Netherlands (1996) 40
6. I.D. Skrypnyk, J.L. Spoormaker, *Modelling of non-linear visco-elastic behaviour of plastic materials*, In: Proceedings of the 5th European Conference on Advanced Materials /Euromat 97/, Materials, Functionality and Design 4 (1996) 4/491-4/495
7. I.D. Skrypnyk, J.L. Spoormaker, P.V. Kandachar, *Modelling of the long-term visco-elastic behaviour of polymeric materials*, Technical Report K369, Faculty of Industrial Design Engineering, Delft University of Technology, Delft, The Netherlands (1997) 48
8. J. Lai., *Non-linear time-dependent deformation behavior of high density polyethylene*, Ph.D. thesis, Delft University of Technology (1995) 157
9. L. Zhang, *Time-dependent behavior of polymers and unidirectional polymeric composites*, Ph.D. thesis, Delft University of Technology (1995) 172
10. M. Henriksen, Computers & Structures 18 (1984) 133
11. W.H. Press et al., *Numerical recipes (FORTRAN version)*, Cambridge Univ. Press (1989)
12. J.G.J. Beijer, J.L. Spoormaker, *Viscoelastic behaviour of HDPE under tensile loading*, In: Proc. of 10th International conference on Deformation, Yield and Fracture of Polymers (1997) 270 – 273
13. I.D. Skrypnyk., J.L. Spoormaker, T. Vasyljkevych, *Modelling of the temperature dependent visco-elasticity in plastics*, Technical Report K381, Faculty of Design, Engineering and Production, Delft University of Technology, Delft, The Netherlands (1998) 40

RESEARCH REPORTS

of the

MATERIALS INSTITUTE

Delft Eindhoven Groningen

## ADVANCED MATERIALS AND CASTING TECHNOLOGY

Delft University of Technology, Laboratory of Materials Science
Rotterdamseweg 137, 2628 AL Delft
phone +31 (15) 2782275, fax +31 (15) 2786730, e-mail ...@stm.tudelft.nl

### PERSONNEL

*Scientific staff*

| | |
|---|---|
| prof.ir. L. Katgerman | (2782249, L.Katgerman@...) |
| dr.ir. J. Duszczyk | (2782218, J.Duszczyk@...) |
| dr. W.H. Kool | (2782224, W.H.Kool@...) |

*Temporary scientific staff*

| | |
|---|---|
| drs. W.A. van den Berg | (2782254, W.A.vandenBerg@...) |
| dr.ir. L. Kowalski (IOP/STW) | (2782414, L.Kowalski@...) |
| ir. E.D. van Vliet | (2784463) |

*Graduate students*

| | |
|---|---|
| I. Apachitei | (2782414) |
| ir. H.J. Brinkman | (2782254, H.J.Brinkman@...) |
| drs. W.M. van Haaften | (2782201, W.M.vanHaaften@...) |
| ir. M.H.M. Huisert | (2785194, M.H.M.Huisert@...) |
| ir. E.N. Straatsma | (2782201, E.N.Straatsma@...) |

*Research students*

R.J. Gouwen
M.T. van den Hoogen
M.E. Pieterse
M.B.C. Spoor
J.W. de Vries
J. Zuidema jr.

*Technical assistants*

| | |
|---|---|
| N.A.M. van den Berg | (2783456) |
| L.A. Borsboom | (2783578) |
| P. Bouter | (2782203) |
| ing. H.J.J. Deen | (2782276, H.J.J.Deen@...) |
| J.J. Jansen | (2782216) |
| H. Kleinjan | (2782193) |
| P. de Ruiter | (2784526) |
| T. Tobi (STW) | (2782242) |

*Managerial assistants*

| | |
|---|---|
| M.A.W. Jacobs | (2782275, M.Jacobs@...) |
| O.M.S. Wens-van Swol | (2783976, O.M.S.Wens-vanSwol@...) |

### RESEARCH AREAS AND OBJECTIVES

The research programme can be divided into different fields of interest:

- Materials
  - Ferrous alloys (spheroidal cast iron, P/M steels)

  - Non ferrous alloys (mainly aluminium alloys)
  - Intermetallic compounds (aluminides, silicides)
- Processing techniques
  - Metal preparation in the liquid phase
  - Computer modelling of the casting process
  - Production of rapidly solidified materials
  - Production of metal matrix composites
  - Strip casting
  - Sintering
  - Extrusion
  - Powder injection moulding
  - Hot isostatic pressing

Three major research areas can be distinguished:

1 *Solidification Processing*

2 *Advanced Materials and Production Technology*

3 *Powder Metallurgy*

FACILITIES

*Foundry*

- Six induction and resistance heating furnaces for ferrous and non-ferrous alloys, capacities from 2-90 l and power-ratings from 15-120 kW
- Heat treatment ovens with or without air circulation, capacities from 10-1500 l, maximum temperatures up to 1200 °C
- One roller, maximum width 30 cm
- One forging hammer
- One vertical semi-continuous casting machine for mainly aluminium alloy billets up to approximately 180 cm with round shape diameter approximately Ø 19 cm and shape 8 cm × 20 cm
- One vacuum furnace (capacity approximately 2 l)
- One low pressure pouring machine for aluminium alloys, computer controlled, inert gas operated, capacity 30 kg
- Two shot blasting machines for glass beads or steel shot. One vibrating container for wet polishing
- Mixers, from 2 to 150 kg, for green (clay bonded) and chemically bonded sand moulds and cores
- Moulding machine, for green (clay bonded) sand moulds
- Gas hardening equipment for chemically bonded sand cores and moulds
- Equipment to produce ceramic moulds (precision casting)
- Equipment to test and analyse green (clay bonded) and chemically bonded sand (Georg Fischer)
- Fully equipped pattern shop for production of patterns for sand moulds including a computer controlled milling machine for production of foam patterns using CAD/CAM-techniques
- Two workstations (HP) for use of several computer simulation programmes (mould filling and solidification)
- Several personal computers for stand alone use (controlling of Low Pressure pouring machines, temperature measurements and place determination of liq-

uid metal in sand moulds, process simulation) and use as a terminal (network) for the workstation
- Water simulation equipment for observation of flow phenomena in water while simulating real casting processes

*Foundry Laboratory*
- A large number of smaller units with inductive or resistance heating are available, power ratings up to ca. 3 kW
- One vacuum furnace (capacity 1 l) and one electron beam furnace with X-Y table
- Extrusion press, max. 500 °C, 60 ton, billet 30 mm diameter x 70 mm length
- One experimental horizontal die-casting machine with transparent dies and cold chamber, for simulation experiments
- Rotating (pen on disk) wear tester
- Equipment for rapid solidification processing
- Dilatometer equipment
- Viscosimeter
- Differential scanning calorimeter

*Powder Metallurgy*
- Processing line for powder injection moulding - PIM (different attritors and ball mills for modification of powder morphology, mixers and kneaders for plastisol fomulation, injection moulding press, BASF debinding oven)
- Vacuum-sinter-debinding oven (1700 °C, $N_2$, $H_2$, Ar) with a unit for fast cooling. The oven is also used for different cycles of phase transformation in steels
- Hot Vacuum Press (2200 °C, 20 Tones, Ø 150 × 200 mm, Ar, $N_2$). The press is also used for diffusion bonding and processing of materials for electronic industry (sandwich capacitors)
- Hot Isostatic Press (2200 °C, 200 MPa, Ø 150 × 300 mm, Ar, $N_2$). HIP is also applied for diffusion bonding, coatings, heat treatment under pressure (for instance nitriding) and post processing in order to close residual porosity (coatings, castings, PIM components)
- Cold Isostatic Pressing (400 MPa, Ø 200 × 1000 mm. CIP is also used for hydrostatic forming techniques of aluminium, steel and metal-polymer laminates
- Horizontal extrusion press (2MN, fully instrumented with conventional liners - 500 °C and high temperature liner water cooled - 750 °C
- Vertical extrusion press (0.8 MN, fully instrumented, liner - 500 °C)
- Carbolite tubular oven (up to 1600 °C)
- Sinter furnace (up to 1200 °C)
- Edwards EQ 80F residual gas analyser
- Degassing unit
- Particle size analyser and BET equipment
- DSC, TGA

## RESEARCH REPORT 1997

### 1 *Solidification Processing*

#### 1.1 *Thin Nodular Cast Iron for Automotive Applications*

Within the PBTS NM95026 project "Thin Nodular Cast Iron for Automotive Applica-

tions" efforts are made to reproduce high quality thin wall (thickness < 3,5 mm) castings out of nodular cast iron. The castings have to be free of carbides and without porosities. Meanwhile the castings need to have a good fatigue resistance. The project is a follow-up on the BRITE-P-2437-5-87 project "Thin Walled Nodular Cast Iron".

### 1.2 *Mould Filling and Solidification of Aluminium Alloys*

As a follow up on the IOP research program "Quality improvement of castings by optimisation of mould filling", a study has been made of the mould filling of a thin wall horizontal horse shoe with aluminium. This research has been conducted to the heat transfer and solidification during mould filling as well as the description of the metal-air surface, including surface tension. Mould filling with liquid metal has been registered using a video camera in moulds with a ceramic glass plate, or using contact measurements in a sand mould. Additionally, temperature measurements have been performed. The experimental results have been compared with computational results obtained with a commercial software package, Flow-3D. Additional to the casting experiments, Particle Image Velocimetry (PIV) measurements were performed in a water model of the horse shoe. This way the velocity field during mould filling was obtained experimentally and could be compared to computations. The experiments have been carried out within a Ph.D. study, in co-operation with the "Kramers Laboratorium voor Fysische Technologie" of Delft University of Technology.

### 1.3 *Lost Foam Technology*

Within the cluster project Lost Foam Technology research has been done on lost foam casting techniques in corporation with the foundries Lovink Terborg and De Globe, TNO Product Centrum Delft and Gemco Lost Foam. During the casting technique an E.P.S. pattern is embedded in non-bounded sand. During the pouring process the molten metal replaces the pattern while vaporising it. Using the lost foam technique difficult high quality castings can be produced without cores and with a smoother surface than conventionally made sand castings. To obtain high quality castings, a fully automated and fully controlled production process from foam pattern design to castings, is required. Therefore it is necessary to apply Computer-Aided-Design, Manufacturing and Engineering techniques (Rapid Prototyping). Mould filling and solidification are very important issues within the process. Therefore investigations are carried out using mathematical computer calculations with software packages like Flow-3D. The computer calculation results are validated with real casting experiments during which the place of the metal in the mould and the local temperatures in moulding material and metal are determined. Also the thermo-mechanical properties of the castings are investigated. During the research, ferrous as well as non-ferrous alloys are examined.

### 1.4 *Low Pressure Sand Casting of Aluminium Composites*

This project is supported by IOP-Metalen. At this moment the castability of aluminium matrix composites has been examined by using a Low Pressure Casting Machine. During the experiments the melt has to be stirred to prevent sedimentation of the composite particles. The composite material is very sensitive to inclusion of oxides and gas. Gas inclusion can be reduced by avoiding turbulence during stirring and pouring of the melt. By the use of ceramic filters the melt can be refined during pouring so the final number of oxides in the castings is reduced. Experiments show that aluminium with SiC particles has a higher Young's modulus, a higher hardness

and a lower elongation.

### 1.5 *Thermomechanical Properties of DC Cast Aluminium Alloys in Relation to Hot Tearing*

Research is carried out within a Brite/Euram programme, EMPACT, which involves six European primary aluminium producers, a software company and several technological institutions. The main aim of this project is to develop predictive tools for control of deformation, cracking and segregation in aluminium casting of rolling ingots and extrusion billets.
Delft University of Technology focuses on two subjects: firstly, the thermophysical and thermomechanical properties of the five selected alloys (AA1050, AA3104, AA5182, AA6063 and AA7075) and secondly, the investigation of the hot tearing mechanism and the formulation of cracking criteria functions for the DC cast ingots.
The main thermophysical properties have been collected from literature and have also been modelled with ALSTRUC by one of the project partners. The thermomechanical properties of AA3104 were determined in a wide temperature range and at low strain rate with a Gleeble thermomechanical simulator. These properties were used to determine the rheological parameters of the modified Ludwig constitutive equation. A literature survey was carried out to investigate the existing cracking criteria functions.

## 2 *Advanced Materials and Production Technology*

### 2.1 *Rapid Solidification Processing of Al Alloys for Recycling or for Advanced Properties*

The rapid solidification technique, as developed by the group and operated through both a laboratory line unit and pilot line unit in industry, approaches the stage of commercialisation. In an EEC CRAFT project, which started in 1996, attention is paid to prototype development of particular finished products to be made from rapidly solidified aluminium alloys.
These products are developed in close co-operation with the producers. The work of the Delft group concentrates on alloy composition, processing procedures and final properties in relation to alloy composition and/or processing procedures. Examples are pistons in automotive engines, high strength alloys used in mountain climbing equipment, light weight ladders, towing brackets etc.

### 2.2 *Formability of Strip Casted Aluminium Alloys*

A single roll stripcaster developed by the TU Delft has been optimised to produce strip with thicknesses between 0.5-10mm. The main problem was to get a strip width of 100 mm with a constant thickness. By studying the liquid flow when connecting the casting drum has resulted in an advanced casting slot. Results proved that there has to be a certain casting pressure, nozzle slot breadth and gap distance to get a constant strip thickness. Also an increased roll speed and casting temperature results in a decreased strip thickness. The microstructure of all stripcast material shows highly orientated columnar crystals originating from the casting roll surface of the strip. A transition from columnar to equiaxed growth is found at $^2/_3$ of the strip thickness. An average SDAS value of 7.07 µm is found for the AA 3004 stripcast material and an average cooling rate of about 1344 °C/s is found for the stripcast process. SDAS and cooling rate are related to the roll speed: a lower roll speed results in a larger SDAS

and thus in a smaller cooling rate of the metal. After the metal is solidified the strip will be directly rolled. Because of the high cooling rate a supersaturation of alloying elements and a fine microstructure occurs and this could give a better formability of sheet material. Experiments are now concentrating on the influence of alloying elements on strip quality, structure and formability properties after the strip has been rolled. This project is supported by IOP-metalen.

## 3 *Powder Metallurgy*

### 3.1 *Processing of Aluminium Alloys and Metal Matrix Composites for Wear-Resistance Applications*

The research work has been supported by national (IOP, FOM and STW), European (COST) and industrial PBTS programmes. A variety of powder metallurgy techniques were employed to process conventional and unconventional aluminium alloys and aluminium alloy based composites, targeting at enhanced wear resistance, lowered thermal expansion coefficient and improved mechanical properties at room and elevated temperatures. For the composites, Al-Si-X pre-alloyed powders, Al-Cu and Al-Fe elementary powders, and Al-Fe-V pre-alloyed powder were selected as starting matrix materials. Ceramic reinforcements (5-20 vol.%), such as $Al_2O_3$ and SiC particles of different median sizes and morphologies and $Al_2O_3$ short fibres, were introduced by mixing them with the matrix alloy powders (the Osprey spray co-deposition was also used as an alternative approach). Subsequent processing was differently conducted, mainly depending on starting materials; for instance, cold isostatic pressing, degassing and hot extrusion were involved in processing Al-Si based composites; uni-axial compaction, degassing, liquid phase sintering, hot extrusion and heat treatment in processing elemental Al-Cu based composites; and uni-axial compaction, reactive sintering and extrusion in processing elemental Al-Fe based composites. Microscopy was carried out to examine structure and to determine the mechanisms of deformation, fracture and wear. Tensile properties at room and elevated temperatures up to 400 °C, hardness, Young's modulus, thermal expansion coefficient and wear resistance were evaluated. As the work covers a wide scope of materials and processes, the following are two examples showing the research on specific composite materials and extrusion process.

- *Aluminium matrix composites with short fibres*
  The composites based on a P/M Al-20Si-X alloy and containing 4.8, 10.0, and 20.0 vol.% d-$Al_2O_3$ short fibres were prepared through dry mixing, compaction, degassing and extrusion. The previous stage of the work was focused on tensile properties as influenced by a post-extrusion heat treatment and by reduction ratio applied during extrusion. Recent work has been on the microstructure at the fibre-matrix interfaces and the fibre chemistry. It has shown that in addition to fragmentation, other forms of less obvious damage are inflicted upon fibres during extrusion such as flaws, cracks and abraded surface, reducing the intrinsic strength of the fibres. The damage is caused by the combined effect of the large volume fraction of hard silicon particles in the matrix alloy and severe shearing involved in extrusion. SEM, TEM and XPS demonstrate the affinity of the d-$Al_2O_3$ fibre to the matrix alloying elements (copper and magnesium). The specific internal texture (porosity and large surface) of the fibres, their surface chemical activity at extrusion temperature and mechanical fragmentation allow rapid hypothetical chemical (redox) reaction. Due to the damage, the reaction

takes place at fibre ends, external surface, abraded surface, flaws and cracks.

- *Extrusion*
  Extrusion has been carried out as an essential step in each of the processing route, to consolidate pre-alloyed powders, sintered elementary powders, mixed composite materials, spray deposited preforms. It has also been considered as a thermomechanical process to understand the mechanical and structural responses of the materials to hot deformation. For each material, it is necessary to specify the correlation between the extrusion pressure requirement and process variables, and to determine the extrudability with respect to the capacity of a press available, and the surface quality, deformation homogeneity, and structural integration of the consolidated materials. Meanwhile, computer modelling of extruding aluminium alloys and composites with the plasticity theory as applied to the specific situation in which volume change occurs along with deformation has also been in progress, with an emphasis on CAD of metallic and ceramic dies especially for difficult-to-extrude materials such as metal matrix composites and intermetallics.

3.2 *Novel Processing, Physical and Mechanical Metallurgy of Ordered Intermetallics*

The research programme, as a continued part of the ongoing projects concerns materials development, novel processing, physical and mechanical metallurgy aspects of several ordered intermetallic compounds ($Ni_3Al$, $Ni_3Si$, $Fe_3Al$ and FeAl based). The main activities and objectives can be summarised as:

(a) Novel processing of ordered intermetallic compounds and intermetallic matrix composites. Several intermetallic compounds based on $Ni_3Al$, Ni-Al-Cr, $Fe_3Al$, FeAl and Fe-Al-Cr have been processed from elemental powders using reactive sintering and reactive hipping techniques. *In situ* forming $Ni_3Al$-$Ti_2B$ composites from elemental powders of Ni, Al, Ti, and B has been studied by means of reactive sintering and self-propagating high-temperature synthesis (SHS) techniques. Although the principle of these techniques is the same, *i.e.*, is based on the highly exothermic nature of the system, considerable differences exist in experimental design and operational mechanism between the reactive sintering/hipping and the SHS processing. In reactive sintering or reactive hipping, the whole volume of the compacts is continuously heated in a furnace or a HIP unit up to the lowest eutectic temperature of the alloy system which is usually much lower than their melting temperature of the compounds, and the reaction completes within a few seconds. While in the SHS process, the reaction is ignited at one end of the compact which gives a combustion reaction wave with a certain wave speed moving through the whole sample and transforming the compacted elemental powders into the final combustion products, compounds or composites.
The research covers both the fundamental aspects and experimental applications. Thermodynamics in relation to reaction mechanisms of the combustion processes are studied by means of DSC analysis at both low and high temperatures (up to 1300 °C) and DTA analysis. The influence of diluent on the thermodynamic properties of the system is also investigated. The reaction phase forming technique for preparing ordered intermetallics or intermetallic matrix composites shows prospective possibility in engineering applications due to its advantages over other conventional processing methods, including the

use of less expensive, readily available and easily compacted elemental powders, lower processing cost and energy savings. Some valuable results have been obtained related to this part of the research. However, some processing controls have to be further studied in order to use this technique for industrial applications.

(b) Study on the microstructures and mechanical properties of the $Ni_3Al$- and $Fe_3Al$-based intermetallics. Microstructures have been investigated using TEM, SEM, optical microscopy. Surface layer structure and grain boundary segregation behaviour of the compounds have been studied using Auger electron spectroscopy and XPS. Room temperature and elevated temperature properties have been investigated with special emphasis on the influence of testing atmosphere (low humidity, inert gas, in petroleum), deformation rate on the mechanical properties.

(c) Processing, microstructures and mechanical properties of the $Ni_3Si$-based intermetallics have been investigated related to the influence of alloying additions of Cr and Ti, as well as different production techniques. This part of the research has provided some useful results for the application of $Ni_3Si$-based intermetallics in off-shore, chemical industries.

### 3.3 *Powder Injection Moulding*

The research on powder injection moulding (PIM) was focused on debinding (the elimination of the binder after moulding) - the most difficult and time consuming stage of the PIM process. As a result of the debinding process, the major part of the binder is removed, while the remainders will be degraded during the subsequent sintering. Three different removal techniques have been investigated, namely thermal degradation, wick debinding and solvent extraction.

Pure thermal degradation proved to be less effective than wick debinding in combination with thermal degradation. For wick debinding, an optimum between wicking time and thermal degradation time has been established. Furthermore, a theoretical model describing the wick process has been developed and confirmed by experimental results. As a result, requirements concerning wick particle size and binder viscosity have been set.

Because of great interest shown by industry, solvent debinding has been introduced. After the first trials based on an extensive literature study, general design rules for a soluble binder system have been set. This enables the development of a new environment-friendly water soluble binder, which allows for a reduction in debinding time of over 50%. At this moment, optimisation and up scaling of the process are the main concerns. The last task will be carried out within a frame of industrial programmes.

### 3.4 *Enhanced Sintering of Ferrous Components*

The influence of sintering parameters (time, temperature and sintering atmosphere) and post-sintering cooling rate on the final properties of Fe-Ni alloys was investigated. Two main issues were thoroughly addressed:

- the influence of debinding-sintering cycle on the final properties of metal injection moulded components;
- homogenisation of Fe-2Ni and its influence on the microstructure and mechanical properties of the final products.

It has been concluded that an addition of 2 wt.% nickel does not depress the pearlite transformation to the extent that causes a noticeable improvement of the micro-

structure and tensile properties of the final parts. The improved mechanical properties can mainly be attributed to the retention of carbon in the alloy and its fine pearlitic structure. Sintering parameters (temperature, time and sintering atmosphere) need, however, to be carefully adjusted; a trade-off between densification mechanisms leading to increased mechanical properties and a grain growth process having a reverse effect on the final properties of the product has to be taken into account. The optimised debinding-sintering cycle with controlled post-sintering cooling allows ultimately an increase of the tensile properties of the sintered products more than twofold.
The investigation on the kinetics of debinding-sintering process related to different particle size distributions of the 316L and 17-4 PH P/M stainless steels has also commenced.

## PUBLICATIONS

D. Bialo, J. Duszczyk
*Influence of Counter-specimen on Wear and Friction of Aluminium Matrix Composites*
In: Advances in Structural P/M Component Production, European Powder Metallurgy Association, Shrewsbury (1997) 529-534

H.J. Brinkman, J. Duszczyk, L. Katgerman
*In situ formation of $TiB_2$ in a P/M aluminium matrix*
Scripta Materialia 37/3 (1997) 293-297

H.J. Brinkman, J. Duszczyk, L. Katgerman
*One step synthesis/densification of in-situ aluminium matrix composites*
In: W. Oleksiuk (ed.), Proc. of the III Konferencja Naukowo-Techniczna "Mechatronika '97", Politechnika Warsawska, Warsaw, 22 November 1997, Oficyna Wydawnicza Politechniki Warszawskiej, Warszawa (1997) 436-440

H.J. Brinkman, J. Duszczyk, L. Katgerman
*Reactive sintering of Al-$TiB_2$ composites*
In: L.A.J.L. Sarton, H.B. Zeedijk (eds.), Proc. 5th European Conf. on Advanced Materials, Processes and Applications (Euromat '97), Maastricht, 21-23 April 1997, Volume 1: Metals and Composites, The Netherlands Society for Materials Science, Zwijndrecht (1997) 351-355

H.J. Brinkman, J. Duszczyk, L. Katgerman
*The use of a reactive diluent in the synthesis of metal matrix composites*
In: Proc 4th International Symposium on Self-Propagating High-Temperature Synthesis, Toledo, Spain, October 6-10, 1997, International Journal of Self-Propagating High-Temperature Synthesis (1997) 147-152

J. ter Haar, J. Duszczyk
*Degradation of $\alpha$-alumina fibre during extrusion of Al-20Si-X P/M composites*
Journal of Materials Science 32 (1997) 2781-2788

L. Katgerman, N.J. Fei, W.H. Kool
*Melt Spinning of SiC Reinforced Aluminium Composites*
In: J. Beech, H. Jones (eds.), Proceedings of the 4th Decennial International Conference on Solidification Processing SP97, Ranmoor House, University of Sheffield,

UK, 7-10 July 1997, Department of Engineering Materials, University of Sheffield (1997) 101-104

J. van de Langkruis, W.H. Kool, S. van der Zwaag
*Relation between the microstructure and the hot deformability of model systems for the aluminium 6XXX alloys*
In: L.A.J.L. Sarton, H.B. Zeedijk (eds.), Proc. 5th European Conf. on Advanced Materials, Processes and Applications (Euromat '97), Maastricht, 21-23 April 1997, Volume 1: Metals and Composites, The Netherlands Society for Materials Science, Zwijndrecht (1997) 273-277

U.T.S. Pillai, J. Duszczyk, L. Katgerman
*Low pressure casting of Aluminium-siliconcarbide composites with high silicon content*
In: E.S. Dwarakadasa, C.G. Krishnadas Nair (eds.), ADCOMP '96, Proc. of the second International Conference on Advances in Composites, 18-20 December 1996, Indian Institute of Science, Bangalore, Allied Publishers Limited, New Delhi (1997) 209-215

S. Sillitto, A. Smolders, C. Testani, J. Duszczyk, H. Paiseley
*Production and Injection Moulding of Nickel Aluminide Powder*
In: Powder Injection Moulding, European Powder Metallurgy Association, Shrewsbury, UK (1997) 199-207

R. van Tol, L. Katgerman, H.E.A. van den Akker
*Horizontal Mould Filling of a Thin Wall Aluminium Casting*
In: J. Beech, H. Jones (eds.), Proceedings of the 4th Decennial International Conference on Solidification Processing SP97, Ranmoor House, University of Sheffield, UK, 7-10 July 1997, Department of Engineering Materials, University of Sheffield (1997) 79-82

J. Zhou, J. Duszczyk. P. Houdijk, H. Zitman, A.J. Walstock
*Extrusion of Aluminium Matrix Composite with Hardmetal Dies*
In: Aluminium 2000, Interall Publications, Modena. Italy, 3 (1997) 19-29

J. Zhou, J. Duszczyk, L. Katgerman
*Effect of Extrusion Speed on Surface Quality of an Aluminium Matrix Composite Profile*
In: T. Chandra, T. Sakai (eds.), THERMEC97, The Minerals, Metals and Materials Society, Warrendale (1997) 1161-1167

## CORROSION TECHNOLOGY, ELECTROCHEMISTRY AND SPECTROSCOPY

Delft University of Technology, Laboratory of Materials Science
Rotterdamseweg 137, 2628 AL Delft
phone +31 (15) 2782196, fax +31 (15) 2786730, e-mail ...@stm.tudelft.nl

PERSONNEL

*Scientific staff*

prof.dr. J.H.W. de Wit
dr.ir. C.J. van der Wekken
ir. G. Bakker
dr. K. Hemmes
dr.ir. M.T.C. de Loos-Vollebregt
dr. E.H. van Veen
prof.dr. B.D. Lichter ( 0.2)
dr.ir. D.H. van der Weijde

*Post-doc's*

dr. L. Gras Garcia (from 1-12 -1997)
dr. R.A. Conte (from 1-12-1997)
dr.ir. R. Hofman (IOP)
dr. J.A. Morales (till 1-4-1997)

*Graduate students*

ir. I. Murris (JRC)
L. Liao, M.Sc. (MP, DUT) (till 15-4-1997)
ir. J.C. Elkenbracht
ir. P.C.H. Ament (STW)
ir.ing. M. Keijzer (0.5)
ir. F. Standaert (0.5, WbMT, DUT)
ir. M. Vreijling (TNO)
drs. R. van der Schoor (IOP, TNO)
drs. M.B. Spoelstra (IOP)
ir. A. Mol (IOP, 0.5)
ir. S. Briot (till 1-6-1997)
ir. M.H.M. Huisert
ir. R. Breur (TNO)
ir. A. de Jong
ir. R. Klumpes
drs. M.A.S. Olivry (research fellow, from 15-10-1997)
ir. F. Schuurman (from 1-10-1997)
dr.ir. W.H.A. Peelen (from 1-4-1997)
dr. N.H.J. Stelzer (till 1-7-1997)
ir. S.F. Au (from 1-4-1997)

*Materials designer*

ir. D. Exalto

*Research students*

B.R.N. Gustama (till 22-4-1997)
A.J. Tijssen (till 22-4-1997)

E. Smaardijk
J. W. van Liere
M. Lauterbach
W. Hamer

*Technical assistants*

ing. P.J.B. Overkamp
L. Norbart
N.J. Schellenbach
ing. J. Padmos
J.P. Koot (till 1-3-1997)
A.H.L.M. Klijnhout

## RESEARCH AREAS AND OBJECTIVES

The electrochemical research is mainly aimed at the clarification of corrosion reaction mechanisms and thereby at the development of better corrosion protection measures. Surface layers play an important role in protecting metals and alloys against corrosion. Therefore an important part of the research program is aimed at a detailed characterisation of these layers and the interface between the layer and the metal, including adhesive properties. The study of the role of passive layers is equally important for our understanding of the environmentally induced fracture of structural materials in aggressive media under an applied stress.
The spectroscopy research is mainly focused on the development of measuring techniques and instruments for atom-spectrometric analysis, with special emphasis on applications in materials science and environmental chemistry.

The research program is subdivided in 5 themes:

1 *Passivity of Materials, Including Film Formation, Passivity Breakdown, Localised Corrosion and Environmentally Induced Fracture*

The general purpose of this research theme is to obtain detailed knowledge of the passive behaviour of both model alloys and commercial materials and to prevent or delay the degradation of materials by localised forms of corrosion as pitting corrosion, stress corrosion cracking and corrosion fatigue. This knowledge will lead to materials selection procedures based on scientific understanding, as opposed to the still common practice of using selection criteria based on poorly understood practical information.

In order to arrive at this long term goal a detailed fundamental model for the passive film is being developed by combining electrochemistry, defect chemistry, fracture mechanics and semiconductor physics.

The different Ph.D. projects coming under this theme are all filling out gaps in our knowledge and are expected to lead eventually to a comprehensive model for the structure and the protective properties of the passive layer, as well as to a fundamental understanding of the role of the passive layer in environmentally assisted failure under mechanical loading conditions in aggressive environments.

2 *Corrosion Protection by Metallic, Inorganic or Organic Coatings*

The general purpose of this theme is the elucidation of the mechanisms that play a role in the protection of substrate metals, in order to arrive at better protection against corrosion and eventually life time prediction of coating systems. The different projects in this theme emphasise different aspects in this wide field.
Part of the work is performed on Al-substrates, mainly focusing on filiform corrosion, which has been a major industrial issue for the last five years due to the increased number of failures in applications.
Another part of the work is directly aimed at life time prediction of organic coatings systems. It is focused on steel substrates, without or in combination with conversion layers and other metallic layers, *e.g.* Zn.
A third part is dealing with inorganic layers to protect metals against high temperature corrosion in complicated aggressive gaseous atmospheres and in molten carbonates.
Emphasis is on a combined materials properties approach for these coated systems. Substrate properties, conversion layers, interfacial phenomena and physicochemical properties of the coating layers themselves in relation with the processing parameters of the total system are studied.
A fourth part of the research is focused on metallic coatings for corrosion protection. Currently the properties of spray deposited metal layers like titanium are evaluated. If these coatings are reliable these materials could be extremely useful for repair work in the process industry.
Besides these four themes also projects are running on microbiological corrosion and metallisation of plastics using conductive polymers.
At the moment several new projects have started in which pre-treatment of aluminium and zinc will be evaluated.
While the background of most projects is very practical, this research is focused mainly on fundamental issues including electrochemical mechanisms and more generally transport mechanisms in relation with microstructure and composition.

3 *High Temperature Corrosion*

The influence of various parameters on the adhesion and growth rate of chromium oxide layers on high temperature alloys is investigated in order to increase the possibilities for application of these alloys in various aggressive gaseous atmospheres. A second major issue is the application of high temperature electrochemistry in order to follow oxidation kinetics *in situ*. This theme has close connections with theme 2, as far as metallic and ceramic coatings are concerned and with theme 4, especially in separator plate research.

4 *Molten Carbonate Fuel Cells*

The electrode reaction mechanisms at the cathode are investigated in relation with cell modelling in order to optimise the cell performance. Also the dissolution/corrosion of the electrode materials and separator plates, including coatings, in molten carbonate is evaluated in order to increase the life time and performance of fuel cells. Understanding the melt chemistry is essential in studying the corrosion and reaction mechanisms. Models have been developed to describe cell performance, *e.g.* as a function of gas utilisation.

5 *Atomic Spectroscopy*

The research has been focused on the study of spectral phenomena, including signal oscillations in graphite furnace atomic absorption spectrometry. Most experimental problems could be solved by applying the same frequency for the power supply of the furnace and for the a.c. magnetic field used in the Zeeman background correction system.
Software was developed for survey analysis in inductively coupled plasma mass spectrometry (ICP - MS). The approach is based on interpretation of the measured spectrum, followed by multicomponent analysis. Several laboratories in the Netherlands are using this software for methods development, in addition to the software provided by the manufacturer of the instrument. At present a similar approach is studied for ICP optical emission spectra.

FACILITIES

- Electrochemical equipment:
  - Various potentiostats/galvanostats, both analogue and digital (ECO, PAR, Gamry)
  - Scanners, sensitive mV meters, electrometer
  - Transient recorder
  - Rotating disk electrodes for aqueous and molten carbonate applications
  - Impedance spectroscopy equipment
  - 5 × Solartron (FRA + electrochemical interface + HP computer + plotter + software)
  - 2 × EG&G equipment, also including potentiostat, lock-in analyser, PC, software and printer
  - Zahner EIS equipment
  - ECO-EIS equipment
  - Digital oscilloscope for noise measurements (Philips)
  - Low noise potentiostat for current transient measurements
  - Fully climatised room (temperature and humidity) for coatings investigations
  - Local measurement techniques: SRET (EG&G), SVET, Kelvin probe, and AFM/STM (Nanoscope III) with electrochemical cell
- Furnaces for oxidation experiments up to 1773 K in a controlled atmosphere
- High temperature cyclic voltammetry equipment
- 25 PC's and mini-computers for measurement control, data management, modelling, electronic mail. Three workstations.
- Equipment for measuring the stress corrosion sensitivity of alloys up to 250 °C:
  - Small autoclaves for quenching experiments
  - Various slow strain rate and constant load test facilities
- MTS corrosion fatigue equipment
- Glove box, with re-circulation of the purified atmosphere for transfer of passivated samples to SAM and XPS high vacuum chamber
- Interferometric ellipsometer, an Ultra-fast Zeeman laser based ellipsometer is being developed
- Three complete Molten Carbonate Fuel Cell Units with furnaces, gas manipulation equipment, electronic controls, etc.
- Three pot-type cells for mechanistic studies in molten carbonate
- Multi-purpose PVD unit

- Potential modulated reflectrometry equipment
- Atomic Absorption and Emission Spectrometers, including X-ray fluorescence, inductively coupled plasma emission, flame and graphite furnace AAS
- Wilhelmy balance for surface tension measurements under potential control
- High temperature Perkin-Elmer thermobalance
- Filiform corrosion test facilities

RESEARCH REPORT 1997

1 *Passivity of Materials, Including Film Formation, Passivity Breakdown, Localised Corrosion and Environmentally Induced Fracture* (L. Norbart, P.J.B. Overkamp, P.C.H. Ament, J.C. Elkenbracht, B.D. Lichter, C.J. van der Wekken, J.H.W. de Wit)

The European project on ultra fast ellipsometry has been largely finished this year. The growth of compact and porous oxide layers on Aluminium and of passive layers on FeCr alloys in corrosive solutions was studied *in situ.*

An important result of the research on stress corrosion cracking (SCC) mechanisms is that in the $\alpha$–brass/nitrite system and in CuAu alloys in chloride solutions, solute transport in the crack solution constitutes the rate determining step in the crack growth mechanism. Experimental evidence suggests for example that the diffusion limited transport of solute species, probably of nitrite ions, to the crack tip region constitutes the rate limiting step during crack growth under anodic polarisation in this system.

The project on the corrosion fatigue behaviour of steel in seawater has now come to a conclusion. The modelling of corrosion fatigue crack growth under anodic polarisation of steel in seawater has been quite successful. Modelling based on computer simulation of the special solute transport mechanism (flow enhanced diffusion) in the crack solution during fatigue cycling was found to lead to a realistic prediction of the behaviour of the crack growth rate as a function of $\Delta K$ and the frequency. In the present model the transport of $H^+$-ions from a location near the crack walls, where the anodic dissolution reaction leads to acidification of the solution, to the crack tip area, results in the creation of an effective source for hydrogen diffusion at the crack tip. From the crack tip, where the hydrogen ions are reduced, and where the hydrogen atoms are adsorbed so that the crack tip can be represented as a moving line source, the hydrogen diffuses into the material. The model relates the strength of this line source to the anodic current density distribution at the crack walls. The hydrogen distribution in the material in front of the moving line source at the crack tip determines the dimensions of a critically embrittled zone and the amount of crack extension per cycle.
The model calculations indicate that during the corrosion fatigue of steel in seawater the crack growth rate per cycle da/dN is determined by the frequency dependent hydrogen ion transport process in the crack solution, as well as by the hydrogen transport mechanism in the material in front of the moving crack tip. In particular the frequency dependence of da/dN is found to be determined to a large degree by the hydrogen transport mechanism in the material in front of the crack tip.
Combining the results for CF under cyclic loading conditions with the findings regarding the stress corrosion cracking under static loading, it appears that the rate of

environmentally assisted crack extension in a variety of systems strongly depends on the rate of solute transport in the crack solution. If hydrogen embrittlement plays a role, the rate of transport of hydrogen ions to the crack tip in the crack solution will determine the hydrogen distribution in the material in front of the moving crack tip and therefore also the crack growth rate.
In general it is clear that the electrochemical conditions in the crack tip region will be strongly affected by the solute transport to or from the crack tip. As a result solute transport may become the rate determining step during environmentally assisted cracking in a variety of systems, under static as well as under dynamic loading conditions.

1.1 *Material Analysis of Björk-Shiley Convexoconcave Heart Valve Prostheses* (P.J.B. Overkamp, J.H.W. de Wit, B.A.J.M de Mol, H.A. Becker)

This project started in September 1996. This research is supported by a grant of the Dutch Heart Foundation.
Scanning electron microscopy investigations of the explanted mechanical heart valves to get a better understanding of the metallurgical features that are important for the evaluation of the valve performance have been continued.
The employed experimental techniques include *in vitro* and *in vivo* acoustic emission experiments. The evaluation of non destructive test methods that should result in an early *in vivo* detection of failures in the valve has been completed. *In vitro* resonance measurements have started. A start has been made with *in vitro* fatigue experiments and with a metallurgical investigation of the explanted valves. The failure of different types of mechanical heart valves has been investigated in co-operation with the Inter University Working Group for Cardiovascular Implant Retrieval Analysis.

2 *Corrosion Protection by Metallic, Inorganic and Organic Coatings* (D.H. van der Weijde, R. Hofman, P.J.B. Overkamp, L. Norbart, M.B. Spoelstra, A. de Jong, R. van der Schoor, M. Keijzer, A. Mol, M. Huisert, D. Exalto, J.H.W. de Wit)

In three projects on filiform corrosion (one with prof. S. van der Zwaag [MIDEG] and one with prof. L. Katgerman [MIDEG]) the research on the mechanism of filiform corrosion is continued. In each project a specific part of the relationships between the aluminium substrate, the pre-treatment and the behaviour of the organic coating is evaluated: one project deals with anodising as a possible replacement for chromate pre-treatments, one project with on the influence of local difference in aluminium composition and one project deals with the effect of the composition and structure of the bulk aluminium alloy.
Although the three project are working on differ themes a close co-operation between the researchers has proven extremely useful. The contacts with national and international research organisations working on this subject are very intensive. This co-operation has the additional advantage that it provides an opportunity to develop an extensive knowledge on the mechanism(s) of filiform corrosion within a short period.

Under the theme "Local Electrochemical Test Methods" a lot of effort has been put in a further development of the Kelvin probe and the SVET. Besides the improvement of the equipment also a considerable effort has been directed at understanding measurements dealing with corrosion processes underneath organic coatings. In co-operation with Hoogovens test systems have been designed and tested to show the

difference between theory and experiment. It is now clear that the theory as presented in literature does not give a complete description of the systems. Especially the height control over organic coatings is still not completely understood.
Electrochemical Impedance Spectroscopy (EIS) measurements were performed on deformed pre-coated metal. These measurements will be combined with the local electrochemical methods.

The metallisation of plastics with conductive polymers has been focused on the neutralisation step. Although the conduction of the polymer layers is still not perfect it is possible to deposit a well adhering copper layer on top of it. With AFM it was shown that the copper is initially deposited on local spots on the polymer. These small spots grow and finally form a dense copper layer. Also other polymers have been tested as a base material.

The IOP project on Spray Deposited Metal coatings has been successfully finished. These types of coatings may have a relatively high porosity. It is therefore important that the quality of an applied coating can be checked easily after application. Within the project a new method, based on electrochemical measurements, was developed which is able to perform this check with a simple, non-destructive and rapid test. It is based on measurements on model systems which showed that some electrochemical parameters of the base material can be measured if pores completely penetrate through the coating. It was shown that the influence of the base material gradually decreases with increasing thickness. If no contribution of the base material is measured no "through-pores" exist and the coating has a sufficient thickness.

3 *High Temperature Corrosion* (R. Klumpes, R. Hofman, S. Briot, N.H.J. Stelzer, L. Norbart, J.H.W. de Wit)

Chromia formers were studied by means of cyclic oxidation studies in ISPRA. During cyclic oxidation two phenomena are important: growth of a protective oxide layer and spallation of the oxide layer. A well known problem in laboratory studies is that spallation at the specimen's edges is favoured above spallation at the remaining specimen surface. As in practical installations alloys the role of edges is less pronounced than in the usually small laboratory samples, a discrepancy exists between practice and laboratory experiments . In the present study a nuclear technique, Thin Layer Activation (TLA), was used to monitor the spallation behaviour. This technique provides the opportunity to activate the test sample locally, *e.g.* only the centre of a specimen surface. This eliminates the above problem, since the spalled material originating from the specimens centre will emit gamma radiation, while material spalled at the specimens edges does not emit any radiation. The studied materials are chromium ODS alloys, produced by powder metallurgy. Research showed that the use of the TLA technique gives precise information of the material loss by oxide spallation. Comparison of the TLA data with the results of conventional mass change techniques show that TLA clearly gives additional information about the spallation process. The investigations show that material loss increases linearly with the number of cycles. The addition of reactive elements reduces the material loss by at least three orders of magnitude. This research is being continued.

A new project, financed by Philips, was started to study glass-metal interactions at high temperatures.

The HCM contract was finished this year. In this project the oxidation/corrosion be-

haviour of various steels was studied in environments corresponding to heat exchangers, which can be used for waste incineration. The alloys were tested in a spring balance at 650 °C in air with 0.1% $SO_2$. The influence of the sodium sulphate deposit on the corrosion resistance was also measured in the spring balance. The tested alloys can be divided in two groups, ferritic steels (9 - 12% Cr) and austenitic steels (Cr > 17%). If no salt deposit is present, it is found that for the alloys with a low chromium content the corrosion rate decreases with increasing chromium content. For the alloys with the higher chromium content this relation does not hold. These alloys contain other alloying elements, which may enhance the chromium activity and may even lead to different corrosion mechanisms. Specimens which were covered by a $Na_2SO_4$ deposit had clearly increased corrosion rates compared to specimens with no salt deposit. Moreover, the corrosion resistance ranking of these alloys appeared to be different. Electrochemical methods, comparable to those used for the studies of separator plates in molten carbonate, were used to obtain kinetic data. The corrosion behaviour of AISI 304 and 12CrMoV were studied by means of polarisation measurements in a molten $Li_2SO_4/Na_2SO_4$ mixture at T = 650 °C under a gas mixture of 15 $SO_2$ in air. The corrosion behaviour of AISI 304 and 12CrMoV changed with exposure time. In the voltage range from -1.2 to 0.8 V several passive regions were found for both alloys. EDX investigations after an exposure of 168 hours to the molten salts showed for AISI 304 an increase in the chromium content and a low iron content in the surface corrosion layer, while for 12CrMoV a high iron content but a rather low chromium content was detected.

4 *Molten Carbonate Fuel Cells* (W.H.A. Peelen, K. Hemmes, M. Keijzer, F. Standaert, J.H.W. de Wit)

A breakthrough was obtained in solving the problem of the dissolution of the NiO cathode. A so-called i-MCFC with a separate supply of $CO_2$ was tested with promising results in which the partial pressure of $CO_2$ can be kept as low as necessary for minimal NiO dissolution also under high pressure operation of the i-MCFC, while still a high current density can be produced by the cell. However, a further reduction of Ohmic losses in the new cells is necessary and the introduction of gas channels in the matrix tiles poses higher demands on the strength of the ceramic tiles.

Corrosion of the SS steel substrate was studied in order to be able to identify any possible failure of the coatings during testing. Although TiN is not stable it was tested and identified as a most promising candidate because it forms a stable coating of Lithium titanate. Following a suggestion in literature we also applied a Ni coating on top of the TiN coating. Hereby a thermodynamically stable coating is achieved for application in anode gas while the TiN acts as a diffusion barrier for Cr diffusion for example.

In co-operation with the Mechanical Engineering department work on fuel cell modelling will be finished in 1998. With a few reasonable approximations an analytical isothermal fuel cell model was derived. It proved to be possible to adapt this model by introducing a suitable co-ordinate transformation to describe also the non-isothermal fuel cell. In co-operation with Tohoku University in Japan the transient behaviour of an MCFC bench cell could be modelled appropriately by a time dependent version of our isothermal fuel cell model.

Porous electrode modelling is approach in several ways. After the work by J.A. Prins-

Jansen, who developed a three phase homogenous model in which all the microscopic details are averaged out, we now instead looked closely at the processes on a detailed microscopic level. In co-operation with dr. Fehribach from WPI we modelled a cross section of a porous cathode by using a new method utilising stoichiometric combinations of electrochemical potentials in the different phases. Hereby the model equations are simplified and numerical calculations using the commercial software package Matlab proved to be possible. Model equations when formulated in conventional terms of concentrations, diffusion constants and exchange current densities are to complicated to incorporate in Matlab or any other commercial package. The Matlab calculations show that the distribution of electrolyte in an actual electrode is far from optimal. Large areas in the electrode do not contribute to the production of current, whereas at other locations (spots) a major part of all the current is produced. A better distribution of the electrolyte as could be obtained easily in the Matlab model showed an increased current density by a factor of at least two. Or in other words: at the same current density polarisation losses can be less than 50% of the present losses.

5 *Atomic Spectrometry*

In ICP optical emission spectrometers based on echelle optics and charge transfer detectors, emission lines of all elements are measured simultaneously. We developed a method of multi component analysis based on model spectra of all elements and the full sample emission spectrum, to achieve fast survey analysis. Software is in operation and initial results are promising.
A microwave desolvation system was tested for the introduction of acidic solutions into the ICP mass spectrometer. The analytical performance is good although typical ICP-MS problems with sulphuric acid, hydrochloric acid and perchloric acid are not solved. Electrothermal vaporisation of the sample solutions seems to be a better approach. The ETV-ICP-MS mass spectra are free from interferences.

PUBLICATIONS

A.J. Bosch, V.J. Gadgil, M. Hoeflaak, J.H. Pennings, M.B. Spoelstra, J.H.W. de Wit
*Corrosion of coated aluminium panels with anodic pretreatment*
In: L.A.L.J. Sarton, H.B. Zeedijk (eds.), Proceedings of the Fifth European Conference on Advanced Materials and Processes and Applications, Vol. 1, Netherlands Society for Materials Science, Zwijndrecht (1997) 767-770

A.J. Bosch, V.J. Gadgil, M. Hoeflaak, J.H.W. de Wit
*Correlation of accelerated corrosion test and outdoor exposure for coated aluminium*
In: L.A.L.J. Sarton, H.B. Zeedijk (eds.), Proceedings of the Fifth European Conference on Advanced Materials and Processes and Applications, Vol. 3, Netherlands Society for Materials Science, Zwijndrecht (1997) 397-407

M. Cassir, B. Malinowska, W. Peelen, K. Hemmes, J.H.W. de Wit
*Identificaton and electrochemical characterization of in-situ produced and added reduced oxygen species in molten $Li_2CO_3$-$K_2CO_3$*
J. Electroanalytical Chemistry 433 (1997) 195-205

J.C. Elkenbracht, B.D. Lichter, C.J. van der Wekken, W.F.Flanagan, J.H.W. de Wit
*Mechanistic Studies of the SCC-Behaviour of Oriented Cu30Zn Single Crystals in*

*NaNO2 Solutions*
In: T. Magnin (ed.), Proc. of the Second international Conference on Corrosion Deformation Interactions (CDI-2), Nice, France, 24-26 september 1996, The Institute of Materials (1997) 45-56

J.D. Fehribach, J.A. Prins-Jansen, K. Hemmes, J.H.W. de Wit
*Internal Resistance Computations for MCFC Using Electrochemical Potentials*
In: J.R. Selman, I. Uchida, H. Wendt, D.A. Shores, T.F. Fuller (eds), Proceedings of the fourth international symposium on Carbonate Fuel Cell Technology, Vol. 97-4: "High Temperature Materials, Battery, and Energy Technology Divisions", The Electrochemical Society, Inc., Pennington, USA (1997) 362-369

V.J. Gadgil, A.J. Bosch, E.G. Keim, J.H. Pennings, M.B. Spoelstra
*Investigation of anodic layer in recycled aluminium alloy*
In: L.A.L.J. Sarton, H.B. Zeedijk (eds.), Proceedings of the Fifth European Conference on Advanced Materials and Processes and Applications, Vol. 3, Netherlands Society for Materials Science, Zwijndrecht (1997) 385-387

K. Hemmes, W.H.A. Peelen, J.H.W. de Wit
*Study of the electro-chemical equilibria in molten carbonate under the MCFC cathode gas atmosphere*
In: J.R. Selman, I. Uchida, H. Wendt, D.A. Shores, T.F. Fuller (eds), Proceedings of the fourth international symposium on Carbonate Fuel Cell Technology, Vol. 97-4: "High Temperature Materials, Battery, and Energy Technology Divisions", The Electrochemical Society, Inc., Pennington, USA (1997) 370-385

R. Hofman, J.H.W. de Wit, M.P.W. Vreijling, G.M. Ferrari
*Electrochemical Characterization of Thermal Spayed Stainless Steel Coatings*
In: L.A.L.J. Sarton, H.B. Zeedijk (eds.), Proceedings of the Fifth European Conference on Advanced Materials and Processes and Applications, Vol. 3, Netherlands Society for Materials Science, Zwijndrecht (1997) 197-200

M. Keijzer, S.F. Au, K. Hemmes, J.H.W. de Wit, J. Schoonman, G. Lindbergh, D. Simonsson
*Corrosion of Stainless Steel 304 in Molten Carbonates*
In: J.R. Selman, I. Uchida, H. Wendt, D.A. Shores, T.F. Fuller (eds), Proceedings of the fourth international symposium on Carbonate Fuel Cell Technology, Vol. 97-4: "High Temperature Materials, Battery, and Energy Technology Divisions", The Electrochemical Society, Inc., Pennington, USA (1997) 296-305

M. Keijzer, K. Hemmes, P.J.J.M. van der Put, J.H.W. de Wit, J. Schoonman
*A search for suitable coating materials on separator plates for molten carbonate fuel cells*
Corrosion Science 39/3 (1997) 483-494

M. Keijzer, P.J.J.M. van der Put, J. Schoonman, S.F. Au, K. Hemmes, J.H.W. de Wit
*Chemical vapour deposition of titanium nitride for corrosion protection in molten carbonates*
In: M.D. Allendorf, C. Bernard (eds.), Proceedings of the Fourteenth International Conference on Chemical Vapour Deposition and EUROCVD-11, Electrochemical Society Proceedings 97-25 (1997) 364-368

D. Li, Y. Ma, B.D. Lichter, W.F. Flanagan, J.P. Wikswo

*Detection of Hidden Corrosion of Aircraft Aluminium Alloys Using a Superconductiong Quantum Interference Device (SQUID)*
Corrosion 53/2 (1997) 93-98

Lun-Zhi Liao
*The application of in exchange membranes in choride related electro chemical technology*
Ph.D. thesis, Delft University of Technology (1997) 142

Y. Ling, J.C. Elkenbracht, W.F. Flanagan, B.D. Lichter
*The Electrochemical Oxidation of Gold in 0.6M NaCl and 0.3M Na2SO4 Solutions*
J. Electrochem. Soc. 144/8 (1997) 2689-2697

M.T.C. de Loos-Vollebrecht, E.X. Vrouwe
*Spectral phenomena in graphite furnace AAS*
Spectrochimica Acta 52B (1997) 1341-1349

J.W. de Man, J.H.W. de Wit
*Real-life Practice of Materials Engineering in Corrosion Education*
In: Proceedings of the European Corrosion Congress EUROCORR'97, 22-25 September 1997, Trondheim, Norway 1 (1997) 609-614

B.A.J.M. de Mol, P.J.B. Overkamp
*Non-destructive Assessment of 62 Dutch Björk-Shiley Convexo-Concave heart valves*
European Journal of Cardio-Thoracic Surgery 11 (1997) 703-709

J.M.C. Mol, D.C.M. Wilms, J.H.W de Wit, S.van der Zwaag
*Filiform corrosion on coated aluminium alloys: the role of microstructural inhomogeneities in the substrate*
In: L.A.L.J. Sarton, H.B. Zeedijk (eds.), Proceedings of the Fifth European Conference on Advanced Materials and Processes and Applications, Vol. 1, Netherlands Society for Materials Science, Zwijndrecht (1997) 27-30

J.M.C. Mol, D.C.M. Wilms, J.H.W. de Wit, S. van der Zwaag
*The influence of copper on filiform corrosion of coated aluminium alloys*
In: H. Terryn, G. Verhoeven (eds.), Proc. Aluminium Surface Science and Technology Symposium 1997(ASST'97 I), Antwerp, Belgium, May 12-15 1997, in: Acta Technica Belgica Volume XXXVII - No. 2-3-4, Benelux Métallurgie (1997) 237-243

W.H.A. Peelen
*Stability and reactivity of oxygen, nickel and cobalt species in molten carbonate*
Ph.D. thesis, Delft University of Technology (1997) 191

W.H.A. Peelen, K. Hemmes, J.H.W. de Wit
*Diffusion constants and solubility values of $Co^{2+}$ and $Ni^{2+}$ in Li/Na and Li/K carbonate melts*
Electrochimica Acta 42/15 (1997) 2389-2397

W.H.A. Peelen, K. Hemmes, J.H.W. de Wit
*Diffusion constants and solubility values of $Co^{2+}$ and $Ni^{2+}$ in Li/Na and Li/K carbonate melts*
In: J.R. Selman, I. Uchida, H. Wendt, D.A. Shores, T.F. Fuller (eds), Proceedings of the fourth international symposium on Carbonate Fuel Cell Technology, Vol. 97-4:

"High Temperature Materials, Battery, and Energy Technology Divisions", The Electrochemical Society, Inc., Pennington, USA (1997) 424-435

W.H.A. Peelen, K. Hemmes, J.H.W. de Wit
*The $CO_2$ reduction in the molten 62/38 mole% Li/K carbonate mixture*
Electrochimica Acta 43/7 (1997) 763-769

W.H.A. Peelen, K. Hemmes, J.H.W. de Wit
*The $CO_2$ reduction in the molten 62/38 mole% Li/K carbonate mixture*
In: J.R. Selman, I. Uchida, H. Wendt, D.A. Shores, T.F. Fuller (eds), Proceedings of the fourth international symposium on Carbonate Fuel Cell Technology, Vol. 97-4: "High Temperature Materials, Battery, and Energy Technology Divisions", The Electrochemical Society, Inc., Pennington, USA (1997) 274-285

G.J.A.M. Plevier, J.A. Prins-Jansen. K. Hemmes, J.H.W. de Wit
*An electrochemical impedance study of the oxygen reduction on non-porous NiO and $LiCo_2$ in molten carbonate*
Polish Journal of Chemistry 71 (1997) 1183-1195

J.A. Prins-Jansen, K. Hemmes, J.H.W. de Wit
*An extensive treatment of the agglomerate model for porous electrodes in molten carbonate fuel cells* - part I: *Qualitative analysis of the steady-state model*
Electrochimica Acta, 42/23-24 (1997) 3585-3600

J.A. Prins-Jansen, K. Hemmes, J.H.W. de Wit
*An extensive treatment of the agglomerate model for porous electrodes in molten carbonate fuel cells* - part II: *Quantitative analysis of time dependent and steady-state model*
Electrochimica Acta 42/23-24 (1997) 3601-3618

J.A. Prins-Jansen, K. Hemmes, J.H.W. de Wit
*Cathodes in Molten Carbonate Fuel Cells: Mathematical Modeling and Experimental Characterization*
In: J.R. Selman, I. Uchida, H. Wendt, D.A. Shores, T.F. Fuller (eds), Proceedings of the fourth international symposium on Carbonate Fuel Cell Technology, Vol. 97-4: "High Temperature Materials, Battery, and Energy Technology Divisions", The Electrochemical Society, Inc., Pennington, USA (1997) 233-237

R.G. van den Schoor, R.M.M. van de Leur, J.H.W. de Wit
*Conducting Polymers as Primers for Galvanic Deposition of Metals on Plastics*
In: L.A.L.J. Sarton, H.B. Zeedijk (eds.), Proceedings of the Fifth European Conference on Advanced Materials and Processes and Applications, Vol. 3, Netherlands Society for Materials Science, Zwijndrecht (1997) 295-298

M.B. Spoelstra, D.H. van der Weijde, A.J.Bosch, J.H.W. de Wit
*An impedance study on anodised aluminium*
In: H. Terryn, G. Verhoeven (eds.), Proc. Aluminium Surface Science and Technology Symposium 1997(ASST'97 I), Antwerp, Belgium, May 12-15 1997, in: Acta Technica Belgica Volume XXXVII - No. 2-3-4, Benelux Métallurgie (1997) 311-315

M.B. Spoelstra, D.H. van der Weijde, A.J. Bosch, J.H.W. de Wit
*Towards a better understanding of filiform corrosion: an electrochemical impedance study on anodised aluminium*
In: L.A.L.J. Sarton, H.B. Zeedijk (eds.), Proceedings of the Fifth European Confer-

ence on Advanced Materials and Processes and Applications, Vol. 3, Netherlands Society for Materials Science, Zwijndrecht (1997) 347

M.B. Spoelstra, T. Zuidwijk, D.H. van der Weijde, A.J.Bosch, J.H.W. de Wit
*The influence of anodising on the filiform corrosion behaviour of aluminium*
In: Proceedings of the European Corrosion Congress EUROCORR'97, 22-25 September 1997, Trondheim, Norway, NTNU-SINTEF-NKF 2 (1997) 345-350

F. Standaert, K. Hemmes, N. Woudstra
*Nernst loss in fuel cells and fuel cell designs in dead-end mode*
In: J.R. Selman, I. Uchida, H. Wendt, D.A. Shores, T.F. Fuller (eds), Proceedings of the fourth international symposium on Carbonate Fuel Cell Technology, Vol. 97-4: "High Temperature Materials, Battery, and Energy Technology Divisions", The Electrochemical Society, Inc., Pennington, USA (1997) 112-119

M.F. Stroosnijder, V.A.C. Haanappel, I. Murris
*The Use of Thin Layer Activation in Cyclic High Temperature Corrosion Studies*
Materials Science Forum 251-254 (1997) 275-282

E.H. van Veen, S. Bosch, M.C.T. de Loos-Vollebrecht
*Quantitative survey analysis by using the full inductively coupled plasma emission spectra taken from a segmented charge coupled device detector: a feasability study*
Spectrochimica Acta 52B (1997) 321 - 337

E.H. van Veen, M.T.C. de Loos-Vollebrecht
*Spectral interpretation and survey analysis in ICP-MS*
In: G.Holland, S.Tanner (eds.), Plasma Source Mass Spectrometry, Developments and Applications, The Royal Society of Chemistry, Cambridge (1997) 77-84

J.P.T. Vossen, R.C. Makkus, J.H.W. de Wit
*Corrosion behaviour of nickel-chromium alloys in molten carbonate*
Mater Corros. 48 (1997) 157-164

M.P.W. Vreijling, E.P.M. van Westing, G.M. Ferrari, R. Hofman, J.H.W. de Wit
*Corrosion protection using Passivating Thermal Spray Coatings*
In: Proceedings of the European Corrosion Congress EUROCORR'97, 22-25 September 1997, Trondheim, Norway, NTNU-SINTEF-NKF 2 (1997) 387-392

D.H. van der Weijde, E.P.M. van Westing, G.M. Ferrari, J.H.W. de Wit
*The use of impedance spectroscopy in life time analysis of organic barrier coatings during prolonged immersion, cyclic tests and outdoor exposure*
In: Proceedings of the European Corrosion Congress EUROCORR'97, 22-25 September 1997, Trondheim, Norway, NTNU-SINTEF-NKF 2 (1997) 387-392

C.J. van der Wekken
*The Effect of the Transport Properties of the Crack Solution on Corrosion Fatigue Crack Growth Rates of Steel in Seawater*
In: T. Magnin (ed.), Proc. of the Second international Conference on Corrosion Deformation Interactions (CDI-2), Nice, France, 24-26 september 1996, The Institute of Materials (1997) 76-85

C.J. van der Wekken
*The Role of Mass Transport in the Stress-Corrosion Cracking Mechanism of Cu-25 At. Pct Au Single Crystals in Chloride Solutions*

Metallurgical and Materials Transactions 28A (1997) 2361-2369

J.H.O. Wijenberg, J.T. Stevels, J.H.W. de Wit
*Galvanic coupling of zinc to steel in alkaline solutions*
Electrochimica Acta 43/7 (1997) 649-657

J.H.W. de Wit, T. Fransen
*Corrosion Studies*
In: P.J. Gellings, H.J.M Bouwmeester (eds.), The CRC Handbook of Solid State Electrochemistry (1997), CRC, Boca Raton, USA (1997) 555-586

J.H.W. de Wit, D.H. van der Weijde, S.D. Meijers, M.J. van Deutekom
*Laboratory experience with the development of combined Kelvin/SVET equipment*
in: Proceedings of the European Corrosion Congress EUROCORR'97, 22-25 September 1997, Trondheim, Norway, NTNU-SINTEF-NKF 2 (1997) 631-637

J.H.W. de Wit, E.P.M. van Westing, D.H. van der Weijde
*Evaluation of Coatings - A Total System Approach*
Materials Science Forum 247 (1997) 69-82

## DESIGN FOR RELIABILITY OF PLASTICS PRODUCTS

Delft University of Technology, Laboratory of Mechanical Reliability
Leeghwaterstraat 35, 2628 CB Delft
phone +31 (15) 2785769, fax +31 (15) 2781700, e-mail ...@io.tudelft.nl

### PERSONNEL

*Scientific staff*

| | |
|---|---|
| prof.ir. J.L. Spoormaker | (2781334, J.L.Spoormaker@...) |
| dr. P.V. Kandachar | (2785769, P.V.Kandachar@...) |
| ir. A.J. Heidweiller | (2784861, A.J.Heidweiller@...) |
| ir. R.P. Koster | (2785977, R.P.Koster@...) |
| ir. W. Smit | (278572, iokolmb@dutrex.tudelft.nl) |

*Graduate students*

| | |
|---|---|
| ir. J.G.J. Beijer | (2785730, J.G.J.Beijer@...) |
| ir. H.D. Hoekstra (till 1-10-1997) | |
| ir. J.J. Horst (till 1-10-1997) | |

*Technical staff*

| | |
|---|---|
| ing. R. van den Boogaard | (2781929, R.vandenboogaard@...) |
| ing. W. Griffioen | (till 1-7-1997) |
| G.J. Schut | (2781929) |
| R.G. Simonis | (2785993, R.G.Simonis@...) |
| ing. D.C.H. Smissaert | (2785993, D.C.H.Smissaert @...) |

### HIGHLIGHTS

The Faculty of Industrial Design Engineering completed internal discussions to formulate a new long term research policy. As a result of this exercise, the research landscape of the faculty is changing. Three main themes have been selected to be elaborated in detail. The themes are:

1. Intelligent products (user oriented design)
2. Product Conceptualisation (processes en methods)
3. Sustainability of products

While all these three themes are being worked out in detail, this group experienced in Design for Reliability of Plastics Products sees close association with the theme: Sustainability of Products. Several research projects are being defined within the framework of the new theme.

Two members of our group obtained a Ph.D. degree from Delft University of Technology in October 1997:

1. Hielke Hoekstra,
2. Jaap Horst.

### RESEARCH AREAS AND OBJECTIVES

A general introduction to the group, research activities and facilities can be found at the Internet site: *http://www.io.tudelft.nl/research/lmb/index.html*

An overview of the research activities of this group can be illustrated as:

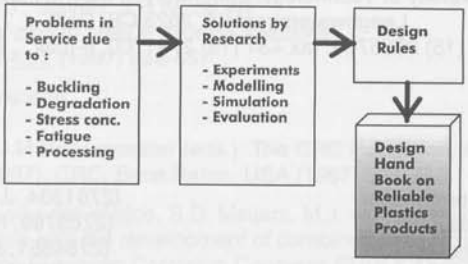


The Faculty of Industrial Design Engineering, to which this research group belongs to, focuses on consumer products and professional apparatus. A large number of these products is designed and manufactured in plastics. Therefore, our research group's emphasis is on "Design for Reliability of Plastics Products".
The different projects within this theme are:

1 *Fatigue of Plastics Products*

Objective: to establish design rules for plastics products subjected to fatigue with consideration of temperature and loading history. The applicability and validity of prediction models are evaluated by fatigue experiments.

2 *UV Degradation of Plastics Products*

Objective: to establish design rules for plastics products subjected to UV radiation. Research is concentrated on the study of the degraded surface layer obtained at different exposure conditions and the effect of the degraded surface layer on the impact behaviour of injection moulded high density polyethylene (HDPE) specimens.

3 *Stress Concentrations in Plastics Products*

Objective: to establish design rules for plastics products with geometry changes resulting in stress concentrations. This research comprises the experimental determination of the loadability of plastics products with stress concentrations and the calculation of stress and strain fields near stress concentrations, taking into account non-linearity and visco-elasticity.

4 *Non-Linear Visco-Elastic Behaviour of Thermoplastic Polymers*

Objective: characterisation of the non-linear visco-elastic behaviour of polymers in order to establish constitutive equations to apply in finite element calculations.

5 *Buckling of Plastics Products*

Objective: to establish design rules for plastics products loaded in compression. This research focuses on thin-walled HDPE products. Column and plate buckling tests will be performed on simple specimens and crates. A model will be determined for numerical simulation to predict buckling with enhanced accuracy.

6 *Effect of Processing on Mechanical Performance of Plastics Products*

Objective: to establish processing-related design rules for plastics products. Research focuses on the effects of flow during injection moulding and frozen-in orientations and stresses on mechanical behaviour of products with well-defined basic geometry. Mechanical evaluation encompasses tensile testing at different strain rates. In addition, brittle specimens will be subjected to impact testing.

7 *Application of the Research Results to Product Design*

Application of the research results in product design projects by students and the staff in co-operation with industry.

FACILITIES

- Fatigue test equipment
  - Multi-purpose electromechanical fatigue equipment for testing plastics products. Maximum load amplitude 400 N. Miscellaneous waveforms including stochastic distributions. Frequency up to 16 Hz. Active specimen temperature control between ambient and +100 °C
  - Multi-purpose hydraulic fatigue facility. Maximum amplitude 13 kN in tension/compression and 50 Nm in torsion. Frequency up to 50 Hz. Specimen temperature between –15 and 60 °C
  - Hydraulic fatigue test equipment for tension loading up to 100 kN. Fatigue test programme with either load, strain or position control; sine, triangle, square or arbitrary waveform. Specimen temperature between –10 and +150 °C
  - Crack growth measurement on centre notched and compact tension specimens
- Environmental testing
  - UV Degradation equipment. Xenon lamp intensity 765 $W/m^2$. Spectrum between 280 and 800 nm. Test area 180 × 250 $mm^2$. Miscellaneous cyclic humidification programmes. Exposure of specimens while bent in prescribed radii
  - Environmental test chamber 1 × 1 × 1 m . Temperature between –40 °C and +100 °C. Relative humidity 0 - 100 %
  - Hydraulic impact tester for tensile and three point flexural impact. Head speed up to 2.5 $m/s$. Registration of force-displacement diagram and fracture energy
  - Notching apparatus for producing precision notches in plastic specimens up to 4 mm wide. Notch depth 0.1 to 1 mm
- Optical microscopes
  - Light optical microscope with polarisation filters. Reflection and transmission mode. Dark-field option. Photographing equipment installed
  - Light optical stereo microscope. Photographing equipment available
- Other equipment
  - Two ovens for heat treatment up to 250 °C
  - Microtome for preparing thin samples from polymer parts, for micro foil mechanical testing and analysis of morphology, crystallinity, etc.
  - Infrared Spectroscope (Perkin Elmer) for dispersive measurements, wavenumbers 4000 to 600 $cm^{-1}$
  - Micro Foil Tester for measuring nominal strain and tensile strength of

plastic foils
- Fontijne hydraulic device for compression moulding; 200 kN
- Klöckner FX75R injection moulding machine. Clamp force 750 kN

- Hardware and Software
  - A cluster of up-to-date SUN and Silicon Graphics workstations, with (colour) printers, tape-streamers, plotters and X-terminals. Several modern Personal Computers
  - Pre- and post-processing software (for use with FEM programmes, developed within the University). Includes both error estimation and remeshing facilities. Software has been developed mainly for thin-walled structures.
  - FEM programmes (developed within the University): includes several types of solution strategies. Elements: Solids, truss, several thick and thin shell elements. All element types possess geometrically non-linear capability. Experience with problems with 50.000 to 100.000 unknowns
  - Optimisation programmes with, among others, interfaces to pre- and post-processors
  - Software for simulation of thermoforming of thin CFRP products. Software for simulation of injection moulding of thin-walled plastic products (MOLDFLOW and C-MOLD)
  - Software for topology design. Software developers tool kits. Software for making graphical presentations and animations
  - Commercial FEM programmes, like ANSYS, MARC, DIANA and GIFTS

RESEARCH REPORT 1997

1 *Fatigue of Plastics Products* (J.J. Horst)

This research area reached a milestone. Horst obtained his Ph.D. degree in October 1997 from Delft University of Technology. The title of his thesis reads: Influence of fibre orientation on fatigue of short glass fibre reinforced Polyamide.

Fatigue failure is an important design criterion for products produced from fibre reinforced plastic. The main objective of his research was to relate the fatigue behaviour of glass fibre reinforced Polyamide 6, with the glass fibre orientation. Lifetime experiments were the main interest, although some crack propagation experiments have been executed as well. Both for lifetime experiments and for fatigue crack propagation, the fatigue strength and the tensile strength showed a correlation. For the designer this is a valuable observation, as he needs to know or predict only the tensile strength in order to estimate the fatigue strength. Studies on fatigue failure revealed that during fatigue, damage is formed at the location of the highest stress, the fibre ends, where voids developed, accompanied by fibre-matrix debonding. These voids join together to form cracks. However, the crack walls remain bridged by matrix material and/or fibres. The bridged crack grows until the residual strength of the specimen is as low as the maximum fatigue stress, when the test specimen fails in the last load cycle.

Based on this research work, guidelines to design for fatigue have been formulated combined with examples of mould design. The fibre orientation can be influenced mainly by the position of the gate(s) in the mould, but also by the design of the part and of the runner system. Some influence on the fibre orientation can also be ex-

pected by the injection moulding parameters, like injection time (equivalent with injection speed or injection pressure) and melt and mould temperatures.

2 *UV Degradation of Plastics Products* (H.D. Hoekstra)

This research area also reached a milestone. Hoekstra obtained his Ph.D. degree in October 1997 from Delft University of Technology. The title of his thesis reads: The Mechanical Behaviour of UV-degraded HDPE: Consequences for Designers.

Products made out of HDPE (High Density Polyethylene), when used outdoors undergo UV-degradation, which can deteriorate the mechanical properties. The focus of his research was to obtain an insight into the effects of UV-degradation on product reliability. The changes in mechanical properties as a result of UV-degradation were the main concern.

In this thesis a two-layer failure model has been proposed, which predicts stable and unstable crack growth in specimens with a brittle surface layer. It is assumed that at a critical load a crack appears in the brittle layer, followed by either an accelerated growth through the inner ductile layer or a decelerated growth and crack arrest. The crack growth characteristics in the ductile part can be calculated using a fracture mechanics approach. If the energy release rate is larger than the critical energy release rate (which is assumed to be a material parameter) unstable crack growth is the result. In this case the mechanical properties of the entire product will be determined by the properties of the embrittled surface layer. If the energy release rate is however lower than the critical energy release rate, stable crack growth results. In this case, the mechanical properties are largely determined by the appearance of a crack in the ductile material.

This model was also experimentally verified by conducting impact studies on UV-exposed HDPE test specimens as well as on plastic tops of a liquid container. Based

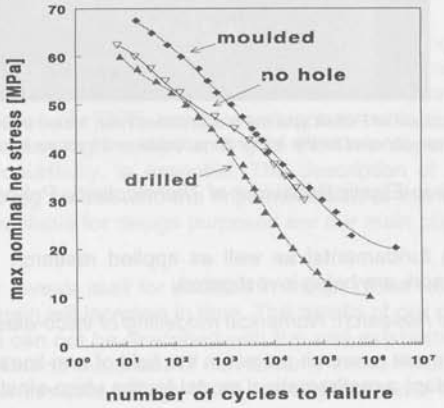


*Figure 1: Results of fatigue tests on ABS specimens. Moulded-in holes are compared to drilled holes showing the effect of orientation due to injection moulding. The extent of redistribution of stresses appeared considerable, even in the case of a brittle material like PMMA. As a result, the linear theory is a safe but very conservative approach for the load carrying-ability of plastics products. It also appeared that injection moulding might have a favourable influence on the load carrying-ability. This result could be related to the fracture mechanism.*

on modelling and experimental study on both laboratory test specimens and real life products, some guidelines have been formulated for designers to take into account the effects of UV-degradation. These guidelines enable designers to estimate (or measure) the properties of an exposed material for a given load, followed by estimating the residual mechanical properties. These properties can be used as a critical limit to which products can be loaded.

3 *Stress Concentrations in Plastics Products* (A.J. Heidweiller)

The effect of geometry transitions on the mechanical load carrying-ability of specimens has been studied. Special attention has been given to a potentially positive influence of the injection moulding process. Tensile tests, three point bending tests and low cycle fatigue tests (see Figure 1) were performed on specimens with either drilled holes or moulded-in holes. The tests were carried out at various temperatures and deformation rates. Two commercial grades of PMMA have been applied. To obtain a better understanding of the fracture mechanism, the fracture surface morphology (see Figure 2) was related to the molecular orientation investigated by the birefringence method and to the results of a finite element method analysis.

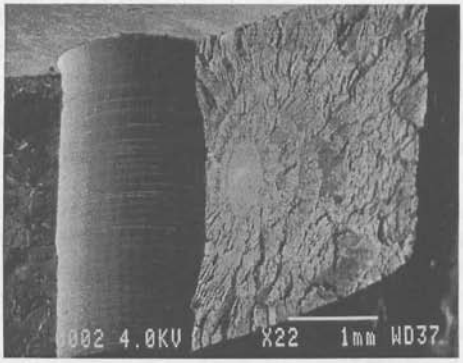


*Figure 2: Fracture surface of PMMA specimen with drilled hole, tested in tensile mode. At the smooth elliptical area, denoted as the mirror zone, craze and fracture initiation take place.*

4 *Non-Linear Visco-Elastic Behaviour of Thermoplastic Polymers* (I.D. Skrypnyk, J.G.J. Beijer)

In this area, both fundamental as well as applied research (specifically aimed at creep behaviour) work are being investigated.

4.1 *Fundamental Research: Numerical modelling of visco-elasticity* (I.D. Skrypnyk)

The aims of the current research project in the field of non-linear visco-elasticity are:

- select and adapt a mathematical model for the visco-elastic behaviour of plastic materials
- develop the implementation of the established model in FEA packages
- verify the developed programme code

with the purpose to use this model for further development of design rules for plastics products as well as to apply it in related research projects, carried out at the laboratory.

During the previous stage of the project (1995-1996) a generalisation of the hereditary integral model of Schapery type has been developed. A parameter identification procedure developed employs the Powell multidimensional minimisation method and allows comparatively fast estimation of model parameters. The "curve fitting" for following polymers have been performed: PMMA, HDPE, PP and NORYL. It has been shown that the parameter identification procedure resulted in a total deviation of less than 1 to 3% between the experimental results and the model.

Further the implementation of the model established into a commercial FEA package MARC and verification of the developed program code have been performed. The numerical algorithm established enables reaching a total deviation of less than 8 to 10 % for the modelling of creep and recovery.

During 1997 main attention has been paid to the modelling of long-term creep and recovery behaviour. For this purpose Struik's theory of physical ageing of polymers has been adapted. The model has been verified using the extended experimental data for long-term creep and recovery of polypropylene (PP), published by the National Physical Laboratory (NPL, Teddington, UK). For this purpose the data set has been split into two parts: first part has been used for the parameter identification, while the second one has been spared for the verification of the model possibility to work with independent experimental data. As a result, model developed has shown good possibility to work with new experimental data for the same material.

Additional attention during this period has been devoted to the elimination of the numerical instabilities, which occur in the algorithmic scheme for non-linear hereditary integral calculations. As a possible way to solve this problem, it is suggested to split up the numerical scheme into two subroutines: for calculation of elastic (instantaneous) part of strain tensor and viscous strains separately.

4.2 *Applied Research: Mechanical behaviour of High Density polyethylene* (J.G.J. Beijer)

Weight reduction of load bearing plastic constructions is becoming increasingly important because of the accompanying cost reduction and environmental benefits. As a consequence the material used will have to perform in the outer limits of its mechanical capability. In case of HDPE, used for instance in bottle crates and containers, this means that a thorough understanding of the time dependent mechanical behaviour, called viscoelasticity, is essential. The description of the behaviour of HDPE in terms of existing models and the implementation of this model description into a FEM package available for design purposes are our main objectives in this research.

Viscoelastic behaviour reveals itself for instance in creep. When HDPE is loaded with a constant force the strain will increase in time. The results of our creep experiments indicate that the strain can not be described with the well established linear description of viscoelasticity. Due to the onset of non-linearity in the mechanical behaviour, already at relatively low stresses, refuge must be sought to more complex nonlinear models.

The creep strain can however be described with the simple principle of separation of variables, meaning that the viscoelastic creep strain is the product of a function of stress and a function of time. For a proper description of the material response to more complex stress histories, the addition of (pseudo) viscoplasticity is necessary.

The influence of temperature on creep strain appears to be very large. For instance rising the temperature from 23 °C to 43 °C will double the creep strain of HDPE. Fortunately the creep strain at a different temperature can be found by the application of time-temperature superposition.

The completion of this research project includes the extension of the model to more realistic three dimensional stress states. The addition of a plastic flow term will enable us to model the material also under high stresses which might occur in stress concentration zones or during failure. Though a numerical description of the material is already operational more must be done for a full implementation into a FEM package. Finally a FEM analysis of a product or product part is needed as a proof of its competence and possibilities.

5 *Buckling of Plastics Products* (T.O. Vasyljkevych, I.D. Skrypnyk)

Plastic products are required to be as light as possible in order to save material and transportation costs. Improved grades of thermoplastics, with high toughness characteristics, are increasingly being applied in plastics products for load bearing applications. Because of the improved characteristics, the failure mechanism of crack initiation and propagation is less dominant for these plastic products. Buckling is becoming more important instead. In the other words, even though these plastic products might not lose their structural integrity, they might lose their shape and functionality because of large (local) deformations. On the other hand, plastics (unlike metallic materials) have very pronounced time-dependent (visco-elastic) behaviour even at room temperature. This makes the behaviour of plastic products even more complex, since buckling (and loss of product functionality) exhibits time-dependant behaviour.

The current project has two objectives:
- investigation of creep buckling behaviour of plastic containers and
- development of methods of product optimisation

with the intention of establishing design rules for development of durable plastic products.

As science and technology carrier, a HDPE bottle-crate has been chosen. When loaded in compression while stacked, a crate can display delayed buckling resulting in the collapse of the whole stack. During the first stage of this project (performed by E.W.G. Zweers) the buckling behaviour of HDPE strips and U-profiles under ramp compressive loading have been studied both experimentally and numerically. The latter work has been performed using the time-dependent plasticity model within the FEA package ANSYS. However, while based on the isochronous curves, the time-dependent plasticity model does not simulate properly the non-linear creep-recovery behaviour of HDPE. In the coming period, it is planned to perform the numerical simulation of buckling phenomenon in strips and U-profiles under ramp loading, using the non-linear visco-elasticity model, implemented recently into FEA package MARC. Besides, it is planned to conduct the compression creep tests on strips and U-profiles, with the purpose of invoking creep buckling and to establish the dependence "compressive force – time to buckling".

6 *Effect of Processing on Mechanical Performance of Plastics Products* (R.P. Koster)

A tensile-impact test installation was set up for the specimens with and without weld-

line at the end of the flow path, which were tested in tensile previous year. A proper specimen clamping system was developed which did not affect test results. During testing, however, it appeared that specimen alignment is still insufficient. Consequently, the mode of the deformation was not pure tension, but an unknown combination of tension and bending. Therefore, the conclusions below are preliminary.

Preliminary conclusions are:

1. melt inlet temperature 230 °C instead of 210 °C results in better performance for all specimens, with and without weldline
2. melt inlet temperature 230 °C instead of 210 °C results in better relative weldline performance: as expected
3. shorter fill time combined with melt inlet temperature 210 °C results in better weldline performance (relative and absolute): probably because of an increased cooling effect with longer fill times
4. higher plasticising back pressure combined with melt inlet temperature 210 °C results in lower relative weldline performance: probably due to lower material density
5. higher mould coolant temperature combined with melt inlet temperature 210 °C results in lower relative weldline performance: apparently there was no beneficial effect from higher mould surface temperature, but a negative effect due to lower material density.

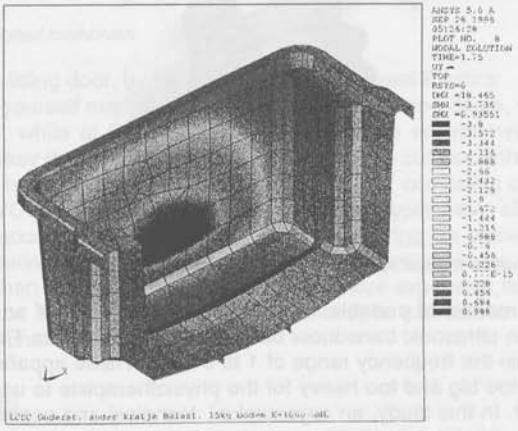

*Figure 3: Finite element analysis of a storage box with 15 kg loaded bottom*

## 7 *Application of Research Results in Product Design* (P.V. Kandachar)

The results from our research are implemented in final year projects of our students, which are carried out in co-operation with the industry. Some examples of undergraduate projects are:

1) GFRP Sluice Gate, by A. Mudde, for the Dutch Ministry of Water & Transport Infrastructure

   A technical and economic feasibility of a glass fibre reinforced polymer (GFRP) sluice gate to replace wooden or steel gates has been carried out, with the objective of reducing maintenance costs and to improve durability. The gate de-

signed consists of standard pultrusion profiles adhesively bonded together. The study has shown that both the investment costs and maintenance costs are much less compared to wooden gates of similar size. Durability is a very important factor affecting economic feasibility. In the proposed design, the adhesive bond could turn out to be the weakest link affecting durability.

2) Mechanical behaviour of storage boxes, by S.W. van Schaik, for Curver
The plastic storage boxes for consumer use are often heavily loaded for long periods of time and are yet supposed not to deform due to creep. This calls for a strong and stiff design. On the other hand, since the cost of materials determine to a large extent the total cost of the product, minimal material application in the design is to be preferred. Some existing storage boxes have been analysed by finite element analysis (see Figure 3), supplemented by some experiments and suggestions for design improvement have been made.

3) Design of a miniature medical apparatus for ultrasonic therapy, by B. Broekman, for Enraf Nonius

*Figure 4: A new miniature medical apparatus for ultrasonic therapy*

The current models of portable medical apparatus consist of an electrical generator and an ultrasonic transducer based on Lead Zirconium Titanate (PZT) to operate within the frequency range of 1 to 3 MHz. These apparatus have been found to be too big and too heavy for the physiotherapists to use in a comfortable manner. In this study, an ergonomical, technical and economical analysis have been carried out to design a new miniature medical apparatus for ultrasonic therapy, complete with a model, a package of technical drawings and cost estimate (see Figure 4).

4) Optimisation and redesign of a 3 planed toothbrush, by K. Martinet, for Tiger Products
A toothbrush with 3 brushes, arranged in three different planes, simplifies the tooth brushing process, as this brush cleans up all the surfaces within minimum time and effort. In this study, an attempt has been made to optimise the stiffness of the different parts of the toothbrush – the brushing area, the fibrils, and the handle - relative to each other. By means of finite element analysis, an optimisation has been arrived at. Using these results a redesign for mass production has been proposed (see Figure 5)

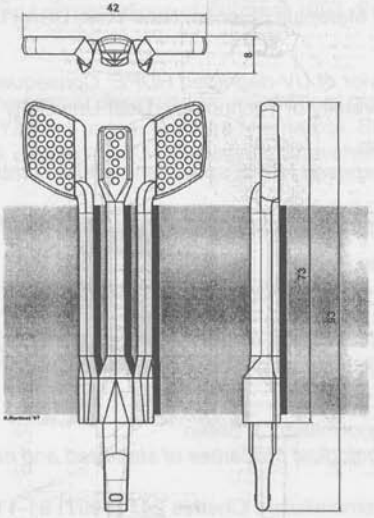


*Figure 5: Redesigned toothbrush*

5) A plastic sliding door, by H. Claessen, for Bruynzeel Plastics
The do-it-yourself market has a need for plastic sliding doors, which are easy to assemble, while at the same time satisfying the environmental requirements such as easy disassembly & reuse or recycle the components. A plastic sliding door has been designed based on a framework consisting of high impact resistant PVC profiles. Strength and stiffness analyses have also been made to take into account the forces during assembly, during the placement of the glass pane & during use (sliding and locking). The design works out to be slightly cheaper than the wooden sliding door, but more expensive than the aluminium sliding door. The plastic sliding doors are easy to maintain and have good heat insulation characteristics.

## PUBLICATIONS

J.G.J. Beijer, J.L. Spoormaker
*Viscoelastic Behaviour of HDPE under Tensile Loading*
In: C.P. Buckley (ed.), Proceedings of 10th International Conference on Deformation, Yield and Fracture of Polymers, Churchill College, Cambridge UK, 7-10 April 1997, The Institute of Materials, London, UK (1997) 270-273

J.C.M. de Bruijn
*Elastics in high temperature quereles of flue gas cleaning units*
In: R. Mourabac, J.E. Niesse (eds.), Proceedings of Corrosion 1997 (Section 353), NACE International, Houston, Texas, USA (1997) 1-10

H.D. Hoekstra
*Mechanical and Morphological properties of stabilized HDPE*

In: G. Klender (ed.), Proceedings of 18th Conference of Degradation of Polymers, 19 June 1996, Institute of Materials Science, New York, USA (1997) 91-110

H.D. Hoekstra
*The mechanical behavior of UV-degraded HDPE: Consequences for Designers*
Ph.D. thesis, Delft University of Technology, Delft University Press, Delft (1997) 133

H.D. Hoekstra, J. Breen
*Fracture behavior of exposed HDPE specimens with an embrittled layer due to UV-exposure*
Die Angewandte Makromolekulare Chemie 252 (1997) 69-88

H.D. Hoekstra, J. Breen
*Fracture Behaviour of exposed HDPE specimens with an embrittled layer due to UV-exposure*
In: G. Klender (ed.), Proceedings of 19th Conference on Degradation of Polymers, Luzern 9-11 June 1997, Institute of Materials Science, New York, USA (1997) 81-100

H.D. Hoekstra, J.L. Spoormaker, J. Breen
*Mechanical and morphological properties of stabilized and non-stabilized HDPE films versus exposure time*
Die Angewandte Makromolekulare Chemie 247 (1997) 91-110

J.J. Horst
*Influence of fibre orientation on fatigue of short glassfibre reinforced Polyamide*
Ph.D. thesis, Delft University of Technology, Delft University Press, Delft (1997) 154

J.J. Horst, J.L. Spoormaker
*Fatigue fracture mechanisms and fractography of short-glassfibre-reinforced polyamide 6*
Journal of Materials Science 32 (1997) 3641 - 3651

I.D. Skrypnyk, J.L. Spoormaker
*Application of non-linear visco-elastic models in FEA of plastic products*
In: A.P.M. van der Veek (ed.), Proceedings of Euromat 1997, Euromat 1997 (1997) 407-410

I.D. Skrypnyk, J.L. Spoormaker
*Modelling of non-linear visco-elastic behaviour of plastic material*
In: L.A.J.L. Sarton, H.B. Zeedijk (eds.), Proceedings of the 5th European Conference on Advanced Materials and Processes and Applications, Volume 4 Characterization and Production/Design, Netherlands Society for Materials Science, Zwijndrecht, The Netherlands (1997) 491-495

I.D. Skrypnyk, J.L. Spoormaker, P.V. Kandachar
*Modelling of the long-term visco-elastic behaviour for polymer materials*
Report to DSM Geleen, K-memo 369, Faculty of Industrial Design Engineering, Delft University of Technology (1997) 48

J.L. Spoormaker
*Construeren van bedrijfszekere en duurzame kunststofproducten*
De Constructeur 6 (1997) 34-39

J.L. Spoormaker

*Establishing Design Rules for Reliable and Sustainable Plastic Products*
In: A.P.M. van der Veek (ed.), Proceedings of Euromat 1997, Euromat 1997 (1997) 401-405

J.L. Spoormaker
*The role of polymer engineering in designing for reliability of plastic products*
In: O.M. Romaniv, S.Ya. Yarema (eds.), Fracture Mechanics, Strength and Integrity of Materials, Jubilee Book devoted to V.V. Panasyuk, Shevchenko Scientific Society, Ukraine (1997) 286-291

## HEAT TREATMENT SCIENCE AND TECHNOLOGY

Delft University of Technology, Laboratory of Materials Science
Rotterdamseweg 137, 2628 AL Delft
phone +31 (15) 2783976, fax +31 (15) 2786730, e-mail ...@stm.tudelft.nl

PERSONNEL

*Scientific staff*

| | |
|---|---|
| prof.dr.ir. S. van der Zwaag | (2782248, S.vanderZwaag@...) |
| dr.ir. J. Sietsma | (2782284, J.Sietsma@...) |
| dr.ir. P. van Mourik | (2781079, P.vanMourik@...) |
| prof.dr.ir. B.M. Korevaar (emeritus) | (2783960, B.M.Korevaar@...) |

*Visiting scientist*

| | |
|---|---|
| S.P. Chen, M.Sc. (NUFFIC, from 1-9-1997)) | (2782268, S.P.Chen@...) |

*Graduate students*

| | |
|---|---|
| ir. J.J. Braam (FOM, till 1-9-1997) | (2783976) |
| drs. T.A. Kop (IOP) | (2782194, T.Kop@...) |
| ir. J. van de Langkruis (STW) | (2782268, J.vandeLangkruis@...) |
| ir. Y. van Leeuwen (Hoogovens) | (2782194, Y.vanLeeuwen@...) |
| ir. J.M.C. Mol (IOP) | (2785194, J.M.C.Mol@...) |
| ir. K.M. Mussert | 2782229, K.M.Mussert@...) |
| ir. S.G.E. te Velthuis (STW) | (2784533, S.teVelthuis@iri.tudelft.nl) |
| ir. F.J. Vermolen | (2783976) |
| ir. S.I. Vooijs (Hoogovens) | 2782197, S.I.Vooijs@...) |

Materials designers

| | |
|---|---|
| ir. P.J. van der Wolk | (2784984, P.J.vanderWolk@...) |
| ir. B. Pennings (till 1-12-1997) | (2783976) |

*Research students*

G. Coolegem
C. Dorrepaal
Y. Fu
G. Krusemeijer
F.A.M. Maas
P.G.W. Remijn
S.I. Vooijs
M.S. Vossenberg
D.C.M. Wilms
J.J. Wits

*Technical assistants*

| | |
|---|---|
| P.F. Colijn (till 1-6-1997) | (2783976) |
| ing. N. Geerlofs | (2784920, N.Geerlofs@...) |
| A.W.J. Gommers | (2782270, A.W.J.Gommers@...) |
| T.L.J. de Haan | (2782198, T.L.J.deHaan@...) |
| E.R. Peekstok | (2782232, E.R.Peekstok@...) |

*Managerial assistants*

| | |
|---|---|
| M.A.W. Jacobs | (2782275, M.Jacobs@...) |

O.M.S. Wens-van Swol (2783976, O.Wens@...)

HIGHLIGHTS

- Ir. Pieter van der Wolk received the ASM-Benelux student award for his M.Sc. thesis on the application of Artificial Neural Networks in metal production. This work was supervised by ir. W.G. Vermeulen.
- Ir. Simone Vooijs received the TU Delft price for the best undergraduate student in Materials Science for her graduation project on interface mobility in Fe-Cu and Fe-Co alloys. Dr.ir. J. Sietsma was her supervisor in this project.
- Ir. Dimphy Wilms received the Borghard price (2nd place) for her M.Sc. thesis on filiform corrosion in aluminium alloys. Ir. J.M.C. Mol was her supervisor.

RESEARCH AREAS AND OBJECTIVES

Research in the Heat Treatment Science and Technology group is centred around the central theme "modelling and controlling phase transformations in ferrous and non-ferrous alloys". The final objective is the development of new thermal and thermo-mechanical treatments on the basis of physical models, resulting in materials and products with improved properties at reduced production costs.

1 *Development of Phase Transformation Models for Low-Alloy Steels*

The phase transformations during the accelerated cooling of the steel strip in the hot-rolling mill play an important role in the generation of the final microstructure and properties of modern lean forming and construction steels. It is the aim of this program to develop detailed models describing these transformations, taking into account effects of the steel composition, (plastic) deformation history and initial microstructure. Both artificial neural network models and physical models are being constructed. Various experimental techniques are being developed to monitor the transformation behaviour quantitatively.

2 *Thermomechanical Processing of Aluminium Alloys for Improved Mechanical and Corrosive Properties*

In order to obtain optimum properties aluminium alloys undergo a number of thermomechanical treatments after solidification. The nature of the relevant metallurgical processes varies considerably and depends on the alloys composition and the order of the mechanical and thermal treatments. In our aluminium research program we study three of these processes which are of great industrial and scientific interest. First of all we study the processes taking place during homogenisation of extrusion alloys and the relation between these homogenisation conditions and the extrudability and the corrosion resistance of the alloy. Secondly, we study inter-critical annealing as a suitable process route for increasing the strength of Al can body stock and finally we study the effect of a heat treatment on the fracture toughness of Al based MMCs.

3 *Surface Treatment of Ferrous Alloys for Improved Fatigue, Wear and Corrosion Resistance*

Surface treatments, such as nitriding or nitrocarburisation, can improve fatigue and

corrosion resistance and reduce wear rate, yielding a considerable extension of the net service life. Our research concentrates on the fundamentals of the internal nitride formation and the relation between nitriding conditions and the fatigue strength. Furthermore, the effects of contaminants on the nitriding kinetics are being investigated.

FACILITIES

- Modern deformation dilatometer (Bähr 805) operating at temperatures up to 1470 K and strain rates up to 10 $s^{-1}$. An additional state-of-the art torsion dilatometer (Bähr 810) with complementary capabilities has been ordered.
- Differential Scanning Calorimeter (Perkin-Elmer, DSC 7) modified for high cooling rates up to 150 K/min), maximum temperature 1000 K
- Furnaces for nitriding, nitro-carburising and carbo-nitriding (temperatures up to 1273 K, quenching facilities, with purified gases and very accurate flow control)
- A special furnace for annealing samples at temperatures up to 850 K with computer controlled specimen handling (10 specimens). Annealing is performed in a controlled gas atmosphere
- Thermal analysis:
  - Thermal Gravimetric Analysis (TGA). Two DuPont horizontal thermobalances (maximum specimen mass 500 mg, sensitivity 20 µg) for TGA measurements during nitriding experiments and a new Netzsch 439 vertical thermobalance (maximum specimen mass 1 g, sensitivity 0.1 µg) for TGA measurements during nitrocarburisation and oxidation
  - Differential Scanning Calorimetry (DTA): a Perkin Elmer high temperature DSC with a maximum operating temperature of 1573 K
  - Thermo-Mechanical Analysis (TMA): a DuPont TMA with a temperature range from 100 K to 873 K, sensitivity 5 ppm
- Reflected light microscopy and metallographic preparation facilities:
  - Several high-quality microscopes, magnifications 50× to 2600×.
  - A modern optical analysis system (Quantimet 550)
  - New metallographic preparation facilities
  - Microhardness testers (0.5 to 25 gram Vickers and 5 to 500 gram Vickers)
  - Scanning Tunnelling Microscopy / Atomic Force Microscopy suitable for measuring both in air and in liquids
- Thermodynamic software for calculating phase equilibria in multicomponent systems (MTData)

RESEARCH REPORT 1997

1 *Phase Transformations in Low-Alloy Steels* (in collaboration with M. Onink, Th.M. Hoogendoorn, A. Bodin [Koninklijke Hoogovens])

The aim of this research is to understand the processes that determine the development of the microsctructure during the transformation of austenite into the low-temperature phases (predominantly ferrite and pearlite) in low-alloy steels. The main line of research is to describe the nucleation and growth of the ferritic phase ($\alpha$) from the austenitic phase ($\gamma$) as a function of temperature and time, considering the material's composition and thermodynamic properties. A number of experimental techniques is being employed in this research. A transformation model on a physical basis is being developed to describe and understand the transformation kinetics.

1.1 *The Development of a Model for Phase Transformations* (Y. van Leeuwen, T.A. Kop, J. Sietsma, S. van der Zwaag)

The austenite-to-ferrite phase transformation is modelled by a model that ascribes the transformation rate as a combined effect of the thermodynamical driving force and the atomic mobility at the $\alpha/\gamma$-interface. In the model, the austenitic microstructure is schematically represented by the tetrakaidecahedron as an austenite grain, for which a grain-size distribution can be applied. During the modelling of a cooling experiment, nucleation takes place at a given rate at the corners of the austenite grains. Each nucleus subsequently grows spherically into the austenite grain, with a velocity that is the product of the free-energy difference between the austenite and the ferrite at the interface, and the so-called interface mobility. The free-energy difference serves as the driving force for the transformation, and it is taken from thermodynamical database programmes. The actual aim of the modelling is to get a better understanding of the interface mobility, and its dependence on composition, temperature, microstresses, etc. The interface mobility is used as a fitting parameter in confrontations of the modelled curves of the fraction ferrite as a function of (decreasing) temperature with experimental ones, determined by means of dilatometry or Differential Thermal Analysis.

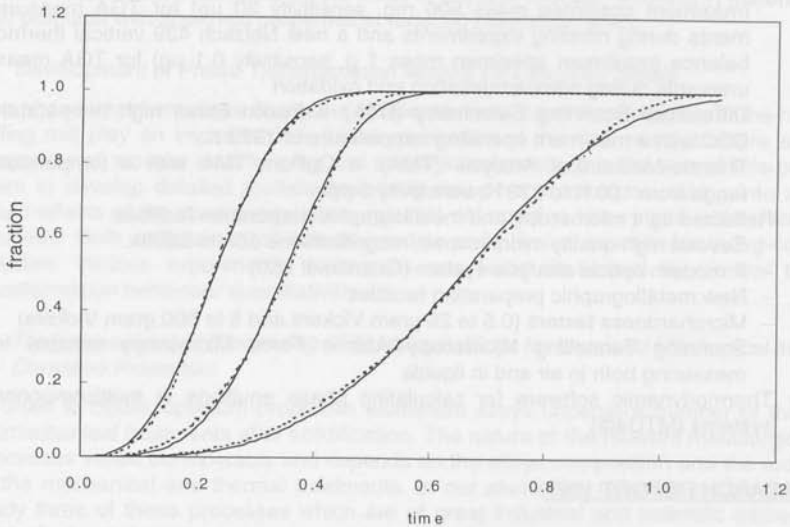


*Figure 1: The fraction ferrite as a function of time in isothermal massive transformations, according to the tetrakaidecahedron geometry (solid lines). The dashed lines represent fits according to the Johnson-Mehl-Avrami kinetics. The curves have been calculated for 1, 12 and 24 nuclei per austenite grain, respectively.*

An extensive study of the effect of the model geometry on the transformation kinetics has shown the similarity with the widely accepted Johnson-Mehl-Avrami kinetics when the tetrakaidecahedron is chosen. The development of the fraction ferrite in isothermal massive transformations with different nucleus densities according to the tetrakaidecahedron model and fits according to Johnson-Mehl-Avrami kinetics is shown in Figure 1. Obviously, in the case of the tetrakaidecahedron the influence of

the microstructural parameters is much clearer. In view of this result, and of the great similarity between tetrakaidecahedron grains and Voronoi tesselations, the tetrakaidecahedron appears to be an outstanding representation of the austenite microstructure.

1.2 *Studies on the Interface Mobility* (Y. van Leeuwen, T.A. Kop, S.I. Vooijs, J.J. Wits, J. Sietsma, S. van der Zwaag)

The modelling scheme sketched in the previous section can be used to reproduce the experimental curves for the fraction of ferrite as a function of temperature during cooling. Assuming a certain undercooling due to nucleation, the modelling of the experimental fraction curves yields the value of the interface mobility *M*. Since the temperature range in which the transformations take place is too narrow to determine the temperature dependence of *M*, an Arrhenian temperature dependence with an activation energy of 150 kJ/mol, reported in the literature for recrystallisation in iron, is assumed. Application of the model to experimental transformation data of several binary iron alloys shows that the interface mobility is distinctly different for iron alloys containing 1 or 2% of one of the alloying elements Co, Cu, Al, Mn, or Cr. A separate study on the lattice parameters of Fe-Co and Fe-Cu at temperatures near the phase transformation has shown that, although Fe-Cu shows a distinct undercooling before transforming and Fe-Co does not, both alloys undergo a change in atomic volume of $1.05 \pm 0.05\%$ upon transforming from $\alpha$ to $\gamma$. At the moment this study is in the stage of gaining a better insight in the nature of the quantities found so far. In other words, it is tried to understand the interface mobility in terms of grain-boundary diffusion properties, the build-up of microstresses, or other circumstances playing a role in the transformation.

1.3 *Dilatometry* (T.A. Kop, J. Sietsma, N. Geerlofs, S. van der Zwaag)

In January 1997 a Bähr 805 A/D deformation dilatometer has been installed, implying an important extension of the experimental facilities available to the steel phase transformation research in Delft. Considerable effort has been devoted to, on the one hand, a meticulous assessment of the accuracy of the instrument, and, on the other hand, the development of the analysis of the dilatation signal in terms of the fractions ferrite and pearlite in the sample. The accuracy of the instrument is most strongly influenced by the temperature distribution over the sample. Measurements of the temperature at two or three places along the surface of the 10 mm long cylindrical sample have shown that, strongly dependent on circumstances like the cooling rate, the cooling medium, the transition through the Curie temperature and the release of transformation heat, significant temperature gradients can occur. An extensive set of experiments has yielded a good picture of the possibilities and the limitations of the equipment.
The aim of a dilatation measurement during the austenite decomposition into ferrite and pearlite is to obtain the development of the fractions austenite, ferrite and pearlite as a function of temperature in a cooling experiment. These experimental fraction curves are confronted to model curves. Two complications occur when using dilatometry for a carbon-containing steel: first, the dilatation effect of the transformation of austenite to pearlite differs from that for the transformation of austenite to ferrite, and secondly during the transformation of austenite to ferrite the austenite itself changes its specific volume due to an enrichment in carbon. These effects have been taken into account, using literature data for the specific volume of Fe-Mn-C al-

loys as a function of temperature. The formation of ferrite and pearlite is assumed to take place in separated temperature ranges, to be indicated by the researcher. Moreover, an adaptable parameter is incorporated to account for instrumental influences.
After this period of development, the dilatometer can now be applied for an accurate determination of transformation kinetics during cooling experiments at high rates. It is therefore a valuable component in the research on steel phase transformations, since the fraction curves derived from dilatometry experiments can be used to test the transformation model that is developed. In 1997 the dilatometer has been used to measure the fraction curves for a set of binary iron alloys (see section 1.2), and for a set of low-carbon Hoogovens steels, the interpretation of which is currently in progress.

1.4 *Ferrite Formation Studied with Neutron Depolarisation* (S.G.E. te Velthuis, F.A.M. Maas, J. Sietsma, S. van der Zwaag; M.Th. Rekveldt [Interfaculty Reactor Institute, Delft University of Technology])

Neutron Depolarisation is a particularly powerful technique for the steel phase-transformation research, since it allows a simultaneous determination of the fraction ferrite that is formed and the average grain size of the ferrite. The technique takes advantage of the magnetic moment of the neutron, and its interaction with ferromagnetic material, which ferrite is and austenite is not, in the sample. In order to allow isothermal experiments on the austenite-to-ferrite phase transformation, in 1997 a two-chamber furnace has been installed. The upper chamber being set at the austenitisation temperature and the lower chamber at the transformation temperature, a pneumatic system moves the sample from the upper to the lower chamber at $t = 0$. Series of isothermal experiments on carbon-manganese steels with carbon contents between 0.22 mass % and 0.60 mass % have been performed at several temperatures. The very strong temperature dependence of the transformation kinetics in these steels has been quantified. For instance, a typical time constant for the formation of ferrite in the 0.36 mass % steel at 1002 K is 500 s, whereas it is 40 s at 938 K. Such data are important for getting to understand the influence of both the driving force and the atomic mobility on the transformation kinetics. The analysis of the data, considering both the translation of the depolarisation parameters in microstructural parameters and the simulation of the formation of ferrite in a three-dimensional model of the microstructure, is still in progress.

1.5 *Transformation Kinetics in a High-Strength Low-Alloy Steel* (T.A. Kop, P.G.W. Remijn, J. Sietsma, S. van der Zwaag)

The elements vanadium, niobium and titanium have a very distinct effect on the strength of steel, even when added in very small quantities (typically 0.02 mass %). The essential aspect of these elements is that they form precipitates (carbonitrides) at relatively high temperatures. The presence of such precipitates inhibits the recrystallisation of the steel in the austenitic phase. The enhanced strength of the steel in the ferritic/pearlitic phase is due to the fine structure that forms when the fine austenitic microstructure transforms during cooling. In order to study the possible direct effects of niobium-carbide precipitates on the austenite-to-ferrite transformation kinetics, a series of Differential Thermal Analysis experiments has been performed on a niobium-containing HSLA steel. The study, involving a range of austenitisation temperatures, provides information on the relations between the amount of niobium

in precipitated form, the grain sizes and the transformation-start temperature. The conclusion is that the precipitates have no direct influence on the nucleation behaviour of ferrite. This can be concluded from the monotonous relation that is found between the austenite grain size and the transformation-start temperatures, without any indication that the amount of precipitated NbC plays a role. The study also shows, however, that the transformation rate is relatively low when during austenitisation at high temperatures, most of the niobium is brought into solution. Presumably the reason for this effect is the precipitation of NbC on the $\alpha/\gamma$-interfaces during the transformation. A pinning effect of the precipitates on the interfaces is expected. Currently this line of research is extended with Secondary Ion Mass Spectrometry at CRM, Liège, and Transmission Electron Microscopy experiments at Glasgow University.

1.6 *Statistical Modelling of Transformation Data by Means of Neural Networks* (P.J. van der Wolk, C. Dorrepaal, J. Sietsma, S. van der Zwaag)

Besides the modelling efforts on a physical basis described in the previous section, transformation data from the literature are also being modelled in a statistical manner, *i.e.* with arbitrary analytical functions that just represent the dependence of the transformation characteristics with composition, rather than explaining the origin of the effects. By far the most extensive set of transformation data in the literature is formed by the Continuous-Cooling-Transformation (CCT) diagrams. These diagrams describe not only the austenite-to-ferrite transformation, but the entire decomposition of austenite into ferrite, pearlite, bainite, martensite for literally hundreds of steel compositions. A CCT-diagram contains phase fields, which for the neural-network modelling are represented by sets of start and finish temperatures. In general, the neural-network technique is capable of modelling most transformation temperatures within an accuracy of 50-80 K. Additional attention is paid to characteristic features like the so-called ferrite and bainite noses. The neural-network models for CCT-diagrams offer the possibility to give an *a priori* estimate of the CCT-diagram of any "new" steel within the composition range of the model. Moreover, it is possible to explicitly study the effect of a variation of a single element. Such studies can offer useful information for the development of more physically based models.

1.7 *Deformation of Two-Phase Microstructures* (A. Bodin, J. Sietsma, S.P. Cornelisse, S. van der Zwaag)

An increasing industrial interest develops in hot-rolling steel plates in the two-phase temperature range, instead of in the austenitic temperature range. Adequate control of this so-called inter-critical rolling requires a detailed knowledge of the phase transformation, since the mechanical properties of austenite and ferrite differ substantially, and therefore the relative amounts of the different phases should be accurately known. Moreover, the reaction of the microstructure on the deformation that is applied (recrystallisation, recovery, internal stresses) can have an important impact on the development of the phase transformation during further cooling. In 1997 a combined research project of Hoogovens and our group has been started to investigate the several aspects of inter-critical rolling. The first part of the research aims at understanding the relation between the microstructural properties of the two-phase material and its deformation behaviour, by means of series of deformation tests on relatively simple steels at different temperatures, at different stages of the transformation. It has become clear from the literature that the two most straightforward parameters, the volumes fractions and the average grain sizes, are not sufficient to un-

derstand the process. The numerous experimental results, both in deformation characteristics and in microstructures that have developed, has given a global picture, but has not yet led to an adequate understanding. Currently Fine-Element modelling is being employed to get a more complete understanding of the influence of different aspects of the microstructure on the deformation behaviour.

## 2 *Thermomechanical Processing of Aluminium Alloys for Improved Mechanical and Corrosive Properties*

### 2.1. *Particle Dissolution During Homogenisation and its Relation to Extrudability*

(F.J. Vermolen, J. van de Langkruis, M.S. Vossenberg, S. van der Zwaag; W.H. Kool [MIDEG]; C. Vuik (Department of Applied Mathematics, Delft University of Technology); M. Sellars [Sheffield University])

The as-cast microstructure of extrudable aluminium alloys is such that these alloys are unsuitable for further mechanical processing, such as hot-extrusion. To improve their microstructure, the alloys are annealed at a temperature just beneath the eutectic temperature. This is called homogenisation.
An important process during homogenisation is the dissolution of particles. These particles may have different geometries: platelets, needles, discs, spheres and they may both occur near the grain centre and at the grain boundaries. To gain a rapid and thorough understanding of the relation between parameters as composition, geometry, temperature-time profile, stoichiometry, casting-conditions and the evolution of the microstructure during the homogenisation, detailed mathematical modelling of the evolution of the microstructure during the homogenisation treatment is necessary.
In a suite of models of increasing physical complexity we consider the dissolution of one or two (different) phases with a fixed stoichiometry, consisting of one or more chemical elements. These phases dissolve in a (aluminium-rich) matrix as a result of diffusion in the matrix. Hence, the second Law of Fick holds in the matrix (*i.e.* the diffusion equation) for each chemical element. The rate of dissolution is proportional to the concentration gradient of each alloying element at the interface between the particle and matrix. Thereby and due to the assumption that the particle stoichiometry is maintained during dissolution, the gradients are linked to each other: they constitute coupled Neumann boundaries at the moving interface. For the presence of n alloying elements, n–1 boundary conditions result.
The other boundary condition results from the thermodynamic consideration that, corresponding to local equilibrium, the concentrations at the interface are coupled via a hyperbolic relationship. For the case of the absence of a phase at the boundary, it is assumed that no flux across the boundary occurs. Having sufficient boundary conditions, the diffusion equation can be solved. We thus are faced with the problem of finding concentration profiles of all chemical elements such that the above stated requirements are met. Having these concentration profiles, the dissolution rate can be calculated. Mathematically this problem is called a vector value Stefan problem. To compute the dissolution rate, numerical software has been developed.
To gain a faster insight into some mathematical implications and problems an asymptotic (semi-) analytical model has been developed too. This model has been tested and for some cases it agrees well with the numerical model. This asymptotic model provides some insight into the possibly existing non-unique solutions of the Stefan problem ('bi-furcation problems'). However, it can also be shown that the so-

lution is unique for those cases considered in metallurgy.
Furthermore, numerical analysis has been done for the accuracy, stability and optimisation of the computational work during the calculation.
The set of models have been linked into a larger model which is capable of calculating the microstructural changes during homogenisation of extrusion billets under industrial conditions.
In this research the influence of the (statistical) particle size (distribution), initial concentration profiles, overall composition, particle geometry and the temperature-time profile on the dissolution kinetics has been studied. Moreover a dimensionless number, 'the non-homogeneity parameter', has been introduced to study the evolution of the magnitude of the concentration differences in the matrix during and after the homogenisation treatment.
As an example, the evolution of the particle volume fraction in a grain as a function of time for several homogenisation temperatures has been displayed in Figure 2. It can be seen in this Figure that the dissolution time may vary an order of two for a temperature difference of 20 K (see the curves for 823 K and 803 K).

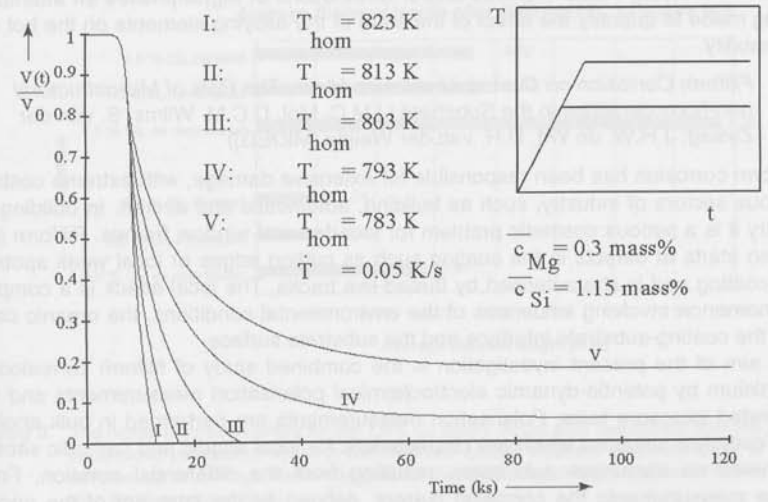


*Figure 2: The dissolution kinetics of a layer of $Mg_2Si$ around a grain for different homogenisation temperatures*

The extrudability of AlMgSi alloys depends on the microstructure of the alloy directly before extrusion, or more in particular on the condition of the alloying elements in the aluminium matrix. For instance, the content of solute Mg and Si in AlMgSi alloys determines the extrusion pressure needed and the maximum obtainable mechanical properties of the extrudate after artificial ageing. Mg and Si containing precipitates formed before extrusion or during cooling after extrusion reduce the available solute. The most important Mg-Si containing intermetallic phases form and dissolve at different temperature ranges with different rates. The formation of these phases during cooling down from the homogenisation temperature is currently being studied as a function of the stoichiometry in the alloy composition and the homogenisation condi-

tions. A detailed description and understanding of the precipitation processes will result in specifications for cooling schedules resulting in the desired microstructure for good extrudability.
This extrudability is currently being investigated using plain strain compression tests using samples in a completely solutionised state and samples where precipitation to a well-controlled degree had taken place.
To describe the hot deformability for aluminium alloys several constitutive equations, such as the Sah-saturation equation, the power law, the exponential law, the Kocks' law and the hyperbolic sine law, have been suggested in the literature. The suitability of each of these models for describing the complete stress-strain behaviour, including the dependency of the flow stress during deformation on the strain, strain rate and temperature, of solutionised samples has been studied in detail. The model with the best performance consists of the Sah-saturation equation and the Sellars-Tegart hyperbolic sine law. The experiments were fitted with an accuracy comparable to the accuracy of the experiments themselves. The effect of solute Mg and Si on the hot deformability is incorporated in the latter equation. By creating different microstructures with varying solute contents and/or distributions of $Mg_2Si$-phases an attempt is being made to quantify the effect of the state of the alloying elements on the hot deformability.

2.2 *Filiform Corrosion on Coated Aluminium Alloys: The Role of Microstructural non-homogeneities in the Substrate* (J.M.C. Mol, D.C.M. Wilms, S. van der Zwaag; J.H.W. de Wit, D.H. van der Weijde [MIDEG])

Filiform corrosion has been responsible for extensive damage, with extreme costs in various sectors of industry, such as building, automotive and aircraft. In building industry it is a serious cosmetic problem for facades and window frames. Filiform corrosion starts at defects in the coating such as cutting edges or local weak spots in the coating and is characterised by thread-like tracks. The local attack is a complex phenomenon involving influences of the environmental conditions, the organic coating, the coating-substrate interface and the substrate surface.
The aim of the present investigation is the combined study of filiform corrosion of aluminium by potentio-dynamic electrochemical polarisation measurements and accelerated exposure tests. Polarisation measurements are performed in bulk anolyte and catholyte solutions which are characteristic for local anodic and cathodic sites in filaments on aluminium substrates, resulting from the differential aeration. From these measurements the corrosion current, defined as the intercept of the anodic and cathodic curves in respectively anolyte and cathodyte, can be determined. The experimental results are also to be compared with results obtained from recent studies on model systems with local enrichments of alloying elements.
The electrochemical and exposure tests are performed on binary Al/Cu, Al/Mg, Al/Si and Al/Zn model alloys as well as typical aircraft alloys, AA2024-T351 and AA7075-T651, with variations of composition, heat treatments and pre-treatments. The pre-treatments range from just degreasing to chromate and cerium based pre-treatments.
The present set of experiments shows good correlation between the polarisation measurements and filiform corrosion propagation during accelerated exposure tests, as shown in Figure 3 for the Al/Cu binary model alloys.

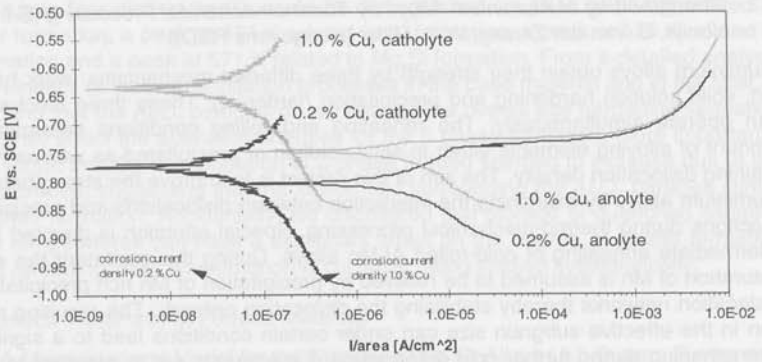


(a)

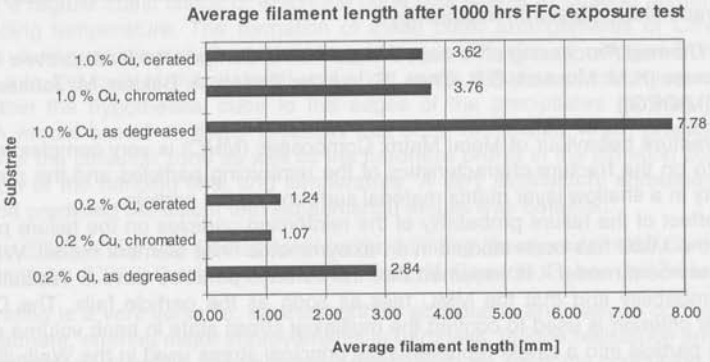


(b)

*Figure 3: The higher corrosion current for the 1.0% Cu binary model alloy determined from the potentio-dynamic polarisation scans in catholyte and anolyte solutions as shown in (a), is in line with the higher average filament lengths for the same alloy during accelerated filiform corrosion tests, as shown in (b)*

Further validation of the filiform corrosion mechanism on aluminium alloys and the anolyte and catholyte as mentioned just above has been done by detailed optical microscopy and videotaping (both real time and time lapse), SEM/EDX analysis, pH-measurements, ICP and colorimetrical analysis of electrolytes and corrosion products in real filaments.

A next step in this research are Kelvin Probe measurements of local corrosion potentials on the investigated aluminium alloys underneath organic coatings and monitoring the filiform corrosion progress during exposition. Recent surface scans of filiform heads and the area around them, give promising results and give insight into the mechanism of filiform corrosion and should eventually lead to insight into the direction dependence of filiform corrosion during propagation.

2.3 *Strengthening of Aluminium Alloys by Thermomechanical Processing* (S.I. Vooijs, S. van der Zwaag; W.S. Miller [Hoogovens R&D])

Aluminium alloys obtain their strength by three different mechanisms: work hardening, solid solution hardening and precipitation hardening. These three mechanisms can operate simultaneously. The reheating and rolling conditions determine the amount of alloying elements either in solid solution or precipitated as well as the remaining dislocation density. The aim of this project is to improve the strengthening of aluminium alloys by examining the interaction between dislocations and precipitation reactions during thermo-mechanical processing. Special attention is devoted to the intermediate annealing of cold-rolled Al-Mn alloys. During this treatment the supersaturation of Mn is assumed to be relieved by precipitation of Mn rich precipitates on dislocation networks thereby stabilising the dislocation network. The resulting reduction in the effective subgrain size can under certain conditions lead to a significant strengthening during further cold deformation. Experiments are in progress to study the effect of initial rolling deformation, intermediate annealing conditions and final rolling conditions. The structural changes during intermediate annealing are being determined using conductivity measurements, thermoelectric power measurements and transmission electron microscopy.

2.4 *Thermal Processing of Al-based Metal Matrix Composites for Improved Toughness* (K.M. Mussert, S.P. Chen, S. van der Zwaag; A. Bakker, M. Janssen [MIDEG])

The fracture behaviour of Metal Matrix Composites (MMC) is very complex, depending a/o on the fracture characteristics of the reinforcing particles and the precipitate density in a shallow layer matrix material surrounding the particle.
The effect of the failure probability of the reinforcing particles on the failure probability of the MMC has been studied in an axisymmetric finite element model. Within the finite element model it is assumed that the ceramic particles have a Weibullian failure probability and that the MMC fails as soon as the particle fails. The Drucker-Prager criterion is used to convert the multiaxial stress state in each volume element of the particle into a single representative principal stress used in the Weibull model. The continuum is considered to consist of a periodic assemblage of hexagonal cylindrical unit cells approximated as circular cylinders. The axisymmetric finite element model contains 350 isoparametric quadrilateral 4-node elements. The MMC is modelled as a matrix of Al6061 (E = 69 GPa, strain hardening coefficient = 0.33, yield stress = 276 MPa), $Al_2O_3$ particles with a diameter of 4 μm (E = 393 GPa, n = 0.27 and a fictitiously high value for the yield stress to ascertain elastic behaviour) and a particle volume concentration of 20%. By plotting the calculated survival probability of an $Al_2O_3$ particle versus the macroscopic axial stresses applied on the MMC, the relation between the failure statistics of the particles and the ensemble can be examined. Based on initial calculations it is concluded that the Weibull parameter m of the reinforcement is only equal to that of the MMC as long as a proportional stress distribution in the matrix surrounding the particle exists and that strong deviations may occur if the stress distribution in the matrix becomes non-proportional, *i.e.* when local plastic deformation occurs. More calculations in which all relevant parameters are varied in a systematic way are in progress. The calculations will be tested against experimental data.
The effect these $Al_2O_3$ particles have on the precipitation kinetics of the Al 6061 matrix alloy have been studied with Differential Scanning Calorimetry. For a heating rate

of 10 K/min four distinct peaks could be distinguished : a peak at 354 K related to cluster formation, a peak at 491 K related to β" formation, a peak at 515 K related to β' formation and a peak at 571 K related to $Mg_2Si$ formation. From a detailed analysis of the kinetics of these precipitation processes in the base material and in the MMC it was found that the $Al_2O_3$ particles do not change the overall age hardening sequence but slightly affect the activation energies for the β phase formation. More importantly it was found that the concentration of β phase formed seemed to increase due to the $Al_2O_3$ particles, suggesting that the stress field surrounding the $Al_2O_3$ particles stimulates their formation. Accidentally, we discovered that storage of quenched samples at low temperatures can have a significant effect on the degree of cluster formation during reheating. This phenomenon is currently being studied systematically.

## 3 *Surface Treatment of Ferrous Materials*

### 3.1 *A Microstructural Model for the Nitriding of Fe-Cr Alloys* (J.J. Braam, S. van der Zwaag)

During the nitriding of Cr containing steels plate-like chromium nitride precipitates form on a regular cubic lattice of which the cube size seems to depend primarily on the nitriding temperature. The formation of these cubic arrangements of CrN precipitates during nitriding involves both long distance diffusion of nitrogen from the surface into the bulk of the material and short range diffusion of chromium atoms from within the hypothetical cube to the edges of the precipitates growing on its faces. A model based on these concepts has been formulated which predicts the build-up of the diffusion zone as well as the hardness profile in the diffusion zone as a function of the nitriding time and temperature. A very satisfactory agreement between the predicted behaviour and experimental results was obtained.

### 3.2 *The Effect of Surface Contaminant on the Nitriding Kinetics of En40B Steel* (B. Pennings, A.W.J. Gommers, T.L.J. de Haan, N. Geerlofs, S. van der Zwaag)

Gas nitriding is a very versatile, environmentally acceptable and easy to control surface treatment, offering major improvements in hardness, fatigue resistance and corrosion resistance. It entails exposing steel products to an ammonia containing gaseous environment at temperatures of about 570 °C. During this nitriding a complex iron nitride multilayer is formed on the surface giving the work piece a dull grey appearance. However, in industrial practice it is occasionally observed that under normal nitriding conditions the compound layer does not form over the entire surface of the product or even does not form at all. Then, the surface remains (locally) shiny. The cause of the phenomenon is not known but is assumed to be related to the chemical or physical structure of the surface of the work piece. In particular traces of cooling, cutting or conserving agents applied during machining or storage are suspected to be responsible for the formation of such passivated surfaces. In an extensive set of experiments involving many industrial cutting and cleaning agents it was established that some of these agents, when not removed properly during cleaning prior to nitriding, do indeed lead to non-nitridable surfaces. By dissimination of their composition and making model cooling fluids containing the critical substance it was shown that sodium salts of (dodecylbenzene) sulfonic acid are very harmful in this respect. The detailed mechanism of the passivation of the surface by this compound still needs to be resolved.

### 3.3 *The Effect of Nitriding Conditions on the Fatigue Behaviour of a Nitriding Steel*
(Y. Fu, A.W.J. Gommers, J. Sietsma)

Earlier work by Braam and Coorens reported in the previous MIDEG Annual report suggested that the fatigue resistance of the engineering steel 42CrMo4 is not uniquely related to the increase in surface hardness in the diffusion zone, but depends very strongly on the interstitial nitrogen concentration too. This phenomenon which had not been reported in the literature has now been studied for a commercial nitriding steel En40B, containing 2.5 rather than 1.0 wt.% Cr. Similar observations were made for this steel too: normal gas nitriding leads to a significant increase in fatigue resistance, denitriding the sample to remove the interstitial nitrogen leads to an almost complete loss of the gain in fatigue strength while subsequent renitriding restores the fatigue strength to its original high value. The hardness profiles in each of these conditions showed only minor changes. However, X-ray diffraction measurements on the samples showed that the de-nitriding led to a disappearance of the compression stresses on the surface of the nitrided samples. Weak tensile stresses in the surface may help to trap hydrogen in the outer surface layer leading to loss of grain boundary cohesion. During renitriding the interstitially dissolved nitrogen atoms rebuild a compressive stress field which repels the trapped hydrogen atoms towards the free surface. The return of compressive stresses and the expulsion of trapped hydrogen are held responsible for the restoration of the fatigue strength.

## PUBLICATIONS

J.J. Braam, S. van der Zwaag
*Fatigue fracture of nitrided steels*
In: L.A.J.L. Sarton, H.B. Zeedijk (eds.), Proc. 5th European Conf. on Advanced Materials, Processes and Applications (Euromat '97), Maastricht, 21-23 April 1997, Volume 1: Metals and Composites, The Netherlands Society for Materials Science, Zwijndrecht (1997) 541-544

J.J. Braam, A.W.J. Gommers, S. van der Zwaag
*The influence of the nitriding temperature on the fatigue limit of 42CrMo4 and En40B steel*
Journal of Materials Science Letters 16 (1997) 1327-1329

L.D. van Ee, J. Sietsma, B.J. Thijsse
*Cooperative atomic motion in metallic glasses*
Phil. Mag. B 76 (1997) 519-527 (on invitation)

L.D. van Ee, B.J. Thijsse, J. Sietsma
*Evidence for two-level states and cooperative atomic jumps in a computer model of amorphous Ni81B19*
Mat. Sci. & Eng. A226-228 (1997) 296-300

P. de Hey, J. Sietsma, A. van den Beukel
*Creation of free volume in amorphous Pd40Ni40P20 during high temperature deformation*
Mat. Sci. & Eng. A226-228 (1997) 336-340

M. de Jong, J. Sietsma, M.Th. Rekveldt, A. van den Beukel
*A neutron depolarization study of internal stresses in amorphous Fe40Ni40B20*
J. Appl. Phys. 81 (1997) 6000-6012

T.A. Kop, J. Sietsma, S. van der Zwaag
*Ferrous phase transformation kinetics: a combined dilatometric-calorimetric approach*
In: R. Asfahani (ed.), Accelerated Cooling/Direct Quenching of Steels, Proc. of Materials Solutions '97 on Accelerated Cooling/Direct Quenching of Steels, Indiana Convention Center, Indianapolis, Indiana, 15-18 September 1997, ASM International, Materials Park, Ohio (1997) 159-165

T.A. Kop, J. Sietsma, S. van der Zwaag
*The transformation kinetics of construction steels; a combined dilatometric and DTA approach*
In: L.A.J.L. Sarton, H.B. Zeedijk (eds.), Proc. 5th European Conf. on Advanced Materials, Processes and Applications (Euromat '97), Maastricht, 21-23 April 1997, Volume 1: Metals and Composites, The Netherlands Society for Materials Science, Zwijndrecht (1997) 537-540

T.A. Kop, F.D. Tichelaar, J. Sietsma, S. van der Zwaag
*In-situ Observation of the Growth of Ferrite from Austenite in the Transmission Electron Microscope*
In: L.A.J.L. Sarton, H.B. Zeedijk (eds.), Proc. 5th European Conf. on Advanced Materials, Processes and Applications (Euromat '97), Maastricht, 21-23 April 1997, Volume 4: Characterization and Production/Design, The Netherlands Society for Materials Science, Zwijndrecht (1997) 39-42

G.P. Krielaart, J. Sietsma, S. van der Zwaag
*Ferrite formation in Fe-C alloys during austenite decomposition under non-equilibrium interface conditions*
Mat. Sci. & Eng. A237 (1997) 216-223

J. van de Langkruis, W.H. Kool, S. van der Zwaag
*Relation between the microstructure and the hot deformability of model systems for the aluminium 6XXX alloys*
In: L.A.J.L. Sarton, H.B. Zeedijk (eds.), Proc. 5th European Conf. on Advanced Materials, Processes and Applications (Euromat '97), Maastricht, 21-23 April 1997, Volume 1: Metals and Composites, The Netherlands Society for Materials Science, Zwijndrecht (1997) 273-277

Y. van Leeuwen, S.I. Vooijs, J. Sietsma, S. van der Zwaag
*Effect of the Geometry in Modelling the Kinetics of Diffusional Transformations in Substitutional Iron Alloys*
In: R. Asfahani (ed.), Accelerated Cooling/Direct Quenching of Steels, Proc. of Materials Solutions '97 on Accelerated Cooling/Direct Quenching of Steels, Indiana Convention Center, Indianapolis, Indiana, 15-18 September 1997, ASM International, Materials Park Ohio (1997) 59-66

J.M.C. Mol, D.C.M. Wilms, J.H.W de Wit, S. van der Zwaag
*Filiform corrosion on coated aluminium alloys: the role of microstructural inhomogeneities in the substrate*
In: L.A.J.L. Sarton, H.B. Zeedijk (eds.), Proc. 5th European Conf. on Advanced Materials, Processes and Applications (Euromat '97), Maastricht, 21-23 April 1997, Volume 1: Metals and Composites, The Netherlands Society for Materials Science, Zwijndrecht (1997) 27-30

J.M.C. Mol, D.C.M. Wilms, J.H.W. de Wit, S. van der Zwaag
*The influence of copper on filiform corrosion of coated aluminium alloys*
In: H. Terryn, G. Verhoeven (eds.), Proc. Aluminium Surface Science and Technol-

ogy Symposium 1997(ASST'97 I), Antwerp, Belgium, May 12-15, 1997, Acta Technica Belgica, Benelux Métallurgie XXXVII (1997) 237-243

K.M. Mussert, M. Janssen, A. Bakker, S. van der Zwaag
*Fracture Toughness of $TiB_2$ Reinforced Aluminium MMC's*
In: L.A.J.L. Sarton, H.B. Zeedijk (eds.), Proc. 5th European Conf. on Advanced Materials, Processes and Applications (Euromat '97), Maastricht, 21-23 April 1997, Volume 1: Metals and Composites, The Netherlands Society for Materials Science, Zwijndrecht (1997) 399-403

C. Qiu, S. van der Zwaag
*Dilatation measurements of plain carbon steels and their thermodynamic analysis*
Steel Research 68/1 (1997) 32-38

G. Ruitenberg, P. de Hey, F. Sommer, J. Sietsma
*Pressure-induced structural relaxation in amorphous Pd40Ni40P20; the formation volume for diffusion defects*
Phys. Rev. Lett. 79 (1997) 4830-4833

G. Ruitenberg, P. de Hey, F. Sommer, J. Sietsma
*Pressure dependence of the free volume in amorphous Pd40Ni40P20 and its implications for the diffusion process*
Mat. Sci. & Eng. A226-228 (1997) 397-400

K. Russew, P. de Hey, J. Sietsma, A. van den Beukel
*Viscous flow of Fe40Ni40Si6B14 amorphous alloy studied by direct creep measurements and relaxation of bend stresses under nonisothermal conditions*
Acta Mater. 45 (1997) 2129-2137

H. Schut, A. van Veen, L.V. Jørgensen, S. van der Zwaag, N. Geerlofs
*Trapping of Nitrogen at the Fe-AlN Precipitate Interface studied by the Position Doppler Broadening Technique*
Materials Science Forum 255-257 (1997) 427-429

S.G.E. te Velthuis, M.Th. Rekveldt, J. Sietsma, S. van der Zwaag
*Neutron depolarization as a tool for studying phase transformations in steel*
Physica B 234-236 (1997) 1027-1029

S.G.E. te Velthuis, F.A.M. Maas, M. Th. Rekveldt, J. Sietsma, S. van der Zwaag
*Phase Transformations in Steels Studied Using Neutron Depolarization*
In: L.A.J.L. Sarton, H.B. Zeedijk (eds.), Proc. 5th European Conf. on Advanced Materials, Processes and Applications (Euromat '97), Maastricht, 21-23 April 1997, Volume 4: Characterization and Production/Design, The Netherlands Society for Materials Science, Zwijndrecht (1997) 175-178

S.G.E. te Velthuis, M.Th. Rekveldt, J. Sietsma, S. van der Zwaag
*A neutron depolarisation study of the austenite to ferrite phase transformation in carbon steels*
In: Y.V. Nikitenko, E.I. Kornilov, E.B. Dokukin (eds.), Proceedings of the International Seminar "Polarized Neutrons for Condensed Matter Investigations", Dubna, June 18-20, 1996 (1997) 114-123

S.G.E. te Velthuis, J. Sietsma, S. van der Zwaag, F.A.M. Maas, M.Th. Rekveldt
*In Situ Studies of the Ferrite Nucleation and Growth in C-Mn Steels*
In: R. Asfahani (ed.), Accelerated Cooling/Direct Quenching of Steels, Proc. of Materials Solutions '97 on Accelerated Cooling/Direct Quenching of Steels, Indiana Con-

vention Center, Indianapolis, Indiana, 15-18 September, 1997, ASM International, Materials Park Ohio (1997) 135-139

W.G. Vermeulen, A. Bodin, S. van der Zwaag
*The prediction of the measured temperature after the last finishing stand using artificial neural networks*
Steel Research 68/1 (1997) 20-26

W.G. Vermeulen, S. van der Zwaag, P.F. Morris, A.P. de Weijer
*Prediction of the continuous cooling transformation diagram of some selected steels using artificial neural networks*
Steel Research 68/2 (1997) 72-79

F.J. Vermolen, H.M. Slabbekoorn, S. van der Zwaag
*The apparent activation energy for the dissolution of spherical Si-particles in AlSi-alloys*
Mat. Sci. & Eng. A231 (1997) 80-89

F.J. Vermolen, C. Vuik, S. van der Zwaag
*Modelling the Microstructural Changes during the Homogenisation of Extrudable Aluminium alloys*
In: L.A.J.L. Sarton, H.B. Zeedijk (eds.), Proc. 5th European Conf. on Advanced Materials, Processes and Applications (Euromat '97), Maastricht, 21-23 April 1997, Volume 1: Metals and Composites, The Netherlands Society for Materials Science, Zwijndrecht (1997) 487-490

F. Vermolen, C. Vuik, S. van der Zwaag
*A numerical analysis for the dissolution of second phase particles in ternary alloys*
In: R. van Kheer, C.A. Brebbia (eds.), Moving Boundaries IV, Computational Modelling of Free and Moving Boundary Problems, Proc. Fourth International Conference on Moving Boundaries "Moving Boundaries 97", Gent, 27-29 August, 1997, Computational Mechanics Publications, Southampton, UK, Boston, USA (1997) 153-162

F.J. Vermolen, P. van Mourik, S. van der Zwaag
*Analytical approach to particle dissolution in a finite medium*
Materials Science and Technology 13 (1997) 308-312

P.J. van der Wolk, A.T.J. van Helvoort, M. van Leeuwen, S. van der Zwaag
*Calculating the hardenability of engineering steels using data from multiple sources*
In: L.A.J.L. Sarton, H.B. Zeedijk (eds.), Proc. 5th European Conf. on Advanced Materials, Processes and Applications (Euromat '97), Maastricht, 21-23 April 1997, Volume 4: Characterization and Production/Design, The Netherlands Society for Materials Science, Zwijndrecht (1997) 525-529

S. van der Zwaag
*Validation of Ferrous Transformation Models: Some Relevant Experimental Techniques*
In: R. Tomellini (ed.), Proceedings ECSC Workshop "Modelling of steel microstructural evolution during thermomechanical treatment", Brussels, 22 January, 1997, ECSC publications, EC DG-SR&D (1997) 159- 174

**MATERIALS SCIENCE AND ENGINEERING**
University of Groningen, Department of Applied Physics
Nijenborgh 4, 9747 AG Groningen
phone +31 (50) 3634898, fax +31 (50) 3634881, e-mail I.De.Hosson@phys.rug.nl

PERSONNEL

*Scientific staff*

prof.dr. J.Th.M. De Hosson (3634897)
dr.ir. P.M. Bronsveld (3634907)
dr.ir. B.J. Kooi (3634896)

*Post-doc*

dr.ir. J.W. Hooijmans (EC) (3634901)

*Graduate students*

ir. D.T.L. van Agterveld (FOM)
ir. P.A. Carvalho (IST-Lisbon)
ir. N.J.M. Carvalho (TNO)
drs. J.W. Chung (FOM)
ir. H.B. Groen (FOM)
ir. J.B.J.W. Hegeman (STW)
ir. J.W.J. Kerssemakers (FOM)
ir. A.B. Kloosterman (IOP)
ir. A. Roos (IOP)
ir. D.H.J. Teeuw (Hoogovens Research)
ir. E. Zoestbergen (IOP)

*Materials designer*

ir. T. Tinga

*Research students*

E.A. Alvarez Otero
D.T.L. van Agterveld
P. Balke
J. de Boer
B. Cordia
A. Garcia Lekue
T.J.J. de Grood
M. Gotink
M.J. de Haas
A. Hibma
J. Kinds
A.R. Westers
J.A. Vreeling
S.R. de Vries

*Technical assistants*

H.J. Bron (3634884)
J. Harkema (3634909)
U.B. Nieborg (3634889)

K. Post (3634906)
O.T. Schutter (3634886)

*Management assistance*
I. De Hosson-Gebhardt (3634898)

## RESEARCH AREAS AND OBJECTIVES

The principal aim of the research projects of the materials science group at the University of Groningen is to search for the relation between the mechanical strength and the microstructure of materials. Defects, like interfaces between dissimilar materials, grain-boundaries and dislocations, form the focal point in microscopic studies.

The work is divided into the following objectives:
1. Interfaces between metals/ceramics: HRTEM and Local Probe Microscopy
2. Interfaces between metals/ceramics: high power lasers
3. Interfaces in nanoceramics and technical ceramics: LV-HRSEM, X-rays
4. Dislocation Dynamics in metallic systems: modelling and NMR

Structural aspects of single metal/ceramic interfaces are considered on different length scales: experiments are performed at an atomic scale on model systems produced by internal oxidation. Metal/ceramic multi-layers on a nanometer scale are manufactured using a novel process called stereostiction, from nanosized particles. At a μm scale metal/ceramic interfaces that find application as protective coatings are studied, being produced by high power lasers (1.5 kW CW- $CO_2$ and 2 kW pulse Nd-YAG). The main experimental tools to unravel the microstructural features are High Resolution Transmission Electron Microscopy (HRTEM, Jeol 4000EX/II equipped with PEELS) and high resolution low-voltage Scanning Electron Microscopy (LV-HRSEM).

On the property-side a rather mesoscopic materials science approach is followed. Parallel to an experimental study using local probe microscopy and LV-HRSEM a computational materials science approach is undertaken. The latter study is carried out in collaboration with prof. E. van der Giessen [MIDEG] and prof. V. Vitek [University of Philadelphia]. The experimental part, using pulse-NMR is carried out in collaboration with prof. O. Kanert [University of Dortmund]. Bonding behaviour of metal/ceramic interfaces and mechanical performance are examined in collaboration with prof. G. de With [MIDEG] and dr. A.J. Huis in 't Veld [TNO].

The principal ideas behind the research projects are the following. Generally speaking, microscopy in the field of materials science is devoted to link microstructural observations to physical properties. In particular mechanical properties of metals and alloys are structure-sensitive. Often it is claimed that advanced microstructural investigations require a microscope with a resolving power in the order of a nanometer or even better. Although the microstructure-property relationship is in itself a truism, the actual linkage between structural aspects of defects in a material studied by microscopy on one hand and its physical property is almost elusive. The reason is that various physical properties are actually determined by the collective behaviour of defects rather than by the behaviour of one singular defect itself. For instance there exists a vast amount of electron microscopy analyses in the literature on *ex situ* deformed metals and alloys which try to link observed dislocation patterns to the mechanical behaviour characterised by stress-strain curves. However, in spite of the enormous

effort that has been put in both theoretical and experimental work, a clear physical picture that could predict the stress-strain curve on the basis of these microscopy observations is still lacking.

There are at least two reasons that hamper a straightforward correlation between microscopic structural information to materials properties: one fundamental and one practical reason. Of course it has been realised already for a long time that in the field of dislocations and interfaces in metals and alloys we are facing highly non-linear and non-equilibrium effects. The defects determining many physical properties are in fact not in thermodynamic equilibrium and their behaviour is very much non-linear. This is a fundamental problem since there doesn't exist an adequate physical and mathematical basis for a sound analysis of these effects.

Nevertheless, the situation is not hopeless since there are two approaches nowadays to circumvent these problems and microscopy still contributes a crucial portion. One has to do with numerical simulations of the evolution of defect structures, which incorporate the behaviour of individual defects as known from both the classical theory and from microscopy observations of individual dislocations, interfaces and interactions between dislocations and interfaces. For example, to have a thorough understanding of the generation of cellular dislocation structures, vein structures, tangles, sub-grain boundaries and persistent slip bands, important input for these numerical simulations on the behaviour of individual dislocations like cross slip behaviour, climb and bipolar structures etc., are provided by microscopy research. Another approach, which is supplementary to these simulations and partly based upon them, is the continuum mechanics approach. It provides a description of the global co-operative behaviour of defects and focuses on the instability transitions and accompanying structural transformations. Also here experimental knowledge provided by electron microscopy, in combination with complimentary techniques, is inevitable.

The situation to correlate the microstructural information obtained by microscopy of an interface to the macroscopic behaviour of polycrystalline solids is even more complex than in the case of dislocations. The reasons are numerous, *e.g.* the limited knowledge of the interface structure, *i.e.* both topological and chemical, at an atomic level of only a small number of special cases, the complexity due to the eight degrees of freedom of an interface and the lack of mathematical-physical models to transfer information learned from bi-crystals to the actual polycrystalline form. It has been shown that in some cases it is crucial to have information on an atomic level available provided by high resolution electron microscopy but surely it is not always necessary and sometimes rather more appropriate to image defects on a μm scale instead to correlate the structural information to physical properties. Actually, new measures can be introduced at a different length scale as well as microscopic features like the radii of gyration and clusters that are joined by like boundaries. Therefore we argue that more quantitative evaluation of the structure-property relationship of materials requires a somewhat de-emphasis of analysis on an atomic scale and a re-emphasis on *in situ* observations.

With the advent of (ultra) high-resolution transmission electron microscopy (HRTEM) it is nowadays possible to derive from the images structural information at an atomic scale. However, still the concept of resolution in HRTEM is not without pitfalls and a thorough understanding of image formation is essential for a sound interpretation. The technique of HRTEM founds it origin in the technique of phase contrast micros-

copy that was introduced by Frits Zernike of this very same University of Groningen for optical microscopy. In 1953 he received the Nobel Prize in physics for this invention. High-resolution TEM imaging is based on the same principles. In reality, however, a HRTEM is not a perfect phase contrast microscope, beams at different angles with the optical axis obtain different phase shifts.

Like in the area of transmission electron microscopes, the more recently commercially available scanning electron microscopes are equipped with a field emission gun (FEG) as well. In 1997 two new microscopes were installed: a Philips XL30-FEG and XL30s-FEG. The high brightness and spatial coherence make these sources excellent for use in high-resolution scanning electron microscopes. The penetration depth of the high-energy electrons will cause the electrons to be trapped in the material. When studying conducting materials, the electrons will be transported away from the point of incidence. However, if the specimen is a non-conducting material, like in our research of ceramic coatings on metals), the excess electrons will cause charging of the surface. The electrostatic charge on the surface deflects the incoming electrons, giving rise to distortion of the image. In order to reduce surface charging effects, it is common practice to sputter a conducting layer of metal, with typical thicknesses 5-10nm onto the surface. This layer will transport the excess electrons, reducing the negative charging effects. However, a negative effect of the sputtered layers is that it may diminish the resolving power of the microscope, since topographical information is no longer gained from the surface of the material, but from the sputtered layer.

A more recent approach is to minimise charging effects by balancing the incoming and emitted electron current. To minimise charging effects, the energy of the primary beam should is chosen usually being typical 2-3 kV. A conducting layer is then not required, and the balancing of the electron yield will prevent the surface from charging. However, charging of the surface is not the only factor determining the resolution of a scanning electron microscope. The width of the electron beam is also an important factor for the lateral resolution. A narrow electron beam results in a high resolution. The spot size however, is a function of the accelerating voltage. The broadening of the spot size is the sum of broadening due to several processes. The first contributor is the beam itself, the brightness of the source, the beam current and its divergence angle. The second part is the contribution due to diffraction of the electrons of a particular wavelength by the size of the final aperture. The last two parts are the broadening caused by chromatic and spherical aberrations. In order to achieve the smallest spot size, all contributions should be as small as possible. Decreasing the accelerating voltage will not only cause the wavelength of the electrons to increase, but also the chromatic aberration, $C_C$ , increases as well, resulting in an increase of the spot size and, as a consequence, a decrease in resolving power of the microscope. A field emission gun has a very high brightness, reducing the contribution in broadening due to the beam itself. The energy spread in the electron energies is also small. Together with the fact that the coefficients $C_S$ and $C_C$ can be reduced by optimising the lenses for low-energy electrons, provides the FEG low voltage scanning electron microscope with very high resolving power. In 1997 a resolution of 1.5 nm at 1-3kV was attained in a special Philips FEG-SEM XL30s equipped at our laboratory with a backscattering Kikuchi diffraction detector. An example of nano-ceramic $SiO_2$ particles on top of fused-quartz, shown in cross section, is displayed in Figure 1.

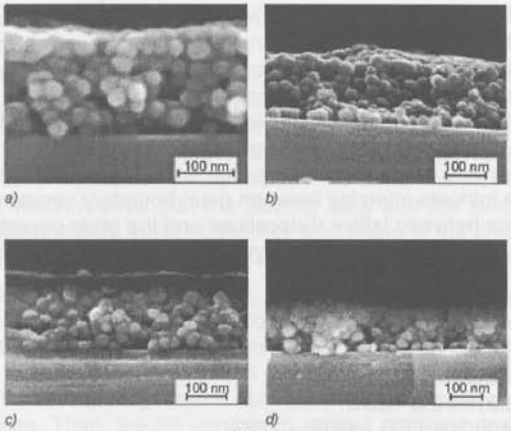


*Figure 1: Nano-ceramic $SiO_2$ particles on top of fused-quartz*

Although conventional scanning electron microscopes (CSEMs) have superior resolution, depth of field, and microanalytic capabilities, they have also a number of limitations since a high vacuum must maintain in its sample chamber. The column requires a high vacuum in order to generate and focus the electron beam. The sample chamber requires a high vacuum to permit the use of available secondary electron detectors. The latter, used in most conventional SEMs is known as the Everhart-Thornley (ET) detector. Because of its exposed high voltage elements, an ET detector can only function in a high vacuum environment. In a gas environment, it too will arc, often damaging or destroying itself in the process. There are two key technologies that differentiate the so-called environmental scanning electron microscope (ESEM) from all other SEMs. The first is its multiple aperture, graduated vacuum system. The second key technology is the environmental/gaseous secondary electron detector, using gas ionisation to detect and amplify the secondary electron signal. Gas ionisation also suppresses charging artefacts on more insulating samples. The detectors are insensitive to light and heat. In 1998 a Philips FEG-ESEM will be installed that may contribute considerably to *in situ* thermo-mechanical studies of metals and alloys since both high-temperature and deformation stages are in principle available.

It is anticipated that in the near future the emphasis of our research in the field of advanced techniques of microscopy will lie rather on the combination of both structural and chemical information. In 1997 a unique JEOL-UHV-7800 combined SEM/SAM was tested to explore impurity segregation and its effect on intergranular fracture. Further, in particular electron energy loss spectroscopy (EELS) will be further integrated in the research projects since it provides information about the density of (un) occupied states, which are relevant for the bonding behaviour along grain-boundaries and interfaces. However, although EELS spectra can be obtained from very small regions, only sub-nanometers across these boundaries, these new methods may be still very disruptive. The electron beam, focused on interfaces, may cause beam-induced motion of the chemical constituents. In addition, from a theoretical point of view the precise nature of 'charge transfer' at the grain-boundaries and interfaces is still rather controversial, although the common opinion is that the

number of d-band electrons of transition metals will change if the atom is placed at the boundary. Therefore, the bonding behaviour is altered which may be estimated from the changed occupancy of the electronic states by EELS. It is quite clear that first many more experimental and theoretical work is needed on the full characterisation, *i.e.* structural and chemical, of special ($\Sigma$) and general boundaries before firm conclusions can be drawn about the correlation between electronic charge transfer, bonding behaviour and properties. In particular for the mechanical properties of metallic systems the intricate interplay between grain-boundary structures and plasticity, *i.e.* the interactions between lattice dislocations and the grain-boundary, becomes an important aspect. For that reason, more dynamic *in situ* studies are planned in 1998.

## FACILITIES

- HRTEM: JEM 4000 EX/II
- CTEM: JEM 200 CX + EDS
- TEM: JEM 2010 FEG +EDS
- Philips SEM-XL30s-FEG + EDS + EBSP
- Philips LV-HRSEM-XL30s-FEG +EDS
- Philips ESEM-XL30-FEG+EDS
- SEM ISI-DS-130 + EDS + WDS
- CW-$CO_2$ laser Spectra Physics 820, 1.5 kW
- Nd-YAG laser system Rofin Sinar CW 20, 2 kW
- Nd-YAG laser Lumonics 300
- FIM - IAP
- FIM - TOF – AP
- Philips PW 1820 $\omega$ goniometer
- Philips X'Prt PW 3040 $\psi$ goniometer
- Instron Tensile machine
- LCF tester
- Logan Acoustic emission
- Ultrasonic attenuation
- SEM/STM combination
- AFM/STM Nanoscope
- High temperature optical microscope HT-OM
- Hardness tester
- Workstations Silicon Graphics/Indigo

## RESEARCH REPORT 1997

1 *Interfaces between Metals/Ceramics: HRTEM and Local Probe Microscopy* (B.J. Kooi, J.Th.M. De Hosson, P.M. Bronsveld)

1.1 *Modification of Metal/Oxide Interfaces by Dissolution of Sb in Oxide Precipitates Containing Metal Matrixes* (A.R. Westers, J.A. Vreeling, D.T.L. van Agterveld, E.A. Alvarez Otero, A. Garcia Lekue, T.J.J. de Grood)

Metal/ceramic interfaces play an important role in many advanced engineering materials. The structure and chemistry of the heterophase interfaces then often govern the performance of these composites. Solute segregation to the hetero-interfaces is known to affect the adhesion at the interfaces. However, in contrast to segregation at

grain boundaries only very few studies have addressed segregation at metal/ceramic interfaces.

In the present study a segregating element, Sb, is dissolved in a metal matrix containing a highly dispersed ceramic phase in the form of oxide precipitates. The influence of this dissolution on the precipitate morphology and interface structure is studied using HRTEM. The following systems were studied: Ag/$Mn_3O_4$, Cu/MgO, Cu/MnO and Ag/ZnO. The oxide precipitates in the metal matrix were obtained by internal oxidation which implies that the starting alloy and the oxidation conditions determine the oxide phase to develop, the size and shape of the precipitates and the orientation relations and interface orientations of the precipitate and the matrix.

To analyse the effect of the Sb dissolution, first the oxide precipitates were grown in the pure metal matrix using internal oxidation. Subsequently the Sb was dissolved in the metal matrix by annealing the composite in an evacuated quartz tube, also separately containing a tiny amount of Sb, at a temperature just above the melting temperature of Sb. The Sb vapour pressure above the molten Sb allows transport of the Sb to the composite. Then, the Sb can be distributed relative homogeneously over the metal matrix via solid state diffusion provided the relative amount of Sb present corresponds to a concentration lower than the solubility limit of Sb in the metal. Since this process of introducing Sb in the alloy generally takes 1 week at a temperature of 650 or 700 °C, the influence of Sb on the precipitates can only be determined if a comparison is made with the effect of annealing the sample under identical conditions but without the presence of Sb. So, three types of samples are compared: as-grown, Sb-dissoluted and vacuum annealed. Below three sections address Ag/$Mn_3O_4$, Cu/MnO+Cu/MgO and Ag/ZnO separately and finally a discussion of the general influence of the Sb dissolution will be given.

*The Ag/$Mn_3O_4$ system*

The $Mn_3O_4$ precipitates in pure Ag were obtained by internal oxidation of Ag - 3at.% Mn in air at 900 °C. This system is well characterised and the precipitates with a size of 10-20 nm have octahedral shape since they are bounded by 8 {111} planes (close packed oxygen planes) of the tetragonal spinel lattice of $Mn_3O_4$. These {111} planes all tend to be parallel to the {111}s of Ag. However, owing to the tetragonal distortion of the $Mn_3O_4$ this parallelism can only be achieved for one pair of {111} facets. Then, at another pair of facets a tilt of $7.6^0$ occurs between the (111)s of $Mn_3O_4$ and Ag, which is accounted for by ledges in the Ag.

The dissolution of 4 at.% of Sb in the Ag matrix showed according to HRTEM observations 2 major effects on the precipitates: (i) a change from a precipitate sharply faceted by solely {111} to a globular shape with sometimes also short {220} and (002) facets and (ii) a partly reduction of $Mn_3O_4$ in MnO for a part of the precipitates. The lower interfacial strain energy for $Mn_3O_4$/Ag with respect to MnO/Ag is probably responsible for the tendency to keep the outer core of the precipitate $Mn_3O_4$. The reduction of $Mn_3O_4$ in MnO can be understood since annealing in Sb vapour will result in equilibrating the sample with respect to the dissociation pressure of Sb-oxide and this pressure is significantly lower than the original oxygen partial pressure used for internal oxidation. To test this explanation, a pure Ag/$Mn_3O_4$ sample was annealed in Zn instead of Sb vapour. The dissociation pressure of ZnO is in-between these pressures for MnO and $Mn_3O_4$ and therefore full reduction of $Mn_3O_4$ in MnO is expected. This expectation was indeed confirmed: only MnO precipitates with {200} truncated

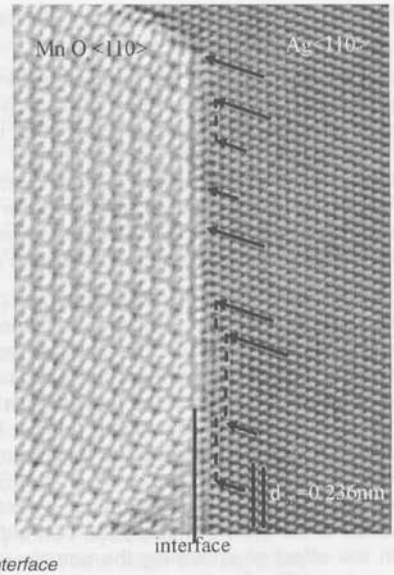


*Figure 2: An Ag/$Mn_3O_4$ interface*

octahedral shapes were observed in the Zn treated sample.

Vacuum anneal of the Ag/$Mn_3O_4$ under identical conditions as used for the introduction of Sb also resulted in some differences with the as-grown case, however, completely different from the changes due to the Sb dissolution: (i) next to the {111} facets of the $Mn_3O_4$ which remained predominant also {200} and (002) facets developed during the anneal for precipitates which did not exhibit growth and (ii) regions where these precipitates without growth were observed adjacent to regions where large (several 100 nm) non-faceted, sometimes poly-crystalline $Mn_3O_4$ clusters had 'consumed' by Oswald ripening all original small precipitates. In the Sb dissoluted samples growth of the $Mn_3O_4$ precipitates was never observed and thus Sb prevents this growth. These results make also clear that Sb is responsible for the spheroidising effect on the precipitates. The absence of {200} and (002) facets for the as-grown precipitates and their presence for the annealed ones indicate that during oxidation precipitate shapes develop which do not correspond to thermodynamic equilibrium but are kinetically determined.

*The Cu/MnO and Cu/MgO system*

The MnO and MgO precipitates in pure Cu were obtained by internal oxidation of Cu - 1at.% Mn, Cu - 3at.% Mn and Cu - 2.5at.% Mg with the so-called Rhines pack method, *i.e.* foil of the alloy together with Cu/$Cu_2O$/$Al_2O_3$ powder is wrapped in Cu-foil and put in an evacuated quartz tube and annealed in a furnace. Both MnO and MgO precipitates currently of interest show parallel topotaxy with Cu and have {200} truncated octahedral shape and have average sizes of 200 nm and 40 nm after 1 week vacuum anneal at 700 °C. Assuming that this anneal results in precipitates with equilibrium shapes the ratio of the {200} and {111} interfacial energy $r$ can be obtained from the relative {200} and {111} facet lengths using the Wulff theorem (in reverse). For Cu/MnO $r = 1.64 \pm 0.04$ is obtained from the average of 10 precipitates

and for Cu/MgO $r$ = 1.27±0.1 [6]. In case during the one week anneal at 700 °C about 2.5 at.% Sb is dissolved in the Cu matrix the ratio of the {200} and {111} interfacial energy appears to be significantly affected and corresponds to $r$ = 1.50±0.06 for Cu(Sb)/MnO (average of 16 precipitate shapes) and to 1.07±0.14 for Cu(Sb)/MgO (average of 14 precipitates). For instance for Cu/MnO this corresponds to an increase of the relative length of the {100} facet with a factor 3. Interesting to note for the Cu/MgO system is that former experiment with 2.5 at.% Au dissolution in the Cu matrix resulted in a decrease of the relative length of the {200} facet and is thus opposite to the effect of the Sb dissolution. In addition for the Cu(Sb)/MnO system small {220} facets arise indicating a ratio of {220} to {111} interfacial energy of 1.19± 0.02 and hence the {220} interface in Cu(Sb)/MnO has a lower energy than the {200} interface. Only in Cu(Sb)/MnO truncation due to the {220} facet is observed, however, if the ratio becomes larger than ½√6 (≈1.225) truncation can not be observed anymore.

*The Ag/ZnO system*

Internal oxidation of an Ag - 1wt.% Zn alloy resulted generally in plate-like wurtzite ZnO precipitates typically with a thickness of 100 nm and a "diameter" of 1000 nm. The predominant orientation relation observed between the Ag and ZnO is <110>Ag//<11-20>ZnO+{111}Ag//{0002}ZnO and these parallel {111}Ag and {0002}ZnO form the dominant pair of facets of the precipitate.

Dissolving 3 to 4 at.% Sb in the Ag matrix of this Ag/ZnO system analogous to the dissolution in the Ag/$Mn_3O_4$ system resulted in dramatic changes of the "diameter" of the precipitates, but without observably affecting the thickness of the precipitates: typically a reduction of the diameter from 1000 nm to 200 nm was observed! Consequently, the number density of precipitates should have increased significantly; this was indeed observed. Next to single wurtzite ZnO plates, a configuration in which sphalerite ZnO is present in contact with 2 wurtzite ZnO plates also appeared frequently as a consequence of the Sb dissolution. The 2 wurtzite plates are parallel to 2 different {111} planes of Ag, but start from a common origin and thus make up a V-shape. The common origin of the 2 plates corresponds to a (geometrically necessary) symmetrical tilt boundary between the wurtzite ZnO. Now, within the confinement of the V-shape sphalerite ZnO is present always showing a parallel topotaxy with the Ag. Interesting to note is that the angle between the wurtzite plates making up the V is always the sharp angle between the {111}Ag of 70.5° and never the obtuse angle of 109.5°. Apparently, this last configuration is unstable and will not be equilibrated during the one week anneal. The reason for the presence of sphalerite is probably caused by the increased number density of precipitates (and thus only an indirect consequence of the Sb dissolution), because this increases the probability that 2 wurtzite plates on different Ag{111} grow together, making the nucleation of sphalerite in the sharp tip of the V-shape advantageously and resulting in a relative stable configuration.

*General influence of Sb metal matrix dissolution on metal/oxide interfaces*

The general picture that arises from the Sb dissolution in the systems Ag/$Mn_3O_4$, Cu/MnO, Cu/MgO and Ag/ZnO is that the original dominant facets of the precipitates as formed by parallel close-packed oxide and metal planes are destabilised by the Sb dissolution. Since we expect the precipitates to have equilibrium shapes after 1 week anneal at 650 or 700 °C the change in shape thus directly reflects the change in relative interfacial energies of different interface configurations. Apparently, the

interfacial energy corresponding to parallel close-packed oxide and metal planes decreases relatively to the ones of the other types of interfaces.

The following possible explanation can be proposed for this change in relative interfacial energies. Sb, which is known to be a strongly segregating element in general and at Ag surfaces in particular, is segregating anisotropically to different interface configurations. The stronger the segregation to a certain interface configuration the larger the decrease in interfacial energy. The destabilising effect of Sb on the parallel close-packed oxide and metal interface can be understood if Sb segregation to this interface is much less compared to (an)other interface(s). Since the atomic radius of (metallic) Sb is larger than the ones of Ag and Cu, Sb will exhibit the tendency to segregate to interfaces with a relative open structure. In general the interface formed by parallel close-packed planes have least open structure and so is not preferable for segregation. This is clearly observed for grain boundaries in metals where for instance segregation of Bi to the symmetrical tilt boundary $\Sigma 3$ {111} in Cu is not observed, but clearly occurs for other boundaries with more open structure such as the symmetrical tilt boundary $\Sigma 5$ {210}. Moreover, segregation to the parallel close-packed plane interfaces is even less preferable for the present metal/oxide interfaces as for fcc metal/metal interfaces. This difference originates from the 2 fcc sublattices, one for the anions and one for the cations present in the oxide compared to one fcc lattice in the metals. The ratio of the number of atoms in the terminating layer of the oxide and in the adjacent first metal layer is, for the parallel close-packed plane interface, equal to the ratio of the lattice constants of the metal and the oxide. For parallel non-polar metal/ oxide interfaces, such as parallel {100}, {110} in NaCl structure-type oxides, this ratio is a factor 2 higher. This factor 2 comes from the fact that only one of the two sublattices in the oxide tends to continue in the metal at the non-polar interface and this results in relative more free volume experienced by the metal layer at the non-polar interface compared to at the polar close-packed interface. Hence, segregation is expected to occur much more strongly to these non-polar than to the parallel close-packed plane interface. This expectation can be verified (hopefully) soon if a new FEG-TEM allowing high spatial resolution elemental analysis (0.5 nm probe EDX) becomes operational in our group in Groningen.

1.2 *High Resolution Electron Microscopy of Metal-Oxide Interfaces* (H.B. Groen)

For many applications like chip packaging and laser cladding the properties of metal-ceramic interfaces are of great interest. The macroscopic properties of the materials depend on the microstructure and chemistry of the interfaces. Little is known about the details of metal-ceramic bonding so a good description is needed. Here, Pd-ZnO interfaces are studied because of the relatively high stacking-fault energy of Pd compared to Ag and the lattice constant being between that of Ag and Cu, both previously observed in combination with ZnO. Internal oxidation of a Pd-Zn alloys is used here and is a simple method to obtain many ZnO precipitates inside a Pd matrix for observation by HRTEM.

Palladium was alloyed with 1.6 and 3.2 at.% Zn by diffusion of zinc vapour into a 100 μm thick Pd sheet at 1273 K for four days in an evacuated quartz tube. After the diffusion treatment the alloy is internally oxidised for 17 h at 1273 K in air. Microscopy is performed using a Jeol 4000 EX/II electron microscope with 0.165 nm point resolution. The average size of the plate-like precipitates is around 1 μm with a thickness of about 100 nm. The majority have a truncated trigonal shape, with large {0001} ba-

sal plane facets parallel to {111} planes in Pd and the [11$\bar{2}$0] direction in ZnO parallel to the [110] direction in Pd.

When observing the ZnO precipitates two striking features show up: (i) on tilted interfaces the tilt is relieved by steps in the ZnO instead of the metal (opposite to Ag-ZnO interfaces) and (ii) the occurrence of sphalerite ('fcc') ZnO surrounded by wurtzite ('hcp') ZnO.

The stepped oxide interfaces can be explained by looking at the shear moduli of the materials, 53 GPa for Pd and 46 GPa for ZnO (wurtzite). This is a rather even distribution compared to the majority of metal-oxide systems where the oxide can be regarded rigid compared to the metal. When we compare Pd-ZnO with the Ag-ZnO system no stand-off dislocations are formed to relieve the small tilt of the interface. This can be explained by the high stacking fault energy of palladium (180 mJ/m$^2$) compared to that of silver (17 mJ/m$^2$).

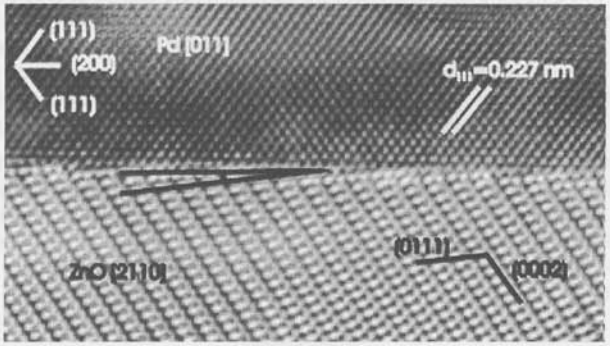


*Figure 3: First pyramidal plane of ZnO in contact with Pd (002). The angle between the two planes is about 6.5°.*

Zinc-oxide exist in a hexagonal (wurtzite) form but it also exists in a metastable cubic (sphalerite) form. Most plate-like precipitates have the hexagonal wurtzite structure. However, for some (small) precipitates it is more favourable to consist of a tetrahedron of four wurtzite ZnO platelets and a nucleus that consists of the cubic sphalerite ZnO. These configurations were also found in internally oxidised Ag-Zn. It is believed that in some cases ZnO nucleates in the sphalerite form and after a certain size the growth is continued as wurtzite ZnO.

Another followed approach is to unravel the detailed interfacial dislocation structure of metal-oxide interfaces. This is done on {111}-type interfaces in Cu-MnO and Cu-MgO systems; a fcc metal in contact with a NaCl-structure oxide. The interfacial structure along the ⟨110⟩ direction has been observed before but to resolve the copper matrix along the ⟨112⟩ direction a microscope is needed with a point resolution of at least 0.128 nm. For this purpose the JEM-ARM 1250, with a point resolution of 0.12 nm, at the Max-Planck institute for Metal research was used. With this microscope it was proven possible to observe the strain fields caused by the predicted network of ⅙⟨112⟩ dislocation at the interfaces. Another effect that could be observed with this microscope is the displacement of individual atomic columns along the ⟨110⟩ direction at the interface.

It is possible to add a segregating element to a internally oxidised metal, in this case

adding a few atomic percent Sb to a Ag/ZnO sample, which is currently under research. The Sb is introduced into the metal by vapour treatment inside an evacuated quartz tube. This segregating element could influence the interfacial energy of the precipitates changing their shape and the structure of the interfaces. The observed result is that the plate-like precipitates change into a more globular shape without losing the facets of the ZnO, possibly caused by the Sb that reduces the step-energy at the interface. This effect is also observed in $Ag/Mn_3O_4$ samples, but here the facets disappeared.

1.3 *Local Probe Microscopy (AFM/STM and FIM)* (J.W.J. Kerssemakers, W. Oele, A. Hibma)

This research deals with certain aspects of the interaction between microscopic systems as it occurs at an atomic level. In this work a prominent part of such a system forms the sharp probing tip of an Atomic Force Microscope (AFM).

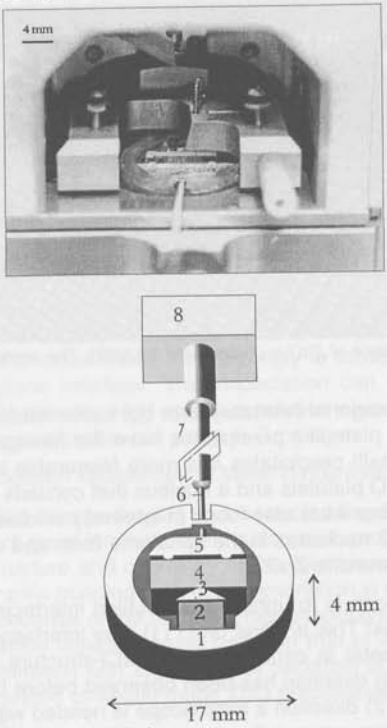


*Figure 4: An in situ three point bending device*
*Upper: Installation of the device in the AFM. The screw can be seen protruding out of the head, just over the XY-position table of the AFM. In this set-up, full utilisation of the AFM is preserved.*
*Lower: Schematic overview: a quarts housing (1) encloses three quarts wedges (3) and (5) clamping a NaCl beam (4). Bending is performed by a piezo (2) or a screw (6). The latter is rotated by a flexible shaft (7) driven by an external stepper motor (8). The flexible shaft still allows for scanning and vibration isolation.*

A detailed knowledge of the mechanical behaviour of this probing tip together with its attached cantilever is essential. The interaction of the tip with the material under investigation leads to forces causing deformation of the cantilever. A full description of this cantilever is feasible with a compact set of elastic moduli.. The actual detection of the cantilever response is done optically. The set of moduli allows for expressing the three-dimensional cantilever response to forces between tip and substrate in a rather detailed fashion.

However, the need for a full description of the cantilever response can be circumvented by following an alternative approach. Experiments are carried out of *in situ* etching and of *in situ* deformation are discussed. A study is presented of the static and dynamic behaviour of line defects (dislocations) as they are encountered on the (001) surface of ionic crystals, like rocksalt. The surface energy that can be associated with such a defect is estimated from morphological arguments. The response of these line defects to stress was investigated with a miniature three-point bending device, installed in the AFM (see Figure 4). It was shown that the observed surface changes stem from the activation of the primary <110>{110} slip system. The density of surface changes was shown to be in reasonable agreement with the applied stress distribution, provided that the non-ideal properties of the bending configuration are properly considered as well.

Details of the cantilever behaviour are of importance and therefore a special form of 'atomic resolution' imaging is investigated as it is captured on certain substrates. This is the so called stick/slip phenomenon, in which the AFM tip performs a jerky-type lateral movement over the substrate. The images produced during this behaviour still display the correct atomic lattice periodicity. This is rather remarkable, as it can be shown that during this stick/slip movement the tip is in contact with the substrate over an area extending over much more than one surface unit cell.

To describe this stick/slip phenomenon, we devised a model in which the process is considered as a rather discrete system. In the model, the AFM tip is thought to perform instantaneous slips between discrete, fixed lattice points. Such a model turns out to give an accurate explanation of features as observed in the actual AFM images. An alternative approach yields the same results, utilising a more physical mechanical description of the AFM configuration. However, the advantage of the discrete model over the mechanical one is that the former allows for an analysis of the detailed slip patterns based on geometrical considerations. The validity of this approach was supported by a more detailed analysis of the slip patterns, in which the relative occurrence of the different kinds of lattice slips was taken as a parameter. This relative occurrence was shown to depend on the various orientations of surface lattice and scan pattern, but also on the magnitude of the maximum sticking force that the substrate may exert on the tip. The strong influence of this latter parameter on the complexity of the slip patterns was shown in a theoretical as well as an experimental sense.

Although the discrete model provides a powerful means to describe the process, it gives no clue on the origin of the phenomenon, or explain why it is most prominently encountered on substrates having a layered structure. Although stick/slip friction is not exclusively linked with materials having such a layered structure, a strong link is clearly present. Examples of such materials are mica or the transition metal dichalcogenides ($MX_2$). These materials are built of sandwich layers of transition metals

(M) surrounded by chalcogen atoms (X), *i.e.* $TiS_2$ . The sandwich structure X-M-X is only weakly bound to the next sandwich layer by Van der Waals forces.

To clarify the underlying processes of stick/slip friction, the concept of surface deformation is examined. To keep in touch with the stick/slip we focus on the sticking phase. We assume that during this phase, the tip is rather tightly connected with the substrate surface. From this point of view, the scan process is considered as a mechanical surface test rather than an imaging process. For such testing, a full description of the cantilever mechanical properties is essential. Therefore a detailed analysis of the cantilever mechanical response is performed. This analysis is based on the set of moduli. The problem of partial visibility of the actual cantilever deformation by the optical detection system was circumvented by the implementation of modified (radial) scan patterns. The procedure can be considered as a lateral stiffness measurement of a part of the substrate surface, namely the nanometer sized area in contact with the tip.

Following this procedure, a marked and consistent difference in lateral stiffness was encountered between anisotropic, layered substrates and those having an isotropic, homogeneous structure. The isotropic materials, Si, NaCl, behave as rigid, whereas investigations on layered $MX_2$ materials, like $TiS_2$, $NbS_2$ and $CdI_2$ , yield a measured lateral stiffness of comparable magnitude as that of the cantilever itself, $\sim 10^{1\text{-}2}$ N/m. However, this is only the case as long as lateral deformations of the total system, *i.e.* cantilever-tip-substrate, are kept small, < 0.05 nm. Larger deformations cause a qualitative difference between the two material classes: the anisotropic materials perform like linear elastic springs up to the point that the tip snaps loose. Markedly different, isotropic materials display a creep like behaviour, resulting in a decreasing stiffness. The point of full rigidity seems linked to the turning points of the scan movement, not to the point of zero lateral force. It suggests irreversible atomistic processes occurring in the tip-substrate interface region.

The combination of cantilever calibration and stiffness measurement allows us to link the occurrence of stick/slip more directly to a surface parameter, *i.e.* stiffness of the contact area, instead of a bulk property (structure). A further interpretation was undertaken from this surface concept by proposing a simple surface 'sheet model'. In this model we account for different atomic bond stiffness in directions parallel and perpendicular to the surface. We explicitly do not assume a commensurate fit of the tip atomic surface structure to that of the substrate, as this proves to be not a necessary experimental condition either. Nevertheless, the model predicts that a nonzero friction force can exist as long as there is local bond deformation possible around the contact area. Furthermore, the difference or anisotropy between surface-parallel and perpendicular bonds promotes an increased correlation of bond strains in the whole contact area, which in turn makes a catastrophic, avalanche like bond breakage event probable. This explains the experimentally observed elastic straining and instantaneous slipping of the tip as observed on layered substrates.

1.4 *Analysis of Dislocation Structures in Tungsten Carbide* (P.A. Carvalho)

Conventional electron microscopy was used to study the microstructure of WC-Co hardmetals and to characterise dislocation structures found in tungsten carbide grains. WC-Co hardmetals are widely used in wear-resistant and cutting applications due to their unique combination of hardness and toughness, and a complete understanding of this exceptional mechanical behaviour can only be achieved through the

study of the microstructures and an analysis of the crystal defects present.

Tungsten carbide has a simple hexagonal crystal structure with $c/a$ = 0.976, space group $P\bar{6}m2$, with tungsten and carbon atoms in the following positions: 1(a) 000 and 1(f)⅔⅓½, respectively. The lattice parameters are $a$ = 0.2906 nm and $c$ = 0.2837 nm. The W-C distance is 0.2197 nm and only the tungsten and carbon atoms are in contact; there is no contact between the tungsten atoms in the basal plane.

Both the carbide grains and the binder metal presented signs of plastic deformation. The relatively high density of dislocations observed in the WC grains resulted from compressive stress states to which the hard phase was submitted during processing. The prismatic planes $\{1\bar{1}00\}$ were identified as the slip planes in the tungsten carbide grains and the most common slip system was found to be $\frac{1}{3}\langle 11\bar{2}3\rangle\{1\bar{1}00\}$.

The prismatic planes $\{1\bar{1}00\}$ were identified as the slip planes in the tungsten carbide grains and the most common slip system was found to be $\frac{1}{3}\langle 11\bar{2}3\rangle\{1\bar{1}00\}$. This is in agreement with information reported by other authors. Dislocations with a $\frac{1}{3}\langle 11\bar{2}0\rangle$ Burgers vector were also commonly encountered. The $\frac{1}{3}\langle 1\bar{1}00\rangle$ displacement vector, which is frequently found in close-packed hexagonal systems, was not observed. Figure 5 presents DF images of a WC grain obtained with different diffracted beams. The determination of the Burgers vectors was accomplished through the invisibility criterion.

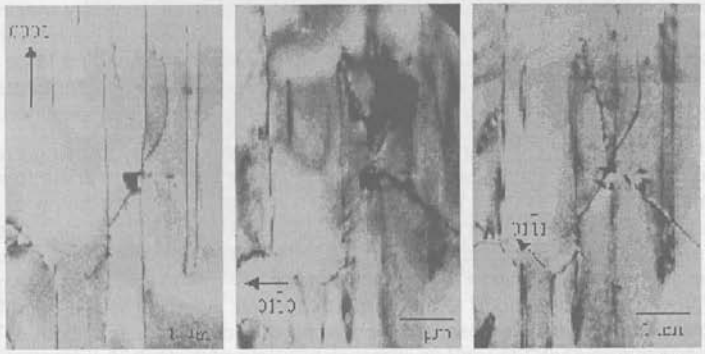

*Figure 5: Dark field TEM images of dislocations in a WC-Co grain obtained with a $[2\bar{1}\bar{1}0]$ beam direction: $\frac{1}{3}[\bar{2}113]$ dislocations are visible in (a), invisible in (b) and visible in (c); $\frac{1}{3}[11\bar{2}0]$ dislocations are invisible in (a), but visible in (b) and (c).*

2 *Interfaces between Metals/Ceramics: High Power Lasers* (J.Th.M. De Hosson, P.M. Bronsveld, B.J. Kooi)

2.1 *Surface Modification of Titanium with Lasers* (A.B. Kloosterman, P. Balke, J. de Boer, M. Gotink, S.R. de Vries)

In engineering applications the material demands often differ between bulk and surface. As a matter of fact, it is beneficial to select two different materials with the appropriate properties, for the bulk and the surface, respectively. Therefore, substantial effort has been devoted to the surface engineering area of research to apply coatings on a wide variety of substrates. This work concentrates on laser surface modification of light weight materials, in particular titanium, in order to enhance its wear

and corrosion resistance under conditions of high contact load.
Despite the numerous advantages of Ti, like the high strength to weight ratio and the excellent corrosion resistance, it exhibits poor tribological properties. Two different routes are presented to obtain a protective coating on Ti, which are aimed at producing a hard phase in a ductile matrix. The research is concentrated at processing control, thermal control and the explanation of both the microstructural features and the mechanical performance. The microstructure is studied in great detail by scanning and transmission electron microscopy. In addition, the novel Kikuchi backscatter technique is applied to obtain information concerning crystal structures in the SEM.

To explain the microstructural properties of the modified layer, it is necessary to know the temperature trajectory during laser processing. The maximum temperature attained is related to the occurrence of phase transitions and chemical reactions. Furthermore, high temperature gradients are involved during cooling down, which determine the size and type of the microstructural features. As the thermal expansion of the applied coating constituents and the substrate material differ, high thermal stresses arise during cooling down, which finally may result in crack formation. An analytical model is presented to predict the temperature profile depending on various process conditions. Therefore, the heat conduction equation is solved by using Green's functions. Temperature fields are calculated for different intensity distributions of the laser beam, possibly including a pulsed laser mode. The model takes into account the finite dimensions of the specimen. This is achieved by making use of image sources, which provide zero heat flux at the boundary. The relevance of image sources is indicated by a case study of Ti and Mo, which exhibit a large difference in thermal conductivity. Finally, a description is presented to incorporate heat loss due to convective and conductive cooling at the boundary of the specimen.

The first route to modify the surface of Ti concerns the laser gas alloying process. Diffusion of nitrogen takes place into the liquid Ti, which finally result in the formation of TiN and N-rich phases. The top layer consists of a thin TiN layer below of which TiN dendrites are present. The TiN top layer exhibits strong {100} texture, caused by the preferred heat transport along the ⟨100⟩ direction, and contained both structures of screw and edge dislocation. The equidistant edge type dislocations stem from cellular growth and correspond to the cellular interface. Adjacent to the dendritic region a plate-like structure is observed, consisting of a combination of both a-Ti and TiN. Inside predominant TiN regions in the plates, incorrect stacked regions are present in a way consistent with an array of $\frac{1}{6}\langle 112\rangle$ Shockley partial dislocations, forming a glissile interface between fcc and cph crystals.

During laser nitriding high thermal stresses will arise, which may induce crack formation. Therefore, the crack behaviour of the TiN laser tracks is studied. The crack frequency can be reduced by preheating the specimen or by using diluted nitrogen during processing. The latter mentioned reduces the number of links between the TiN dendrites, which is favourable with respect to the stress conditions. Furthermore, it is found that the crack frequency increases with increasing laser scan velocity. In order to explain this behaviour the temperature gradients are measured by an optical pyrometer. It is found that there is no significant change in gradient within the applied range of laser scan velocities. Therefore it is concluded that the crack formation is mainly caused by the thermal stress due to the different thermal expansion coefficients between Ti and TiN.

An alternative route is scrutinised to modify the surface of titanium using the laser particle injection process. This process is found to be very sensitive for the positioning of the powder injection, the interaction time of the particles with the laser and the amount of powder used. By changing the injection position in the negative x-direction relative to the laser beam, the time the particles spent in the liquid Ti decreases. In addition, the temperature of the region where the particles penetrate into the melt pool is lower. Both effects result in a decrease of the degree in which the injected particles dissolve in the matrix. As a consequence of the dissolution of SiC, new phases will be formed in the matrix, like the eutectic structure, strongly faceted $Ti_5Si_3$ grains and TiC dendrites. Furthermore, a reaction layer of TiC is formed around the SiC particle. The thickness of this layer increases with increasing interaction time and temperature. A distinction can be made between the relatively thin cellular and thick irregular type of reaction layer, which correspond respectively to growth of TiC from the SiC surface and from the melt towards the surface of SiC. The dissimilarity is caused by the different temperature conditions during solidification. The latter situation results in the presence of $Ti_3SiC_2$ plates in the reaction layer, which represents a ceramic with plastic-like behaviour (see Figure 6).

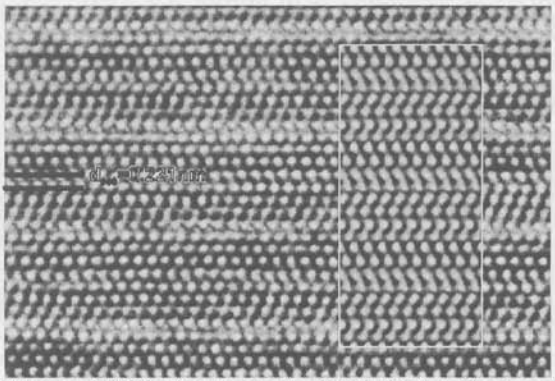

*Figure 6: HRTEM image of $Ti_3SiC_2$ viewed along the ⟨1120⟩ direction. The inset displays the simulated structure.*

The mechanical performance strongly depends on the degree of dissolution and the type of reaction layer. Therefore, hardness indentations are performed to examine the crack initiation and propagation behaviour. As the aim is to produce a hard phase into a ductile substrate, the dissolution of SiC should be minimised to avoid matrix embrittlement. This is confirmed by the ability to initiate cracks, which is found to be hard for small amounts of dissolution and can be explained by the high tensile strength of Ti-6Al-4V relative to the ceramic phases. In case of the cellular reaction layer the cracks propagate straight through this layer into the SiC particle without deflection at the interface. For the irregular reaction layer the cracks propagate along the pores and possibly deflect along the interface before penetrating into the SiC particle. The latter indicates a less good bonding between SiC and TiC, which is explained by the different growth mechanism of the irregular layer during solidification.
The modified layers are subjected to abrasive and sliding wear tests. The sliding wear tests under boundary lubrication conditions exhibit a specific wear rate close to or below 0.01 $10^{-6}$ $mm^3/Nm$ for both the laser alloyed and embedded type of layers.

Therefore, practical applications as bearing material should be within reach. In particular, the SiC particles in Ti-6Al-4V and the laser gas nitrided titanium coatings are promising.

2.2 *Analysis, FE-modelling and Design of Wear Resistant Coatings on Tool Steel* (T. Tinga)

This research project is part of the educational program for designer in materials science and technology. The research was aimed at improving the scientific insights in the relationship between the microstructure of the coating and properties on one hand and its performance on the other. The basic idea is to apply this knowledge to design an appropriate coating for specific application, *i.e.* in this case a wear resistant coating on deep-drawing tools.

The investigations consisted of two part: One part is an experimental analysis of a number of different coating, carried out in collaboration with TNO-industry in Apeldoorn, the other part consisted of finite element (FE) modelling of layered systems.

The coatings that are analysed are the ceramic coatings TiN and TiCN, diamond like carbon (DLC), DLC with an addition of W (WC/C) and a TiN coating with a $MoS_2$ layer on top. The wear test is a sliding test, in which a coated ring is sliding over a sheet of steel or aluminium in such a way that always virgin material is encountered. The sliding distance is measured over which the friction coefficient stays lower than a certain value. Afterwards the wear test rings are analysed with a scanning electron microscope. Combination of the wear test results and the microscopical analyses show that the TiN and TiCN perform very well, providing that a lubricant is used. The DLC and WC/C coatings are worn away layer by layer during the test, but the friction remains at a very low level, even when no lubricant is used. The TiN+$MoS_2$ performs very weakly, that is to say after only a half a meter of sliding the friction increases rapidly, probably because the $MoS_2$ layer is completely removed.

In combination with the FE modelling the effects of two design parameters are examined, namely the coating thickness and the ratio of the elastic moduli of the coating and substrate. Their effects are studied by looking at the shear stress at the interface and at the development of plastic strain. This provides some general design rules for the coatings. The effects of the various design parameters are the following: the plastic deformation decreases upon increasing the layer thickness, whereas a thick layer results in a relatively low value of the shear stress at the interface. Further, the shear stress at the interface decreases with decreasing ratio of the elastic moduli, layer vs. substrate. If this ratio lies between one and two the plastic strain seems to be minimised. The best coating for the underlying tool steel and applications is a well- bonded, thick DLC layer.

2.3 *Characterisation of Interfacial Fatigue in TiN PVD Tool Steels* (N.J.M. Carvalho)

During the last few years there has been an increasing interest in Titanium-nitrogen films deposited by physical vapour deposition methods. In this study TiN films were deposited on different tools steel substrates by a BAI 640R unit, using a triode ion plating (e-gun) with high plasma density.

The coated substrates are submitted to an interfacial fatigue test technique to obtain some clarification of the mechanism of rolling contact fatigue. This mechanism can be characterised by observation of plastic deformation in rolling contact, analyse of

growth of fatigue cracks and flakes, and measurements of fatigue durability under rolling contact. Analytical techniques including light microscopy, high resolution low voltage scanning electron microscopy and high resolution transmission electron microscopy in conjunction with parallel electron energy loss spectrometry are used to characterise the microstructure and the phase composition of the coatings.

The TiN coatings with a thickness of 5 μm have a dense morphology as can be seen in Figure 7a. Tests were run using PVD coated rings finished by polishing and grinding to produce different surface roughness. From the results it appears that the fatigue durability is at lower stress levels significantly influenced by both the pre-treatment and final surface roughness of the material. The polished and smoother surfaces are associated with longer life. However, at higher contact stress there appears to be very little influence of pre-treatment and surface roughness.

Two mechanisms of crack propagation under pure rolling conditions were found, depending of the hardness of the substrate. Figure 7b shows a micrograph for a lower substrate hardness where the cracks propagates perpendicular to the surface. This type of crack appears fairly frequently in this type of material. In a harder material, as shown in Figure 7c, the cracks generally originates above the interface and progresses parallel to the surface at a distance below it corresponding to the point of maximum shear stress. From these results if does appear that differences in micro plastic deformation most probably are responsible for the observable macro plastic deformation and fatigue behaviour differences of these two materials.

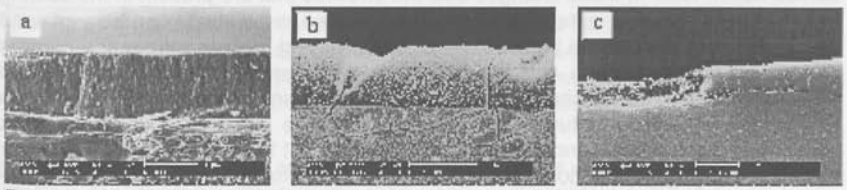


*Figure 7: Cross-sectional SEM micrographs of the coating-substrate interface. (a) region free of rolling contact; (b) coating on substrate hardness of 50 HRc. The crack propagation is perpendicular to the interface; (c) coating on substrate hardness of 60 HRc. The cracks first propagate parallel to the interface and then secondary cracks growth to the surface.*

2.4 *Bonding of Brittle Layers on a Ductile Metallic Substrate* (E. Zoestbergen; E. van der Giessen, G. de With [MIDEG])

The research is concentrating on TiN and Ti(C,N) PVD coatings on tool steel and TiN layers on hard metals. The coatings on tool steel were deposited onto substrates with three different surface roughnesses. For the TiN layers that are deposited onto a hard metal substrate the deposition parameters; the bias voltage and the concentration between Ti and N, were the variables.

For the samples the residual stresses, the texture and structure of the coating were investigated. This was done with the use of XRD, TEM and SEM.

For the coatings deposited on the tool steel all the samples have a one-degree {111} orientation. The surface roughness has a very small influence on the texture development. It is difficult to compare the results of the TiN with the results for the Ti(C,N) sample, as there is a large difference in the thickness of the coatings. For both systems there is however an influence of the surface roughness. Decreasing the surface roughness will increase the residual stresses in the coating. For the Ti(C,N) coating

there is also found that there exist a stress gradient in the coating.

The stresses in PVD coatings are usually made up out of two components. An extrinsic component, due to the differences in the expansion coefficients between the coating and the substrate. This introduces a tensile stress in the part with the highest expansion value and a compressive stress in the one with the lowest, when the system is cooled to room temperature. And an intrinsic part, which can be due to a lot off different reasons: chemistry (reaction Ti en O), microstructural changes below the growing area, and particle bombardment. The particle bombardment is a kind of atomic peening process. The deposit particles have a kinetic energy and will hide the coating, so the coating wants to expand, but this is restricted by the substrate. This introduces an additional compressive stress in the coating. This plays an important role during the deposition of PVD coating.

It is not yet clear why the surface roughness has an influence on the stresses that are present in the coating and what the driving force behind the stress gradient in the coating is.

The measurements done on the TiN coatings on a hard metal show that when then bias voltage is increased, the stresses increase. But that there is also a change in the texture. At low bias voltages, there is a two-degree {220} orientation, which a very rough surface where the {200} planes are the outside planes. At higher voltages the texture changes to a one-degree {111} orientation. Next to this the surface also becomes flatter. Next to these changes also the stresses that are present in the coating increase when the bias voltage is higher. The increase in the stress can be explained with the idea of the particle bombardment. By increasing he bias voltage the number of ions hitting the surface and their average kinetic energy will increase and the stresses will increase. In literature this idea of increasing strain energy is used, to explain the change in texture. The minimisation of the strain energy will dominate over the surface energy and the strain energy for a {111} texture TiN layer is lower then for any other orientation. This is, however, doubt full as for Cu layers, the texture also changes to a {111} orientation at higher bias voltages, but he strain energy for the {111} orientation is higher then for another orientation.

Changing the concentration between Ti and N also has an influence on the texture in the coating, by increasing the Ti concentration the texture changes from the two degree {220} orientation, to an one degree orientation with a tendency towards a {111} plane.

So to be able to explain the texture that is present in the TiN coatings it is not enough to look at one variable only. But is necessary to take all the deposition parameters into consideration.

2.5 *The Quality of the Surface Condition of Ground Inorganic Materials* (J.B.J.W. Hegeman; G. de With [MIDEG])

Grinding may influence the surface layers at the machined surface and therefore it may effect the mechanical and functional properties of the ground inorganic material. The relation between the processing parameters such as Wheel speed, infeed, depth of cut and the functional parameters such as residual stress, magnetic properties, induced damage and surface roughness is being investigated. The grinding process can be modelled using the superposition of multiple scratches of the abrasive grains on the surface. The single elasto-plastic scratch of one abrasive grain on

the surface, including chip formation, can be used as a building block of the statistical model.

The aim of the project is to postulate a model that describes the grinding process and which can be used to optimise the grinding process. The model will experimentally be verified

The grinding experiments have been performed using a D213 C75 MN790, ∅ 200 mm grinding wheel. For different wheel speeds, sample speeds and cooling conditions the residual stress states and the surface condition was analysed using X-ray diffraction, SEM and AFM. From Figure 8 it can be concluded that the grinding mechanism for ferrite is mainly by cracking and for WC-Co, the material is mainly removed by plastic deformation and pull out of WC grains.

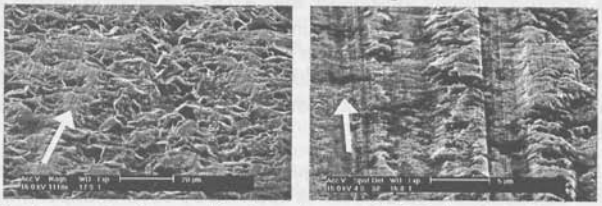

*Figure 8: SEM micrographs of ground ferrite and ground WC-Co hardmetal from an angle of 70°. From the micrographs the fractal surface of ferrite and the deformed surface of WC-Co can be shown (the arrows show the grinding direction).*

AFM can be used for roughness analysis of the ground surface. The samples that were cooled during the grinding experiments show a lower roughness than the surfaces that were ground without cooling. Because of the heat the material will be softened. The abrasive grains on the grinding wheel will remove more material, leaving deeper traces.

X-ray stress analyses show an increase in residual stress state after grinding. Before grinding, the (thermal) stress in the WC grains of the sintered WC-Co samples is −1373 ± 60 MPa. After grinding the stress is on average −2205 ± 57 MPa. No correlation's between the wheel speed, table speed and the residual stress are found yet. It should be noted that the residual stress state of the samples that were ground without cooling is much lower −1625 ± 97 MPa. Probably the local heat has a stress relieving effect on the surface.

Cross sections of the ground samples will be analysed for dislocation structures and crystal defects near the surface using TEM. Also the stress will be measured in cross section.

2.6 *Segregation and intergranular fracture* (D.T.L. van Agterveld)

The current project started at the end of 1997 and will focus on *in situ* fracture experiments and accompanying segregation at the fracture surface in UHV-SEM/SAM. Segregation and interphase formation at metal/ceramic interfaces are of great technological importance, because they have large influence on the properties, *e.g.* the strength and interface toughness. Also from a scientific point of view it is a great challenge. For instance an atomistic study on segregation on metal/ceramic interfaces and its influence on orientation relations between metal and ceramic, relative stability of the various facets existing between metal and ceramic, defect structure

near and at the interface, particularly the network of misfit dislocations by performing HRTEM have not yet scrutinised. However, due to the indirectness and difficulty to obtain chemical information in the JEOL 4000EX/II equipped with PEELS on a very local scale (*e.g.* via comparison with image simulation), other analytical techniques which can accurately provide chemical information on segregation would be essential.

Requirements for such an analytical technique is not only a high surface sensitivity, but a high spatial resolution and possibility to prepare samples, *e.g.* by breaking, in ultra-high vacuum. Then, after cleavage of the specimen in UHV, analysis with high depth and lateral resolution can be performed near/at the metal/ceramic interface. Technique thought to be most suited for this task is a UHV Scanning Electron microprobe (SEM) which is directly integrated with a UHV Scanning Auger microscope (SAM). An electron beam as excitation source can be focused well and in a state-of-the-art SAM a lateral resolution of 15 nm is achieved at low acc. voltage (with a depth resolution of typically 4 nm, but with a predominant weight on the outmost monolayer) and in the SEM mode due to lower currents even 5 nm can be achieved at low acc. voltage.

The principal cause for concern is the question if interfaces are indeed close to thermodynamic equilibrium. This concern is sparked by several experimental results. In some metal-oxide systems that have been prepared by various methods, *e.g.* Cu-MgO, the resulting orientation relations and interfaces were found to be different . Also for Nb-$Al_2O_3$, a system that very often forms with the same orientation relation, an interface was found with different atomic structures. The structure of a vapour deposited sample and a diffusion bonded sample differed, but there were also differences between apparently equally treated vapour deposited samples. In general metal-oxide interfaces are not stable and may undergo diffusional reactions. These reactions are thought to be of major technological importance. Segregation of impurities, mutual dissolution and interphase formation may occur. The reaction products are difficult to predict as the kinetics rather than the equilibrium phase diagram dominate.

In this case and, as a matter of course, in the case of segregation and interphase formation concentration gradients can be expected locally which can be determined well with UHV-SEM/SAM by performing line scans and depth profiling on surfaces fractured in UHV and on cross sections. Depth profiles can be obtained destructively via ion sputtering and non-destructively via angular-resolved measurements. With a high energy resolution information about chemical environment of element probed can be obtained. Performing EDS in the UHV-SEM/SAM can also benefit from the small diameter of the electron beam, but the analysis volume probed can never effectively be reduced to the small size as for SAM. Segregation studies have been performed for almost 25 years, but hardly on metal/ceramic interfaces and in conjunction with high resolution microscopy and atomistic calculations. Needless to say that UHV SEM/SAM can be very useful for the other studies performed by us on interfaces between similar and dissimilar materials, ranging from metal/ceramic to ceramic/ceramic

3 *Interfaces in Nanoceramics and Technical Ceramics: LV-HRSEM, X-rays* (J.W. Hooijmans, J.Th.M. De Hosson)

3.1 *Densification of Nano-Ceramics* (R. Popma; in collaboration with Philips Research)

A large part of the work was related to the analysis of the sol-gel layers. This enhances the description of the layer and the interaction layer-substrate. Also crystal phases in the coatings have to be recognised and the stress present in the layers has to be measured. At the start of the project the work has been concentrating on silica, titania and alumina based sols. Later work has also taken into account zirconia sols. Samples tested were made by Philips-CFT, Sandvik and ISC.

The description of the sol-gel coatings is done using a scanning electron microscope (SEM). Used is the Philips XL30S FEG SEM, which is equipped with a special electromagnetic lens, which can deal with the magnifications necessary to make images of the particles in the coatings. Unfortunately charging and contamination of the sample takes place when using the SEM, and as a result all specimens have to be sputtered with a very thin palladium layer before any examination can be made. The palladium islands on the samples, created by the sputtering make interpretation of the images harder. A way to prevent this, either by using cleaner samples or by sputtering thinner coatings, needs to be found.

The crystal phases and stresses were determined using XRD.

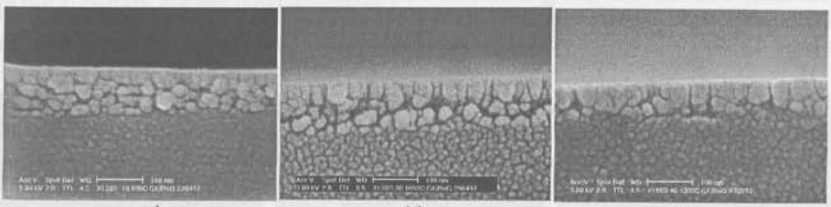

a) b) c)

*Figure 9: Furnace treated $Al_2O_3$-sol coating on quartz. a) 700°C/ 30 min., $d_0$ = 100 nm b) 1100°C/ 30 min., $d_0$ = 100 nm c) 1300°C/ 30 min., $d_0$ = 100 nm*

Most work on sintering of sol-gel layers until now has been carried out with quartz as substrate. The quartz substrates coated with an alumina sol ($Al_2O_3$, supplied by Merck) and both furnace and laser treated, were systematically investigated. The furnace-cured sample underwent a treatment of 30 minutes with temperatures of 700, 900, 1100 and 1300 °C. Figure 9 shows SEM images of furnace treated samples. In the figure, $d_0$ represents the original coating thickness.

The images show a great similarity between different samples: in all situations, the top 40 to 60 nm of the alumina coating appears to have densified. An increase in the depth with increasing temperature can be found, but is not very distinct. The part of the layer lying underneath still consists of not-sintered, 20 nm, $Al_2O_3$-spheres. This is true for all layer-thicknesses.

Almost no complete densification has been obtained. Only one coating shows nearly complete densification: the 100 nm thick layer, treated at 1300 °C. Probably, either longer heating treatments or higher temperatures should be used to complete sintering throughout the coating.

The laser treatment of alumina on quartz resulted in a variety of results. In Figure 10 the SEM images of the results are shown, with again $d_0$ the original coating thick-

ness. With high heat input there is no coating visible. The coating seems to delaminate from the substrate because of the intense treatment. With low heat input no densification is apparent. The laser treatment has had no impact, but for some shrinkage. With intermediate heat input the coating seems to be sintered at some places, but at other places blisters have been formed or the coating delaminated from the substrate.

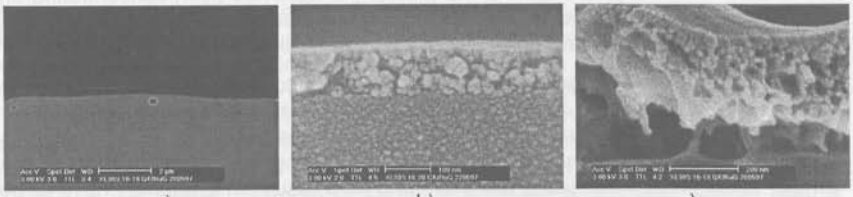

a) b) c)

*Figure 10: Laser treated $Al_2O_3$-sol coating on quartz. a) 25 W/ 800 mm/s, $d_0$ = 500 nm b) 25 W/ 2700 mm/s, $d_0$ = 100 nm c) and d) 25W/ 1800 mm/s, $d_0$ = 500 nm*

The zirconia samples reacted differently. It was much easier to make good layers. In most cases a densified layer was formed after laser sintering. When the heat input of the laser was too low, the grains were very small and the layer seems to be very loosely attached to the substrate. When the fluence increases the layer seems to be sintered more, but the layer is very easily separated from the substrate (see Figure 11).

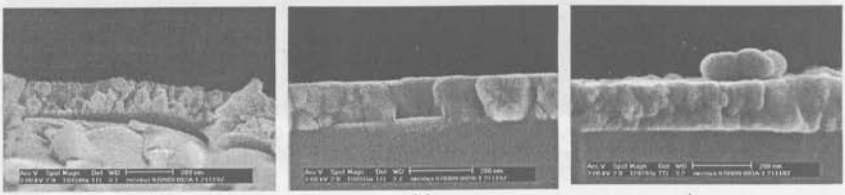

a) b) c)

*Figure 11: Laser treated $ZrO_2$-sol coating on quartz. a) 100 W/ 150 mm/min., $d_0$ = 450 nm b) 100 W/ 75 mm/min., $d_0$ = 450 nm c) 80 W/ 37 mm/min., $d_0$ = 420 nm*

Only with a high fluence a completely sintered layer is formed which is very well attached to the substrate. But it still seems difficult to repeat the results obtained.

Because the maximum thickness of the zirconia layer is 150 nm, work has been done to find better sol-gels which can form thicker layers. As a result hydrothermally treated zirconia was developed. With this hydrothermally treated zirconia layers of 300 to 500 nm seem to be possible.

*Phase identification and stress measurements*

A suitable method to determine whether the coating is crystalline or not, is provided by the use of X-ray diffraction. Beside phase identification, more information can be obtained by using X-ray diffraction, as grain size and texture. Also residual stress measurements on the sol-gel coatings can be carried out.

The phase identification of the alumina sols was not possible. Until now no peaks were found. This is the case for both the furnace treated as with the laser treated samples. Also furnace treatment of alumina sol-gel on cemented carbide did not re-

sult in any crystal phase. It is still not clear why no crystal phases seem to be formed or whether the measurements are not sufficient.

In the case of zirconia all samples seem to crystallise. There are three crystal phases possible: monoclinic, tetragonal and cubic. Both monoclinic (the regular low temperature phase) as cubic crystal phases were determined, but it is still not clear what influences the formation of the two phases. Only in the case of hydrothermally treated sol the layer seems to be crystallised for a large extend.

Stress measurements were until now only possible with furnace treated titaniumoxide. Only then the peaks are high enough to make any realistic measurements. In the case of alumina and zirconia no measurements were done until now. The results with hydrothermally treated zirconia sol indicate that stress measurements on these layers is a possibility.

*Temperature model for a finite, laser treated, sol-gel coated sample*
Temperature modelling of laser treated sol-gel coatings is performed to make a comparison between laser and furnace treatment in sol-gel processing. The model developed is applicable for finite laser treated sol-gel coated silicon substrates. A number of assumptions have been made, from which the neglect of the absorption of the layer and the assumption that the coating has the same temperature as the top of the substrate are the most important.

3.2 *Engineering Ceramics and Thermal Stresses* (D.H.J. Teeuw, B. Cordia, M.J. de Haas, J. Kinds)

In this work the relation between processing and residual stress states in ceramic materials is studied. Various materials are considered, bulk ceramics derived from powder compacts as well as thin ceramic layers derived using a sol-gel technique. The influence of the processing techniques on the eventual residual stress state of the material is studied.

Material properties may be altered by microstructural modifications. This holds for a large range of materials, metals as well as ceramics. In this work, the influence of a second phase added to a homogeneous matrix is studied. The addition of $ZrO_2$ to an $\alpha$-alumina matrix increases the fracture toughness of the composite ceramic with 160%. The increase in toughness is achieved through the tetragonal to monoclinic phase transformation which takes place upon cooling of the specimen, or is induced by high tensile stresses ahead of a crack tip.

The addition of a second phase in a matrix also is a means for tailoring the final particle distribution of the material. Grain growth is controlled by dispersed second phase particles through the forces these particles exert on moving grain boundaries in the matrix. Addition of a second phase leads to a grain size in the matrix controlled through the radius of the second phase particles and the volume percentage added. The measured grain sizes in the specimens studied correspond well to the expected limited grain sizes in the matrix.

Diffusion bonding the two-phase ceramic layer to a layer of homogeneous $\alpha$-alumina is performed using different processing routes. A method to derive these specimen is to mould and sinter the specimen in one process. The precursor powders are pressed simultaneously and consequently sintered to high relative densities. A problem using this approach is the difference in shrinkage during the sintering process,

resulting in debonding of the two layers. Therefore, an alternative approach is used in which the layers are formed separately. These layers are then pre-sintered, hence pre-shrunk, and consequently placed in contact and sintered to high relative densities.

Problems encountered in this process are stresses arising in the specimen as a consequence of dissimilar shrinkage upon cooling of the specimen induced by differences in thermal linear expansion coefficients of both layers. The thermally induced stresses are calculated using analytical as well as finite elements methods. The finite elements approach provides insight in the total residual stress state of the specimen, whereas the analytical approach yields values for the maximum expected stresses across the interface. Both methods indicate that the two-phase layer, exhibiting a larger thermal linear expansion coefficient, is in tension after the curing process, and the homogeneous layer is in compression. The magnitude of the evolving stresses are typical of the order of ~50-100 MPa. In the bulk of the specimen the radial and tangential stress components are equivalent in sign and magnitude, at the free edges the radial component can not be sustained by the free surface and drops to zero. The tangential component, however, reduces in magnitude but a gradient is still present over the interface.

The determination of the residual stress state in the samples using x-ray residual stress analysis, requires for the x-ray elastic constants to be known. For typical applications, it is appropriate to use the macroscopical materials properties, Young's modulus and Poisson's ratio. Since the x-ray elastic constants for the two-phase material are unknown, they are determined experimentally using an especially designed *in situ* loading device. In contrast to experimental methods commonly used, employing a tensile loading state, here a device is constructed in which the material is stressed compressively. The advantage of this loading mode is that the material under investigation is in uniaxial compression. For materials exhibiting brittle like crack behaviour, the compressive mode enables the loads to reach values higher compared to experiments performed in tension. Experimental determination of the x-ray elastic constants for ceramics may thus be performed over a range of stresses larger than when using a tensile loading mode, resulting in more accurate values. The uniaxial character of the stress state secures that no corrections to the measured lattice strains are required. The x-ray elastic constants for the $\alpha$-alumina compare to the determined constants for the two-phase material.

In the determination of the residual stress fields in the composite ceramic products, the experimentally derived x-ray elastic constants are used. The residual stress fields measured throughout the samples compare well to the stress values evaluated using finite element methods. At the locations of interest, *i.e.* the interface, the comparison between measured and calculated is best. Using an alternative approach for residual stress determination , the hole drilling evaluation technique, delivers similar results as the x-ray stress analysis method.

Sol-gel derived thin ceramic layers are studied using various techniques. Scanning electron microscopy is used to reveal the microstructure and morphologies of the layers. The differences in curing processes appeared to dictate the final morphologies of the layers. For the $TiO_2$ layers grain growth is observed for the furnace as well as the laser cured layers. The activation energy for grain growth of these layers is determined and corresponds to other studies concerning these type of sol-gel lay-

ers. Furnace curing the ceramic layers results in dense layers.

X-ray diffraction methods are used to evaluate crystallisation and stress evolution in the $TiO_2$ layers. For the various cured specimen it proved that the as spun layers are amorphous. They crystallise during the heat treatment, provided that the curing temperatures and times suffice for crystallisation to take place. For the furnace cured specimen, the temperature at which crystallisation is observed is 700 °C. Increasing the curing temperature to 900 °C and 1200 °C, respectively, results in further crystallisation of the layers and a transformation from the anatase to the rutile phase takes place. Using x-ray residual stress analysis, the residual stress state is determined for specimen which experienced dissimilar heat treatments. The stress values in the specimen are compared to the expected stresses which arise as a result of thermal expansion misfit in the layers. From this comparison it is concluded that the stresses in the layers are thermally induced.

Tensile stresses evolve in the layers during the spinning and drying stage. Due to capillary forces as a result of the evaporation of liquids in the solid network, tensile stresses evolve in the layer. This results in cracks in the layers. For the highly porous layers a model is derived which describes the thickness of the layer in terms of the crack resistance factor. A crack pattern is expected for layers of various thicknesses, depending on this thickness. Thick layers, that is for $Al_2O_3$ layers thicknesses exceeding 500 nm, are expected to delaminate, layers with lower thicknesses will exhibit channelling crack like behaviour. For layers of low thickness, typical below 200 nm, only sub-micron sized surface cracks are expected and observed in the layers.

3.3 *Surface Engineering with High Power Lasers* (J.A. Vreeling)

The main target of this project is to improve the corrosion resistance and mechanical properties of metals by producing clad layers of hard and chemically inert (ceramic) materials. The lifetime of machine parts, made out of steel and operating in acid environment, is reduced by high corrosion. In this research we concentrate on protecting Duplex steel against phosphoric acid at higher temperatures. Duplex stainless steels have high chromium content (± 25 wt.%) and low amounts of nickel (± 7 wt.%) and generally contain molybdenum and manganese. The microstructures of Duplex are approximately 50% ferrite and 50% austenite. Therefore, Duplex combines the features of these two phases.

It turns out that SiC is the only corrosion resistant material against phosphoric acid at 573 K. So, a poreless SiC coating on Duplex steel will extend the lifetime of Duplex machine parts, operating in phosphoric acid at higher temperatures.

A high power YAG laser is used to clad the corrosion resistant and hard coating on Duplex steel substrates. An advantage of using a laser is the possibility of producing a coating on a complicated shape such as a cog. Another advantage is that laser-cladded layers can have thicknesses up to several hundreds of micrometers.

In the laser-cladding process the laser melts the upper layer of a substrate while simultaneously a powder of the desired coating is added into the melt pool. In this process there are many important parameters like laser power, scan velocity, powder feed rate, position of particle injection with respect to the laser beam and characteristics of the cladded powder. These parameters and the properties of the materials involved determine the quality of the coating. The quality depends on the purpose of the coating. Generally, a measure of the quality can be the thickness, adhesion, po-

rosity, crack formation and dilution. Dilution is a measure of the amount substrate elements dissolved into the coating during the melting process.

The problem we have to deal with is the fact that SiC dissolves into the Duplex steel matrix. A possible solution is to make use of an intermediate layer of another material like Ti or Ni. This intermediate layer has to form a separation between the steel matrix and the SiC coating, so SiC cannot dissolve into the matrix.

Another possible solution is adding a second powder in the laser-cladding process. Cladding both SiC and Ti results in deformation of SiC and formation of high amounts of TiC. This layer, consisting of TiC particles in Duplex steel, is also a possible intermediate layer. Producing a dense TiC layer with additionally cladded SiC particles will be the first step towards the desired corrosive resistant coating.

Another target is to get a better understanding in the melt and solidification processes during laser treatment. In the laser-cladding process the temperature of the upper layer of the substrate and powder is quickly increasing and subsequently decreasing. These abrupt melt and solidification processes cause interesting microstructures and phase changes. Also chemical reactions can occur when the elements of the powder react with elements of the substrate. Both Scanning and Transmission Electron Microscopy are used to study these phenomena.

3.4 *Mesoscopic Materials Science: Computer Modelling* (J.W. Chung; E. van der Giessen [MIDEG])

The modelling work is aimed at finding a relation between the mechanical strength of porous media and its microstructure. In previous investigations we have used 2-D and 3-D lattice models, *i.e.* artificial networks of linear springs that in a loose sense attempt to incorporate the microstructural stiffness. In such models, there is not a direct physical relationship with the actual microstructure; the sole purpose of the models is to mimic the stochastic heterogeneity of porous materials at the size scales of individual pores. In previous work we have used geometrically regular networks where all elements had identical properties. In this project, we will extend these models to investigate the effects of random geometry and/or of variable (stochastic) material properties of the elements.

In addition to these 'stochastic' models, the project is aimed at developing an alternative, more 'deterministic' model in which there is a more direct relationship between the elements of the model and the porous microstructure. This will allow for more or less direct mapping of the random geometric cellular structure as observed experimentally to the network properties. The more 'deterministic' models seem to be essential to study local deformation mechanisms in porous solids. Aspects that can be studied include the effects of residual stresses and possible plasticity in the ligaments. Also they will allow for a detailed study of the influence of pore shape etc. which cannot readily be accounted for in the existing network models.

Our current attention is focused on the ultimate strength of porous materials, and the influence of the size scale. For a more complete understanding of the failure process, fundamental insight in the actual failure development (percolation of microcracks) in the course of the process is needed. Does failure occur in a rather localised region, leading to a sharp propagating crack, or does failure occur more in the form of spatially diffuse damage? And what is the relation with the observed size scale effect? Little is known in general for porous materials. Lattice models poten-

tially offer interesting possibilities to simulate this process on the appropriate mesoscopic scale. In this course of this project we hope to be able to generate some more fundamental knowledge on these matters.

The ultimate aim is to develop models spanning a length scale from 5-200 nm (pore size diameter) to single extrudates (length 1 cm and 1 mm in diameter) to agglomerates of extrudates (bulk). Typical bulk model properties are: length distribution of the extrudates, bending distribution of the extrudates and reactor shape contributions. As a start we will use overlapping spheres to represent our extrudates on macro length scale. Our mesoscopic model uses dynamical Lennard-Jones system to generate a correlated sphere distribution. The sphere configurations will be converted into a 3-Dimensional spring network. The bulk model uses a set of macro-model extrudates in a box. The system will be generated by dynamical densification of a randomly oriented extrudate. This will generate a configuration distribution of how extrudates are positioned in a reactor. At the moment we are investigating a mesoscopic model using a dynamical mode to generate a distribution of 10 000 sphero-cylindrical particles to represent the extrudates. In the description the attractive and the repulsive part of the particles are parametrised and monitored.

Finally, the new methodology will be extended to study the size effect of non-homogeneous systems as well, *i.e.* systems that contain two different sets of elastic constants. Further the geometric networks considered will also be analysed by computational structural mechanics techniques, especially the finite element method. The important difference with the present approach from a computational point of view, is that these finite element methods involve a more efficient method to incorporate bending and torsion, but the number of degrees of freedom in a given network is twice as large as in the present approach. These aspects have to evaluated in more detail.

4 *Dislocation Dynamics in Metallic Systems: Modelling and NMR* (J.Th.M. De Hosson)

4.1 *Dislocation Dynamics at High Strain Rates* (A. Roos; E. van der Giessen [MIDEG])

In 1997, the equations for the stress and displacement fields of fast-moving dislocations have been implemented in a computer program in collaboration with Van der Giessen en Cleveringa. These equations are needed for the description of the formation of shear bands. The code has been optimised for speed, and new visualisation programs have been created in order to be able to assess the output of the simulations.

In the simulations the attention is focused on the formation of dislocation pile-ups, in the process of which the dislocations are allowed to achieve high velocities. The maximum velocity is the velocity of sound in the material, or the shear wave velocity. As a result, the dislocation stress and displacement fields transform according to a Lorentz transformation, in an analogous fashion as in special relativity.

The total stress state is decomposed into a contribution from the finite linear elastic body and a complementary contribution arising from discrete dislocations in an infinite medium. From the simulations it is seen that at very high strain rates the dislocations do indeed reach the high velocities that significantly alter the stress and dis-

placement fields locally. However, the number of dislocations that do so is small, even at high strain rates and low obstacle densities. The overall stress-strain curve, which is calculated by averaging over the top- and bottom surface, is therefore not influenced significantly by the local changes.

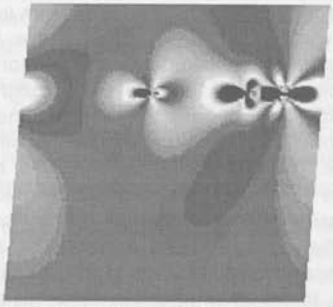

*Figure 12: Calculated interacting stress fields $\sigma_{xy}$ between moving edge dislocations*

At the tip of the pile-up, the local stresses can reach high enough values in order to initiate a microcrack. Simulating the formation of pile-ups at high strain rates can yield insight into where and under what conditions these cracks are formed. The influence of the relativistic stress fields on the stress state at the tip of the pile-up is investigated. The exact dependence is not clear yet, but locally the fast-moving dislocations can affect the stress state significantly. At high dislocation velocities, the processes that damp the dislocation motion change in character and magnitude. Phonon damping, for instance, will play a dominant role. Dislocation pinning by point defects (Cottrell atmosphere), which is the dominant term at low velocities, will be rendered inactive. This is due to the fact that the interaction time for the point defects to move to the dislocation core is too short. Furthermore, the gradients of the fields, along which the defects migrate, are no longer leading to the core of the dislocation.

Analysis of the physical damping mechanisms has led to a new drag relation. This drag relation closely resembles the Gillis/Gilman/Taylor drag relation, which is usually postulated in order to keep the dislocation velocities below the speed of sound.

A part of the research focuses on the interaction between dislocations and different types of obstacles and nucleation sites. For example, the interaction with forest dislocations is fundamentally different from the interaction with (shearable or non-shearable) precipitates or grain boundaries. Nucleation sites can generate dislocations in pairs of opposite signs (Frank-Read sources), or a single dislocation (at a grain boundary). Dislocations can also be generated by small local fluctuations of the bare lattice at very high velocities, due to the change in sign of the dislocation fields at the slip plane. These effects can have a profound influence on the movement of dislocations, and therefore on the total deformation. At this moment, the computer programs are being augmented to be able to take them into account.

The damping of dislocation movement results in a transformation of mechanical energy into heat. Due to the short time span in which the process takes place, the heat is confined to a very small region (before it spreads by thermal conduction to other regions of the material). The temperature may rise several hundreds of degrees (K) locally, and sometimes even reaches the melting point. The temperature rise softens

the material, thereby promoting strain instabilities, such as a shear band.
The methodology of discrete dislocation plasticity lends itself well for coupling to the thermal field. Work is being done in order to obtain a precise model in which the effect of temperature can be captured on a mesoscopic level.

4.2 *Dislocation Dynamics in Metallic Systems using Nuclear Magnetic Resonance*
(in collaboration with O. Kanert [University of Dortmund])

Critical strain to serrated flow in solid solution alloys is due to strain-induced vacancy production. The dynamical behaviour of point defects in metals is usually characterised by investigating annealing kinetic following extensive cold work. The recovery of induced plastic deformation is monitored using various techniques such as electrical resistivity, positron life times, perturbed-angular correlation, Mossbauer spectroscopy, ultrasonic attenuation, etc. In contrast to these two-step experiments, it is desirable to be able to investigate this kinetics *in situ* during deformation of materials in a single step. The plethora of non-destructive experimental techniques notwithstanding, very few of them are useful in the investigation of the dynamical properties of these defects. This is in particular true in the investigation of the diffusion of point defects and the motion of dislocations.

Nuclear magnetic resonance (NMR) techniques can be used to monitor *in situ* the dynamical behaviour of both point defects and dislocations during deformation, and these techniques are non-destructive and non-invasive. A new NMR pulse sequence method was developed and tested allowing an accurate evaluation of the strain-enhanced vacancy diffusion and consequently the excess vacancy concentration during deformation as a function of strain, strain rate and temperature. Due to skin effect problems in metals at high frequencies, thin foils of Al were used. The experimental results were correlated with models based on vacancy production through mechanical work (vs. thermal jogs), while *in situ* annealing of excess vacancies is noted at higher temperatures. These correlations made it feasible to obtain explicit dependencies of the strain-induced vacancy concentration on test variables such as strain, strain rate and temperature.

The experiments were performed on Al foils (skin effect). The choice is based on the fact that it is a very suitable nucleus for magnetic resonance studies. In addition the thermal vacancy concentration is well established and the dynamic strain ageing studies of aluminium alloys have been prevalent. In addition the effect of stress on the activation energy for creep has been widely studied to drive the strain and strain-rate effects on non-equilibrium vacancy concentrations.

PUBLICATIONS

J. Aué
*Fractals and Fracture*
Ph.D. thesis, University of Groningen (1997) 126

J. Aué, J.Th.M. De Hosson
*Influence of atomic force microscope tip-sample interaction on the study of scaling behavior*
Applied Physics Letters. 71/10 (1997) 1347-1349

R. Beye, M.G.M. Verwerft, R. Gronsky, J.Th.M. De Hosson

*Characterization of Novel Ti-A Al-O phases*
Acta mater. 44 (1997) 4225-4233

P.M. Bronsveld, Y.G. Wang, J.Th.M. De Hosson, B. Djuricic, D. McGarry, S. Pickering
*About boehmite and beyond: the transition aluminas revisited*
In: 5th European Conference on Advanced Materials and Processes and Applications - Materials, Functionality & Design (EUROMAT 97), The Federation of European Materials Societies (1997) 73-76

J.Th.M. De Hosson
*Metals and Alloys*
In: S. Amelinckx (ed.), Handbook of Microscopy, Chapter 1.1, Verlagsgesellschaft m.b.H., Germany (1997) 5-111

J.Th.M. De Hosson, J.L. De Mol van Otterloo
Surface engineering with lasers of co-base materials
In: M.H. Aliabadi, C.A. Brebbia (eds.), Third International Conference on Computer Methods and Experimental Measurements for Surface Treatment Effects Surface Treatment 97, Surface Treatment, Computational Mechanics Publications, Southampton, UK / Boston USA (1997) 341-359

J.Th.M. De Hosson, J.L. De Mol van Otterloo, B.M. Boerstoel, A.J. Huis in 't Veld
*Surface engineering with lasers: an application to Co-base materials*
In: 5th European Conference on Advanced Materials and Processes and Applications - Materials, Functionality & Design (EUROMAT 97), The Federation of European Materials Societies (1997) 85-90

J.Th.M. De Hosson, W.P. Vellinga, H.H. Groen, B.J. Kooi
*Metal-ceramic interfaces studied with high-resolution transmission microscopy*
In: 5th European Conference on Advanced Materials and Processes and Applications - Materials, Functionality & Design (EUROMAT 97). The Federation of European Materials Societies (1997) 11-16

J.L. De Mol van Otterloo, J.Th.M. De Hosson
*Microstructural features and mechanical properties of a cobalt-based laser coating*
Acta mater. 45/3 (1997) 1225-1236

J. Kerssemakers
*Concepts of interactions in atomic force microscopy*
Ph.D. thesis, University of Groningen (1997) 165

J. Kerssemakers, J.Th.M. De Hosson
*A quantitative analysis of surface deformation by stick/slip atomic force microscopy*
J.Appl.Physics. 82/8 (1997) 3763-3770

A.B. Kloosterman, J.Th.M. De Hosson
*Cellular growth and dislocation structures in laser nitrided Titanium*
J.Mat.Sci. 32 (1997) 6201-6205

A.B. Kloosterman, J.Th.M. De Hosson
*Ceramic particle injection during laser treatment of Titanium*
In: M.H. Aliabadi, C.A. Brebbia (eds.), Third International Conference on Computer Methods and Experimental Measurements for Surface Treatment Effects Surface

Treatment 97, Surface Treatment, Computational Mechanics Publications, Southampton, UK / Boston USA (1997) 287-294

A.B. Kloosterman, J.Th.M. De Hosson
*Solidification structures in TiN laser coatings*
In: 5th European Conference on Advanced Materials and Processes and Applications - Materials, Functionality & Design (EUROMAT 97), The Federation of European Materials Societies (1997) 161-164

B.J. Kooi, J.Th.M. De Hosson
*$Mn_3O_4$ precipitates in Ag and Cu studied with HRTEM: orientation relations and tetragonal twinning*
In: 5th European Conference on Advanced Materials and Processes and Applications - Materials, Functionality & Design (EUROMAT 97), The Federation of European Materials Societies (1997) 17-22

B.J. Kooi, H.B. Groen, J.Th.M. De Hosson
*Atomic structure of interfaces between $Mn_3O_4$ precipitates and Ag studied with HREM*
Acta mater. 45/9 (1997) 3587-3607

B.J. Kooi, H.B. Groen, J.Th.M. De Hosson
*Misfit dislocations at Ag/$Mn_3O_4$, Cu/MnO and Cu/$Mn_3O_4$ interfaces*
Acta mater. 46 (1997) 111-127

W.F. Oele, J. Kerssemakers, J.Th.M. De Hosson
*In-situ generation and atomic scale imaging of slip traces with atomic force microscopy*
Rev.Sci.Instrum. 68/12 (1997) 4492-4497

G.D.W. Smith, A. Cerezo, S.J. Sijbrandij, T.J. Godfrey, P.J. Warren, F.M. Venker, J.Th.M. De Hosson
*Applications of a high-resolution three dimensional atom probe*
In: 5th European Conference on Advanced Materials and Processes and Applications - Materials, Functionality & Design (EUROMAT 97), The Federation of European Materials Societies (1997) 5-5

D.H.J. Teeuw
*Engineering ceramics and thermal stresses*
Ph.D. thesis, University of Groningen (1997) 165

W.P. Vellinga, J.Th.M. De Hosson
*Atomic structure and orientation relations of interfaces between Ag and ZnO*
Acta mater. 45/3 (1997) 933-950

W.P. Vellinga, J.Th.M. De Hosson, V. Vitek
*Misfit dislocations: An atomistic and elastic continuum approach*
Acta mater. 45/4 (1997) 1525-1534

## MECHANICAL BEHAVIOUR OF MATERIALS

Delft University of Technology, Laboratory of Materials Science
Rotterdamseweg 137, 2628 AL Delft
phone +31 (15) 2785418/2782235, fax +31 (15) 2786730, e-mail ...@stm.tudelft.nl

### PERSONNEL

*Scientific staff*

| | |
|---|---|
| prof.dr.ir. A. Bakker | (2785418, A.Bakker@...) |
| dr.ir. M. Janssen | (2785866, M.Janssen@...) |
| A.R. Wachters, B.Sc. (0.8) | (2782244, A.Wachters@...) |
| dr.ir. J. Zuidema | (2782208, J.Zuidema@...) |

*Graduate students*

| | |
|---|---|
| ir. P.C.H. Ament (STW) | |
| C.H.L.J. ten Horn (from 15-7-1997, DIOC 10) | (2784765, C.H.L.J.tenHorn@...) |
| ir. A.H.M. Krom | |
| ir. K.M. Mussert | (2782229, K.M.Mussert@...) |
| ir. G. Pape (STW) | (2784721, G.Pape@...) |

*Research students*

M.I. Arbouw (till 1/10/97)
C.J. Boone
A.C. van Gorp
C.E. Wijnmaalen

*Technical staff*

| | |
|---|---|
| A. Budding | (2782210) |
| B.W. Oude Engberink | (2782346, OudeEngberink@...) |
| S.T. Smit | (2782202, S.T.Smit@...) |
| Th.M. van Soest | (2782220, Th.M.vanSoest@...) |

### RESEARCH AREAS AND OBJECTIVES

The research performed in the group Mechanical Behaviour of Materials can be divided into 4 themes:

- fatigue
- creep and creep-fatigue interactions
- environmental effects
- failure

#### 1 *Fatigue*

##### 1.1 *Fatigue of Aluminium*

Fatigue crack growth in aluminium is studied experimentally during constant load amplitude, constant stress intensity amplitude ($\Delta K$) and various forms of block loading. Particular attention is paid to the effect of:

- shear lip development and shear lip roughness,
- crack closure level changes,
- the crack tip plastic zone,
- the effect of the environment and loading frequency.

The aim is to develop models for predicting fatigue crack growth in aluminium.

### 1.2 *Fatigue of Thin Nodular Cast Iron*

Recent developments have enabled the production of thin-walled (≈ 2 mm) nodular cast iron. This material contains a large number of small-sized nodules, which is expected to increase the ductility. Due to the low thickness in combination with the high ductility of the nodular cast iron, applications become within reach that traditionally are manufactured in steel. In these cases, *e.g.* automotive applications, the fatigue limit is an important design criterion.
The fatigue limit is experimentally determined for cast iron with different nodule densities and sizes and also with different matrices, varying from ferritic to perlitic. Furthermore, attention is paid to the effect of the cast skin on the fatigue limit. Additionally, threshold stress intensity values and crack growth rates will be determined. The objective is to optimise the production of thin nodular cast iron with respect to the fatigue properties.
This work is part of the PBTS-project *Thin Nodular Cast Iron for Automotive Applications.*

## 2 *Creep and Creep-Fatigue Interactions*

### 2.1 *Crack Growth in Asphalt*

Fatigue crack growth and creep crack growth at different loading conditions are studied for a number of asphalt concrete mixtures. Particular attention is paid to the effect of:

- the load frequency,
- the ratio between minimum and maximum load (R-value),
- the specimen geometry and thickness,
- load or displacement control.

The aim is to develop a method for classifying asphalt concrete mixtures as far as their sensitivity for crack growth is concerned.
This work is sponsored by *Dienst Weg- en Waterbouwkunde* (DWW, Rijkswaterstaat) and carried out in conjunction with both DWW and the *Netherlands Pavement Consultancy.*

## 3 *Environmental Effects*

### 3.1 *Corrosion Fatigue of Structural Steel*

Fatigue crack growth in steel will occur at a higher rate in seawater than in an air environment. An important role is played by the transport of aggressive solution species from the crack mouth to the crack tip. A model for the transport mechanism has been proposed by C.J. van der Wekken. The basis of this model is that transport to the crack tip will be enhanced by the diffusion of species between laminar flowing layers having different speeds. Such layers are caused by the cyclic opening of the crack.
This so-called *flow enhanced diffusion* mechanism is verified by performing laboratory experiments in artificial seawater using compact tension specimens of Fe E355-KT (Euronorm 113-72), a structural steel of a type often used in offshore constructions. The long term objective is to develop a new cathodic protection method on the basis of the proposed transport mechanism.
This project is financially supported by STW.

### 3.2 *Hydrogen Embrittlement in Steel*

The term "hydrogen embrittlement" is used in the literature for a wide variety of hydrogen related phenomena. The degradation of the mechanical properties of materials caused by the presence of hydrogen in the microstructure has been and is the subject of extensive research. The general perception is that hydrogen embrittlement is the result of the interaction of hydrogen with the formation and movement of dislocations, thus reducing the potential for plastic deformation. However, the phenomenon is not completely understood despite extensive research. Hydrogen embrittlement generally refers to macroscopic toughness parameters such as strain at fracture, tensile strength and fracture toughness.
Fracture mechanics experiments on hydrogen charged specimens do not result in a unique critical fracture toughness, as the fracture toughness is strongly dependent on the strain rate. To model the strain rate dependency, thus reducing the need for expensive experimental work in the future, a sophisticated computer model using the finite element method is under development.

## 4 *Failure*

Research is performed into the mechanical failure of structural materials, mainly using a fracture mechanics approach. Fracture mechanics offers a number of parameters, such as stress intensity factor ($K$), energy release rate ($G$), crack tip opening displacement ($\delta_t$) and the $J$-integral, to characterise overall fracture behaviour. Besides, local fracture criteria can be used in order to account more specifically for the fracture mechanisms that actually occur in the material.

The focus is on the following topics:

- Less-material-consuming mechanical testing
  Often the amount of available material is not sufficient for determining mechanical properties such as fracture toughness or the stress strain curve. Therefore the possibility is examined of performing tests which use less material. An additional objective is to come to cheaper tests.
- Fracture Toughness of Thin Nodular Cast Iron
  As mentioned above the production of thin-walled ($\approx$ 2 mm) nodular cast iron has recently become feasible. Due to the large number of small-sized nodules this material is expected to have a relatively high ductility. In the applications which are obvious for this type of cast iron knowledge about the fracture toughness is essential.
  The standard test procedures for evaluating fracture toughness prescribe specimen dimensions for this thin material which are too small to be practical. Therefore an alternative specimen geometry is tested and the results are compared to standardised test methods. Using these results, the effect of the number and size of the nodules on the toughness of the cast iron is investigated.
  This work is part of the PBTS-project *Thin Nodular Cast Iron for Automotive Applications.*
- Fracture Behaviour of Metal Matrix Composites
  The favourable properties of metal matrix composites (MMCs), *i.e.* a high stiffness and load-bearing capacity, are somewhat hampered by the relatively low fracture toughness of this class of materials. In order to optimise existing MMCs for specific applications and to develop new types, insight in the conditions that

lead to an optimal toughness is essential. For this purpose both fracture mechanics experiments as well as finite element computations are performed on aluminium-based MMCs. Work is performed on an $Al_2O_3$ reinforced MMC with a precipitation hardening aluminium alloy as matrix and a $TiB_2$ reinforced aluminium based MMC which is produced *in situ*. Eventually this must lead to a micromechanical model, which relates fracture toughness to material parameters, such as matrix alloy, ageing condition, particle volume fraction and particle size.

- Prediction of Fracture Initiation using Local Fracture Criteria
  In order to diminish the vulnerability of welded steel structures by a suddenly applied heavy load and also for safety reasons, knowledge about the failure behaviour of dynamically loaded structures is of prime importance. For this reason research is being performed to predict fracture initiation in these structures at various strain rates. Experiments are carried out to obtain the necessary material behaviour data, which are subsequently used in a local fracture criteria model to perform predictions.
  This work is carried out in conjunction with TNO Rijswijk (Prins Maurits Laboratory) and is mainly sponsored by STW.
- Micromechanical based critical flaw size prediction
  The objective of this project is to apply and further develop micromechanical models for the prediction of critical flaw sizes in welded structures.

FACILITIES

- Seven computerised hydraulic fatigue machines (350, 2×250, 3×100, 25 kN)
- Four electro-mechanical tensile testing machines (3 × 100, 50 kN)
- High capacity hydraulic tension testing machine (2 MN) and compression testing machine (5 MN)
- Fast hydraulic mechanical testing machine (10 $^{m}/_{s}$ at 50 kN, 17 $^{m}/_{s}$ at zero load), including a high speed photo camera (maximum 224 pictures and 35 000 picture/s)
- Digital imaging systems for recording crack growth and plastic deformation
- Ten creep machines for metals ($T < 1000$ °C)
- Two creep installations for polymers ($+20 < T < +90$ °C, 10 specimens each)
- Climate chamber for mechanical testing in various gaseous climates (400 × 500 × 600 mm; $-150 < T < +250$ °C)
- Oven for tensile testing at high temperature (250 × Ø60 mm; $T < 1200$ °C)
- Chamber for mechanical testing at low and elevated temperatures (345 × 330 × 600 mm; $-180 < T < +80$ °C)
- Instrumentised drop-weight tower: Dynatup 8000A with digital oscilloscope and PC for data acquisition
- Various equipment for the mechanical characterisation of materials: Charpy impact tester, hardness measurement equipment, etc.
- Various ultrasonic measurement equipment, including a set-up for acoustoelastic stress measurements
- DEC 3400 workstation running MARC finite element program and MENTAT pre-and-post processor
- DEC 6/333 workstation running MARC finite element program and Matlab
- DEC 5/400 workstation running MARC and ABAQUS finite element programs and MENTAT pre-and-post processor

RESEARCH REPORT 1997

## 1 *Fatigue*

### 1.1 *Fatigue of Aluminium* (J. Zuidema, Th.M. van Soest)

Further progress has been made in an extensive experimental program studying the fatigue crack growth rate in aluminium alloys. Special emphasis has been given to effects of environment and frequency on the crack growth rate in Al 2024.
Multiple underloads and overloads with constant $\Delta K$ have been carried out using centre-cracked tension specimens. The aim is to study the effect of crack closure changes on the crack growth rate. Progress on synergetic effects of different fatigue crack closure mechanisms is reported on the second ASTM symposium on advances in Fatigue Crack Closure Measurement and Analysis, held in November 1997 in San Diego.

### 1.2 *Fatigue of Thin Nodular Cast Iron* (C.E. Wijnmaalen, J. Zuidema)

A large number of tests are performed to measure the fatigue limit stress at 4 million cycles. For this purpose the stair case procedure is used. An important issue is the geometry of the specimens, since this can affect the initiation of fatigue cracks, and therefore the resulting fatigue limit, significantly. Relevant aspects are crack initiation at corners or at the cast skin.
Furthermore "normal" S-N curve testing is performed in order to obtain an overall impression of the stress dependence of the fatigue life.
Additionally, crack growth experiments under constant amplitude loading were performed and threshold values, $\Delta K_{th}$, were measured.

## 2 *Creep and Creep-Fatigue Interactions*

### 2.1 *Crack Growth in Asphalt* (M.I. Arbouw, J. Zuidema; R.L. Krans [Dienst Weg- en Waterbouwkunde, Rijkswaterstaat, Delft]; F. Tolman [Netherlands Pavement Consultancy])

The study is continued on the fatigue crack growth rate behaviour of asphalt with a special emphasis on the creep-fatigue interactions in this material. Fatigue and creep crack growth experiments in sand asphalt specimens have been carried out in centre-cracked tensile set-ups at 0 °C. Specimen thickness, frequency and $R$-value (load ratio) have been varied. Most of the tests were constant load experiments, but a constant $\Delta K$ experiment was carried out also.
Paris law, relating crack growth rate $da/dN$ and $\Delta K$, describes the results well. Results of tests at different frequencies $f$ can be reduced to a single scatter band by plotting $da/dt$ ($= f \cdot da/dN$) instead of $da/dN$ versus $\Delta K$. It is concluded that the dominant crack growth mechanism in this type of asphalt and under the investigated circumstances is creep. A model has been developed for the prediction of creep-fatigue interactions as a function of the stress ratio $R$ and the frequency $f$. The tests are performed on two kind of asphalt materials: fine sand asphalt material (with 2 mm stones max.) and dab 08 (with 8 mm stones).

## 3 *Environmental Effects*

### 3.1 *Corrosion Fatigue of Structural Steel* (P.C.H. Ament, M. Janssen, Th.M. van Soest, J. Zuidema; M. Corbeels, C.J. van der Wekken [MIDEG])

Corrosion fatigue experiments were performed according to ASTM E-647-93 in deaerated artificially seawater which was prepared according to ASTM D-1141-90. Crack lengths were determined by the four-point potential-drop technique. A reasonable insight has been obtained in the corrosion fatigue behaviour of the structural steel FeE355-KT in deaerated artificial sea water by performing constant load amplitude tests at frequencies ranging from 10 to 0.1 Hz, *R*-values of 0.3, 0.5 and 0.7, and maximum loads of 20.4, 35.4 and 40.4 kN. In all cases an anodic potential was chosen of –500 mV (versus Ag/AgCl). It has been shown that while decreasing the frequency one order, the crack growth rate increases a factor 3. The corrosion fatigue crack growth rate at a frequency of 10 Hz is already a factor 3 higher than fatigue of this type of steel in laboratory air. Schematically the result are shown in Figure 1.

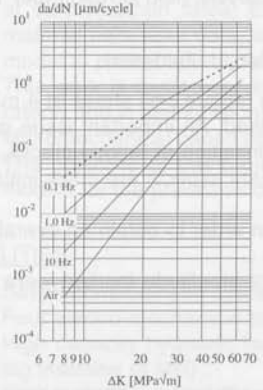


*Figure 1: Generalisation of the crack growth rates for corrosion fatigue of FeE455-KT in deaerated artificial seawater for frequencies of 10, 1 and 0.1 Hz, together with the curve for fatigue in air*

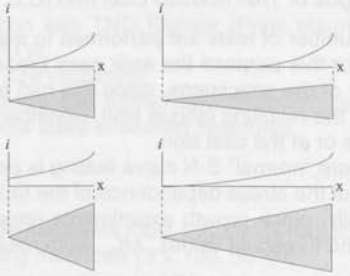


*Figure 2: Effect of the physical crack size and crack mouth opening displacement on the $H^+$ source strength (in terms of the current density i) at the crack flanks*

Numerical simulations were performed based on the Flow Enhanced Diffusion model using the following assumptions. First, the flow of the solution in the corrosion fatigue crack is assumed to be laminar under all circumstances. Secondly, only two dimensional diffusion is considered, *i.e.* diffusion normal to the crack length and crack opening directions is assumed to have no effect on the final result. The crack tip is blunted and the geometry of the corrosion fatigue crack is therefore a trapezoid. Due to the anodic polarisation $H^+$ ions are formed along the crack flanks. The source strength of these $H^+$ ions is assumed to have a parabolic distribution along the crack flanks, with the highest value at the crack mouth. There is a certain penetration depth of the source distribution, which is assumed to be proportional to the average crack mouth opening displacement. This penetration depth is shown in Figure 2.

The results of the numerical simulations for constant amplitude tests showed that the number of $H^+$ ions reaching the crack tip increases one order if the frequency is lowered one order. The simulations also showed no effect of the maximum load.

It is assumed that the crack growth rate, d*a*/d*N*, is proportional to the number of $H^+$

ions reaching the crack tip per unit time and inversely proportional to the root of the frequency. Using superposition, *i.e.* adding the crack growth due to $H^+$ ions and the crack growth due to the mechanical load, the numerical results can be correlated to the experimentally obtained crack growth rates. At high $\Delta K$ values there is a good agreement, but at low $\Delta K$ values, especially at low frequencies, there is an overestimation of the crack growth rate. An example is shown in Figure 3.

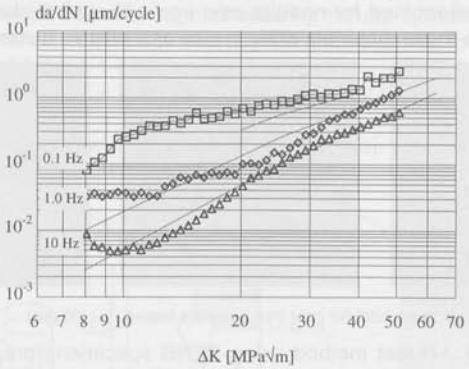


*Figure 3: Crack growth rate da/dN as a function of the stress intensity range ΔK, experimental and superposition results, frequencies of 0.1, 1 and 10 Hz, $P_{max}$ = 35.4 kN, penetration depth is 400 times the average crack mouth opening displacement.*

3.2 *Hydrogen Embrittlement in Steel* (A.H.M. Krom, A. Bakker; R.W.J. Koers [Shell Research, Amsterdam])

Hydrogen transport in uniaxial tensile specimens is modelled. The model includes the effect of trap sites formed as a result of plastic deformation and the effect of a hydrostatic stress state. Finite element calculations suggest that a high strain rate causes a low hydrogen concentration in lattice sites, and *vice versa*. In tensile tests a similar tendency is found: a high strain rate results in a high fracture elongation, whereas the opposite effect is found at low strain rates. This suggests that a low elongation at fracture corresponds to a high hydrogen concentration in lattice sites.

This project is terminated in 1997 and the results will be reported in a Ph.D. thesis by A.H.M. Krom.

## 4 *Failure*

4.1 *Less-material-consuming mechanical testing* (C.H.L.J. ten Horn, A. Bakker; R.W.J. Koers [Shell Research, Amsterdam])

This project, which was completed in April 1997 with a graduate report, comprised the determination of:

- $J_{Ic}$ using circumferential cracked cylindrical specimens
  It was found that the eccentricities observed after precracking of the specimens were caused by eccentricities in the machined notch of the specimen. A procedure was put forward to correct for the eccentricities. The data found using the circumferentially cracked cylindrical specimens coincided with those obtained using Single Edge Notched Bend specimens.
- the true stress-strain curve from hardness measurements

Equations proposed by Tabor were found to describe the first 14% strain of the true stress-strain curve well. Furthermore, Meyer's law could be used to obtain the power law parameters. The yield strength and the ultimate tensile strength could be estimated using these power law parameters.

4.2 *Fracture Toughness of Thin Nodular Cast Iron* (C.J. Boone, M. Janssen)

The *J-R* curve is determined for nodular cast iron with wall thicknesses 2, 4 and 7 mm. The nodules in these materials differ in size and relative distance (Figure 4)

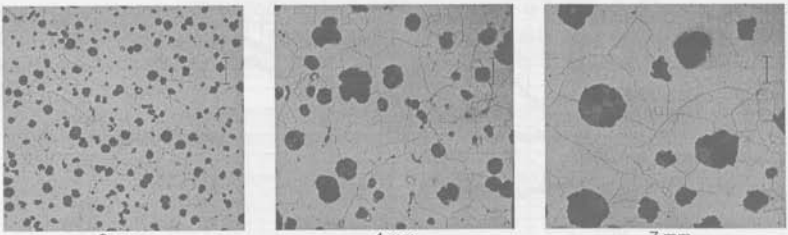


*Figure 4: Structure of the three nodular cast iron samples tested (⌶ = 20 μm)*

Since the standard *J-R* test method using SENB specimens prescribes very small dimensions for 2 mm thick material, tests are performed using a Single Edge Notched Tensile (SENT) geometry. These specimens are tested in combination with special fixtures. Figure 5 gives an outline.

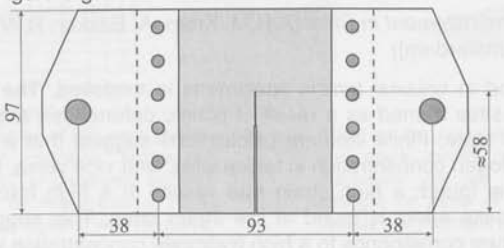


*Figure 5: Geometry of the SENT specimen and the fixtures used*

An important result is that *J-R* curves determined on 4 mm thick SENT specimens correspond to those determined with the standardised SENB specimens. This enables fracture toughness determination on thin material.

The experimental results indicate that fracture toughness of the cast iron decreases as the thickness decreases. These results can be related to the nodule morphology, using a fracture model developed by Rice and Johnson. Their model predicts the CTOD required for void growth and coalescence as a function of void size and distance to the crack tip. Assuming the nodules mechanically behave like voids, critical *J*-values can be calculated for the current three nodule morphologies. The model predicts a decreasing fracture toughness for smaller nodules which are closer to each other, which is in agreement with the tendency found in the experimental results.

4.3 *Fracture Behaviour of Metal Matrix Composites* (K.M. Mussert, A.C. van Gorp, M. Janssen, A. Bakker; S. van der Zwaag [MIDEG])

Fracture in an Al 6061 based metal matrix composite (MMC) containing 20 vol.% $Al_2O_3$ particles is modelled using an axisymmetrical finite element model and a statistical approach for calculating strengths of ceramic via Weibull's model. Within the finite element model, it is assumed that the MMC fails as soon as the particle fails and variables such as particle volume fraction, particle size and matrix alloy properties can be varied. The continuum is considered to consist of a periodic assemblage of hexagonal cylindrical unit cells approximated by circular cylinders, which allows for a simple axisymmetrical calculation whereby the finite element mesh consists of 350 isoparametric quadrilateral 4-node elements, see Figure 6. The MMC is modelled with a matrix of Al 6061 ($E$ = 69 GPa, $\nu$ = 0.33, $\sigma_{ys}$ = 276 MPa) and $Al_2O_3$ particles with a diameter of 4 μm ($E$ = 393 GPa, $\nu$ = 0.27, $\sigma_{ys}$ = 2000 GPa, this is a fictitious high value to prevent plastic deformation in the particle). The triaxiality, *i.e.* the ratio $\rho = \sigma_{rr}/\sigma_{zz}$, is kept constant during the loading history.

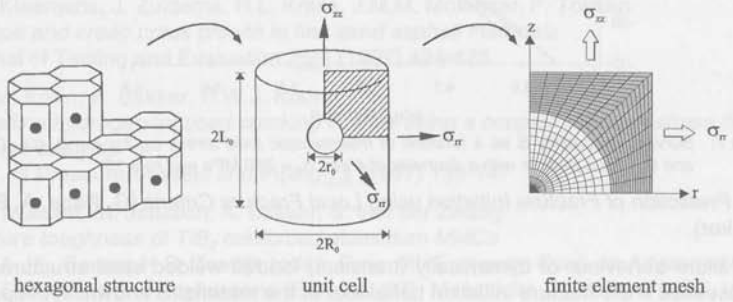


*Figure 6: Micromechanical modelling of a matrix containing a spherical particle*

In case of a uniform stress distribution, the survival probability $S$ of a ceramic particle can be calculated with the following equation:

$$S = \exp\left(-\frac{\sigma}{\sigma_0}\right)^m$$

where $\sigma$ is the applied stress, $m$ is the Weibull modulus and $\sigma_0$ is the stress at which $S = 1/e$. Manipulation of this equation allows a straight-line representation of gradient $m$, when $\ln \ln 1/S$ is plotted versus $\ln \sigma$.

$$\ln \ln \frac{1}{S} = m \ln \sigma - m \ln \sigma_0$$

By plotting the calculated survival probability of an $Al_2O_3$ particle versus the macroscopic axial stress applied on the whole MMC, the applicability of Weibull statistics on these type of new materials is checked, see Figure 7.

It can be concluded that, knowing the stress distribution in a ceramic particle, Weibull's model can be used to calculate the survival probability of ceramic particles in ductile matrices, however, the Weibull modulus becomes meaningless when a non-proportional stress distribution in the matrix occurs. More calculations have to be done to investigate other $m$ and $\sigma_0$ values, particle sizes and to incorporate surface defects and interface strengths. Furthermore, when more experimental data become

available, the model has to be adjusted in terms of particle volume fraction, particle size and matrix alloy properties.

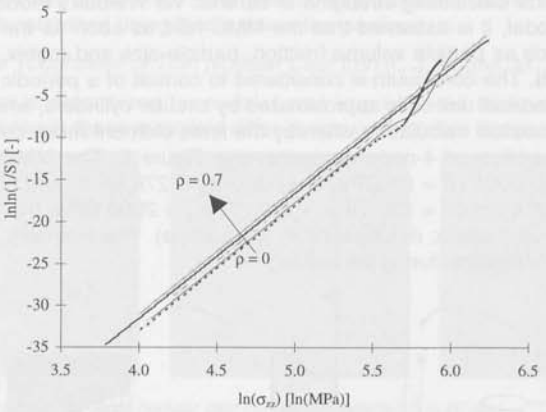


*Figure 7: Survival probability S as a function of macroscopic axial stress $\sigma_{zz}$ for $\rho$ = 0, 0.1, 0.3, 0.5 and 0.7, for a particle with a diameter of 4 μm, $\sigma_0$ = 350 MPa and m = 15*

4.4 *Prediction of Fracture Initiation using Local Fracture Criteria* (G. Pape, A. Bakker)

The failure behaviour of dynamically (transient) loaded welded steel structures can be assessed if the fracture initiation behaviour of the material is known. An important aspect in this assessment is the effect of high strain rates on the fracture initiation process. The different material properties of the weld and HAZ have to be taken into account also.
High rate tensile tests will be performed on specimens taken from the steel plate, the weld material as well as the heat affected zone. The resulting data will be used as input for finite element calculations. In these calculations use will be made of a local fracture criterion which accounts for the accumulated damage during deformation. Using this local fracture criterion, a prediction can be made of the initiation of fracture.
In order to verify the used local fracture criteria model, the laboratory experiments (tensile tests) will also be simulated and the results compared. Another verification follows from predicting failure in (scaled down) structural components that will be tested experimentally.

4.5 *Micromechanical Based Critical Flaw Size Prediction* (C.H.L.J. ten Horn, A. Bakker; G. den Ouden, E. van der Giessen [MIDEG])

An introductory literature study was carried out in order to find the most promising micromechanical models which are available for predicting ductile and cleavage fracture.

PUBLICATIONS

D.M. Li, A. Bakker
*Fracture toughness evaluation using circumferentially-cracked cylindrical bar speci-*

*mens*
Engineering Fracture Mechanics 57 (1997) 1-11

D.M. Li, A. Bakker
*Shear fracture mechanisms in a rapidly-solidified aluminium scrap alloy*
Journal of Materials Science 32 (1997) 259-266

D.M. Li, A. Bakker
*Shearing and toughening mechanisms in an RSP recycled aluminium alloy*
Acta Materialia 45 (1997) 2407-2415

M. Janssen (ed.)
*Research in Materials Science and Technology - Annual Report 1996*
Delft University Press (1997) 277

C.P. Kleemans, J. Zuidema, R.L. Krans, J.M.M. Molenaar, F. Tolman
*Fatigue and creep crack growth in fine sand asphalt materials*
Journal of Testing and Evaluation 25/4 (1997) 424-428

A.H.M. Krom, A. Bakker, R.W.J. Koers
*Modelling hydrogen-induced cracking in steel using a coupled diffusion stress finite element analysis*
Int. J. of Pressure Vessels and Piping 72 (1997) 139-147

K.M. Mussert, M. Janssen, A. Bakker, S. van der Zwaag
*Fracture toughness of $TiB_2$ reinforced aluminium MMCs*
In: L.A.J.L. Sarton, H.B. Zeedijk (eds.), Proc. 5th European Conf. on Advanced Materials, Processes and Applications (Euromat '97), Maastricht, 21-23 April 1997, Volume 1: Metals and Composites, The Netherlands Society for Materials Science, Zwijndrecht (1997) 399-402

A.C. Riemslag
*Crack Growth in Polyethylene*
Ph.D. thesis, Delft University of Technology, Delft University Press, Delft (1997) 128

L. Varkoly, J. Zuidema
*Studium vplyvu frekvencie zazazovania na rychlosz sirenia a uzatvaranie unavovych trhlin v hlinikovej zliatine Al2024*
Materialove in Zinierstvo 10 (1997) 59-64

L. Varkoly, J. Zuidema
*Study of frequency of loading influence on fatigue crack growth rate and fatigue crack closure in Al 2024 alloy*
Materialove Inzinierstvo 4 (1997) 59-64

L. Varkoly, J. Zuidema, B. Varkolyova, M. Chalupova
*Fatigue failure of Materials - Theory and Solved Examples*
Zilina University Press, Zilina, Slovak Republic (1997) 235

J. Zuidema, J.P. Krabbe
*The effect of regular and irregular shear lips on fatigue crack growth in Al 2024*
Fatigue and Fracture of Engineering Materials and Structures 20/10 (1997) 1413-1422

## MICROMECHANICS OF MATERIALS [1]

Delft University of Technology, Laboratory for Engineering Mechanics
Mekelweg 2, 2628 CD Delft
phone +31 (15) 2785733, e-mail ...@wbmt.tudelft.nl

### PERSONNEL

*Scientific staff*

| | |
|---|---|
| prof.dr.ir. E. van der Giessen | (2786500, E.vanderGiessen@...) |
| J. Booij, M.Sc. | (2786504, J.Booij@...) |

*Post-doc's*

| | |
|---|---|
| dr. S.M. Schlögl (from 1-5-1997) | (2786509; S.M.Schloegl@...) |
| dr. B.-N. Nguyen (from 1-12-1997) | (2786509; B.N.Nguyen@...) |

*Graduate students*

| | |
|---|---|
| A.A. Baqi, M.Sc. | (2786547; A.A.Baqi@...) |
| ir. M.W.D. van der Burg (till 1-2-1997) | (2786509, M.vanderBurg@...) |
| ir. H.H.M. Cleveringa | (2783522, H.H.M.Cleveringa@...) |
| ir. P.R. Onck | (2786509, P.R.Onck@...) |
| drs. K.G.W. Pijnenburg (since 1-3-1997) | (2786506; K.G.W.Pijnenburg@ ...) |
| ir. A.C. Steenbrink (till 1-4-1997) | (2786506, A.C.Steenbrink@...) |
| ir. M.G.A. Tijssens | (2786547, M.G.A.Tijssens@...) |

### RESEARCH AREAS AND OBJECTIVES

#### 1 *Plasticity of Metals*

The objective is the development of a class of models that provides a quantitative link between the structure of the material and, ultimately, its macroscopic elastoplastic behaviour. Models are considered at several length scales. Polycrystal behaviour is formulated on the basis of so-called crystal plasticity models which describe the elastoplastic response of individual crystals. These models are based on a description of slip on discrete slip systems, and provide a solid and natural basis for accounting for microstructural phenomena as *e.g.* texture development. On a smaller scale, models are explored to describe plasticity on the basis of discrete dislocations. These models serve as "input" for the crystal plasticity models, but also provide a means to study small-scale plasticity problems where a continuum description of dislocations breaks down.

#### 2 *Deformation and Fracture of Polymers and Blends*

Within this theme, a number of projects are concerned with the deformation and fracture of polymers (including rubbers and polymer blends). As far as deformation behaviour is concerned, current emphasis is on the long term behaviour of rubbers, as well as on the viscoplastic behaviour of amorphous polymers and of semicrystalline polymers. In addition, the development of failure in these polymers and associ-

[1] Part of the work reported here has been carried out within the "Onderzoeksschool Polymeren PTN" or in the "Onderzoekschool Engineering Mechanics".

ated polymer blends is studied. Modelling typically follows a micromechanical approach.

3 *High-Temperature Failure of Polycrystalline Materials*

Fracture of polycrystalline metals, alloys and ceramics at elevated temperatures often occurs by the nucleation, growth and coalescence of microscopic cavities at grain boundaries. A comprehensive micromechanical model of creep rupture is being developed, which aims at quantitatively relating microstructural properties on the scale of cavities or grains to the macroscopic creep fracture parameters. In addition to creep conditions, cyclic loading and the influence of the environment (*e.g.* hydrogen) is studied.

4 *Failure of Brittle Materials and Coatings*

Fracture in materials that are inherently brittle, like ceramics, or that behave in a brittle manner under certain conditions, is often much more complicated than the simple textbook notions assume. As a rule, brittle fracture is characterised by the occurrence of micro-cracking and strongly serrated crack propagation paths, involving crack branching, crack kinking, etc. In the case of coatings, these features interact with other failure mechanisms, such as delamination along the interface with the substrate. In this field, we are interested in the physical factors controlling these fracture features, their mechanistic description and the resulting overall characteristics.

## FACILITIES

- a cluster of workstations: Silicon Graphics Indigo 4000, Indys, Challenge M, Indigo2 Extreme and O2s;
- a five-node Silicon Graphics Challenge L server.

## RESEARCH REPORT 1997

1 *Plasticity of Metals*

1.1 *Crystal Plasticity Modelling* (E. van der Giessen; K.W. Neale, P.D. Wu [Université de Sherbrooke, Canada])

The influence of texture development on the behaviour of metals during large plastic strains, as in for instance forming processes, is still an important issue. During recent years we have developed a procedure to predict Forming Limit Diagrams (FLD) on the basis of polycrystal plasticity models. This has been done within the framework of the Marciniak-Kuczynski (MK) approximation, and using the elastic-viscoplastic crystal plasticity model for FCC crystals. Initial textures and uniaxial stress-strain data are input for the analysis, which then predicts a complete FLD. The model is capable of revealing much more details and more accurate predictions than the phenomenological plasticity models used so far in industry. During 1997 we have used the model to study the influence of strain path changes on the FLD. Commonly, an FLD is constructed assuming proportional straining, but practical sheet forming operations usually involving more complex strain paths. Without any further adjustable parameters, the model predicted effects on the FLD of sudden strong strain path changes which

show good qualitative agreement with the few experimental results available in the literature.

1.2 *Discrete Dislocation Plasticity* (H.H.M. Cleveringa, E. van der Giessen; A. Needleman [Brown University]; D. Srolovitz [University of Michigan]; J.Th.M. De Hosson [University of Groningen])

In this research, plastic deformation is studied at length scales of the order of microns. At this length scale, a continuum plasticity theory involving a smeared-out description of dislocations may no longer be appropriate. Therefore we have developed a model to treat dislocations as discrete entities in an otherwise elastic medium. The collective behaviour of these dislocations determines the plastic flow. The difference with other models describing plastic flow using discrete dislocations is that our model allows for the solution of boundary value problems. The dynamics of the dislocations are governed by a linear drag relationship, while also creation and annihilation are incorporated. Furthermore, the pinning of dislocations at obstacles and their subsequent release is included in the model. The boundary conditions are accounted for by means of a finite element discretisation of the elastic continuum in which the dislocations are embedded.
In our first applications, reported on last year, dislocations were treated on parallel slip planes, so that no crossing of dislocations occurred and plastic deformation was only possible in shear. To incorporate plastic deformation in multiple directions, though still in two dimensions, the model is extended for multiple slip, *i.e.* glide planes at different angles. One of the difficulties in implementing this is how to handle junctions of the two slip planes. Much is known about the intersection of dislocations in 3D, but this cannot be readily taken over to 2D. Currently, we let the dislocation interaction near junctions of slip planes be controlled solely by the long-range elastic interactions. Special numerical procedures have been developed to maintain numerical stability. They involve the use of a cut-off value for the dislocation velocities. In this way we loose some local information on the exact position of dislocations at a junction, but the speedup is several orders of magnitude. The global response is not affected by this.
As an example, Figure 1 shows the result of a simulated tensile test on a specimen of 12 × 6 μm. Uniform horizontal displacements on the sides of the specimen are applied; anywhere else, the tractions vanish. We use slip planes in three different

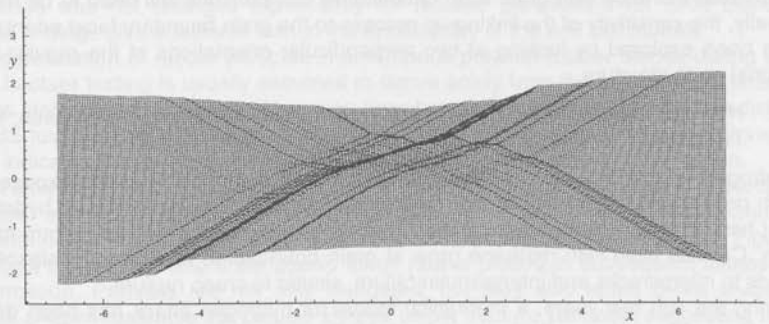


*Figure 1: Deformed mesh of a specimen subjected to uniaxial tension, analysed using discrete dislocation plasticity. The material contains three active slip systems. The deformation is 5% and displacements are magnified 10×.*

orientations with a spacing of 125 Burgers vectors. The material parameters used are typical for aluminium. We start with an initial random distribution of dislocations, so that they can act as obstacles for each other at slip plane junctions. The figure shows the deformed mesh at a deformation of 5%. The left-hand side is seen to be lower than the right side. This is caused by the randomness in the initial dislocation structure and the fact there are no constraints in the y-direction. At the stage shown, the dislocation density in the specimen is more than $10^{10}/cm^2$. To be able to efficiently handle this large number of dislocations we use a Fast Multipole Method.
The model for single slip developed previously is now being used in the group of prof. J.Th.M. de Hosson (University of Groningen) for the simulation of high-speed localised shearing; this work will be reported in the Chapter elsewhere in this Report.

## 2 *High-Temperature Fracture*

### 2.1 *Creep Rupture in Polycrystalline Materials* (P.R. Onck, B.-N. Nguyen, E. van der Giessen)

In structural materials at high temperatures subjected to low stationary loading, failure occurs by intergranular fracture. The underlying physical mechanisms are the nucleation and growth of cavities on the grain boundaries, dislocation creep inside the grains and grain boundary sliding. Coalescence of cavities leads to microcracks, and final failure occurs when those microcracks link up with the macroscopic crack.
Last year, a microstructural model has been developed for the investigation of the initial stages of creep crack growth. The grains in the polycrystalline material are represented discretely. This enables the simulation of the actual linking-up process of discrete microcracks with the macroscopic crack. Full account is given to the relevant micromechanisms, such as viscous grain boundary sliding, the nucleation and growth of cavities, and micro-cracking by cavity coalescence.
This year we continued our investigations by studying the effect of crack tip blunting on crack growth behaviour. The computations show a general trend that while an initially sharp crack tends to propagate away from the original crack plane, crack tip blunting renders the crack to grow more in the plane of the crack.
In addition, size effects have been investigated. In particular, we have been interested in the influence of the ratio between specimen size and grain size. Our computations tend to confirm the experimental findings that the crack growth rate and brittleness increase with grain size. Quantitative comparisons still need to be made.
Finally, the sensitivity of the linking-up process to the grain boundary facet orientation has been explored by looking at two perpendicular orientations of the regular hexagonal grain structure.

### 2.2 *Hydrogen Attack* (M.W.D. van der Burg, S.M. Schlögl, E. van der Giessen; V. Tvergaard [Technical University of Denmark])

Hydrogen attack is a material degradation process occurring in steels exposed to high pressures of hydrogen at temperatures above 200 °C. The dissolved hydrogen that has diffused into the material reacts with the carbides of the steel to form methane. Cavities filled with methane grow at grain boundaries, and cavity coalescence leads to microcracks and intergranular failure, similar to creep rupture.
During the last few years, a theoretical model for hydrogen attack has been developed, culminating in the Ph.D. thesis by M.W.D. van der Burg (May 1997). The modelling is performed on three different length scales: cavity size, grain size and speci-

men size scale. Last year we focused once again on the model on the smallest length scale, the so-called single cavity model, including the thermodynamical relationships used to compute the methane pressure from the hydrogen-carbide reaction. One of the reasons was to compare this model with a model used by API (American Petroleum Institute) RP 941. We have revealed the differences regarding the void growth relations and the calculation of the methane pressure. Further, we have extended the single cavity model to be able to compute the methane pressure resulting from the equilibrium reaction of Fe-Cr-Mo-V alloy carbides with the hydrogen. This was necessary since, besides the standard 2.25Cr1Mo-steel, new steel grades are used in the petrochemical industry which are modified with vanadium.

## 3 *Deformation and Fracture of Polymers*

### 3.1 *Failure of Polymer-Rubber Blends* (A.C. Steenbrink, K.G.W. Pijnenburg, E. van der Giessen; R.J. Gaymans [Twente University])

Many brittle glassy polymers are toughened by way of blending in small rubber particles. The basic mechanism is that when the material is deformed, plasticity is initiated at the rubber particles and takes place in a larger volume, increasing the energy dissipation. The deformation mechanisms and the relation of particle properties and toughening efficiency has been the subject of many studies, but still the precise mechanisms are not well understood. Moreover, a quantitative description of the deformation processes at a microscale is lacking. The objective of this project is to investigate the deformation processes in well-defined blends of styrene-acrylonitril (SAN) with various core-shell rubber particles following a combined experimental-modelling approach.

To explain and describe the aforementioned interaction of rubber particle cavitation and matrix plasticity, we had developed a micromechanical model during previous years, which was based on the idea of a unit cell representation. The particular unit cell considered until then corresponded to a square (in 2D) or square/hexagonal (in 3D) packing of identical particles. Real material obviously are not periodic. In order to obtain some feeling for the influence of the assumed packing we developed an alternative 2D model with a different, *viz.* hexagonal, packing. It was found that local plasticity in the matrix was still governed by essentially the same two types of shear bands as found for the other packings. Also we found that the overall stress-strain response was not changed significantly for realistic parameters for SAN blends. These findings give additional faith in the applicability of the unit cell models.

The deformation of rubber particles in amorphous polymer-rubber blends during impact fracture testing is usually assumed to derive solely from the predominant tensile stress state ahead of a crack. However, the observed shapes of deformed particles in ABS just beneath the fracture surface do not seem to be consistent with this view. This indicates that another mode of deformation might be involved in this region.

In an attempt to explain this behaviour we studied the response of a blend subjected to shear instead of tension. Assuming a periodic packing of the particles, a band of material deforming in simple shear was analysed with a finite element model. Figure 2 shows the results, where the plastic strain rate is plotted in subsequent stages of deformation. Particles are not only elongated, but they also attain S-like shapes. These shapes resemble the particle shapes below fracture surfaces, suggesting that substantial localised shearing of the material next to the propagating crack takes place.

The material parameters used in the calculations are typical for SAN. For comparison, computations were done using parameters that are more representative for polycarbonate and for materials that show no intrinsic softening in their stress-strain behaviour. A decrease in localisation of the plastic flow within shear bands is observed as the softening decreases.

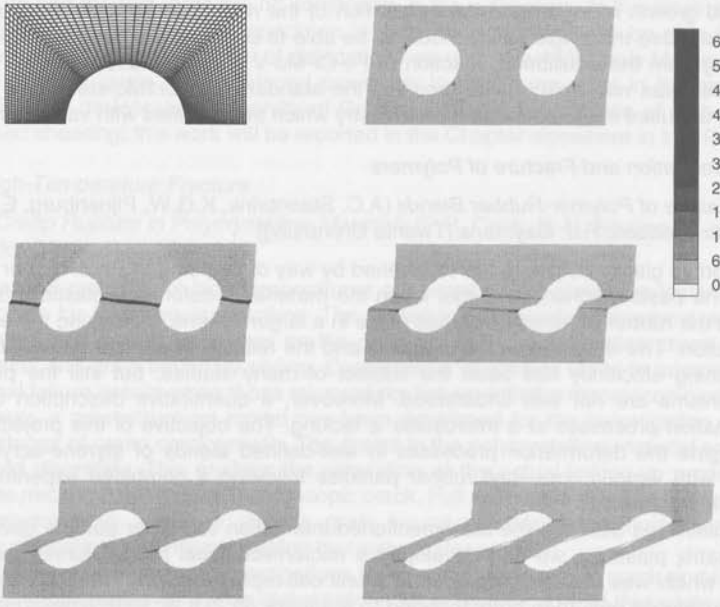


*Figure 2: Undeformed mesh and contour plots of the rate of plastic flow at increasing macroscopic shear (left to right and top to bottom). The shear rate has been normalised with a convenient parameter. Because of periodicity and (point) symmetry, only one quarter of the figures shown was actually modelled (see mesh).*

3.2 *Fracture of Polymers under Impact Conditions* (E. van der Giessen; R.J. Gaymans, M. Hamberg [Twente University])

The objective of this project is to predict the macroscopic fracture or crack growth characteristics in terms of appropriate macroscopic constitutive models, involving plasticity through the 'shear yielding' mechanism, crazing, and possibly cavitation of blends, all in dependence of the local temperature and strain-rate. In particular, the purpose is to give an explanation for the unexpected toughening phenomena at high strain-rates observed experimentally.

An experimental program has been carried out in the group of Gaymans (Twente University) to carefully study the fracture behaviour of polycarbonate, a well-defined polymer that does not easily craze but deforms well plastically (by shear yielding). Careful examination of the test results, especially the fracture surfaces, has revealed that the dependence of the fracture phenomenon on the applied loading rate is a complex one. This is caused by the fact that, dependent on the loading rate, different fracture mechanisms are active at various stages of crack propagation. This implies that the standard simple distinction between a brittle regime in strain-rate or tem-

perature space, or a ductile one may be less accurate than people tend to believe.
The theoretical/numerical part of the project has been very limited owing the fact that it has shown very difficult to find a post-doc for this work. There has been some progress related to adiabatic heating near the crack tip due to plastic dissipation. The change of temperature due to plastic dissipation was incorporated in the constitutive model. Also the evolution of the network parameters to describe the orientation hardening, as a function of temperature was modelled, adopting the approach of Raha and Bowden (1973). The deformation process was assumed to be either completely isothermal or adiabatic, so heat conduction was not considered. It was shown that the temperature in a typical glassy polymer (SAN) may rise by approximately 60° under adiabatic loading conditions, thus raising the room temperature up to the glass transition temperature. A limited parameter study revealed that whether or not the glass transition temperature can be reached depends not only on the dissipated energy up to the limit strain, as is generally assumed, but also depends on how rapidly the yield stress drops with increasing temperature. Materials that have a lower temperature dependence of the yield stress tend to favour the possibility of local 'melting'.
There has also been very limited progress with the numerical micromechanical model for craze growth. Most effort here went into implementing surface energy in the finite element model. Preliminary studies however suggest that the influence of surface energy on craze drawing is very mild.

4 *Discrete Decohesion Modelling of Brittle Fracture* (M.G.A. Tijssens, E. van der Giessen; L.J. Sluys [Faculty of Civil Engineering and Geosciences, Delft University of Technology])

In applications where a high fracture toughness is required, engineering composites are used because of the possibility of massive plastic deformation during overloading. However, polymer and ceramic based composites also fail in a brittle manner. The deformation is localised in crack-like defects and the bulk material experiences no plastic deformation. However, the interaction of defects with the bulk material still leads to a higher fracture toughness and is therefore of practical importance.
The present project aims at obtaining a better understanding of the problem of brittle fracture in heterogeneous materials through micromechanical modelling of the fracture process. The central idea is to make use of finite element techniques in which the standard discretisation of the continuum is supplemented by a high density of cohesive surfaces which are dispersed in between the continuum elements. The interaction of the elastic bulk material and the behaviour of the cohesive surfaces leads to a characteristic decohesion problem governed by material behaviour and the fracture processes.
This year we studied the problem of purely elastic fracture. It was assumed that no energy dissipation was present other than the energy needed to create new fracture surfaces. The formulation of the traction-separation law was taken from work by Xu and Needleman. It is a phenomenological description, but is motivated by the universial binding law.
Anticipating a high density of cohesive surfaces and therefore a very large number of equations to accurately represent the overall fracture path, considerable effort has been put in the development of dynamic relaxation schemes in order to solve the system of equations economically. The nature of the elastic fracture problem however, leads to several distinct problems regarding the numerical solution. One has to

do with the large difference in stiffness of the initial cohesive surfaces compared to that of the bulk. The second problem for purely elastic fracture is the associated local 'snap-back' behaviour in a region around the crack tip. A lot of effort has been put into trying to relieve these difficulties, but so far without sufficient success. Therefore the work on purely elastic fracture has been temporarily stopped until better solutions to the problem become available. From the beginning of 1998, this project continues with brittle fracture of polymers through crazing.

PUBLICATIONS

M.W.D. van der Burg, E. van der Giessen
*A continuum damage relation for hydrogen attack cavitation*
Acta Materialia 45 (1997) 3047-3057

M.W.D. van der Burg, V. Shulmeister, E. van der Giessen, R. Marissen
*On the linear elastic properties of regular and random open-cell foam models*
Journal of Cellular Plastics 33 (1997) 31-54

H.H.M. Cleveringa, E. van der Giessen, A. Needleman
*Comparison of Discrete Dislocation Plasticity and Continuum Plasticity Predictions*
Acta Materialia 45 (1997) 3163-3179

E. van der Giessen
Localized plastic deformations in glassy polymers
European Journal of Mechanics A/Solids 16 (1997) 87-106

E. van der Giessen, J. Lai
*A numerical study of craze growth*
In: Deformation, Yield and Fracture of Polymers, Proceedings of the 10th International Conference, Cambridge, April 7-10 1997, The Institute of Materials, London, 35-38

E. van der Giessen, P.R. Onck, M.W.D. van der Burg
*Some effects of random microstructural variations on creep rupture*
Engineering Fracture Mechanics 57 (1997) 205-226

J. Lai, E. van der Giessen
*A numerical study of crack-tip plasticity in glassy polymers*
Mechanics of Materials 25 (1997) 183-197

P.R. Onck, E. van der Giessen
*Analysis of intergranular creep crack growth by means of grain-elements*
Computational Mechanics 20 (1997) 109-114

P.R. Onck, E. van der Giessen
*Influence of microstructural variations on steady state creep and facet stresses in 2-D freely sliding polycrystals*
International Journal of Solids and Structures 34 (1997) 703-726

P.R. Onck, E. van der Giessen
*On the simulation of creep crack growth by means of grain-elements*
In: J.C. Earthman, F.A.Mohamed (eds.), Creep and Fracture of Engineering Materials and Structures, The Minerals, Metals & Materials Society (1997) 471-480

A.C. Steenbrink, E. van der Giessen
*A Numerical Study of Cavitation and Yield in Amorphous Polymer-Rubber Blends*
Journal of Engineering Materials and Technology 119 (1997) 256-261

A.C. Steenbrink, E. van der Giessen
*Deformation and fracture of styrene-acrylonotril copolymer-rubber blends: microscopy studies of deformation zones*
Journal of Materials Science 32 (1997) 5505-5511

A.C. Steenbrink, E. van der Giessen
*Void growth in glassy polymers: effect of yield properties on hydrostatic expansion*
International Journal of Damage Mechanics 6 (1997) 317-330

A.C. Steenbrink, E. van der Giessen, R.J. Gaymans
*Modelling of cavitation and yield in amorphous polymer-rubber blends*
In: Deformation, Yield and Fracture of Polymers, Proceedings of the 10th International Conference, Cambridge, April 7-10 1997, The Institute of Materials, London, 266-269

A.C. Steenbrink, E. van der Giessen, P.D. Wu
*Void growth in glassy polymers*
Journal of the Mechanics and Physics of Solids 45 (1997) 405-437

**PHYSICAL CHEMISTRY OF THE SOLID STATE**
Delft University of Technology, Laboratory of Materials Science
Rotterdamseweg 137, 2628 AL Delft
phone +31 (15) 2782207, fax +31 (15) 2786730
e-mail J.E.M.Kerklaan-Koene@stm.tudelft.nl

## PERSONNEL

*Scientific staff*

| | |
|---|---|
| prof.dr.ir. E.J. Mittemeijer | (2782207) |
| dr. A.J. Böttger | (2782243) |
| dr.ir. R. Delhez | (2782261) |
| dr.ir. Th.H. de Keijser | |
| dr.ir. W.G. Sloof | (2784924) |
| dr.ir. M.A.J. Somers (till 1-10-1997) | |
| dr. H.W. Zandbergen | (2782266) |

*Post-doc's*

dr. P.J. Kooyman (SON)
dr. J. Jansen (NWO)
dr.ir. F.D. Tichelaar (FOM/SON)
dr.ir. H. Yang (EEG)

*Research fellows*

dr. V. Svetchnikov (Intas, from 15-9-1997)

*Graduate students*

drs. R.M.J. Bokel (SON)
ir. T.C. Bor (FOM)
drs. R.C. Currie (STW)
ir. P.C.J. Graat
drs. L.P.H. Jeurgens (FOM)
ir. J.-D. Kamminga (IOP)
drs. M.M.W. Peeters (FOM, from 1-9-1997)
drs. M.I. Pekelharing (FOM)
drs. L. Velterop (IOP)

*Guests*

dr. S.S. Malinov (Nuffic, from 1-9-1997)
Xia Ruidong (Nuffic, from 1-9-1997)

*Research students*

S.J. Everstein
M.C. Huisman (till 1-8-1997)
A.T.W. Kempen (till 1-1-1998)
M. van Leeuwen (from 1-9-1997)
L. Mol (from 1-11-1997)
M.R. Paulissen (till 1-8-1997)

*Technical assistants*

C.G. Borsboom
ing. E.J.M. Fakkeldij

C.D. de Haan
J. Helmig
T.R. de Kruijff
J.F. van Lent
ing. N.M. van der Pers
G.J.M. Sprong (till 1-7-1997)

## RESEARCH AREAS AND OBJECTIVES

1 *Thin Surface Layers and Interfaces*
- 1.1 Microstructure of, stress development, diffusion and phase transformations in multilayer systems
- 1.2 Formation, microstructure and internal stresses of surface layers
- 1.3 Structure of grain boundaries in ordered alloys

2 *Phase Transformations in Iron-Based Interstitial Alloys*
- 2.1 Ageing and tempering of iron-based interstitial martensites
- 2.2 The austenite-ferrite transformation in Fe-C alloys

3 *Microstructural Imperfections and Diffraction-Line Broadening*

4 *High Resolution Electron Microscopy for Structural Analysis*

## FACILITIES

- Scanning electron microscope (Jeol, JSM 6400 F) equipped with a field emission gun and provided with a large specimen analysis chamber. This microscope is also equipped with an energy-dispersive X-ray microanalysis system (Noran Voyager III).
- Electron probe X-ray microanalyser (Jeol, JXA-733) equipped with four wavelength-dispersive spectrometers and one energy-dispersive system. This instrument is provided with Noran Systems TN5500 and TN5600 for instrument control, data acquisition and data analysis.
- Fully automated equipment for scanning Auger electron spectroscopy (PHI 4300 SAM). The system offers the possibility of Auger depth profiling, secondary electron imaging, back-scattered electron imaging and scanning Auger microscopy.
- Fully automated equipment for X-ray photoelectron spectroscopy (PHI 5400 ESCA). The instrument is provided with a dual anode X-ray source and an ion-gun for depth profiling. The system offers the possibility of small area analysis, angle-resolved photoelectron spectroscopy and low energy Ion Scattering Spectrometry (ISS).
- HP/Apollo workstations (DN 3500) for instrument control, data acquisition and data analysis of the PHI 4300 SAM and the PHI 5400 ESCA systems.
- An UHV specimen processing chamber coupled to the PHI 5400 ESCA system. This chamber is provided with an ion-gun, two quadrupole mass spectrometers, a specimen heating device and a unit for controlled admission of reactive gases. One quadrupole mass spectrometer (Balzers QMG 112) is used for control and analysis of the gas composition. The other quadrupole mass spec-

trometer (Balzers QMG 422) is used for Secondary Ion Mass Spectrometry (SIMS).

- A Philips CM30T high-resolution transmission electron microscope (HREM) equipped with a twin lens. It can also be used in scanning mode (STEM) and quantitative X-ray micro-analysis (LINK system) can be applied.
- A Philips CM30UT-FEG 300 kV high-resolution transmission electron microscope equipped with an ultratwin lens and a field emission gun (FEG). Quantitative X-ray analysis (LINK system) can be applied. Both an off-axis CCD camera (for real time image acquisition) and a slow scan 1024×1024 pixel camera (for high quality image and diffraction acquisition) are present.
- EM400 transmission electron microscope (TEM) equipped with a twin lens. It can also be used in the scanning mode (STEM) and quantitative X-ray micro-analysis (Tracor system) can be applied.
- On-line and off-line image processing facilities (TIETZ system, Macintosh, IBM) are available for both CM30 microscopes.
- A IBM RS6000 58H computer is used for the collection and processing of through focus series of images and for structure reconstruction from electron diffractograms and HREM images.
- An advanced system to prepare and manipulate specimens, and to bring specimens into the microscope under a controlled atmosphere.
- Electrochemical polishing equipment (Struers) for specimen preparation.
- Ion-mills (Gatan, Barna, Baltec) for the preparation of TEM samples.
- Automated X-ray powder diffractometers: two Siemens D-500 (one with a scanning position sensitive detection system; both D500's will be replaced in the near future)/and a Siemens D5000 with Eulerian cradle. The present X-ray powder diffraction software is the Siemens Diffrac AT program package and rather comprehensive packages written in our laboratory for data collection, stress determinations and line profiles analysis (size-strain analysis). Most of the software will be updated along with the replacement of the diffractometers.

## RESEARCH REPORT 1997

### 1 *Thin Surface Layers and Interfaces*

#### 1.1 *Microstructure of, Stress Development, Diffusion and Phase Transformations in Multilayer Systems*

##### 1.1.1 *Growth Conditions, Microstructure and Stress Development in Multilayer Systems* (H. Yang, A.J. Böttger, E.J. Mittemeijer; group of J.-E. Sundgren [Linköping University, Sweden]; O. Thomas [University of Marseille, France]; B. Chenevier [Ec. Nat. Sup. de Grenoble, France]; F. Roux [Ion Beam Systems, Gréasque, France]; D. de Boer [Philips, Eindhoven])

The influence of the growth conditions on the state of stress in thin films (200 nm) and multilayers of sublayer thicknesses of 1-5 nm is investigated. Magnetron sputtered layers were prepared by using different Kr sputter gas pressures (1 to 8 mTorr) and a constant bias voltage. The macrostress of the crystalline layers has been established using the $\sin^2\psi$-method. All the layers show a strong <111> fibre texture which restrict the possible $\psi$-tilt angles. Because of these restrictions and the relatively weak intensity of the peaks the following methodology was used. To increase

the reliability of the peak positions obtained by fitting, the background (measured for an identical oxidised Si<100> wafer under the same conditions, $\psi$ and $2\theta$ ranges as the measurements for the specimens) is subtracted from the measured profile. Thereafter the peak positions were corrected for systematic errors using ZnO as a reference. Ni and Ag films (200 nm thickness prepared at various sputtering pressures) were measured. The average stresses of the pure Ni films change from tensile to slightly compressive with decreasing sputtering gas pressure. The stress of the pure Ag films, however, is slightly tensile and seems independent of the sputtering gas pressure. The stress values obtained by the $\sin^2\psi$ method are in good agreement with those obtained by substrate curvature measurements (University of Marseille). Line-profile analysis of the {111} Ag and {111} Ni reflections indicate that the grain size is decreasing with the increasing of the sputtering gas pressure for both Ag and Ni. In Ni films micro strain increases with increasing sputtering pressure. Also the macro stress in Ag/Ni multilayers were investigated using the same experimental methodology as used for the pure Ni and Ag layers. Because of the low intensities of most of the reflections a reliable determination of the peak positions is very difficult and no conclusive results have be obtained so far.

### 1.2 *Formation, Microstructure and Internal Stresses of Surface Layers*

#### 1.2.1 *The Interaction of Stresses and Phase Transformations in Surface Layers*
(R.C. Currie, L. Velterop, A.J. Böttger, R. Delhez, Th.H. de Keijser, E.J. Mittemeijer)

The incentive for this project is the frequent occurrence and the presumed mutual effects of stresses and phase transformations in layers and their substrates.

##### 1.2.1.1 *Configuration and Behaviour of Dislocations in Metal Layers under Stress*
(R.C. Currie, R. Delhez, A.J. Böttger, E.J. Mittemeijer; J.F. Jongste [DIMES/TN, Delft University of Technology])

In a previous Ph.D. project the relaxation of thermal stress in Al layers on oxide-covered Si single-crystal wafers was studied. A decrease of diffraction-line breadth coupled to the decrease in thermal stress was observed that was explained quantitatively. In this project Ag is chosen as model system due to the low stacking fault energy and high elastic anisotropy as compared to Al. Ag layers of thickness 100, 250 and 500 nm were deposited on Si wafers covered with natural oxide by means of electron beam evaporation at AMOLF Amsterdam. The layers possess a fibre texture consisting of a "matrix" of crystallites with a {111} plane oriented parallel to the plane of the layer and a substantial amount of growth twins with a {511} plane parallel to the layer-substrate interface. During annealing at temperatures above 523 K severe recrystallisation effects result in the formation of holes throughout the layer.
During thermal stress relaxation at room temperature a dependency between the decrease in X-ray diffraction peak breadth and the stress state within the layer is observed. Interpretation of the diffraction data with the biaxial stress state model yields resultant tensile stresses decreasing within several days from 160 MPa to 30 MPa in the matrix crystallites and a slower relaxation of the tensile stress from 170 MPa to 50 MPa in the twin crystallites. Simultaneously with the decrease in stress the microstrain (*i.e.* diffraction-line breadth) decreases significantly for both texture fractions. The relationship between the decrease of stress and the diffraction-line breadth indicates that the stress relaxation is governed by movement and subsequent annihilation of defects in the layer. Orientation- and reflection-dependent de-

crease of the diffraction-line breadth indicates that the mechanism responsible for the relaxation of the applied tensile stress is different for the matrix crystallites and the twin crystallites.
To assess the effect of elastic anisotropy of Ag on the observed stress relaxation 1000 nm thick Al layers were deposited onto oxidised Si wafers by sputter deposition at DIMES-TN at Delft University of Technology. The first stress relaxation experiments confirm the reflection- and orientation dependency of the decrease of diffraction-line breadth and the relationship between the stress state and diffraction-line breadth for all reflections. Attention will be paid to the initial stage of the stress relaxation to extract more detailed information on the relaxation process.
Monte Carlo calculations of the Fourier coefficients of diffraction-line profiles are currently performed to gain insight in the relationship between the reflection-dependent line breadth and the defect configuration during the strain relaxation process.
An Al standard suitable for the correction of instrumental effects in measured X-ray diffraction profiles was developed. This standard consists of spherical Al particles with a diameter smaller than 5 mm annealed for 10 hours at 550 °C in an Ar filled rotating quartz tube.

1.2.1.2 *Phase Transformations in Anisotropic Metastable Alloy Films* (L. Velterop, M.R. Paulissen, R. Delhez, Th.H. de Keijser, E.J. Mittemeijer, A. Buis; D. Reefman [Philips])

This project is performed in co-operation with (and financially supported by) Philips Research, Eindhoven and Philips Analytical, Almelo; project co-ordinator from Philips is dr. D. Reefman.
The word "anisotropic" in the title of the project means that the (elastic, magnetic, etc.) behaviour of the system depends on the direction with respect to the crystallographic and / or specimen axes. Appropriate anisotropic metastable alloy layers are Ag-rich Ag-Co and Ag-Ni thin layers. The precipitation in these layers can be rather well controlled.
The thin Ag-Co and Ag-Ni alloy layers were made (by Philips) by magnetron sputtering of 500 identical periods of 10 Å consisting of sublayers of 1, 1.5 or 2 Å Co or Ni plus 9, 8.5 or 8 Å Ag, respectively. The periodicity of 10 Å could not be detected by XRD, only reflections of a silver-rich phase were detected. XRD and transmission electron microscopy revealed that only a silver-rich phase was present and indicated that the Co or Ni was (non-homogeneously) dissolved in the Ag. The silver matrix exhibited a {111} fibre texture. From the shift of XRD reflections it was calculated that very high strains are present in the as-prepared Ag-Ni and Ag-Co layers: up to 0.5 %, whereas a pure Ag layer has no strain.
Details of the structure of the as-prepared Ag-Ni layers are still under study with TEM/HREM. It was reported last year that a large density of small twins (of a width of tens of nm) is present in the as-prepared alloy layers (not in the pure Ag layer). Upon heating of the alloys at 723 K the amount of twins decreased, the strains decreased (and the alloy decomposed). It was assumed, that twins would influence the positions of XRD reflections like stacking faults do: these cause peak shifts with a magnitude that depends on their amount, on their orientation and on the reflection considered. These peak shifts have to be excluded when calculating the strain in the layers. A method to do this has been developed. Further it has been shown that not only stacking faults, but also twins can cause peak shifts. In the literature approximations were performed that are justified only for low twin content, but for higher twin

contents (as occur in the present alloy layers) the peak shift sharply increases. For small twin widths the final formulae cited in the literature do not hold: this case still has to be explored.
Further HRTEM and CTEM work on the Ag-Ni layers is still in progress and mainly concerns the possible relation between the twins and the dislocations observed.
To investigate the influence of the non-homogeneity of the starting material, a start has been made with the examination of thin Mo-Ti layers. The layers were made at DIMES by magnetron sputtering of 1000 periods of 5 Å, each period containing 0.5 Å Ti and 4.5 Å Mo. It is expected that these layers can be homogenised by heating them at 900-1000 K (in accordance with the Mo-Ti phase diagram) to be able to perform several decomposition experiments on the same sample.
No low angle XRD reflections corresponding to a 5 Å periodicity were observed in the as-prepared layers. Only reflections of a Mo-rich bcc phase were detected, the peaks of which were rather symmetric. This suggests that the layers were indeed homogeneous. TEM and XRD observations indicate that the layers exhibit a {110} texture with a weak in-plane preferred orientation.
Upon heating, decomposition of the layers takes place. A BCC Ti phase is formed, although the stable modification of Ti at < 1150 K is HCP. TEM observations show that in the thinner parts of the TEM foil the BCC Ti has relaxed to an HCP structure.

1.2.2 *Coatings on Steel Tools; Relation between Deposition Parameters, Microstructure and Wear* (J.-D. Kamminga, R. Delhez, Th.H. de Keijser, E.J. Mittemeijer)

This project is part of the project IOT94005 as a co-operation of six research groups under auspices of the IOP-Oppervlakte Technologie (Surface Technology): (i) the group Inorganic Materials of TNO-TPD in Eindhoven (drs. C.I.M.A. Spee and dr. A.D. Kuypers), (ii) the group Materials Technology of TNO-MI in Apeldoorn (dr.ir. A.J. Huis in 't Veld), (iii) the Laboratory of Applied Inorganic Chemistry of the Delft University of Technology (prof.dr. J. Schoonman), (iv) the group Tribology of the Faculty of Mechanical Engineering of the University of Twente (dr.ir. D.J. Schipper), (v) the group Tool Production and Automation of the Faculty of Mechanical Engineering of the Technological University of Eindhoven (dr.ir. A.J. Dautzenberg) en (vi) the Section Physical Chemistry of the Solid State of the Laboratory of Materials Science of the Delft University of Technology (dr.ir. R. Delhez, dr.ir. Th.H. de Keijser, prof.dr.ir. E.J. Mittemeijer). In each of the groups mentioned under (i), (iv), (v) and (vi) an Ph.D. student works. The project has a duration of four years and started officially on November 1, 1994.
For the work presented here TiN PVD layers have been prepared by the group of dr.ir. J.H. Dautzenberg. The TiN layers usually have thicknesses of 1 - 5 mm, and are deposited under various circumstances on a tool steel, a cermet and on stainless steel foils.
In our research the average macrostresses are determined using an X-ray diffraction method, the so-called $\sin^2\psi$ method, which uses spacings of crystal lattice planes as a "strain gauge". The magnitude of the average (compressive) macrostresses obtained

(i) is of the order of –1 to –10 GPa (using for TiN a Young's modulus equal to 600 GPa and a Poisson constant $\nu = 0.25$),
(ii) depends on the substrate material used,
(iii) is the lower the thicker the TiN layer concerned and

(iv) varies with the nitrogen concentration in the layers.

The stresses in these layers are considered to consist of a "thermal" component and a component caused during growth of the layer, the "growth" stress. The thermal stress is caused by the difference in thermal shrink of substrate and layer after cooling from the deposition temperature (~570 K) to room temperature. The growth stresses in the layers can be ascribed to atoms "peened" into the layer during sputter-deposition (the so-called "atomic peening" mechanism). The stress caused by the introduction of misfitting particles into the layer, yielding interstitial or substitutional point defects, has been modelled. From the model it follows that the high growth stresses may be caused by about 1 at.% titanium atoms on nitrogen sites in the TiN lattice. Predictions from the model for the lattice spacing show a good agreement with the measurements made.

The dependence of the growth stress on layer thickness has been described accurately by stress gradients in the layers. Although the stress gradients correlate with a change in microstructure with depth in the layer, the origin of these stress gradients is yet unclear.

Further research aims at a description of the microstrains in the layers. Microstrains are caused by faults in the lattice and are revealed by broadening of the peaks measured by X-ray diffraction. For the present layers the XRD peaks are very broad. The effect of the strain fields of point defects on the XRD peak width has been modelled and it has been shown that point defects do not lead to significant peak broadening. Now our attention is focused at the description of peak broadening caused by dislocations. The first results show that the strain fields of dislocations do induce significant peak broadening.

### 1.2.3 *Oxidation of Metals*

#### 1.2.3.1 *Initial oxidation of Fe and Fe-N Phases* (P.C.J. Graat, M.A.J. Somers, H.W. Zandbergen, E.J. Mittemeijer)

Polycrystalline $\alpha$-Fe and polycrystalline $\varepsilon$-$Fe_2N_{1-x}$, with nitrogen contents at the surface ranging from 25.0 at.% and 28.4 at.% (*i.e.* x = 0.21-0.33), were oxidised at oxygen pressures of $8 \cdot 10^{-5}$ and $10^{-4}$ Pa and at temperatures ranging from 300 K to 600 K. Prior to oxidation the surfaces of the samples were either sputter cleaned with $Ar^+$ ions, or sputter cleaned followed by annealing to remove the sputter-induced damage.

*XPS analysis*

From analysis of XPS N 1s spectra of $\varepsilon$-$Fe_2N_{1-x}$ it was shown that the sputter cleaning pre-treatment of $\varepsilon$-$Fe_2N_{1-x}$ leads to a reduction of the N concentration in the surface region and that subsequent annealing at 573 K leads to restoration of the N concentration by suppletion of N from the bulk. A linear relation was observed between the nitrogen concentration in the substrate and the binding energy of N 1s electrons, which is attributed to transfer of negative charge from iron atoms to nitrogen atoms, due to the stronger electronegativity of nitrogen as compared to iron. It was found that upon oxidation of $\varepsilon$-$Fe_2N_{1-x}$, most of the nitrogen atoms, which are released as Fe atoms are incorporated in the oxide film, accumulate underneath the oxide film. For $\varepsilon$-$Fe_2N_{1-x}$ oxidised at temperatures $\geq$523 K the released nitrogen atoms rapidly diffuse from the nitride-oxide interface into the bulk of the $\varepsilon$-$Fe_2N_{1-x}$ layer. For $\varepsilon$-$Fe_2N_{1-x}$ oxidised at temperatures $\leq$423 K the released nitrogen atoms are taken up in the part of the $\varepsilon$-$Fe_2N_{1-x}$ substrate adjacent to the oxide. If the nitrogen

concentration underneath the oxide film exceeds the maximum solubility of nitrogen in $\varepsilon$-$Fe_2N_{1-x}$, which is the case for sputter cleaned + annealed $\varepsilon$-$Fe_2N_{1-x}$, an additional peak appears in the XPS N 1s spectrum. This peak is associated with the nitrogen atoms in excess of the maximum solubility, which are assumed to be "adsorbed" at the nitride-oxide interface and to have a relatively large negative charge.

The procedure for quantitative analysis of XPS spectra containing overlapping peaks, previously developed in our group, was applied to Fe 2p spectra of oxidised $\alpha$-Fe and $\varepsilon$-$Fe_2N_{1-x}$. The procedure provides a full reconstruction of the experimental Fe 2p spectra from reference spectra for $Fe^0$, $Fe^{2+}$ and $Fe^{3+}$ taking the thickness of the thin oxide film and the $Fe^{2+}$ and $Fe^{3+}$ concentrations in the films as fitting parameters. It was verified that the values obtained for the oxide-film thickness agree with thickness values determined from the intensity of the corresponding O 1s spectra and with the thickness values resulting from an ellipsometric analysis during oxidation. The sensitivity of the reconstruction procedure with regard to film thickness and film composition was tested.

It was shown that the composition of the oxide films changes with film thickness from approximately FeO to a composition close to $Fe_3O_4$, irrespective of the pre-treatment applied or the nitrogen content in the substrate. For a certain oxygen exposure, the oxide-film thickness was observed to decrease with increasing nitrogen concentration in the substrate, which is ascribed to an increase of the net positive charge on the iron atoms in the substrate due to transfer of negative charge to nitrogen atoms. Thus, upon oxidation of the iron atoms to iron cations, less electrons can be released, and consequently less oxygen atoms adsorbed at the oxide surface are reduced to oxygen anions. This may induce a smaller potential difference over the film and consequently a slower oxidation rate.

*Ellipsometric analysis*

Ellipsometry was performed at Utrecht University (provided by dr. A.M. Vredenberg) and applied for *in situ* monitoring of the oxide-film thickness as a function of oxidation time. Also, the optical properties of the substrates and the oxide films were determined. It was shown that the thickness and (real) refractive index of an iron-oxide film growing on either an $\alpha$-Fe substrate or an $\varepsilon$-$Fe_2N_{1-x}$ substrate can both be calculated from the ellipsometric parameters, $\Delta$ and $\Psi$, which are determined continuously during oxidation. The linear dependence of $\Delta$ on the oxide-film thickness, which followed from the present treatment, agrees well with earlier experimental results. It was shown that accounting for the effect of surface and interface roughness leads to a higher value for the film thickness and to smaller value of the (real) refractive index of the oxide.

The refractive index and the extinction coefficient (respectively the real and the imaginary part of complex index of refraction) of both the $\alpha$-Fe and $\varepsilon$-$Fe_2N_{1-x}$ substrates, were observed not to be modified by an annealing treatment after sputter cleaning. This implies that the optical constants of the substrates do not strongly depend on the amount of sputter-induced defects and on the nitrogen content. The (real) refractive index of the oxide film growing on an $\alpha$-Fe substrate was found to be equal to that for the oxide film growing on an $\varepsilon$-$Fe_2N_{1-x}$ substrate, irrespective of the pre-treatment of the substrate. This observation is consistent with the XPS results, in that the oxide-film composition does not depend (strongly) on the substrate composition or pre-treatment.

The evolution of the oxide-film thickness on $\alpha$-Fe as a function of time was earlier

successfully described with the model due to Fromhold and Cook, and has now also been applied to the oxidation of $\varepsilon$-$Fe_2N_{1-x}$. The most sensitive parameters in the model, which presumes coupled currents of ions and electrons, are the energy barrier for cation motion in the oxide film and the energy barriers for electron transport, *i.e.* the substrate-oxide work function, $\chi_0$, and the oxygen-oxide work function, $\chi_d$. At the lower temperatures an excellent agreement of experimental and calculated oxidation curves was obtained by adopting a time-dependent difference of the metal-oxide and the oxide-oxygen work functions, $\Delta\chi$. It was concluded that layer-growth kinetics is governed by electric field enhanced cation transport through the oxide film. Further, it was demonstrated that tunnelling is the dominant electron transport mechanism at the lower temperatures (<400 K) and oxide films thinner than about 3 nm. At the higher temperatures and oxide films thicker than 3 nm thermal emission is the dominant electron transport mechanism.
The condition of the substrate surface prior to oxidation has a strong effect on the initial oxidation rate. The initial oxidation rate of sputter cleaned + annealed $\alpha$-Fe was observed to be lower than of sputter cleaned $\alpha$-Fe, which is associated with a less negative value of $\Delta\chi$. The initially less negative value of $\Delta\chi$ is ascribed to the presence of segregated nitrogen at the substrate surface and/or to a smaller amount of sputter-induced defects in the metal substrate. The initial oxidation rate of sputter cleaned + annealed $\varepsilon$-$Fe_2N_{1-x}$ was observed to be lower than of sputter cleaned $\varepsilon$-$Fe_2N_{1-x}$. This is attributed to the higher nitrogen concentration of sputter cleaned + annealed $\varepsilon$-$Fe_2N_{1-x}$ and the associated smaller potential difference over the oxide film. For sputter cleaned + annealed $\varepsilon$-$Fe_2N_{1-x}$ this effect is enhanced because during oxidation the maximum solubility of nitrogen in $\varepsilon$-$Fe_2N_{1-x}$ is exceeded and negatively charged nitrogen atoms accumulate at the nitride-oxide interface. Upon prolonged oxidation the oxidation rate of sputter cleaned + annealed $\varepsilon$-$Fe_2N_{1-x}$ was found to exceed the oxidation rate of sputter cleaned $\varepsilon$-$Fe_2N_{1-x}$. This is attributed to the development of $Fe_{1-\delta}O$ with a relatively large grain-boundary density, which can support a relatively large flux of Fe cations. At 472 K the difference between the oxidation rates for sputter cleaned $\varepsilon$-$Fe_2N_{1-x}$ and sputter cleaned + annealed $\varepsilon$-$Fe_2N_{1-x}$ was found to be smaller than at lower oxidation temperatures. This is attributed to the (partial) replenishment of nitrogen in the sputter-affected region from the bulk of the sputter cleaned $\varepsilon$-$Fe_2N_{1-x}$ sample, which occurs on heating to 472 K and on subsequent oxidation at this temperature.

*HREM analysis*

The constitution and morphology of the oxide layers, as observed with HREM and XRD, were found to depend on the substrate composition and the pre-treatment. The results for oxidised $\alpha$-Fe were described earlier. For $\varepsilon$-$Fe_2N_{1-x}$ it was found that oxidation at 400 K at $p_{O_2}=8\cdot10^{-2}$ Pa after sputter cleaning leads to the formation of a thin oxide film which is constituted mainly of relatively large $Fe_3O_4$ grains. The oxidation of sputter cleaned + annealed $\varepsilon$-$Fe_2N_{1-x}$ at 400 K leads to the formation of an oxide film which is constituted of relatively small $Fe_{1-\delta}O$ and $Fe_3O_4$ grains. The $Fe_{1-\delta}O$ grains were observed to be present adjacent to the $\varepsilon$-$Fe_2N_{1-x}$ substrate grains and had a preferred orientation with respect to these grains. $Fe_3O_4$ was found throughout the oxide film. The oxidation of $\varepsilon$-$Fe_2N_{1-x}$ at 573 K at $p_{O_2}=8\cdot10^{-2}$ Pa and $10^5$ Pa leads to the formation of an oxide layer which is constituted mainly of relatively large $Fe_3O_4$ grains, and contains also $Fe_{1-\delta}O$ and $\alpha$-$Fe_2O_3$ grains. The stability of $Fe_{1-\delta}O$ at temperatures lower than the temperature at which this phase is stabile in the Fe-O system can be a consequence of the preferred orientation relation between

$Fe_{1-\delta}O$ and $\varepsilon$-$Fe_2N_{1-x}$ grains and an associated low interfacial energy for an $\varepsilon$-$Fe_2N_{1-x}$-$Fe_{1-\delta}O$ interface as compared to an $\varepsilon$-$Fe_2N_{1-x}$-$Fe_3O_4$ interface.

1.2.3.2 *The Initial Stage Oxidation of Aluminium* (L.P.H. Jeurgens, W.G. Sloof, F.D. Tichelaar, C.G. Borsboom, E.J. Mittemeijer)

*Growth kinetics and oxide-film structure*

The initial stages of oxide-film growth on pure Al were studied by exposing a clean Al single crystal substrate to varying amounts of $O_2$(g) at a constant temperature, $T$, and oxygen pressure $P(O_2)$. In particular, the role of the composition and microstructure of the developing oxide-film upon the oxide-layer growth kinetics, is investigated. In order to understand the mechanism for oxide-film growth, a physical model for the dry, thermal oxidation of Al will be developed, describing the oxide layer growth kinetics as a function of its oxidation conditions and developing oxide-film microstructure.

Oxidation series as a function of total oxygen exposure were performed on sputtered clean Al(110), Al(112) and Al(115) crystal grains, at constant temperatures and oxygen pressures of 305 K, 573 K, 673 K and $1.0\times10^{-6}$ Torr and $1.0\times10^{-7}$ Torr, respectively. An UHV specimen processing chamber, equipped with an ion-gun, quadrupole mass spectrometer, specimen heating device and a unit for controlled admission of oxygen, was specially developed and built for these type of experiments. This UHV specimen processing chamber is directly coupled to our PHI 5400 ESCA analysis system.

The oxide-film thickness and composition of the oxide layers grown were obtained from the Al 2*s*, Al 2*p*, O 1*s* and C 1*s* photoelectron spectra (*i.e.* binding energy $E_B$ vs. electron intensity $I$) as recorded with X-ray Photoelectron Spectroscopy (XPS). The corresponding oxide-film microstructures were resolved by studying cross sections of several oxidised Al substrates, using High Resolution Electron Microscopy (HREM).

Investigation of the oxide growth kinetics (*i.e.* oxide-film thickness vs. total oxygen exposure) showed that at relative low oxidation temperatures, continued oxide-film growth is limited by the diffusion of cations through the developing oxide film. After 500 L (*i.e.* 1 L $\equiv 1\times10^{-6}$ Torr.s) total oxygen exposure, $Q$, at 305 K and $1.0\times10^{-6}$ Torr, the oxide-film thickness is independent of $Q$, and a 0.5 nm thick oxide-film has formed. At 673 K and $1.0\times10^{-6}$ Torr, oxide-film growth is completed after $Q$ = 10000 L, and a 3.9 nm thick oxide-film has formed. At a relative low oxygen pressure of $1\times10^{-7}$ Torr, linear oxide-film growth kinetics are observed, suggesting that oxygen transport from the gas phase to an active cation adsorption site on oxide-gas interface is rate-limiting at the initial stages of oxidation. At higher oxygen pressures, logarithmic type of growth kinetics are observed, suggesting that diffusion of cations through the developing oxide-film is rate-limiting.

XPS analysis shows a decrease in O/Al atomic ratio of the oxide-film with increasing oxidation temperature and increasing oxide-film thickness, towards the stoichiometric ratio of 1.5 of the crystalline $Al_2O_3$ phase. This also hints at outward diffusion of Al cations through the chemisorped oxygen layer.

Investigation of the HREM cross sections showed that in all studied cases an amorphous oxide-film with uniform thickness up to 4 nm is formed even at a high oxidation temperature of 773 K. The uniform thickness is a direct consequence of its amorphous structure, as there are no grain boundaries present acting as paths of easy cation (or anion) diffusion. Localised on the oxidised Al substrate, relative large (*i.e.* in the order of 30 nm) crystalline islands of $\gamma$-$Al_2O_3$ were also found. However, it is not

yet clear if these islands nucleated during oxide-film growth, or were already present on the sputtered clean surface prior to oxidation.

*Quantitative XPS Analysis of Thin Oxide Overlayers on a Metal Substrate*
For a correct quantitative XPS analysis of thin oxide overlayers grown on the Al substrate, it is necessary to accurately determine the primary photon excited electron intensity of each core-level photoelectron line separately, from the measured core-level XPS spectra of the oxidised specimen.
Each primary core-level photoelectron spectrum, consisting of the zero-loss peak plus its associated intrinsic fine-structure, is a direct result of the photoemission process itself and *intrinsic* excitations upon the creation of a localised core hole potential in the photoemission process. Due to the possibility of inelastic scattering of the primary photoelectrons in their passage through the solid and escape through the surface (*i.e. extrinsic* energy loss), this primary photon excited electron spectrum will be altered. In order to retain the original primary core-level photoelectron spectrum from the XPS spectrum measured at the sample surface, the correct background of inelastically scattered electrons must therefore first be calculated and subtracted from the measured XPS spectrum.
In the case of Al, where plasmon excitations are the dominating energy losses process, intrinsic and extrinsic bulk (BP) and surface plasmon (SP) excitations produce successive lines at the same series of energies with the extrinsic plasmon excitations constituting approximately 90% of these lines. Since a detailed knowledge of the differential cross section for inelastic electron scattering is lacking, it is difficult to separate the intrinsic fine-structure from the large extrinsic contribution to the BP and SP in the Al metal.
To this end, a new method was developed to indirectly retrieve the total Al(2*s*) and Al(2*p*) intrinsic BP and SP energy loss intensities from measured XPS spectra of the oxidised and sputtered clean Al metal. With this method the relative contribution of intrinsic BP and SP excitations to the total intrinsic plasmon excitation probability can be determined, separately. The method can easily be adapted to the case of other free-electron like metals covered by a thin overlayer (*e.g.* Si-oxide on Si-wafer).

1.3 *Structure and Properties of Interfaces* (R.M.J. Bokel, C.D. de Haan, F.D. Tichelaar, H.W. Zandbergen, F.W. Schapink)

The investigations on the structure and properties of grain boundaries in ordered alloys during the last year can be subdivided as follows:

a) Structure of incoherent twin boundaries in $L1_2$-ordered alloys
The structure of incoherent twin boundaries in CuPd(17%) alloys has been investigated by HREM, employing the exit-wave reconstruction method. In the disordered f.c.c. structured material, obtained by quenching, the boundaries showed an extended structure equivalent to the so-called 9R structure of incoherent twin boundaries in some f.c.c. metals. In this boundary structure, a rhombohedral layer of approximately 1 nm wide is present between the two crystals. The average boundary normal deviates approximately 8° from the {112} mirror plane of the bicrystal. In the ordered material a similar structure has been observed, but the influence of the change from the disordered structure to the s.c. ordered structure upon the structure of the boundary has not been resolved yet. In one case ordering could be discerned within the reconstructed image of the boundary area, but in other cases the ordering seemed to be absent at the boundary. Factors which influence the reconstructed image

are: 1) local foil thickness variations due to the specimen preparation procedure, 2) deviation of the electron beam direction from the [110] direction common to both crystals, and 3) electron beam orientation differences on either side of the boundary of unknown origin, In order to evaluate the influence of these parameters on the HREM imaging of grain boundaries, the method of exit wave reconstruction is being applied, see the next section and Section 4.1.

b) Influence of beam tilt on the exit-plane wave reconstruction of grain boundaries, obtained by HREM.
A general problem in the determination of boundary structures by HREM is the influence of very small deviations of the electron beam direction away from a crystallographic direction common to both crystals, on the image or the reconstructed exit-plane wave. This is especially true for thin metals foils which tend to bend within the electron microscope. In order to study this problem experimentally, BP whiskers grown on Si, containing numerous twin boundaries, are being studied by the exit-plane wave reconstruction. In this study small variations of the electron beam are introduced and the effect on the reconstruction is recorded. Large effects of seemingly negligible deviations of the beam direction on the reconstructed boundary structure are observed.

c) Convergent beam electron diffraction (CBED) at vertical grain boundaries.
The intersection configuration of deficit HOLZ lines g in the CBED central disc can be employed to determine structure factors $U_g$ in a small area of a specimen, since a probe as small as 1 nm in diameter can be located on the specimen. Previously, we have studied the relatively simple case of 3-beam dynamic diffraction in single crystals, both experimentally and analytically. Splittings of symmetrical HOLZ-lines g and h have been correlated to the structure factors $U_g = U_h$, and $U_{g-h}$. Now, we have studied CBED patterns obtained from grain boundaries in Si and CuPd(17%) with the electron beam aligned parallel to the boundary plane, such that HOLZ line g is positioned symmetrically to h with respect to the boundary plane. A splitting of HOLZ lines could not be observed when the cross-over region of the convergent beam was located on the boundary area. On the contrary, although positioning of the cross-over region has been proven to be very difficult, some HOLZ lines seemed to disappear completely. Evaluation of the results is in progress by computer simulation of CBED at vertical boundaries, and by analysing the beam geometry at the location of a grain boundary aligned vertical to this boundary.

2 *Phase Transformations in Iron-Based Interstitial Alloys: Thermodynamics of Fe-N phases and the Fe-N phase diagram* (M.I. Pekelharing, A.J. Böttger, S.S. Malinov, M.A.J. Somers, E.J. Mittemeijer; A.M. van der Kraan, M. Steenvoorde [IRI, Delft University of Technology]; C. Tang [SRS, Daresbury, UK])

*Thermodynamics of Fe-N(-C) phases: Ordering of N atoms in $\gamma$- and $\gamma'$ $Fe_4N_{1-x}$*
The tetrahedron approximation of the cluster variation method (CVM) is applied to describe the $\gamma/\gamma'$ phase equilibrium in the Fe-N system taking into account short-range ordering (SRO) and long-range ordering (LRO) of N and vacancies on the interstitial sublattices in $\gamma$-Fe[N] and $\gamma'$-$Fe_4N_{1-x}$. Usually the CVM is applied to substitutional (alloy) systems, however, in the present calculation the Fe-N phases have been conceived as consisting of a fully occupied Fe sublattice and an interstitial sublattice occupied by N atoms and vacancies. The $\gamma/\gamma'$ phase equilibrium in the Fe-N system was calculated by assuming that no changes occur in the Fe sublattice and

by describing the interactions in the Fe-N ($\gamma$, $\gamma'$) phases through effective Lennard-Jones (L-J) pair-potentials for the binary (N,V) system. The effective L-J parameters for V-V interaction are estimated using the enthalpy of formation and the lattice parameter of $\gamma$-Fe[N] without N, the N-N and N-V interaction parameters were optimised such that the best fit with the experimental data for the $\gamma$/ $\gamma'$-phase boundary was obtained. The CVM calculation also yields information on the lattice parameters, LRO and SRO. A comparison of the calculated and experimental lattice parameters shows that the calculated values are about 3 to 8 % smaller than the experimental values. In $\gamma'$ pronounced LRO is present, LRO increases with decreasing T and increasing N content. The results are consistent with those obtained previously by using the Gorsky- Bragg -Williams approximation to describe absorption isotherms. In $\gamma$ no LRO is present, but there are some indications for SRO in $\gamma$–Fe[N] *e.g.* non-Henrian behaviour of solubility data and discrepancies from random distribution of N atoms obtained from Mössbauer spectra. Comparing calculated results and Mössbauer data indications. The results from CVM show that there is a preference for N-V nearest neighbours over N-N or V-V nearest neighbours. Information on SRO deduced from Mössbauer spectra available in the literature show a similar tendency.

*Thermodynamics of Fe-N(-C) phases: Ordering of N atoms in $\varepsilon$-$Fe_2N_{1-z}$*

$\varepsilon$-$Fe_2N_{1-z}$ consists of an h.c.p. Fe lattice in which N atoms occupy octahedral interstices. It has been suggested on the basis of experimental nitrogen absorption isotherms and by modelling using the Gorsky-Bragg-Williams approximation that two types of long-range ordering of N atoms would occur: an A configuration for $\varepsilon$-$Fe_3N$, a B configuration for $\varepsilon$-$Fe_2N$ and a two phase region for intermediate compositions. Up to now there exist only weak and indirect indications, as obtained by Mössbauer experiments, that both types of ordering occur. To replenish the available set of experimental data, a series of homogeneous $\varepsilon$-$Fe_2N_{1-z}$ powders with a nitrogen content of 26-31 % is prepared at 450 °C and Mössbauer data are recorded (at liquid He temperature) at the IRI. Since conventional X-ray and neutron diffraction experiments could not distinguish in a conclusive manner between both types of ordering, the specimens used for the Mössbauer experiments were also used to obtain diffraction patterns at the Synchrotron Radiation Source (Daresbury, UK). This allowed to observe also the weak superstructure reflections due to ordering of interstitial N atoms.

*Phase Transformations of Fe-N Phases below 300 °C*

The iron-nitrogen phase diagram is not well established for temperatures below 300 °C. Starting from homogeneous iron-nitrogen powders prepared at a relatively high temperature, annealing experiments at temperatures below 300 °C were performed in order to provide information about the stability of phases and their composition at. Highly porous pure iron samples were nitrided to obtain homogeneous $\gamma$-Fe[N], $\gamma'$-$Fe_4N_{1-x}$ and $\varepsilon$-$Fe_2N_{1-z}$ with a varying nitrogen content. Several samples, consisting of either homogeneous $\gamma$-Fe[N], $\gamma'$-$Fe_4N_{1-x}$ or $\varepsilon$-$Fe_2N_{1-z}$ with a nitrogen content smaller than 20 at.%, were annealed in the temperature range 100-190 °C. X-ray diffraction analysis was used for identification of the appearing phases. Local enrichment of the $\varepsilon$-$Fe_2N_{1-z}$ phase was observed prior to the decomposition into $\gamma'$-$Fe_4N_{1-x}$ and $\alpha''$-$Fe_{16}N_2$.

3 *Microstructural Imperfections and Diffraction-Line Broadening* (T.C. Bor, R.C. Currie, L. Velterop, A.T.W. Kempen, R. Delhez, Th.H. de Keijser, E.J. Mittemeijer, N.M. van der Pers)

In principle, X-ray diffraction line broadening analysis is a powerful technique for studying all kinds of crystal imperfections, like crystallite size, stacking faults, dislocations. Successful application to powders of very small (<100 nm) undeformed crystallites is well known. In the 'remaining' and technologically very important class of deformed polycrystalline specimens much still has to be done.

The new "strain field" method of J.G.M. van Berkum (see his Ph.D. thesis, Delft, June 1994) will be considered in more detail and applied in some of the current projects along with other methodological developments in the field of diffraction-line broadening that are induced by the present projects.

3.1 *Analysis of Strain Fields in Solids; X-ray Diffraction-Line Broadening and Micromechanics* (T.C. Bor, A.T.W. Kempen, M.C. Huisman, R. Delhez, Th.H. de Keijser, E.J. Mittemeijer; E. van der Giessen [MIDEG])

The macroscopic behaviour of crystalline materials is strongly influenced by imperfections, such as dislocations and precipitates. Quantitative information about these imperfections is necessary to predict for example macroscopic mechanical material properties. These predictions are possible using micromechanics, which calculates the material behaviour on a local (mesoscopic) scale in a small volume element, that is representative of the microstructure of the material, using continuum mechanics. This representative element and its behaviour is then used to calculate the overall materials properties.
X-ray diffraction (XRD) analysis is in principle a powerful non-destructive technique to study crystal imperfections. Measurements of crystal reflections show line broadening which is a direct result of strain fields associated with the kind and number of imperfections. However, the nowadays available interpretations of measured line broadenings (for example: Warren-Averbach analysis) do not provide the characteristics of the imperfections that can be used directly in current physical models.
We already reported about the first steps to be made in the development of a line-broadening analysis method that approaches the analysis of line broadening from the opposite angle. Local strain fields are calculated by means of micromechanical models of the microstructure of the material. From these strain fields XRD line profiles are calculated and these can then be compared with measured ones. Then in principle, by adjusting the parameters of the micromechanical model, calculated profiles can be found that fit the measured XRD line profiles best, resulting in the determination of necessary microstructural information.
This year finite element calculations have been done for a 2D-representation of a material containing a periodic distribution of precipitates to obtain the displacement fields (elastic strains) around the precipitates. The results were compared with Eshelby's description of the strain field around a misfitting spherical inclusion in a continuum. It was shown that the average strain of the periodic description is equal to the average strain of Eshelby's description until high particle fractions (up to 40 %) even in the case of clustering of neighbouring particles. The average strain calculated on the basis of the shift of the centroid of the simulated XRD line profiles shows approximately equal behaviour.
However, a distinct difference exists between the mean square strain of both descriptions: the mean square strain of the periodic description shows direction dependence, related to the ordering of the particles, whereas the circularly symmetric Eshelby description is direction independent. This direction dependence is also reflected in the broadening of the simulated XRD line profiles resulting in the observa-

tion that the broadening of the simulated XRD line profiles is proportional to the product of the order of reflection and the root mean square strain in the specific crystallographic direction.
As model specimens for the project thin strips have been made (last year) of Fe alloys containing 2 at.% V and the Fe-V alloy strips are being nitrided under such circumstances that only VN precipitates are formed (and no Fe-nitride). Transmission electron microscope experiments are carried out to determine the VN precipitate dimensions and their spatial and size distribution, and to characterise the strain fields around them. The VN size and spatial distribution were shown to be dependent on the nitriding conditions (nitriding temperature and potential) which was also reflected in the measured XRD line profiles (shift and broadening). From simulation of the contrast in bright field of the strain fields in the Fe matrix surrounding the VN-precipitates it was possible to obtain an estimate of the precipitate matrix misfit.
Ball milled powders are a second type of deformed specimens that are under investigation. Mo powder is ball milled for 30 minutes up to 64 hours in a low impact ball mill in co-operation with the group of H. Bakker [University of Amsterdam]. Scanning Electron Microscopy pictures suggested that after short milling times still undeformed Mo starting powder is present in the ball milled powder. This was confirmed from X-ray diffraction-line profile measurements using a special, newly developed, diffraction-line deconvolution procedure. By applying this procedure the volume fraction undeformed Mo-starting powder in the ball milled powder was obtained with an accuracy of about 1 vol.%. Now the development of the volume fraction of undeformed

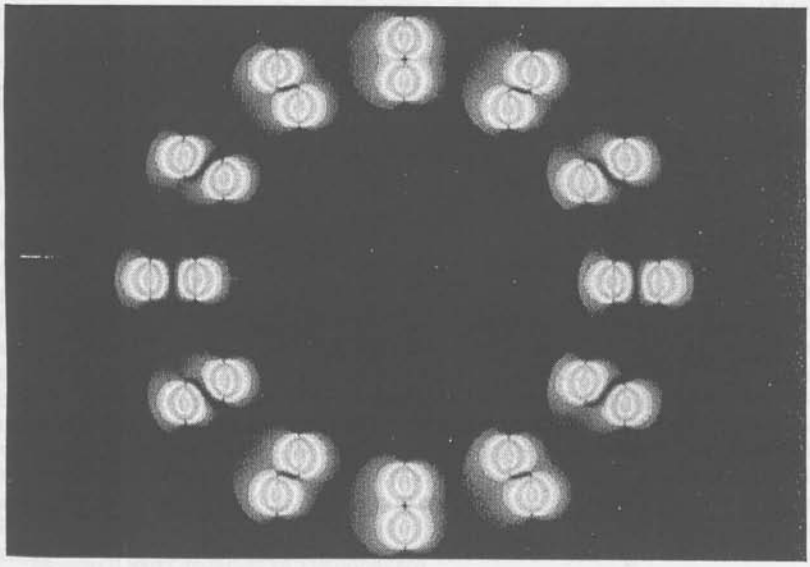

*Figure 1: Simulated Transmission Electron Microscopical dark field images of identical, parallel, misfitting, lenticular precipitates in a ferrite matrix (300 kV, 200 dark field). Both precipitates are 200 Å wide and have a misfit of 7 Å maximum perpendicular to the midplane of the precipitates. The precipitates have been rotated clockwise around each other. The contrast is shown for various amounts of rotation in cases arranged according to a circle.*

Mo-powder and the broadening of the deformed Mo-powder as a function of ball milling time is under investigation with emphasis on the development of a micromechanical model.

3.2 *The Problem of the "Appropriate" Standard Line Profile* (T.C. Bor, R.C. Currie, L. Velterop, R. Delhez, Th.H. de Keijser, N.M. van der Pers, G.J.M. Sprong)

In X-ray powder-diffraction analysis there is a need to know the shape of the line profile due to the non-ideal optics of the diffraction equipment and the wavelength distribution of the radiation used. Last year we reported that the most reliable way to obtain it, is to measure it using a general purpose standard as developed in our group (Powder Diffraction 10 (1995) 129-139) and that the line profiles (or the values of its parameters) at desired $2\theta$ values then should be obtained by an accurate interpolation procedure (see the Annual Report over 1996).
We have continued our efforts and are preparing an efficient, transportable procedure that can be published.

3.3 *X-ray Diffraction Software Development* (L. Velterop, J.-D. Kamminga, R. Delhez, Th.H. de Keijser, E.J. Mittemeijer; V.A. Kogan [Philips Analytical, Almelo])

We continued the elaboration of a PC program for performing the "Delft Truncation Correction" (as a part of the project described in Section 1.2.1.2). The aim is a to incorporate the program in (Philips) X-ray diffraction software. We are still involved in the further development in co-operation with Philips Analytical, Almelo, of PROFIT, "our" computer program for Total Pattern Fitting and of LPA, "our" program to determine crystallite size and microstrains from X-ray diffraction-line broadening.

4 *High Resolution Electron Microscopy for Structural Analysis*

4.1 *Structure Determination using Through Focus Exit Wave Reconstruction from a Series of HREM Images* (J. Jansen, R.M.J. Bokel, H.W. Zandbergen; D. van Dyck [RUCA, Antwerp])

The through focus exit wave reconstruction uses the focus dependence of the image distortion by the electron microscope to restore the distortion by the microscope optics. Using algorithms developed in a Brite-Euram project all useful information is extracted from a series of high resolution electron microscope images taken at different defocus values with known defocus increments. The result is the exit wave function which contains amplitude as well as phase information up to the information limit of the microscope. The exit wave function - or shortly exit wave - is the electron wave at the exit plane of the specimen. Since the electron wave passing through the crystal is continuously changed, the exit wave function is still thickness dependent, but not dependent on the distortion introduced by the electron microscope. As such it provides a major advantage over conventional high resolution electron microscopy (HREM), yielding a more reliable starting model for the electron diffraction refinement. The through focus exit wave reconstruction allows the determination of atomic positions with an accuracy up to the information limit of the microscope, which is about 1 Å for the high end electron microscopes. Because the shapes of the atoms are known this would allow determination of the atomic positions with an accuracy better than 0.1 Å.
Since the reconstructed exit wave contains amplitude and phase information one has also information about the disorientation of the crystal fragment from which the exit

wave is obtained. Such information is essential for detailed analysis of the atomic structures at grain boundaries, since very frequently the grains on the two sides of the grain boundary are not both in a perfect orientation. Likewise the thickness is an important parameter. We have developed a software package which allows the refinement of the misorientation and the thickness of very small areas (of the order of a unit cell). An important difficulty in this refinement was that the exit wave reconstruction does not take into account the mechanical vibration of the specimen. Simulations have been carried out in order to quantify the effects of such a vibration on the exit wave reconstruction and the subsequent refinement of the thickness and the orientation of a given area. The simulations show that for anisotropic specimen vibrations as occur in our microscopes, the exit wave cannot be used for a reliable refinement of the thickness and orientation. Consequently the exit wave reconstruction has to be changed such that mechanical vibration is taken into account.

4.2 *Structure Determination using Electron Diffraction in Combination with HREM* (J. Jansen, D. Tang, H.W. Zandbergen; H. Schenk [University of Amsterdam])

In 1993 an STW project was started aiming at the development of the use of Direct Methods in the structure determination from electron diffraction data, using HREM information as a starting set. In the first year two methods (a. using statistics for normalised structure factor and b. using misorientation induced differences in equivalent reflections) for the determination of the thickness of the specimen have been evaluated, both giving acceptable results.
In previous years a software package was developed in which the effect of dynamic scattering was explicitly included. Once a crude structure model is available (obtainable from the high resolution image or the reconstructed exit wave), a refinement is done of the atomic positions and the thermal parameters as well as the specimen thickness and crystal mistilt. The software package is called multi-slice-least-squares (MSLS). About 12 structures (partly of known compounds and partly of unknown compounds) have been determined using this MSLS program. Typical R values obtained in these refinements are 2-7 %, which are well comparable with the R values obtained with X-ray single crystal diffraction. The atomic positions obtained using MSLS refinement are in good agreement with those obtained from X-ray single crystal diffraction or neutron powder diffraction methods. Based on the know-how associated with the MSLS program, collaborations have been intensified with several groups in the field of electron diffraction (D. van Dyck [RUCA, Antwerp]; I. Voigt-Martin [University of Mainz]; D. Dorset [Buffalo]) which until now have been applying kinematic electron diffraction theory for structure analysis of inorganic as well as organic compounds.
In the last year we focused our attention on the further improvement of the method and on more complicated structures like the multiple twinned compound $La_{1-x}Ca_xMnO_3$ (see 4.11). In particular the use of chemical information (like bond lengths and bond angles) has been included in the software.

4.3 *Development of Equipment for Vacuum Transfer of Specimens* (H.W. Zandbergen, P.J. Kooyman; R. van Santen [Eindhoven University of Technology], J.A. Moulijn [Delft University of Technology])

This research program had as goal the realisation of specimen vacuum transfer from a manipulation chamber into the electron microscope (about $10^{-7}$ Torr). In the course of the project several new specimen holders were developed and built, which

allow specimen transfer at about $10^{-3}$ Torr. These specimen holders are now used routinely.
A completely new transfer system, allowing specimen handling at about $10^{-7}$ Torr, has been designed. This transfer system will be fixed to the electron microscope. At present a transfer vessel to allow transfer of specimens from the electron microscope to other equipment is being designed. Also a specimen preparation chamber, which allows thermal treatment of the specimen in a chosen atmosphere as well as additional ion milling of the specimen is being designed. At present the electron microscope has been adjusted for the new transfer system. During 1998 the electron microscope will be equipped with the transfer system after which evaluation experiments will be performed.
This project has initiated some proposals for the further use of the developed equipment (an STW proposal for a study of Raney-like catalysts and a SON proposal for detailed studies of grain boundaries and clean surfaces have been granted recently).

4.4 *Structures and Microstructures of Superconductors* (V.L. Svetchnikov, C. Treaholt, H.W. Zandbergen; S. Amelinckx, G. Tendeloo [University of Antwerp]; J. Aarts, R.J. Griessen [Vrije Universiteit, Amsterdam]; P.H. Kes [University of Leiden]; A.A. Menovsky [University of Amsterdam]; H. Rogalla [Twente University]; R.J. Cava [AT&T Bell Labs, Princeton]; V.M. Pan [Institute of Metal Physics, Kiev]; A.R. Kaul, I.E. Graboy [Moscow State University]; C. Chaillout [Laboratoire de Cristallographie, Grenoble]; S. Barillo [Minsk]; H. Fuess, G. Wirth [Hochschule, Darmstadt]; P. Rogl [Vienna].

Like in previous years, research activities were focused on three subjects: i) determination of structures and microstructures of materials which could be superconducting, ii) study of defects and intergrowths to correlate the presence of these defects with the properties, and to obtain ideas about possible new compounds, and iii) characterisation of devices containing superconducting components.

4.4.1 *Characterisation of Compounds which could be Superconducting*

This research is done predominantly in collaboration with R.J. Cava [AT&T Bell Labs, Princeton] and C. Chaillout [Laboratoire de Cristallographie, Grenoble]
Cava and co-workers have been preparing oxide compounds on which they have performed physical measurements, whereas the structure and microstructure has been determined in our group. In particular Cu and Co containing oxides were investigated. No new superconductors have been discovered.
Chaillout has provided several samples of $Ba_2Ca_3Cu_5O_{10+\delta}$ and $Ba_2Ca_2Cu_4O_{8+\delta}$ which were prepared by high pressure synthesis. We have continued our analysis of the structure and the superstructure by exit wave reconstructions and electron diffraction.

4.4.2 *Characterisation of Thin Superconducting Films and Devices*

Like previous years a considerable effort has been put into the characterisation of thin films of $YBa_2Cu_3O_7$ and $Bi_2Sr_2CaCu_2O_{8+\delta}$ on various kinds of support. This research has been mainly performed by V.L. Svetchnikov, C. Treaholt and I.E. Graboy (post-doc from Moscow). The thin layers and devices which were studied, were obtained from the P.H. Kes [University of Leiden], R.J. Griessen [Vrije Universiteit, Amsterdam], V.M. Pan [Institute of Metal Physics, Kiev], H. Fuess [Hochschule, Darmstadt], and A.R. Kaul [Moscow State University].

Major topics in these investigations are: i) the presence of extra phases, ii) the orientation of the grains in the superconducting films and iii) the substrate/film interface. In particular the microstructures of buffer layers between the substrate and the superconducting thin film and their effect on the quality of the superconducting thin film have been studied. Also sapphire substrates with double sided covering with superconducting film (*e.g.* $YBa_2Cu_3O_7$/sapphire/$YBa_2Cu_3O_7$) have been analysed. Finally multilayers of superconducting compounds with compounds showing a giant magnetoresistance have been analysed.

4.4.3 *Characterisation of Flux Pinning Defects and Weak Links*

The collaborations with P.H. Kes [University of Leiden] and G. Wirth [Hochschule, Darmstadt] on the characterisation of irradiation defects in thin films of $YBa_2Cu_3O_7$ and $Bi_2Sr_2CaCu_2O_8$ and single crystals of $Bi_2Sr_2CaCu_2O_8$ have been continued. The shape of the amorphous tracks along the whole trajectory of the fast ion has been the subject of the collaboration with Wirth. The aim of the analysis was to determine whether the theoretical calculations for minimum and maximum energy of the high energy ions for which amorphous tracks are formed are in agreement with the experiments. The experiments showed a reasonable agreement with the calculations based on TRIM software.
It has been investigated further whether defects like the antiphase boundaries occurring in Ti doped $Bi_2Sr_2CaCu_2O_8$ single crystals could be introduced in bulk materials. Although occasionally such defects (for instance in Nb doped $Bi_2Sr_2CaCu_2O_8$) are observed, their occurrence is far too small to result in an appreciable enhancement of the critical current.

4.5 *HREM on Catalysts* (P.J. Kooyman, C.D. de Haan, H.W. Zandbergen; R. van Santen [Eindhoven University of Technology], J.A. Moulijn, A.D. van Langeveld, A.M. van der Kraan, H. van Bekkum, J.C. Jansen [Delft University of Technology], A.J. Bliek, E.K. Poels [University of Amsterdam]; J. Lercher [Twente University]; V. Ponec, B.E. Nieuwenhuis, R. Louw [Leiden University]).

Practically all research on catalysts has been performed as part of a collaboration with or as service for other catalysis research groups in the Netherlands.
The vacuum transfer system to prepare specimens for transmission electron microscopy and transport them to the microscope while excluding air (developed in the framework of an STW project; see Section 4.3) has found many applications. Case-studies on Mo- and W-based sulphided hydrotreating catalysts showing nanometer and sub-nanometer sized particles, were continued. The various types of small species (ranging in size from 0.5 to several nanometers) were found to have distinctly different catalytic performances for various catalytic reactions. In collaboration with Van Santen the influence of preparation parameters on the stacking of the slabs for sulphided Mo on various supports has been studied. The distribution of various sulphided metals in and on zeolites has been studied in collaboration with Van der Kraan and Van Santen.
The collaboration with Van Bekkum on the catalytic applicability of the new microporous material MCM-41 has been continued. Extensive studies on new types of mesoporous materials are being conducted in collaboration with Van Bekkum and Jansen. Promising results using new templating materials have been obtained.
The effects of microwave heating on supported Ni-catalysts is being studied in collaboration with Bliek and Poels. Novel Au-based catalysts are studied in collaboration

with Ponec and Nieuwenhuis. Various types of Pt-based catalysts have been characterised in collaboration with both Louw and Lercher. The redispersion of noble metal catalysts in reductive dechlorination reactions has been proven in collaboration with Moulijn.

4.6 *Nitriding of Fe Layers with and without Oxide on Si, Coated with Ni* (F.D. Tichelaar, T.R. de Kruijff; D.K. Inia [Atomic and Interface Physics, Debye Institute, Utrecht University])

Microstructural analysis of iron nitrides by Transmission Electron Microscopy (TEM) has been performed. Nitriding was done by exposing ~280 nm iron layers on Si, covered by a ~40 nm Ni layer, to pure $NH_3$ at 1 atm. The microstructural evolution during nitriding was studied by nitriding with different exposure times at 275 °C and at 325 °C. In some cases the iron layer was oxidised before depositing the Ni layer. The nitrided layers were subjected to different analysis techniques, of which the TEM results are reported here. Cross sectional TEM analysis was done by bright-field imaging and local diffraction of separate grains with a 12 nm spot. It was found that the original columnar $\alpha$-Fe grains transform into smaller, more spherical, $\gamma'$-$Fe_4N$ grains which subsequently transform into larger $\varepsilon$-$Fe_{3-x}N$ grains. The formation of the $\gamma'$ grains occurs throughout the entire depth of the Fe layer, or preferentially at the Ni/Fe interface when an iron oxide layer is present at this interface. By comparison of nitrided and unnitrided layers in the TEM, it could be concluded that the nitriding did not induce extra porosity in the iron layers.

4.7 *Thin Film-Silicon for Application in Solar Cells* (F.D. Tichelaar, T.R. de Kruijff; A.J.M.M. van Zutphen [ECTM/DIMES, Delft University of Technology])

For the fabrication of photo active film-silicon layers on cheap substrates, at DIMES the thermal chemical vapour deposition (CVD) process is employed. Different substrates have been used, like single crystal Si, single crystal Si covered with Si oxide, and Si-Al(4%) ceramic material. Transmission Electron Microscopy (TEM) has been used for the microstructural characterisation of the deposited layers. It was found that on the $SiO_2$ covered substrate amorphous Si grows with polycrystalline Si islands growing into larger crystals (1-2 μm) at the surface of the layer (12 μm thick). The amount of amorphous material could be reduced to practically zero by choosing the right process parameters. When the oxide barrier layer was interrupted by periodically etched lines, oriented Si could be grown which showed, however, numerous twin related orientations with respect to the substrate. On the porous ceramic substrate (~50% porosity), a ~50 μm Si layer could be grown which consisted of large Si grains, up to 30 mm, and contained numerous twins and stacking faults.

4.8 *Metallic Point Contacts* (T.R. de Kruijff, F.D. Tichelaar; N.N. Gribov, J. Caro [DIMES/TN, Delft University of Technology])

Nanofabricated metallic point contacts are produced at DIMES by depositing metal films on both sides of a $Si_3N_4$ or a Si membrane (100 nm) containing ~50 nm × 50 nm holes. One of the layers can also be a multilayer. This is the case for the fabricated Cu/Co multilayer point contacts which yield giant magneto resistance signals. Various procedures (dry and wet etching, e-beam lithography) and chronology of procedures to create the holes and the metal layers have been tried to obtain suitable point contact, *i.e.* a high quality and flat interface between the two metal layers at the holes. A major problem for the microstructural characterisation of the layers

and the interface at the point contact turned out to be specimen preparation for cross sectional TEM analysis. The membrane is susceptible to damage during preparation, and the metallic layers adhere poorly to the membrane, *i.e.* when the specimen reaches electron transparent thicknesses, the layers disconnect from the membrane. A technique has been developed to circumvent mechanical damage of the membrane, and model materials (Cr and Al) have been chosen which do adhere sufficiently. This system is prepared in the same way as the Co/Cu multilayer contacts, and can be prepared for cross sectional TEM analysis. Final experiments are underway to demonstrate the high quality interfaces at the point contacts.

4.9 *InAsP Layers on Misoriented (100) InP* (F.D. Tichelaar, T.R. de Kruijff; T. Marschner, M.R. Leys [Eindhoven University of Technology])

In Eindhoven, InAsP layers of 40 nm and 400 nm thickness have been grown on InP substrates with a 0.5° deviation from (100) towards (111)B. Relaxation measurements of the layers by XRD predicted dislocation densities for $\alpha$ and $\beta$ dislocations (line directions $[1\bar{1}0]$ and [011] respectively) on the assumption that glide of these dislocations have relaxed the InAsP layers. An analysis of the dislocations at the interface between layer and substrate was attempted by Transmission Electron Microscopy (TEM) to measure dislocation densities. To this end plane view specimens were prepared for TEM by ion milling away the substrate partly. Moiré fringes caused by the overlap of substrate and layer complicated the analysis severely. The densities of dislocation of type $\alpha$ and $\beta$ found in TEM could therefore not be determined unambiguously. For example, the $\alpha$ dislocations seemed to be split in pairs, and surface steps also give a line like contrast, similar to dislocations. In addition, in the 400 nm layer specimen, dislocations were also found with line directions [010] and [001]. The density of these dislocations is comparable to that of the $\alpha$ and $\beta$ dislocations. Therefore the assumption that only $\alpha$ and $\beta$ type dislocations are responsible for relaxation is not always valid.

4.10 *SiGe Growth on Si: Quantum Wells and Single Layers* (F.D. Tichelaar, T.R. de Kruijff; P. Luckey, A. Suslov, J. Caro [DIMES/TN, Delft University of Technology]; J. Shi [DIMES/ET, Delft University of Technology])

A SiGe quantum well consisting of several Si SiGe layers has been deposited on Si at DIMES. With Transmission Electron Microscopy (TEM) the layer thicknesses, and the defect density and character at the SiGe/Si interfaces have been determined. The defects consisted of 60° dislocations dissociated into partials lying on a {111} plane inclined to the {100} type interfaces. The single layer structures vary in thickness between 3 and 200 nm. The Ge content of the layers varied between 30 and 67 at.%, depending on the growth conditions of the CVD process (growth time, temperature, and pressure). By TEM the layer morphology and defect structure was investigated. For layer thicknesses larger than ~10 nm at 50 at.% Ge, relaxation of the lattice mismatch between SiGe and the substrate has been observed to occur by two mechanisms: misfit dislocations at the interface and island formation. Also stacking faults have been observed within the islands.

4.11 *Characterisation of Various Materials* (P.J. Kooyman, C.D. de Haan, H.W. Zandbergen; S.J. Andersen [Trontheim, Norway]; J. Aarts [Leiden University])

a) In the last four years manganese oxides played a crucial role in the research hype of the giant magnetoresistance (GMR). Magnetoresistance the effect that

the resistance of a material depends on the magnetic field applied. Since magnetoresistance is widely used (*e.g.* reading heads in computer hard disks) there is a strong technological interest for GMR, in particular as films. Very thin films are of special interest because they are most suitable for multi-layer devices, for instance with superconductors. But the properties of films of 4-12 nm are quite different from those of films which are thicker than 50 nm, although they can all be made such that they are very smooth, single phase and well crystalline. To understand this behaviour we have started a detailed study on the structure and microstructure of 6 nm and 12 nm thin films of $La_{0.7}Ca_{0.3}MnO_3$ on $SrTiO_3$ substrates. Electron microscopy revealed important differences between the (micro-)structures of the thin and thick films of $La_{0.7}Ca_{0.3}MnO_3$. The main differences for the thin films are i) the size of the unit cell is constrained by the substrate, ii) the film is (almost) uniformly b-axis oriented, iii) twin boundaries occur with a high density; iv) the tilts of the $MnO_6$ octahedra are smaller and different, v) the $MnO_6$ octahedra are Jahn-Teller distorted. In particular the last two differences are probably responsible for the different properties and since they are imposed by the substrate they can only be prevented by changes in the substrate (like other material, deliberate surface roughness).

b) Small precipitates in commercial Al-Mg-Si alloys play a crucial role in increasing their mechanical strength. The composition and structure of the b" phase, occurring as precipitates of typically 4×4×50 $nm^3$, which are associated with a particularly strong increase in mechanical strength, has been determined. Element analysis using a small electron beam probe indicates the composition to be $Mg_5Si_6$. A rough structure model was obtained from exit waves reconstructed from high resolution electron microscopy images. The structure was refined with electron nano-diffraction data (overall *R*-value of 3.1 %) using a recently developed least squares refinement procedure in which dynamic diffraction is fully taken into account.

c) The synthesis of zeolites is studied in collaboration with Van Bekkum [Delft University of Technology]. Thus, materials resulting from new synthesis methods for (substituted) BEA have been studied for crystallinity, crystallite size and surface (amorphous) deposits. Also, totally new mesoporous materials prepared using new templates are yielding promising results.

d) New processes for the preparation of ceramic powders are being developed in the group of Scarlett [Delft University of Technology]. The characterisation of these powders is focused on the particle morphology and size distribution in correlation with particle composition. The relation between these data and the preparation condition is studied.

PUBLICATIONS

R. Benedictus
*Solid state amorphisation: Thermodynamics and kinetics*
Ph.D. thesis, Delft University of Technology (1997) 137

T.C. Bor, R. Delhez, E.J. Mittemeijer, E. van der Giessen
*Simulation of X-ray diffraction-line broadening for a material containing misfitting precipitates*
Materials Science & Engineering A 234/6 (1997) 896-899

R.J. Cava, H.W. Zandbergen, J.J. Krajewski, T. Siegrist, H.Y. Hwang, B. Batlogg
*$Ln_3Cu_4P_4O_2$ a new lanthanide transitia metal pnictide oxide structure type*
J. Solid State Chem. 129 (1997) 250-256

B. Dam, C. Traeholt, B. Stäuble-Pümpin, J. Rector, D.G. de Groot
*The relation between the defect structure, the surface roughness and the growth conditions of $YBa_2Cu_3O_{7-\delta}$ films*
Journal of Alloys and Compounds 251 (1997) 27-30

P.J. French, P.M. Sarro, R. Mallee, E.J.M. Fakkeldij, R.F. Wolffenbuttel
*Optimization of a low-stress silicon nitride process for surface-micromachining applications*
Sensors and Actuators A: Physical 58 (1997) 149-157

M.J. van Genderen, A. Böttger, E.J. Mittemeijer
*Formation of $\alpha$"-iron nitride in FeN martensite: nitrogen vacancies, iron-atom displacements, and misfit-strain energy*
Metallurgical and Materials Transactions A 28A (1997) 63-77

M.J. van Genderen, M. Isac, A. Böttger, E.J. Mittemeijer
*Aging and tempering behavior of Iron-Nickel-Carbon and Iron-Carbon martensite*
Metallurgical and Materials Transactions A 28A (1997) 545-561

M.J. van Genderen, S.J. Sijbrandij, A. Böttger, E.J. Mittemeijer, G.D.W. Smith
*Atom probe analysis of initial decomposition of Fe-N martensite*
Materials Science and Technology 13 (1997) 806-812

M.J. van Genderen, S.J. Sijbrandij, A. Böttger, E.J. Mittemeijer, G.D.W. Smith
*Atom probe analysis of the first stage of tempering of Iron-Carbon-Nitrogen martensite*
Zeitschrift für Metallkunde 88 (1997) 401-409

P.C.J. Graat, M.A.J. Somers
*Quantitative XPS analysis of thin iron-oxide films effect of elastic electron scattering*
In: Ecasia 97. European Conference on Applications of Surface and Interface Analysis. John Wiley & Sons Ltd., Chichester, U.K. (1997) 805-808

P.C.J. Graat, M.P.H. Brongers, H.W. Zandbergen, M.A.J. Somers, E.J. Mittemeijer
*HREM investgation of the constitution and the crystallography of thin thermal oxide layers on iron*
In: Microscopy of Oxidation, Vol. 3, The Institute of Materials, London (1997) 503-514

P.C.J. Graat, M.A.J. Somers, E.J. Mittemeijer
*XPS investigation of the initial oxidation of $\varepsilon$-$Fe_2N_{1-x}$*
In: Ecasia 97. European Conference on Applications of Surface and Interface Analysis. John Wiley & Sons Ltd., Chichester, U.K. (1997) 317-320

P.C.J. Graat, M.A.J. Somers, A.M. Vredenberg, E.J. Mittemeijer
*On the initial oxidation of iron: Quantification of growth kinetics by the coupled-currents approach*
Journal Applied Physics 82 (1997) 1416-1422

I.E. Graboy, N.V. Markov, V.V. Maleev, A.R. Kaul, S.N. Polyakov, V.L. Svetchnikov, H.W. Zandbergen, K.H. Dahmen

*An improvement of surface smoothness and lattice match of $CeO_2$ buffer layers on R-sapphire processed by MOCVD*
Journal of Alloys and Compounds 251 (1997) 318-321

R.H. Jutte, B.J. Kooi, M.A.J. Somers, E.J. Mittemeijer
*On the oxidation of α-Fe and ε-$Fe_2N_{1-z}$: I. Oxidation kinetics and microstructural evolution of the oxide and nitride layers*
Oxidation of Metals 48 (1997) 87-109

B.J. Kooi, M.A.J. Somers, R.H. Jutte, E.J. Mittemeijer
*On the oxidation of α-Fe and ε-$Fe_2N_{1-z}$: II. Residual strains and blisters in the oxide layer*
Oxidation of Metals 48 (1997) 111-128

P.J. Kooyman, P. van der Waal, H. van Bekkum
*Acid dealumination of ZSM-5*
Zeolites 18 (1997) 50-53

A. Lagerwaard, K.J. Volkers, D. Camelot, P.J. Kooyman, J. van Geel
*Preparation and characterization of micrometer size nuclear material particles for analytical studies: a need for definition*
In: Workshop on The Status of Measurement Techniques for the Identification of Nuclear Signatures, Proceedings, Office for Official Publications of the European Communities, Brussels, Belgium (1997) 115-119

T.W. Li, R.J. Drost, P.H. Kes, C. Traeholt, H.W. Zandbergen, N.T. Hien, A.A. Menovsky, J.J.M. Franse
*Enhanced flux pinning in Bi-2212 single crystals by planar defects introduced via Ti-substitution*
Physica C 274 (1997) 197-203

J.W.H. Maes, J. Caro, C.C.G. Visser, T. Zijlstra, E.W.J.M. van der Drift, S. Radelaar, F.D. Tichelaar, E.J.M. Fakkeldij
*Novel post-etching treatment of small windows in oxide for selective epitaxial growth*
Applied Physics Letters 70 (1997) 973-975

J.W.H. Maes, P.W. Lukey, T. Zijlstra, C. Visser, J. Caro, E.W.J.M. van der Drift, F.D. Tichelaar, S. Radelaar
*Preparation of nanometer-scale windows in $SiO_2$ for selective epitaxial growth of Si based devices*
Microelectronic Engineering 35 (1997) 321-324

O.C. Mantel, H.S.J. van der Zant, A.J. Steinfort, C. Dekker, C. Traeholt, H.W. Zandbergen
*Thin films of charge density wave oxide $Rb_{0.3}MoO_3$ by pulsed laser deposition*
Phys. Rev. B 55 (1997) 4817-4824

T. Marschner, R.T.H. Rongen, M.R. Leys, F.D. Tichelaar, H. Vonk, J.H. Wolter
*Effects of tensile strain and substrate off-orientation on the growth of GaInAs/InP multiple quantum well structures by CBE*
Journal of Crystal Growth 175 (1997) 1081-1086

T. Marschner, F.D. Tichelaar, M.R. Leys, R.T.H. Rongen, C.A. Verschuren, H. Vonk, J.H. Wolter

*Epitaxial layer morphology of highly strained GaInAs/InP multiple quantum well structures grown by CBE*
Microelectronics Journal 28 (1997) 849-855

E.J. Mittemeijer, M.A.J. Somers
*Thermodynamics, kinetics, and process control of nitriding*
Surface Engineering 13/6 (1997) 483-497

S.V. Samoylenkov, O.Yu Gorbenko, I.E. Graboy, A.R. Kaul, S.V. Svetchnikov, H.W. Zandbergen
*MOCVD of high quality $LuBa_2Cu_3O_{7-\delta}$ thin films*
Acta Physica Polonica A 92 (1997) 243-248

S.V. Samoylenkov, O.Yu Gorbenko, A.R. Kaul, Ya.A. Rebane, V.L. Svetchnikov, H.W. Zandbergen
*Metalorganic chemical vapour deposition of high quality $LuBa_2Cu_3O_{7-\delta}$ thin films. Peculiarities of growth and superconducting properties*
Journal of Alloys and Compounds 251 (1997) 342-346

W.G. Sloof
*Microstructural characterization of surface layers by combined application of various analytical methods - Analysis of chemically vapour deposited TiC coatings*
In: L.A.L.J. Sarton, H.B. Zeedijk (eds.), Proceedings of the Fifth European Conference on Advanced Materials and Processes and Applications, Vol. 4, Netherlands Society for Materials Science, Zwijndrecht (1997) 87-90

M.A.J. Somers, B.J. Kooi, L. Maldzinski, E.J. Mittemeijer, A.A. van der Horst, A.M. van der Kraan, N.M. van der Pers
*Thermodynamics and long-range order of interstitials in an h.c.p. lattice Nitrogen in $\varepsilon$-$Fe_2N_{1-z}$*
Acta Mater 45/5 (1997) 2013-2025

C. Traeholt, H.W. Zandbergen, T.W. Li, R.J. Drost, P.H. Kes, A.A. Menovsky, N.T. Hien, J.J.M. Franse
*TEM analysis of planar defects induced by Ti doping in Bi-2212 single crystals*
Physica C 290 (1997) 239-251

A.P. Voskamp
*Microstructural changes during rolling contact fatigue: Metal fatigue in the subsurface region of deep groove ball bearing inner rings*
Ph.D. thesis, Delft University of Technology (1997) 211

A.P. Voskamp, E.J. Mittemeijer
*State of residual stress induced by cyclic rolling contact loading*
Materials Science and Technology 13 (1997) 430-438

A.P. Voskamp, E.J. Mittemeijer
*The effect of the changing microstructure on the fatigue behaviour during cyclic rolling contact loading*
Zeitschrift für Metallkunde 88 (1997) 310-320

H.W. Zandbergen
*Electron microscope techniques*
In: T.L. Blundell (ed.), 26th Course Electron Crystallography "Ettore Majorana", Cen-

tre for Scientific Culture, Erice, Italy (1997) 33-44

H.W. Zandbergen
*Electron microscopy techniques*
In: D.L. Dorset et al. (eds.), Electron Crystallography, Kluwer Academic Publishers, Dordrecht (1997) 41-54

H.W. Zandbergen, S.J. Andersen, J. Jansen
*Structure determination of $Mg_5Si_6$ particles in Al by dynamic electron diffraction studies*
Science 277 (1997) 1221-1225

H.W. Zandbergen, J. Jansen
*Least squares refinement of structures from dynamic electron diffraction data*
In: T.L. Blundell (ed.), 26th Course Electron Crystallography "Ettore Majorana", Centre for Scientific Culture, Erice, Italy (1997) 157-167

H.W. Zandbergen, J. Jansen
*Least squares refinement of structures from dynamic electron diffraction data*
In: D.L. Dorset et al. (eds.), Electron Crystallography, Kluwer Academic Publishers, Dordrecht (1997) 231-241

H.W. Zandbergen, C. Traeholt
*Small particles*
In: S. Amelinckx , D. van Dyck (eds.), Handbook of Microscopy, Applications in Materials Science, Solid-State Physics and Chemistry, VCH, Weinheim, Germany (1997) 691-737

**PHYSICAL MATERIALS SCIENCE**
Delft University of Technology, Laboratory of Materials Science
Rotterdamseweg 137, 2628 AL Delft
phone +31 (15) 2782221/2782285, fax +31 (15) 2786730, e-mail ...@stm.tudelft.nl

## PERSONNEL

*Scientific staff*

dr. B.J. Thijsse (2782221, Thijsse@...)
dr.ir. J. Sietsma (0.2) (2782284, Sietsma@...)

*Graduate students*

ir. L.D. van Ee
ir. P.G. de Hey

*Research students*

T.P.C. Klaver

*Technical staff*

G.T.W.M. Bekking (0.7)

## RESEARCH AREAS AND OBJECTIVES

The group's central research theme is the study of atomic-scale processes in materials far from equilibrium. Defects and atomic transport, resulting either from thermal excitation of the material (diffusion, structural relaxation) or from excitation by energetic particle collisions, are the key subjects under study. The two main areas of research are (1) structural dynamics in metallic glasses and (2) ion-beam assisted deposition of thin films. Whereas our main interest lies in fundamental materials science, the relation with materials properties, for many of which defects play an important role, is never left out of sight. Experimental work forms the main part of the group's research effort. However, over the years computational simulation methods have become a second major research tool, both in its own right and as a supporting technique for the experimental work. Development of dedicated and general software is a third major part of our group's activities.

## FACILITIES

- Equipment for accurate measurement of creep, viscosity, tensile strength, electrical resistivity, and sound velocity.
- A combined apparatus for Ion Beam Assisted Deposition (IBAD) and Thermal Desorption Spectrometry (TDS), see Figure 2. The ultra high vacuum system contains as main parts: a quartz-crystal controlled electron beam evaporator for film deposition, two ion sources to generate He, Ar, or other ion beams, two electron beams for sample heating, and a quadrupole mass spectrometer to measure the desorption curves. A load lock and translator are part of the sample manipulation system.
- Most apparatuses are fully computer controlled. Together with the group's five Unix-based workstations and several other smaller computers, they form an integrated networked environment. Various types of mass-storage media and a

large collection of software are available.

## RESEARCH REPORT 1997

A research report over 1997 is not available.

## POLYMER TECHNOLOGY

Delft University of Technology, Department of Polymer Technology
Julianalaan 136, 2628 BL Delft
phone +31 (15) 2781828, fax +31 (15) 2787415, e-mail poltechsecr@stm.tudelft.nl

PERSONNEL

*Scientific staff*

| | |
|---|---|
| prof.dr.ir. A. Posthuma de Boer | (2786946) |
| prof.dr. T. Odijk | (071-5145346) |
| prof.dr. W.J. Mijs (part-time) | (2782630) |
| prof.dr. J. van Turnhout (part-time) | (2785090) |
| dr.ir. R. Addink (part-time 0.6) | (2782621) |
| dr.ir. J. van Dam (part-time 0.8) | (2782623) |
| dr.ir. A.E.M. Keijzers (part-time 0.5) (part-time) | (2782621) |
| dr.ir. K. te Nijenhuis | (2782630) |
| dr. A.D. Gotsis | (2786940) |
| dr. M. Wübbenhorst | (2786940) |

*Temporary scientific staff*

M. Chen (Chinese government), M.Sc.
dr. W.F. Jager (KNAW fellow)
dr. I. Krakovský
dr. M.A. Odriozola (OZS-PTN)

*Graduate students*

drs. ing. R.H. Bode (TWAIO)
ir. A. Boersma (SON/STW)
ir. H.J.A. Breur (TNO, with prof. De Wit)
ir. K.F.J. Denys (Cie. Beek)
drs. A. Duijndam
ir. F. van Eeten(TWAIO)
drs.ing. M.W.C.P. Franse
ir. G.J. Klap (FOM)
drs. P.H.J. Kouwer
ir. A.M. Romijn
drs. J.B. Ubbink (SON)
drs. H. Veenstra
drs. E.G.M. Veldman (Cie. Beek)
drs. R.J. de Vries (FOM)
ir. R.C. Willemse (IOP-Recycling)
S. Zohrevand, M.Sc. (IOP-Verf)

*Research students*

E. van de Berg
R. Cai
Y. Go
M. Groote Schaarsberg
R.P. Gulickx
A. Hensens

M.J.E. Kersten
S.M. van Klooster
B. van Lent
C.H. van de Pol
A.L. de Rooij
M.E. Schippers
A. Speijer
R.E. Staal
P.C.J. Verkooijen

*Technical staff*

| | |
|---|---|
| ing. H.J. van Benschop (part-time 0.6) | (2784603) |
| A.H. van Keeken | (2782629) |
| B. Norder | (2784262) |
| E. Sedlick (part-time 0.5) | (2782618) |
| G. de Vos | (2782622) |

*Secretaries*

M. Roodenburg-van Dijk (part-time 0.6)
A.J. Verheul-Mentink (part-time 0.5)

## RESEARCH AREAS AND OBJECTIVES

### 1 *Polymerisations*

The objectives of this part of the research programme of the group are: finding synthetic routes for the preparation of new polymers, obtaining understanding of the relations between chemical structure and physical properties, both with the ultimate aim of producing new macromolecular materials. The subjects of research are a/o: synthesis of new polymers with reactive side groups, mesogenic side groups, fluorescent chromophores or electron donor-acceptor side groups, connected to the main chain by spacers of variable length; preparation of networks by controlled cross-linking. Changes in the fluorescent characteristics of fluorescent probes, that can be built in into a polymer, give insight in polymerisation kinetics and network formation. Electrical and rheological properties as well as phase behaviour of the polymers will be investigated.

### 2 *Physical Chemistry and Rheology*

a) Development of models to describe the network formation in high molecular weight polymers. Application to kinetics of cross linking reactions and to structures of networks.
b) Film formation in water borne polymer dispersions and their rheology.
c) Rheology of dilute solutions of ultra high molecular weight polymers through porous beds

### 3 *Materials and Processing*

These investigations are aimed at obtaining understanding of properties of polymers required for creating new materials by blending and for rational processing. The research on blending is focused on formation, stability and properties of special poly-

mer blends, *i.e.* co-continuous and self-reinforcing polymer blends. The processing studies include structure evolution, rheology and processing properties of thermotropic liquid crystalline polymers.

4 *Electrical Properties*

This part of the research programme is aimed at the use of electric fields to investigate polymers and as a means to induce structural changes. Dielectric spectroscopy is explored for studying network formation, the properties of liquid crystalline main- and sidechain polymers, and the microstructure and properties of polymer blends. Dielectric spectroscopy is further applied for characterising the durability of coatings. Structural changes induced in polymers by an electric field are studied by measuring the electromechanical response of liquid crystalline elastomeric networks. Heat wave techniques have been developed which allow the measurement of the thermal properties of polymer films and of coatings during cross linking or polymerisation. The properties of polymeric nanostructures incorporated in zeolite crystals are analysed as well. Finally, hybrid structures consisting of a porous polymer film filled with an electro-active inorganic powder are synthesised and examined.

5 *Theory of Complex Fluids*

Statistical theory of complex fluids (DNA, proteins, membranes, polymers, liquid crystals, fibres, turbulence).

FACILITIES

1 *Characterisation*
- Two differential scanning calorimeters
- Fourier-transform infrared spectrometer
- Infrared microscope
- Three microscopes (polarisation and fluorescence)
- Small angle X-ray apparatus
- 2 Dynamic-mechanical-thermal analysers
- 2 Dielectric-thermal analysers
- Three tensile testers
- Torsion pendulum
- Deformation calorimeter
- Heat distortion temperature tester
- Scanning electron microscope
- Gel Permeation chromatograph
- Gas chromatograph
- Two Thermal gravimetric Analysers
- Pendulum Izod Impact tester
- Photothermal microcalorimeter

2 *Rheology*
- Two high pressure capillary viscositymeters
- Dynamic rheometer
- Rheometrics mechanical spectrometer
- Advanced rheometric expansion system for fluids

- Rotational viscometer
- Ubbelohde viscometer
- Extensional flow viscositymeter

3 *Processing*
- Injection moulding machine
- Two transfer moulding machines
- Four single screw extruders of various sizes
- Double screw extruder
- Three two-roll mills
- Two hydraulic presses
- Four-roller apparatus
- Cone-flow apparatus
- Spinning-drop apparatus

RESEARCH REPORT 1997

1 *Polymerisations*

1.1 *Fluorescent Probes for Polymer Characterisation and Monitoring (Photo)polymerisation Processes* (W.F. Jager)

Fluorescent probes can be employed as mobility probes since their emission spectra can be highly sensitive to the mobility of molecules in the medium that surround them. Suitable fluorescent probes can be employed for monitoring neat polymerisation processes, in which the medium changes from a low viscous liquid into a hard and glassy material throughout the process. Another application of fluorescent probes that is currently under investigation is the detection of phase transitions in polymeric media. Those phase transitions can be monitored by means of changes in the emission of fluorescent probes that have been added to, or covalently attached on the polymer. Among the objectives of our research is to find structure-property relationships for fluorescent probes by a systematic variation of their molecular structure. Functionalisation of fluorescent probes and covalent attachment to polymeric systems is another objective that will be actively pursued.

1.2 *Discotic Liquid Crystalline Polymers, Bearing Electron Donors and Electron Acceptors as Mesogenic Groups* (P.H.J. Kouwer)

In a mixture of two compounds, one electron donor, the other electron acceptor, both with a specific geometry (disk-like), the compounds can order into long columns. These composites can exhibit liquid crystalline mesophases, even if the original compounds are not liquid crystalline. If the structures are incorporated into a polymer, a stable, easy processable material is obtained. The objectives of our research is to study the supra-molecular structure as well as the physical properties of the composites by means of various characterisations.

2 *Physical Chemistry and Rheology*

2.1 *Formation of a Gel-Network of Liquid Crystalline Side-Chain Polymer Solutions* (M.W.C.P. Franse)

The preceding work of ir. P.M. Cordfunke is momentarily being continued. Typical

features of this project are 1) the hard synthesis of the liquid crystalline side-chain polymers and 2) rheological end small angle x-ray spectroscopic (SAXS) measurements of polymeric solutions forming a gel. A Statistical model for gel-network formation has been derived and is momentarily being tested on a somewhat simpler gel-system. In a later stage this model will be tested on the liquid crystalline side-chain polymer gels.

2.2 *Interaction of Multiphase Fluid Flow* (K.F.J. Denys)

One phase-core-flow experiments have been conducted in order to measure the influence of the water pH and salinity on the permeability of a porous medium (packed PMMA beads) pre-adsorbed with a polyelectrolyte (HPAM). This polymer is relevant in enhanced oil recovery techniques like polymer flooding and water shut-off. Attempts have been made in order to correlate the resulting permeability with the adsorbed layer extension.

2.3 *Film Formation from Water-Borne Polymer Dispersion* (S. Zohrevand)

We used turbidity measurement in order to study the film formation process Turbidity is defined based on two optical phenomena: Raleigh scattering and multilayer interference. The ageing, annealing and application of some additives in paint formulation cause some influences on film properties. In this project, these influences are investigated with the aid of turbidity method.

3 Materials and Processing

3.1 *Polymer Blends* (H. Veenstra)

In this project we investigate the influence of the molecular form and the rheological properties of the components on the formation and stability of network structures in polymer blends. It is found that block co-polymers may form such morphologies in a wide range of compositions when blended with common polymers. Blends with co-continuous morphologies present the best combination of the properties of their components and improved barrier properties.

3.2 *Interpenetrating Polymer Blends* (R.C. Willemse)

The goal of this project is to improve the mechanical properties of a mixture of waste plastics by creating an interpenetrating network. The main issue of the project is the study of the morphology development in a polymer blend (in general) in order to describe the effect of the process parameters on the formation of such interpenetrating networks for a wide composition range.

3.3 *Extensional Rheology of Polymer Melts* (A.D. Gotsis, M.A. Odriozola)

The resistance of polymer melts to extensional flow is examined in uniaxial elongational flow and in complicated flows, where both elongation and shear occur. Polymers with different molecular architecture are studied: Linear flexible chains, chains with different degrees of branching, block co-polymers and liquid crystalline polymers. The goal of this study is to find the association between the differences in response and the molecular forms and (super)molecular structures in the melt. The project was part of the "OZS polymeren PTN". The project will continue.

4 *Electrical Properties*

4.1 *Electrostriction in Rubber* (A.M. Romijn)

Electromechanical properties of rubbers are examined with a variety of methods; elongation parallel and perpendicular to an electric field are measured capacitively on a nanometer scale. Thermomechanical properties of rubbers are studied in a Perkin Elmer DMA7. Combination of these measurements yields valuable insight in the theory of rubber elasticity .

4.2 *Electrical Properties of Self-Reinforcing Polymer Blends* (A. Boersma)

In the processing of polymer blends, the morphology (size and shape of the inclusions) has a significant influence on the properties of the final product. Using dielectric spectroscopy, it was possible to obtain information about the morphology of a blend of thermotropic liquid crystalline polymer particles in a thermoplastic matrix.

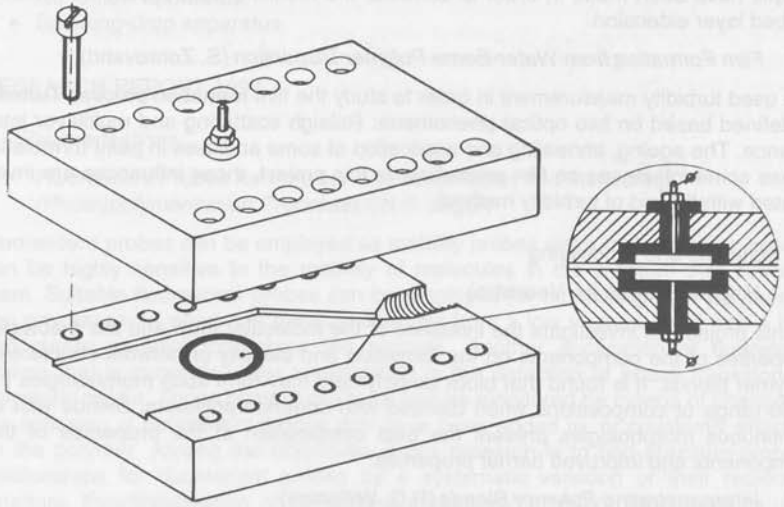

*Figure 1: Sheet extrusion die used in the dielectric analysis of the morphology of polymer blends during extrusion*

4.3 *Electrical and Optical Investigations on Liquid Crystalline Polymers* (M. Wübbenhorst)

Side chain liquid crystalline polymers based on a polysiloxane (collaboration with prof. Vancso [Twente University]), and poly(maleic acid) (collaboration with prof. Sudhölter [Wageningen Agricultural University]) backbone have been studied with dielectric relaxation spectroscopy. Besides the detection of various phase transitions and glass transitions we have found a relation between the local order parameter $S_I$ in smectic A phases and specific relaxations in the glassy and LC state. The molecular dynamics of highly ordered $S_E$ en hexatic B-phases has been elucidated.

4.4 *Nanostructures of Conjugated Polymers in Zeolite Crystals* (G.J. Klap)

In collaboration with the department of Organic Chemistry and Catalysis (prof. Van Bekkum/dr. Jansen) pyroelectric experiments have been done on zeolite single

crystals, loaded with several (a)polar molecules. The measurements reveal the polarity of the $AlPO_4$-5 lattice and give an explanation for the specific adsorption behaviour and the formation of long dipole chains (see Figure 2). Furthermore, the crystallographic inclusion of monomers in the zeolite lattice was studied with polarised FTIR microscopy.

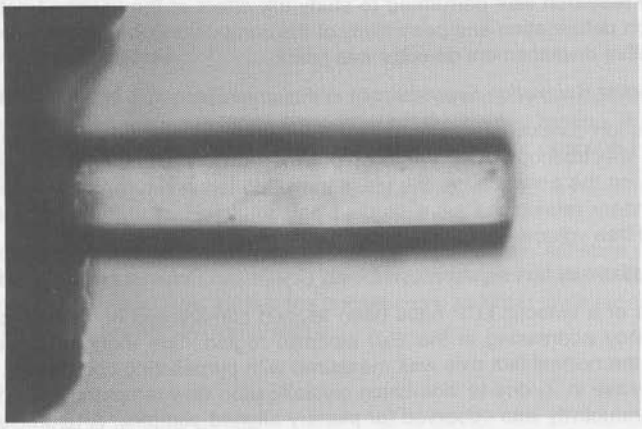

(a)

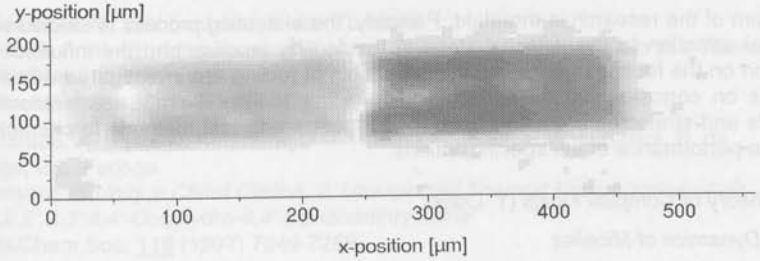


(b)

*Figure 2: (a) Micrograph of an $AlPO_4$-5 crystal on an electrode*
*(b) Scanning pyroelectric micrograph of an $AlPO_4$-5 crystal loaded with p-nitroaniline(pNA), in which blue denotes a negative and red a positive alignment of the pNA-molecules.*

### 4.5 *Pyroelectric Investigations on NLO Active Guest-Host Materials* (M. Wübbenhorst)

In co-operation with the university of Bern (prof. Hulliger) pyroelectric studies on NLO active organic co-crystals (clathrates) have been performed. Based on the newly developed Scanning Pyroelectric Microscope (SPEM) with improved lateral resolution of 10µm the 3-dimensional structure of polar domains in several host single crystals was ascertained. Typical polarisation reversals in the crystal core support a new model for a specific crystal growth mechanism.

4.6 *Electromechanical Properties of Polymer Composites* (E.G.M. Veldman)

Polymer composites based on polyurethane and polyphosphazene loaded with ceramic powder have been manufactured by means of rolling and film casting. The investigated semi-crystalline poly[bis(trisfluoroethoxy)phosphazene] was synthesised through ringopening polymerisation and substitution method. Electromechanical and dielectrical research was performed to study the effect of the volume fraction of the ceramics on deformation and permittivity of the composites. In these studies a sensitive capacitive displacement detector was used.

4.7 *Dielectric Relaxation Spectroscopy of Polymer Electrolytes* (M. Wübbenhorst)

Amorphous ion conducting poly(ether esters) have been characterised with dielectric relaxation spectroscopy. The effect of polymer structure and the complexing salt (LiX, NaX) on the conductivity, the glass transition temperature, as well as two specific secondary relaxations were studied and analysed in terms of physical cross linking and free volume.

4.8 *Photothermal Investigations on Liquid Crystalline Polymers* (M. Wübbenhorst)

Thin layers of a smectic LCP have been aligned planary and homeotropically using two-frequency addressing in the $S_A/I$ biphasic region. The thermal conductivity $\lambda_3$ parallel to the normal film axis was measured with pyroelectric calorimetry. Beside a strong increase in $\lambda_3$ due to side-chain crystallisation (low temperatures) the highest thermal conductivity was observed for planary aligned samples. A tentative model is proposed, invoking an essential contribution of intramoleculare phonon transport along the polymeric backbone layers.

4.9 *Prevention of Marine Biofouling of Materials* (H.J.A. Breur)

The aim of the research is threefold. Primarily, the biofouling process is studied with special attention to the different steps in the fouling process and the influence of season on the fouling rate. Secondly, the effects of fouling are investigated with emphasis on corrosion processes resulting from the fouling. Thirdly new antifouling agents and strategies are being developed together with test methods to characterise the performance of the specific options.

5 *Theory of Complex Fluids* (T. Odijk)

5.1 *Dynamics of Micelles*

The dynamic sedimentation of polymer-like micelles is described by a nonlinear transport equation. Because diffusion is a minor perturbation, it can be neglected. The resulting nonlinear equation exhibits a rarefaction wave and this allows the micelles to be readily characterised.

5.2 *Supercoiled DNA*

A theory valid for all types of external forces, has been developed for supercoiled plectonemic DNA. A general formula for the dimensions of the coil has been derived and is extremely useful for supercoiled DNA under general conditions.

5.3 *Charged Membranes*

For salt-free lamellar phases, the ion distribution is coupled to the undulation of the charged membranes. A full statistical mechanical theory is given invoking the Pois-

son-Boltzmann equation.

5.4 *Osmotic Compaction of Supercoiled DNA in Bacteria*

The protein concentration in bacterial cells is high enough to cause the collapse of the supercoiled DNA genome. Thermodynamic equilibrium imposes coexistence equations which agree with microscopic measurements of the nucleoid dimensions in bacteria.

5.5 *Buckling of Microfibrils*

It is often the case that compressive failure in fibres is caused by the buckling of individual microfibrils. Because the latter are perturbed by thermal motion, a statistical mechanical theory has to be set up. The elastic environment is described by a harmonic potential.

5.6 *Protein-Polymer Mixtures*

The semi-dilute polymer distribution around an array of protein satisfies a Laplace equation. In this way, a statistical theory can be formulated for depletion force in polysacharide protein mixtures. Unlike the colloid case, polymer is never completely forced out of the voids between the proteins.

PUBLICATIONS

F. Beekmans, A.D. Gotsis, B. Norder
*Influence of the flow history on stress growth and structure changes in the termotropic liquid crystalline polymer Vectra B950*
Rheol Acta 36 (1997) 82-95

A. Boersma, M. Wübbenhorst, J. van Turnhout
*Dielectric Analysis of the Breakup of Liquid Crystalline Polymer Fibers in a Thermoplastic Matrix*
Macromolecules 30 (1997) 2915-2922

N. Harada, A. Saito, N. Koumura, D.C. Roe, W.F. Jager, R.W.J. Zijlstra, B. de Lange, B.L. Feringa
*Chemistry of Unique Chiral Olefins. 2. Unexpected Thermal Racemization of cis-1,1',2,2',3,3',4,4'-Octahydro-4,4'-biphenanthrylidene*
J.Am.Chem.Soc. 119 (1997) 7249-7255

N. Harada, A. Saito, N. Koumura, H. Uda, B. de Lange, W.F. Jager, H. Wynberg, B.L. Feringa
*Chemistry of Unique Chiral Olefins. 1. Synthesis, Enantioresolution, circular Dichroism, and Theoretical Determination of the Absolute Stereochemistry of trans- and cis-1,1',2,2',3,3',4,4'-Octahydro-4,4'-biphenanthrylidenes*
J.Am.Chem.Soc. 119 (1997) 7241-7248

J. Hulliger, P. Rigin, A. Quintel, P. Rechsteiner, O. Koenig, M. Wübbenhorst
*The Crystallization of Polar, Channel-Type Inclusion Compounds: Property-directed Supramolecular Synthesis*
Adv. Mater. 9 (1997) 677-679

W.F.Jager, A. Lungu, D.Y. Chen, D.C Neckers
*Photopolymerization of Polyfunctional Acrylates and Methacrylate Mixtures: Charac-*

*terization of Polymeric Networks by a combination of Fluorescence Spectroscopy and Solid State NMR*
Macromolecules 30 (1997) 780-791

G.J. Klap, M. Wübbenhorst, J. van Turnhout, J.C. Jansen, H. van Bekkum
*Modification of a pyroelectric detector by controlled electrocrystallization of thin zeolite layers*
Progress in Surface Science and Catalysis 105 (1997) 2093

C.L. de Korte, E.I. Cespedes, A.W.F. van der Steen, B. Norder, K. te Nijenhuis
*Elastic and acoustic properties of vessel mimicking material for elasticity imaging*
Ultrasonic Imaging 19 (1997) 112-126

H.C. Langelaan, R. Jansen, M. van Uffelen, Y.N. Bronkhorst, A.D. Gotsis, A. Posthuma de Boer
*Influence of the flow history on Stress Growth and Structure Changes in the Thermotropic Liquid Crystalline Polymer Vectra B950*
Rheologica Acta 36 (1997) 82

A.G.C. Machiels, J. van Dam, B. Norder, A. Posthuma de Boer
*Stability of Blends of Thermotropic Liquid Crystalline Polymers with thermoplastic Polymer*
Polymer Engineering and Science 37 (1997) 1512-1525

A.G.C. Machiels, K.F.J. Denys, J. van Dam, A. Posthuma de Boer
*Effect of Processing History on the Morphology and Properties of Polypropylene/Thermotropic Liquid Crystalline Polymer Blends*
Polymer Engineering and Science 37 (1997) 59-72

J.J.A. Mertens, M. Wübbenhorst, L.W. Jenneskens, B.B. Wentzel, J. van Turnhout, R.H.M. van de Leur
*Polyesters with 3,4,7-trioxanonyl segments in their main chain. Novel ion-conducting matrices*
Acta Polemerica 48 (1997) 314-318

K. te Nijenhuis
*Thermoreversible Networks. Viscoelastic Properties and Structure of Gels*
Springer-Verlag Berlin Heidelberg New York, Berlin Heidelberg (1997) 267

T. Odijk
*Depletion around a Protein Sphere Interacting with a Semidilute Polymer Solution*
Langmuir 13 (1997) 3579-3581

T. Odijk
*Many-body depletion interactions among protein spheres in a semidilute polymer solution*
J.Chem.Phys. 106/6 (1997) 3402-3406

T. Odijk,Ilya M.Lifshitz
*An Appreciation*
Phys. Report 288 (1997) 9-12

M.A. Odriozola, A.D. Gotsis
*Extensional rheology of flexible and liquid crystalline polymer melts*
Kalfoglou, Transcripts of the 4th Pantellenic Polymer Congres, November 1997, Uni-

versity of Patras, Patras (1997) 167-170

W. Schuddeboom, M. Wübbenhorst
*Validity of the extrapolation to lower temperatures in high temperatures storage life (HTSL) testing of plastic encapsulated IC's*
In: B. Michel, T. Winkler (eds.), Proceedings of the Micro Materials 97, Druckhaus Dresden GmbH, Dresden (1997) 294-297

P.A.M. Steeman, J. van Turnhout
*A numerical Kramers-Kronig transform for the calculation of dielectric relaxation losses free from Ohmic conduction losses*
Colloid Polym Sci 275 (1997) 106-115

R.J. de Vries
*Thermal undulations in salt-free charged lamellar phases; Theory versus experiment*
Phys.Rev.E. 56 (1997) 1879-1886

M. Wübbenhorst, E.M. van Koten, J.C. Jansen, W.J. Mijs, J. van Turnhout
*Dielectric relaxation spectroscopy of amorphous and liquid-crystalline side-chain polycarbonates*
Macromol. Rapid Commun. 18 (1997) 139-147

**PRODUCT DEVELOPMENT, PRODUCTION AND MATERIALS SCIENCE**
Delft University of Technology, Faculty of Aerospace Engineering
Kluyverweg 1, 2629 HS Delft
phone +31 (15) 2785340, fax +31 (15) 2781151, e-mail L.B.Vogelesang@Lr.tudelft.nl

## PERSONNEL

*Scientific staff*

| | |
|---|---|
| prof.ir. L.B. Vogelesang | (2785145) |
| prof.dr.ir. J. Schijve (0.4) | (2781341) |
| ir. J. Sinke | (2785137) |
| ir. M.J.L. van Tooren | (2784794) |
| dr.ir. A. Vlot | (2787158) |

*Temporary staff*

| | |
|---|---|
| ir. R.A.M. Coenen (STW) | (2786279) |
| ir. P.W.C. Provó Kluit | |
| ir. Soerjanto Tjahjono (Garuda) | (2785164) |
| ir. T.J. de Vries (Cie Beek/NIMR) | (2785492) |
| ir. G.J. Bakker (GTO) | (2788232) |
| ir. A. van den Berg (IOP) | (2786395) |
| ir. J.J. Homan (GTO) | (2788230) |
| ing. N.H. Jalving (GTO) | (2788454) |
| ir. P.L. Kuijpers (GTO) | (2788454) |
| ir. A. Kwakernaak (Adhesion Institute) | (2785353) |
| ir. A. Longhi (DIOC 6) | (2788233) |
| ir. P.J.M. Nijssen (GTO) | |
| ir. H. Panday (GTO) | (2788232) |
| ir. T.C. Wittenberg (STW) | (2788232) |

*Technical assistants*

| | |
|---|---|
| ing. B.A. Grashof | (2782083) |
| M. Badoux | (2786397) |
| F.G.C. Oostrum | (2786700) |
| C.G. Paalvast | (2786396) |
| ing. J. Snijder | (2782083) |
| J.H. Weerheim | (2786395) |

## HIGHLIGHTS

- Start of the Airbus A3XX fuselage project in co-operation with SLI, NLR and Airbus (GTO project)
- Start of a project for the development of a compression shear test set up for full scale fuselage panels (STW)
- Development of GLARE as a repair material for aircraft structures in co-operation with the USAD and GARUDA
- Start of the DIOC 6 programme on damage tolerance of large fuselages

## RESEARCH AREAS and OBJECTIVES

The work performed in the Structures and Materials Laboratory consists of most of the research in the disciplinary group B2 and part of the research in the disciplinary group C. The laboratory is specialised in the development of advanced materials, structural design and manufacturing techniques for light-weight structures.

The research efforts of the laboratory have three major corner stones:

- Fundamental scientific research. Successful application of new materials and design strategies can only be achieved if based on a thorough scientific understanding of the mechanical, physical and chemical aspects of materials and the optimal lay-out of structures.
- Integration of various disciplines. The laboratory has the knowledge, skills and equipment to cover the complete development of a structure: from materials science, structural design and manufacturing techniques to the fabrication and testing of full-scale components.
- Close co-operation with the industry. The laboratory has a strong application oriented approach. Input and questions from the industry are essential to guide the research, which is directed at gathering of engineering knowledge for the solution of practical problems.

The expertise of the laboratory covers an area from micro-mechanics of materials, via design and manufacturing techniques, up to full scale testing of components. A thorough knowledge of and insight into the relation between micro-structure and macro-properties of materials is of increasing importance to optimise the application of materials in constructions. This relation is pursued experimentally, in combination with model development. The material behaviour which has been investigated includes the resistance against mechanical loading, both static and dynamic, durability, workshop properties, forming and environmental consequences like recycling.

Although the research is divided into specific research topics there is a strong co-operation between the staff members and students integrating different areas. The major research topics of the group can be summarised as follows:

- Fibre reinforced polymers (thermosets, thermoplastics and elastomers)
  The emphasis in the research of fibre reinforced polymers is on the development of new structural concepts and suitable manufacturing techniques.
- Fibre-Metal Laminates
  This new group of damage tolerant materials was developed in our laboratory and is still under development. All kind of aspects of the laminates are investigated: from fabrication and inspection to optimising these materials and the application in aerospace structures.
- Light-weight Metal Alloys
  Light-weight alloys, especially aluminium alloys still play an important role in the aircraft industry. Acquired knowledge, theories, new alloys, etc. are evaluated, tested and compared to improve understanding and to aid the search for future aircraft materials.
- Jointing Techniques
  Joints are very important in aircraft structures. Joints can be made using bolts, rivets or adhesives. The laboratory has a close co-operation with the Adhesion Institute, of which the Faculty of Aerospace Engineering is one of the founding Faculties.

The tendency towards more advanced materials, more powerful computational tools,

modern design methods, more flexible and computerised manufacturing techniques and last but not least destructive and non-destructive inspection, requires an integration of the various disciplines involved. There is a strong interrelationship between material selection and properties, structural design and processing.

## FACILITIES

The Structures and Materials Laboratory is well equipped with all kind of test machinery and devices to perform the tests required for the research described in the paragraphs above. The research facilities encompass:

*Fatigue machines, computer controlled, hydraulic*

- MTS 1000kN
- MTS 100 kN
- Amsler/MTS 200kN
- Schenck 60 kN
- MTS (300 Hz) 10 kN
- MTS/Fokker 200 kN

*Fatigue machines, low frequency, pneumatic*

- Four tension machines
- Barreltest set-up (2 bar)
- Fuselage skin simulation set-up (1 bar)

*Static testing machines; hydraulic*

- Mohr & Federhaff 40 kN

*Static testing machines; mechanical*

- Zwick 20 kN
- Three Tensometer 20 kN
- Minimat 200 N

*Compression machines*

- Special design 800 kN
- Special design 150 kN

*Torsion machine, mechanical*

- Amsler 1500 Nm

*Production equipment*

- Installations for anodising and chemical milling
- Autoclave (Scholz) $1.5 \times 0.9$ m$^2$, 350 °C, 25 bar
- Hot press (Fonteijne) 180 kN, 200 °C, $23 \times 36$ cm$^2$
- Hot press (Fonteijne) 600 kN, 400 °C, $50 \times 50$ cm$^2$
- Hot press (Fonteijne) 1000 kN, 400 °C, $50 \times 50$ cm$^2$
- Hot press (Heckler & Koch) 60 kN, 250 °C, $20 \times 50$ cm$^2$
- Two Fast closing presses (Alfamatic), 210 kN
- Fast closing press, infrared unit (Fonteijne), $1.5 \times 0.8$ m, 4000 kN
- Press-clave, 450 °C, 30 bar, nitrogen
- NC filament winding machine (Bear), 4 axes, $l = 3$ m; $d = 2$ m
- Deep drawing machine (Roell & Korthaus), 400 kN

*Special material test equipment*

- Two salt spray cabinets
- Scanning electron microscope (Jeol 840A),
- Several potentiostats equipped with energy dispersive X-ray analysing corrosion behaviour system (TRACOR)
- Zeiss microhardness tester
- Heat treatment equipment
- Medium energy impact tester
- Laser extension meter
- EC tester for crack detection
- Six constant load machines for stress corrosion
- Three slow strain rate machines for stress corrosion (max. load 20 kN)
- Test cells for different environments, vacuum, high temperatures
- Ultrasonic C-scanner with data processing
- Ultrasonic delamination detector (SONIC)
- Low energy impact tester with data processing
- High velocity impact tester with data processing

*Computers*

- HP laboratory computer
- HP network server
- Terminals of the University computer network
- CAD/CAM installation (SUN workstations)
- Several HP 286, 386 and 486 personal computers
- CAD/CAM installation (Silicon Graphics workstation)

RESEARCH REPORT 1997

1 *GLARE Application in Ultra High Capacity Aircraft A3XX* (A. Vlot, L.B. Vogelesang, J. Sinke, R.A.M. Coenen, T.J. de Vries, H. Panday, T.C. Wittenberg, A. Longhi, N.H. Jalving, J.J. Homan, G.J. Bakker, P.L. Kuijpers, P. Boersma)

Fibre Metals Laminates like GLARE are very suited for application in large aircraft because of their high inherent safety. Last year the material was optimised for this type of structures. A new method was developed to laminate and cure large panels in one autoclave cycle, including all structural details like doublers and splices. In this way a very cost effective structure can me manufactured by reducing joints and eliminating crack stoppers and production steps like chemical milling. Large aircraft like the Airbus A3XX leads to skin thicknesses in the order of 4 mm instead of the 1 to 2 mm skin thickness of the laminates that were tested for smaller aircraft. This leads to new design concepts and methods.
In a joined program called 'GLARE Technology Ontwikkeling' (GTO) Structural Laminates Industries , NLR and NIVR are working on the technology readiness of GLARE for large aircraft like the Airbus A3XX. Several working groups are established: qualification and processes, methods, design concepts, maintenance and manufacturing. Many preliminary studies were carried out by a group of twenty students covering burn through resistance, residual strength, blunt notch, impact, C-scan quality control, etc.

2 *Part Through Cracks and Oblique Through Cracks in Riveted Lap Joints* (S.A. Fawaz, J. Schijve, L.B. Vogelesang)

Finite Element (FE) calculations were made to obtain stress intensity factors for hole edge cracks under different loading conditions: unidirectional and biaxial tension, bending and pin loading. Small quarter elliptical part through cracks and oblique through cracks with an elliptical crack front were considered. A large amount of results is now evaluated for prediction purposes. The FE technique is discussed in report LR-805 by S.A. Fawaz. The co-operation with NASA (dr. Newman) should be acknowledged.
In parallel, the development of cracks in riveted lap joints is now studied by fractographic observations in the electron microscope. Marker loads are used for this purpose.

3 *Three Dimensional Finite Element Analysis of Three Rivet Row Lap Splice Joint* (S.A. Fawaz, J. Schijve)

In this analysis a Finite Element is used of which a quarter is composed of 1764-20 noded, isoparametric solid elements for both sheets and pins, in combination with 364 non-linear gap elements defining the interaction between sheets and pins. Both sheet and pins are assumed to be 2024-T3. The MSC/PATRAN pre/post processor is used, and the MARC finite element analysis program for solving the model. Two cases are considered, one representing a low squeeze force (LSF), and the other one a high squeeze force (HSF). In the latter case there are two stress systems, (i) the remote stress system, and (ii) a residual stress system created by rivet squeezing. The residual stress system represents the residual stresses created by expanding the rivet in the hole during rivet squeezing. The most important result so far is the reduction of the cyclic stress by a factor of 3.2 as a result of the residual stress system in the HSF analysis. Due to rivet tilting in the LSF case, the rivet is losing contact with the bore of the hole at the net section of the joint, thereby moving the point of maximum stress away from the net section. In the HSF case, the rivet tilting is restricted due to the residual stress system. Additional analyses are underway with the inclusion of a quarter circular corner crack. More information on this topic is given in a paper at the Symposium. The work is done in co-operation with NLR (A.U. de Koning).

4 *Fatigue of Riveted 2024-T3 and GLARE Lap Joints* (R.P.G. Müller)

Research of R.P.G. Müller described in the previous review was documented as a Ph.D. thesis. It included both experimental and an analytical research on the fatigue behaviour of fuselage riveted lap joints. The most important outcome of the research is that the rivet squeeze force has a dominant effect on the crack initiation life of riveted joints. Therefore the squeeze force (and not the diameter of the driven head or the stroke during squeezing) should be carefully controlled during production. The squeeze force has two effects: (*i*) On the residual stress distribution around the rivet hole and (*ii*) on the geometrical imperfections of the sheet around the rivet holes which will have a large influence on the load transfer as well as the secondary bending of the sheet in this area. Imperfection may lead to *crack initiation in the nominally less critical bottom row*, which is not visible at the outside of the fuselage. Glare shows a similar response to the riveting parameters as 2024-T3, however, the fatigue life is much longer and crack growth is very slow, even at a high stress level.

## 5 *Fatigue investigation of Structural Laminates Company, SLC* (G. Roebroeks [Structural Laminates Company])

### 5.1 *Influence of the Internal Stress in GLARE® 1 on the Fatigue Behaviour*

The fatigue behaviour of unstretched GLARE® 1, based on 7475-T761 aluminium sheet is relatively poor compared to that of the other 2024-T3 based GLARE® materials. To overcome this problem GLARE® is post stretched, reversing the internal stress in the layers of the material: compression in the aluminium layers and tension in the fibre layers. It considerably improves the fatigue properties. There are two possibilities to define the stretching operation:

- stretching to a constant permanent strain
- stretching to a constant internal stress

The first procedure is based on a more simple definition. However, the second one leads to more uniform properties for different lay-ups.

### 5.2 *Environmental effects on the fatigue behaviour of GLARE®*

If there is an environmental effect, a frequency effect should also be expected. Fatigue crack growth experiments were carried out at a frequency as low as 0.0033 Hz (one cycle in 5 minutes). The effect of moisture was also investigated. It turned out that the load frequency and the humidity have a rather small influence on the fatigue crack growth rates.

The effect of the environment on the behaviour of riveted lap joints was investigated with tests in distilled water and salt water immersion in order to study the fatigue behaviour and residual strength after fatigue. Tests on 2024-T3 lap joints were carried out as base line data. Environmental effects were observed indeed. However, in each environment the GLARE® lap joints showed a similar superiority if compared to the behaviour of 2024-T3 lap joints. It appears that the environmental effects are related to effects on the aluminium layers, but the advantage of the fibre-metal laminates concept is maintained.

### 5.3 *Thermal behaviour of GLARE®*

Various aspects of the thermal behaviour of GLARE® are investigated:

- thermal conductivity (through the thickness of the material),
- thermal expansion and
- thermal fatigue.

The thermal fatigue behaviour of GLARE® was studied by exposing the material to a cyclic temperature range from –50 °C to +80 °C, up to a maximum of 1000 cycles (one cycle in 46 minutes). The purpose of the tests was to see whether it might cause any physical damage or material degradation. In addition to two standard laminates (GLARE 2-3/2-0.3 and GLARE 3-3/2-0.2) two non-standard lay-ups were tested in order to get more excessive residual stresses in the metal and the layer after production. High residual stresses were introduced by post-stretching GLARE 3-3/2-0.2 to 0.6%. High residual compressive stresses in the fibres were obtained by manufacturing GLARE 2-2/1 with two 2024-T3 layers of a large thickness (2.6 mm). After exposure to the thermal fatigue conditions, the specimen were investigated using the C-scan, the scanning electron microscope and ILSS tests. None of the investigations showed material degradation for any of the variables studied.

### 5.4 *Fatigue Behaviour of Spliced GLARE® Configuration*

A spliced GLARE® panel was developed for the A340. In 1995 the full analysis of the configuration was completed. The tests included tensile strength, residual strength, blunt notch, off-axis behaviour, shear buckling, riveting issues, quality but also fatigue crack initiation and growth. An important type of cracking of GLARE® structures is fatigue crack initiation in an outer aluminium sheet of the laminate at the edge of a doubler. The splice configuration for the A340 side panel uses a GLARE® doubler bonded over the splice to locally reduce the stress for preventing delamination initiated by the interrupted aluminium layers. The crack initiation behaviour at the doubler edge was evaluated in experiments. Also crack growth from large saw cuts (25 mm and 75 mm) at the doubler edge was studied.
The test results show that crack initiation did not occur for the thickness step used for the splice area. Damage was not found after 400 000 fatigue cycles from 6 to 120 MPa. Also the proposed doubler configuration around the windows in the GLARE® side panel did not cause crack initiation. The fatigue crack growth tests on configurations with saw cuts at the doubler edge showed lower crack growth rates than those found for the basic GLARE 3-3/2-0.3 skin material. The study showed that fatigue crack initiation and growth is not a critical aspect for the splicing geometry chosen for the A340 side panel.

5.5 *Fatigue Crack Growth Prediction in GLARE®*

The fatigue crack growth behaviour of Fibre Metal Laminates (FMLs) has been modelled by R. Marissen. The calculation method uses crack growth data of the metal sheet in ARALL® or GLARE®. Because of the low K values due to crack bridging fibres, the relation between crack growth rate (da/dN) and the stress intensity factor should be available at these low K values for the thin aluminium sheet used in FMLs to calculate the crack growth rates. This relation was believed not to be available with sufficient accuracy. A crack edge loading specimen was used to generate new crack growth data for the thin aluminium sheet in the required K range. These results were used in Marissen's model to calculate the fatigue crack growth behaviour in various GLARE® materials. Reasonable correlation between prediction and measurement was found. Discrepancies can be associated with shortcomings of the prediction model.

6 *Repair Techniques for Pressurised Aircraft Fuselages* (A. Vlot, R.S. Fredell, C.B. Guyt [United States Airforce])

An important issue concerning the structural integrity of ageing aircraft is the damage tolerance of fuselage repairs. The investigation focuses on the analysis and testing of existing repair methods and develops two improvements [1,2]. The first one, which is called 'soft patching', makes use of the high strength and moderate modulus of GLARE 3 Fibre Metal Laminates. For riveted repairs this material attracts less loads and shows lower rivet loads in the first critical rivet row, due to its relatively low stiffness. GLARE 3 patches extend the fatigue life of riveted repairs significantly. A structural repair carried out with GLARE is also cheaper because a taper of the patch is not necessary.
The second technique involves bonded crack patching of fatigue cracks in fuselage skins. An analysis program called CALCUREP was developed for the optimisation of bonded patches. The program calculates the reduction of the stress intensity factor in the cracked skin for a bonded elliptical patch and takes temperature effects (due to differences in thermal expansion coefficients and the difference between the tem-

perature at the ground and at cruising altitude) and also shear deformation in the adhesive layer and the tapering of the patch into account. Analysis and fatigue tests showed that bonded GLARE 3 is preferable over boron/epoxy, carbon/epoxy, titanium and monolithic aluminium. Especially the temperature effects have a large negative influence on the crack closing capability of the boron/epoxy material.
In the near future fatigue tests will be carried out under a combined cycling of the mechanical load and the temperature of the specimen. Flight tests will be performed on bonded GLARE 3 patches in the Lockheed C5 Galaxy.

7 *Automated Laminate Inspection System* (R.A.M. Coenen, J. Vos, D.W.W. Krul [Aerospace Engineering, Delft University of Technology])

The Automated Laminate Inspection System (ALIS) has been designed for the ultrasonic evaluation of composites and fibre Metal Laminates (FML). These laminates generally consist of thin (0.3 mm) layers of metal or epoxy-fibre prepreg. The most known varieties are Glare, with glass-fibre and Arall with Aramid fibre. Besides FML, ALIS can also be used for full composite laminates and adhesive bonded plate structures. ALIS has recently been expanded to include complete structural components.

7.1 *Image Analysis*

Apart from the classical method of analysing the image directly it is also possible to analyse the image in the frequency domain. To do this the image has to be transformed from space into the Spatial Frequency Domain (SFD). Where an analysis of the spectrum can be performed. This way the ratio's of fibre directions can be determined and other repetitive patterns can be found.

7.2 *Image Processing*

The SFD image can be processed to filter out unwanted effects. These include dominant fibre direction, honeycomb cells, curved surfaces. This will facilitate the recognition of defects and anomalies on a "noisy" background. A low pass filter can be used to reduce high (spatial) frequency noise when the spatial bandwidth (spot size) of the specific transducer is known.

7.3 *Signal Processing*

In a three-dimensional volume-scan, a series of measurements is obtained for each point. Recording starts after a wave is generated at the transducer. The pressure field at the surface of the transducer is measured at regular time-steps. Instead of making decisions based on one value for each point only, we develop a system that uses the whole time-trace in its processing. The plane-wave theory is used to calculate the properties of the layers by analysing the time-trace.

8 *Space Materials Research* (T.J. van Baten)

With Fokker Space and TNO research is done on structures of space re-entry vehicle. Both thermal protected and so called hot structures, made of refractory metals of special alloys, are investigated. For a given thermal load the results with computational models and from experiments with the quartz lamp heating test set-up are compared. The test set-up is also used for material coatings research at high temperatures up to 1300 °C.

9 *Cumulative Fatigue Damage Aspects* (J. Schijve)

Fractographic research was carried out on specimens fatigue tested under variable-amplitude load histories. The load sequences selected were primarily constant-amplitude base line cycles combined with different types of periodically applied overload cycles. Fractographic observations in the scanning electron microscope have given detailed information on delayed crack growth retardation following high loads. Such information cannot be obtained from records of visual crack growth measurements. Two aluminium alloys (2024-T3 and 7075-T6) were used, but in a co-operation with prof. Skorupa of the University of Mining and Metallurgy (Faculty of Mechanical Engineering and Robotics) in Krakow, fatigue fractures of similarly tested steel specimens were also studied.

10 *Fatigue of Riveted Lap Joints* (S.A. Fawaz, J. Schijve, L.B. Vogelesang, A. Vlot)

The research on this topic was continued and documented in the doctor thesis of S.A. Fawaz. The development of small fatigue cracks in a riveted lap joint were studied by adopting fractographic observations obtained by using marker loads. Crack growth data were obtained for cracks as small as about 100 μm, followed by crack growth up to 5 mm. The correlation with stress intensity factors obtained with FE calculations were partly promising, but there are still some difficulties involved to obtain qualitatively accurate results. The shape of the fatigue cracks is part-elliptical.

PUBLICATIONS

R.A.M. Coenen
*Laminate quality assessment through multi-dimensional ultrasonic C-scan analysis*
In Proceedings of World Congress on Ultrasonics, August 1997, Yokohama, Japan (1997) 66-67

S.A. Fawaz
*Fatigue crack growth in riveted joints*
Ph.D. thesis, Delft University of Technology, Delft University Press (1997)

S.A. Fawaz, J. Schijve, A.U. de Koning
*Fatigue crack growth in riveted joints*
In: Proceedings of the 19th ICAF Symposium, Edinburgh, 18-20 June 1997

H. Haaksma, A. Vlot, H. van Riessen
*Pionier van de filosofie van de techniek*
Algemeen Nederlands Tijdschrift voor Wijsbegeerte 89/1 (1997) 26-43

M. Papakyriacou, J. Schijve, S.E. Stanzl-Tschegg
*Fatigue crack growth behaviour of fibre-metal laminate GLARE-1 and metal laminate 7475 with different blunt notches*
Fatigue Fract. Engng Mater. Struct. 20/11 (1997) 1573-1584

W. Poelman, J. Sinke
*Revival van metaalplaat. De mogelijkheden en beperkingen van rubberpersen en voorgelakte plaat*
Tijdschrift voor Industriële Productontwikkeling 5 (1997) 33-34

P.W.C. Provó Kluit

*In-situ foamed sandwich panels*
In: Proceedings of the 5th European Conference on Advanced Materials and Processes and Applications. Materials, Functionality & Design, Characterization and Production/Design, EUROMAT 97, Maastricht, 21-23 April 1997, Netherlands Society for Materials Science 4 (1997) 2/91-2/94

P.W.C. Provó Kluit
*The development of in-situ foamed sandwich panels*
Ph.D. thesis, Delft University of Technology, Delft University Press (1997)

P.W.C. Provó Kluit, K.J. Volkers, Z.I. Kolar
*Replacement of acetone in acetone-swollen polyehterimide (PEI) foils with 1,1,1-trichloroethane or ethanol: An [$^{14}$C]acetone aided radiotracer study*
Journal of Radioanalytical and Nuclear Chemistry 219/1 (1997) 47-50

J. Schijve
*Four lectures on fatigue crack growth*
In: R.J. Sanford (ed.), Selected papers on Foundations of Linear Elastic Fracture Mechanics, SEM Classic Papers, The Society for Experimental Mechanics CP 1 (1997) 587-637

F. Soetens, IJ.J. van Straalen, B.W.E.M. van Hove
*Aluminium, light weight and durable load-bearing structures*
In: Proceedings of the 5th European Conference on Advanced Materials and Processes and Applications. Materials, Functionality & Design, Characterization and Production/Design, EUROMAT 97, Maastricht, 21-23 April 1997, Netherlands Society for Materials Science 4 (1997) 4/353

IJ.J. van Straalen, F. Soetens, J. Wardenier, L.B. Vogelesang
*Structural adhesive bonded joints in engineering - drafting design rules for aluminium applications*
In: Proceedings of EUROMECH 358 'Structural Mechanical behaviour of adhesive joints - Analysis, testing and design', September 1997

IJ.J. van Straalen, J. Wardenier, L.B. Vogelesang, F. Soetens
*Structural adhesive bonded joints in building engineering - principles and requirements of design*
In: Proceedings of the 5th European Conference on Advanced Materials and Processes and Applications. Materials, Functionality & Design, Characterization and Production/Design, EUROMAT 97, Maastricht, 21-23 April 1997, Netherlands Society for Materials Science 4 (1997) 4/357

A. Vasek, J. Schijve
*Residual strength of cracked 7075 T6 Al-alloy sheets under high loading rates*
Delft University Press (1997) 70

A. Vlot
*Recensie van: E. Schuurman, 'Perspectives on Technology and Culture'*
Algemeen Nederlands Tijdschrift voor Wijsbegeerte 89/1 (1997) 91-92

A. Vlot, E. Kroon, G. La Rocca
*Impact response of Fiber Metal Laminates*
In: J.K. Kim, T.X. Yu (ed.), Impact Response and Dynamic Failure of Composites and Laminate Materials, Int. J. Key Engineering Materials 141-143 (1997) 235-276

A. Vlot, M. Krull
*Impact damage resistance of various fibre metal laminates*
Journal de Physique 7 (1997) C3-1045-1050.

L.B. Vogelesang
*Glare (Fiber-Metal Laminates technology) and safety*
In: Proceedings IASC-97, International Aviation Safety Conference 1997, Rotterdam, 27-29 August 1997, 14

L.B. Vogelesang, A. Vlot, J.W. Gunnink
*Fibre Metal Laminates and Aircraft Safety*
In: Aviation Safety - Proceedings of the International Aviation Safety Conference, Rotterdam, 27-29 August 1997, 471-479

## SOLID STATE CHEMISTRY AND MATERIALS SCIENCE

Eindhoven University of Technology
PO Box 513, 5600 MB Eindhoven
phone +31 (40) 2474947, fax +31 (40) 2445619, e-mail ...@chem.tue.nl

### PERSONNEL

*Scientific staff*

| | |
|---|---|
| prof. dr. G. de With | (2474947, G.deWith@...) |
| prof. dr. R. Metselaar (0.2) | (2474947, tgtvrm@...) |
| prof. ir. F.J.J. van Loo (0.3) | (2473331, tgtvfl@...) |
| dr. H.T. Hintzen | (2473113, tgtvbh@...) |
| dr.ir. G.F. Bastin | (2473049, tgtvgb@...) |
| dr. A.A. Kodentsov | (2472314, tgtvak@...) |
| dr.ir. P.G.Th. van der Varst (0.8) | (2474946, vdvarst@sg5.chem.tue.nl) |

*Graduate students/Post-doc's*

| | |
|---|---|
| S. Markovski, M.Sc. | (2473034, tgtvsm@...) |
| ir. S. Jansen | (2473034, tgtvsj@...) |
| drs. J.W.H. van Krevel | (2473132, tgtvjk@...) |
| ir. G. Boon | (2473053, tgtvgb2@...) |
| ir. M.A.H. Donners | (2474945, tgtvmd@...) |
| ir. M.A. Verspui | (2474945, tgtvmv@...) |
| A.A. Kudyba, M.Sc. | (2473053, tgtvak2@...) |
| ir. R. Bruls | (2473132, tgtvrb@...) |
| ir. P.J.T.L. Oberndorff | (2473034, tgtvpo@...) |
| dr. S. Shulepov | (2473059, tgtoss@sg17.chem.tue.nl) |
| dr. V. Bondarenko | (2473041, tgtvvb@...) |
| dr. ir. J.D.B. Veldkamp | (2473057, tgtvdv@...) |
| ir. M. van Dal | (2473053, tgtvmd2@...) |
| Ldo E. Jimenez-Pique | (2473041, tgtvep@...) |
| M.E. Velazquez-Sanchez, M.Sc. | (2473132, tgtvmv@...) |

*Technical support*

| | |
|---|---|
| L. van Loon | (2472770, Linda@...) |
| ir. H.J.M. Heijligers | (2473051, tgtvhh@...) |
| ing. J.A. van Beek | (2473040, tgtvhb@...) |
| ing. D. Klepper | (2473051, tgtvdk@...) |
| ing. M. Hendrix | (2474967, tgtvmk@...) |
| H. van der Palen | (2473058, tgtvhp@...) |
| ing. A. Delsing | (2473041, tgtvad@...) |
| ing. N. Lousberg (temporarily) | (2472967, tgtvnl@...) |

### HIGHLIGHTS

- During the 5th ECerS conference, Versailles, France, June 22-26, 1997, prof. R. Metselaar was presented with the "The International ECerS Award".
- Due to substantial funding by SON an Orientation Image Microscope (OIM) was installed. In fact this is an attachment to an electron microscope annex micro-probe. This provides an opportunity to study on a scale of about 0.1 μm, not

only the chemistry but also the crystallography of the materials under investigation.

- New oxynitride materials based on the Ba-Al-O-N system have been discovered (See Figure 9). Incorporation of a limited amount of nitrogen in the oxide lattice compensates for the defects and results in significantly improved thermal conductivity. Moreover the materials exhibit high quantum yield luminescence.

## RESEARCH AREAS AND OBJECTIVES

The laboratory of *Solid State and Materials Chemistry* (SVM) is active in inorganic materials science and technology, in particular in research on solid state processes and microstructure related properties, with the aim to obtain insight in the relation between chemical and physical properties and the composition and microstructure of materials. The emphasis is on interfacial mechano-chemistry of inorganic materials (including metals), that is the chemistry related to interfaces and mechanical aspects. In this research the use of classical and irreversible thermodynamics as a unifying methodology will be pursued. The application of this methodology is focused on the meso-level, that is that level that is determining the macro-behaviour but itself is determined by the micro-level. While chemistry and kinetics are an important part of the micro-scale, the macro-scale refers to the phenomenological material parameters. The research is therefore situated at the junction of three axes: the material, the concept and length scale axis, as illustrated in Figure 1.

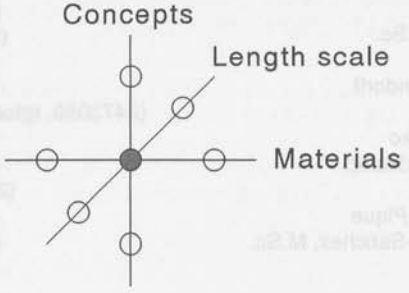


*Figure 1: Research in the department SVM at the junction of the concepts, the length scale and the materials axes*

The identification of the thermodynamic internal variables with relevant microstructural parameters requires intensive co-operation with a characterisation activity. Electron beam based characterisation of inorganic materials is an important activity. Since in the research programme a focus has been given to interfacial aspects, an attempt is made to incorporate these characterisation activities in the programmes. This means that for the characterisation activity the emphasis is more on materials aspects than on methodology development. In particular the relation to the thermodynamic modelling and material characteristics dependent on the process is crucial. Consequently the research has been organised along two main programmes: 'Solid state processes' and 'Microstructure related properties'. Each programme contains clusters related to the main theme. Most clusters contain more than one project.

1 *Solid State Processes*

The area of processing in inorganic materials is wide. Roughly speaking, one can distinguish raw materials, shaping and properties. For polycrystalline inorganic materials (ceramics) for instance, this means powders, consolidation/sintering and the whole range of properties of materials that can be imagined. We do not put an emphasis on raw materials. Instead we try to focus on the shaping and property area and co-operate with third parties in the overlap area. Processing also includes the joining of two different materials, in which the possible reactions between the materials have to be assessed. Moreover, the final shape of the materials in their applications has to obey tightly bound tolerances, often only reachable by abrasive processing techniques. Here also the possible chemical reactions play an important role in the fundamental understanding of these processes. The programme *Solid state processes* is focused on processes dominated by interfacial aspects, such as diffusion reactions, phase relations, morphology, textures and reaction kinetics in metal/metal and metal/ceramic systems, consolidation and abrasive processing. The present activities in this programme are therefore divided in three clusters (in brackets the researchers involved):

- Reactions (Kodentsov, Oberndorff, Markovski, Van Dal, Van Loo, De With),
- Particulate Processing (Hintzen, Kudyba, Metselaar, De With) and
- Abrasive processing (Verspui, Shulepov, De With).

2 *Microstructure-Related Properties*

The area of properties of inorganic materials is also wide and can of course not be covered completely. A simple distinction can be made between intrinsic properties of a material and the extrinsic, that is microstructurally related, properties of a material. While intrinsic material properties are related mainly to the compound used to produce a material, the extrinsic properties are largely determined by the microstructure of the material. In this respect we define the microstructure, along with Exner, by the type, the structure and the number of phases, by the number, the geometric appearance (size, shape, etc.) and the topological arrangements of the individual phase regions and their interfaces and by the type, structure and geometry of lattice defects. The programme *Microstructure related properties* aims at establishing relations between microstructure and properties of inorganic materials dominated by interfacial aspects. In particular we concentrate on modelling of mechanical performance in relation to chemistry. To support the extreme demands on microstructural analysis we also develop electron microscopic methods for quantitative element analysis of bulk materials and thin films. The present activities in this programme can therefore be divided in three clusters (in brackets the researchers involved):

- Oxynitrides (containing preparation and characterisation) (Hintzen, Kudyba, Jansen, Bruls, Van Krevel, Metselaar, De With),
- Failure (fracture and damage mechanics of both monoliths and bi-material systems) (Van der Varst, Donners, Van Gils, Bondarenko, Dortmans, Jimenez-Pique, Velazquez-Sanchez, De With) and
- Characterisation (mainly with electron based methods) (Bastin, Boon, Metselaar, De With).

Historically a significant part of the work on technical ceramics has been done in cooperation with TNO-TPD within the Centre for Technical Ceramics (CTK). This cooperation is still quite active but the interest of both parties has become wider than technical ceramics only and a considerable effort is made to increase the mutual in-

teraction. This has led to a wider perspective of inorganic materials processes and properties in which the emphasis will be shifted at TNO-TPD still more towards applications and at TUE-TVM more towards fundamental processing and property problems. This co-operation has created the possibility to interact with industrial companies, for which a short time scale is becoming more and more important, without sacrificing long term projects.
In the Section RESEARCH REPORT an overview of the various projects is given except for those researchers who only recently joined the group.

FACILITIES (jointly with TNO-TPD within the CTK)

*General processing*
- Dip coating
- Attrition milling (small and large batches)
- Atmospheric slip casting
- Pressure slip casting
- Injection moulding
- Cold isostatic pressing
- Uniaxial pressing
- Various CVD apparatus

*Characterisation*
- Powders and suspensions
- Mercury porosimetry
- BET
- Sedigraph (particle sizes between 0.1 and 100 μm
- DTA/TG/DTG/DSC ($T_{max}$ = 1675 °C)
- X-ray diffraction
- High temperature X-ray diffraction
- Mass spectrometer
- Viscometers

*Sintering and metal-ceramic joining*
- Air sintering furnaces, maximum temperature 1750 °C
- Hot press, 10 kN, maximum temperature 2000 °C
- Horizontal tube furnaces, maximum temperature 1650 °C
- Vacuum sintering furnaces, maximum temperature 2000 °C
- Nitriding furnace, maximum temperature 2000 °C
- Gas pressure furnace, maximum temperature 2200 °C, maximum gas pressure 100 bar
- Furnace for binder removal, weight loss rate controlled, maximum temperature 1100 °C
- Thermocompression apparatus, maximum load 50 kN, maximum temperature 700 °C
- Thermocompression apparatus, maximum load 8 kN, maximum temperature 1400 °C

*Green and sintered ceramics*
- Several dilatometers, maximum temperature 1600 °C
- Dilatometer for sintering studies, maximum temperature 2000 °C
- 3 and 4 point bend test, maximum temperature 1600 °C

- Universal mechanical testing machines, maximum 10 kN
- Biaxial bending in controlled atmosphere, maximum 1600 °C
- $K_{Ic}$ measurement in controlled atmosphere
- Abrasive particle testing machine
- Hardness measurements
- Nano-indentation
- Subcritical crack growth test jigs, max. 600 °C
- Oxidation measurements in controlled atmosphere, maximum temperature 1600 °C
- Measurement of AC and DC conductivity in controlled atmosphere, maximum temperature 1500 °C
- Tribology: pin-on-plate, pin-on-disk

*Coatings*

- Profilometer
- Scratch tester
- Electrographic printing
- Vickers/Knoop microhardness tester

*General*

- SEM, scanning electron microscopy
- TEM, transmission electron microscopy
- Microprobe
- Optical microscopy

## RESEARCH REPORT 1997

### 1 *Solid State Reactions* (A.A. Kodentsov)

Substantial efforts in 1997 were concentrated on study of the interactions at the contact surfaces between TV-screen glass and chromium steel, and interfaces formed by refractory metals (Mo, W, Re) with fused silica. The work is conducted in co-operation with (and financially supported by) Philips Centre for Manufacturing Technology. The fundamentally oriented part of the program includes a number of interconnected projects. They focus primarily on chemical aspects of the interfacial phenomena.

#### 1.1 *Interaction in metal/metal systems*

A diffusion kinetic model, based on the use of integrated diffusion coefficients and mobilities was developed for describing the layer growth of intermetallic compounds between metal conductor and Pb-free solder. The model was verified on the ternary substrate/solder system Cu/SnBi. (Further development of work on Pb-free solders, see in the report of P. Oberndorff).

#### 1.2 *Reactions of metals and ceramics/compound semiconductors*

Chemical reactions at the interfaces between monocrystalline SiC (4H SiC, 6H SiC) and non-carbide forming metals (Co, Ni, Re, Pt) were studied. These material systems generate considerable technological as well as scientific interest. The former is related to the fabrication of stable contact to wide-gap semiconductor, the latter is connected with a peculiar phenomenon in solid state chemistry: the formation of a

periodic (in time and space) layered reaction zone in diffusion couples (see the report of S. Markovski).

1.3 *Gas-solid interactions in multiphase systems*

A project on the nitrogen permeation through nickel originates from the problems experienced in developing joints between $Si_3N_4$-ceramics and Ni-based alloys. Significant advances have been made to understand the kinetics and thermodynamics of the nitriding process. As a result, suitable nickel alloys and conditions of nitridation have been selected which make it possible to obtain permeability data.

In general, the chemical interaction between dissimilar materials is governed by the thermodynamics and diffusion kinetics of the system under consideration. However, it was recognised that a point of view entirely focused on purely chemical aspects of interactions is somewhat biased since it fails to account for the considerable effect of mechanical stresses induced during mass transport and chemical reaction.

In this respect, a new project on mechano-chemistry of interfaces has been initiated, and since mid September Marc van Dal started his Ph.D. work on this subject.

2 *Pb-Free Solder* (P.J.T.L. Oberndorff)

The last years there has been an increasing interest from industry for substitutes of the eutectic Sn-Pb solder. The main reason for this interest is that a ban on lead is expected to come into existence within a few years.

After some empirical research one acknowledged that fundamental research is needed to come up with decent alternatives. This is why our laboratory is involved in this project. We are studying phase diagrams, thermodynamics and kinetics of systems that could be used as alternative solders, and the interaction of these systems with substrate materials.

One of these systems is the Sn-Ag-Sb system. We investigated this system with the help of the diffusion couple technique and with equilibrated alloys. By studying the microstructure with light microscopy, electron microscopy and XRD we determined an isothermal cross-section of this system at 220 °C. Also an attempt has been made to calculate the phase equilibria in this system with the help of the Thermo-

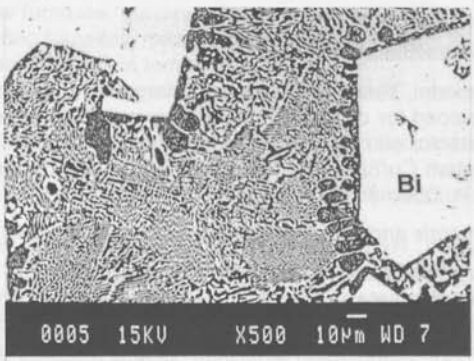


*Figure 2: Microstructure of a solidified hypereutectic Sn-Bi alloy, showing the formation of a Sn-rich halo around primary Bi-crystals*

Calc data bank. Furthermore we investigated the interaction of near eutectic Sn-Ag-Sb with Cu, a commonly used substrate material.

Another very interesting candidate as an alternative solder material is the Sn-Bi system. Besides investigating the microstructure of alloys of this system we also studied the interaction with Ni.

In order to find evidence that the formation of intermetallic compounds in the vicinity of substrate/solder interface is mediated by the mechanism of isothermal solidification rather than reactive diffusion we started studying liquid-solid interaction and compared that to solid-solid interaction. This is being done with the help of the Sn-Au system. Here Sn represents the solder material and Au the substrate. This investigation is currently being conducted.

3 *Chemical Interactions in Metal-III-V Compound Semiconductor Systems* (S. Markovski)

In general, solid state electronic devices require low resistance Ohmic contacts to allow communication with the external circuit via the flow of current. The most common and familiar use of metal films in semiconductor technology is for surface wiring. The materials, methods and process of "wiring" the component parts together is generally referred to as metallisation. The electrical properties of a metal contact to a compound semiconductor depend strongly upon the chemistry of the metal-semiconductor interface. Ohmic contacts have usually been formed by an alloying process which often results in undesirable interfacial reactions, massive interdiffusion and lateral non-uniformity of the contact region. These processes may also cause embrittlement due to formation of intermetallics, or reduced bondability and even the catastrophic delamination of the contact metallisation.

In the past year, metal/III-V compound semiconductor interfaces have been investigated intensively in order to find suitable metallisation scheme meeting the performance, reproducibility and stability criteria. Solid state equilibria at 500 °C in the Ga-Ni-

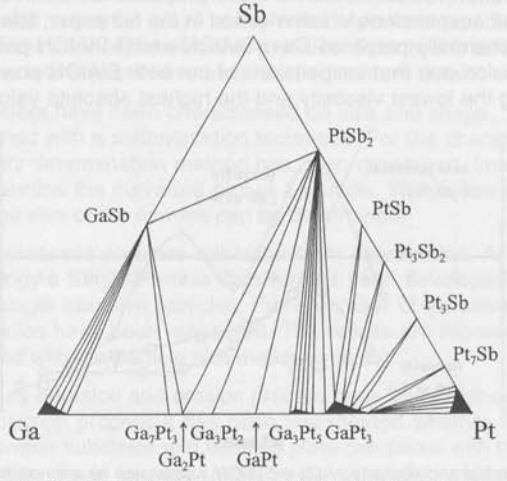


*Figure 3: Isothermal cross section at 500 °C of the Ga-Pt-Sb phase diagram*

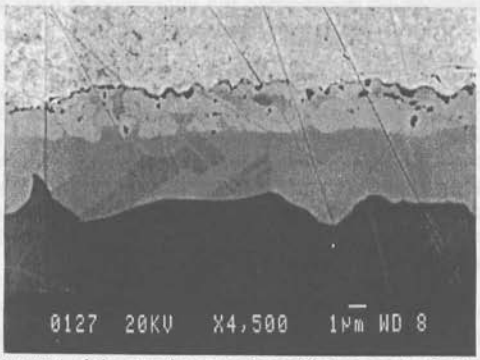


*Figure 4: Microstructure of the reaction zone in a diffusion couple GaPt/Pt annealed at 500 °C for about 100 h*

Sb, Ga-Co-Sb and Ga-Pt-Sb systems have been experimentally determinate. In the course of the work substantial efforts were concentrated on studying the solid state transformations in the constituent binary systems, for *e.g.* the new temperatures of transformation and phase boundaries in the Ni-rich part of the Ga-Ni diagram has been suggested. The $GaPt_2$ phase at 500 °C in the binary Ga-Pt system was not present, contrary to previous reports in the literature. The resulting Ga-Pt-Sb isothermal cross section at 500 °C is shown in Figure 3. The microstructure of the reaction zone in a diffusion couple GaPt/Pt annealed at 500 °C for about 100 h is given in Figure 4.

4 *Aqueous Processing of SiAlON Powders* (A.A. Kudyba)

The objective is the investigation of the influence of suspension parameters and processing conditions on mechanical properties of green compact and sintered product. Work performed on carbo-thermally prepared Ca-α-SiAlON and β-SiAlON powders and their suspensions is summarised in the full paper, titled "Aqueous processing of carbo-thermally prepared Ca-α-SiAlON and β-SiAlON powders". The most important conclusion was that suspensions of our both SiAlON powders behave very similarly showing the lowest viscosity and the highest absolute values of zeta poten-

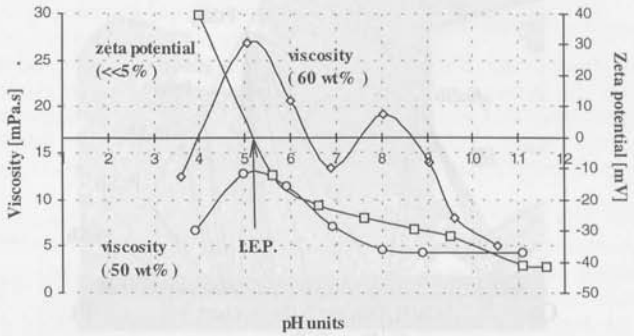


*Figure 5: Zeta potential and viscosity of Ca-α-SiAlON suspension as a function of the pH. The solid content is indicated in the figure*

tial at pH 10-11. As an example Figure 5 shows such a behaviour of a Ca-α-SiAlON suspension and also the good correlation between used different techniques: at the isoelectric point (I.E.P., zeta potential is zero) the viscosity is the highest due to flocculation. The second maximum in viscosity (Figure 5) measurement was checked and appeared to be reproducible and is assigned to particle-particle interaction.

A more focused study on the influence of different treatments and additives on the suspension behaviour of β-SiAlON (graduation project), showed the significant role of sintering additive ($Y_2O_3$). The heterocoagulation of oppositely charged β-SiAlON and $Y_2O_3$ particles (between pH 4.6 and 9.0, isoelectric points respectively) and coagulation of β-SiAlON particles and the dissolution of $Y_2O_3$ below pH 6 exclude the possibility of preparing the suspension at pH below 9.

Expecting that similar suspension behaviour of the investigated SiAlON powders is caused by similar surface composition we performed X-ray Photoelectron Spectroscopy measurements on Ca-α-SiAlON and β-SiAlON powder. The interpretation of the obtained results is in progress.

Over four months were spent on full time teaching at Silesian University of Technology, Katowice, Poland. The courses and lecturing concerned properties, behaviour and use of ceramics within the Materials Science and Engineering Course and Metallurgy Course.

5 *Fracture Characteristics of Abrasive Particles* (M.A. Verspui)

Three-body abrasion of glass is an important industrial process in finishing x-ray tubes, lenses and prisms. Another abrasive process is the erosion process, which in recent years has been developed as an industrial process. This technique produces small holes and channels in thin glass plates. The descriptions of both three-body abrasion and erosion are based on the indentation fracture theory.

The objective of the investigation is to develop a simulation model for abrasive processes starting from the indentation theory. In this model the interaction between abrasive particle and substrate plays a key role. Important aspects are the shape and degradation behaviour of the abrasive particles. Prior to the development of the simulation model, a few aspects have been studied in more detail.

The abrasive powders have been characterised on size and shape. The particle size has been determined with a sedimentation technique. For the characterisation of the shape an angularity determination method has been developed. Image analysis has been used to determine the curvature plot of a particle. With a few selection criteria the number and the size of the corners can be determined.

During abrasive processes particles will suffer from degradation. At Eindhoven University of Technology a Single Particle Crusher has been developed to measure the fracture force of single abrasive particles. For a number of abrasive powders about one hundred particles have been measured. The results are represented in Weibull plots and compared with the particle size measurements.

Then the three-body abrasion and erosion process have been further investigated. In the three-body abrasion process it has been investigated whether the experimental bed thickness between substrate and backing plate compares with the present theories. This information would be very useful in the simulation model. In the erosion

process the theoretical erosion map for spherical particle impact has been verified with single impact experiments on a soda-lime and a borosilicate glass.

The studies described above support the Monte Carlo simulation model. In the model of the erosion process an abrasive particle with a certain mass and velocity (both drawn from a Gaussian distribution) hits the surface, which is represented by a line. Depending on the kinetic energy of the particle a chip will break out. This so-called 'unit event' will be repeated many times. The simulation program determines the amount of removed material and the surface roughness. The results are compared with the performed erosion experiments. Finally, some remarks on how to adjust the model to make it suitable also for three-body abrasive processes will be made.

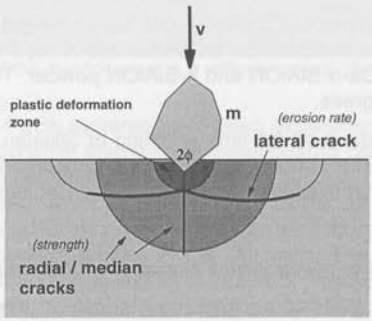


*Figure 6: The deformation and fracture pattern of a brittle material due to impact with a hard angular particle*

6 *Quality of the Surface Condition of Ground Inorganic Materials* (S. Shulepov)

A new project related to the modelling and optimisation of the grinding process. Grinding belongs to one of most important technological processes concerning abrasive processing and shape forming of different materials. It involves a lot of different parameters which may influence such characteristics as quality of the surface, state of the sub-surface stresses, power consumed during the process, etc. There is an empirical knowledge about such parameters as the wheel speed and velocity of the work piece, depth of cut etc. Values of these parameters are usually estimated on the basis of averaged characteristics describing the grinding wheel topography, grinding method, coolant used, etc. Moreover, they are tightly tied to the properties of a material ground.

However, deviations from those averaged characteristics may cause a significant, local "damage" of the work piece ground, leading to a degradation of important properties of materials, such as magnetic susceptibility in ferrite-based ceramics, for example. Also, they may significantly influence the power losses during the process. To optimise the grinding process, it should be looked at the time scale of a unit event. Relating to the wheel topography, the unit event describes an engagement of one grain of the grinding wheel with work piece. Such an engagement can be described on the basis of indentation, where both normal and tangential components are present (scratch). Deviation from averaged characteristics of such an indentor may strongly influence very important properties of the process as forces acting during

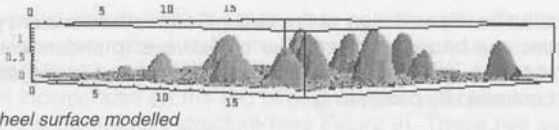

*Figure 7: The wheel surface modelled*

the grinding, integrity of the gage ground, rate of the removal process, power consumed during the process, etc.

In with theoretical modelling of this process at the level of the unit event, an experimental part of the investigation includes characterisation of the wheel topography (which serves as an input for theoretical simulations), and an assembly of the measuring platform for recording forces and moments during the process. This equipment must be able to cover all time scales being important for the grinding process. In terms of frequencies, this latter corresponds typically to about 500-900 kHz for a unit event (depending on the grain concentration and size), about 1-10 kHz – for eigenfrequency of the grinding wheel (depending on the wheel size), etc.

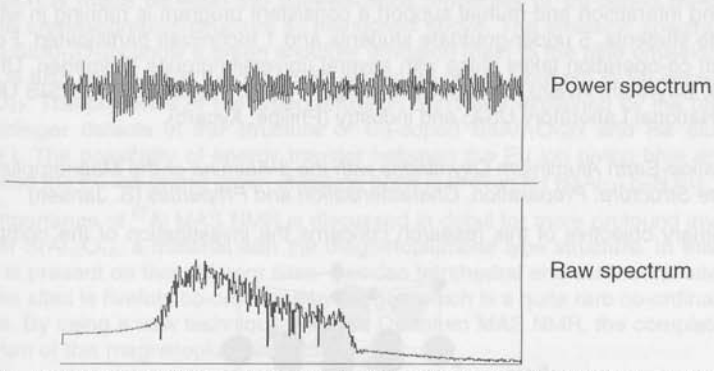


*Figure 8: A typical result of AE measurements. A filter with the band path 450-950 was applied to filter out signals from individual grains.*

Topography measurements are used as input in Monte Carlo-like simulations. Considering engagements of all the simulated grains during the grinding process, various characteristics can be predicted, *e.g.*, forces, grinding power, work piece topography, etc.

Utilising acoustical emission (AE) technique combined with piezo-accelerators, a dynamical part of these engagements can be followed and analysed experimentally. The absolute, "static" values of these characteristics can be extracted using more traditional methods (3-way dynamometers, for example).

7 *Materials Chemistry of Oxynitrides* (H.T. Hintzen)

In the cluster 'Oxynitrides' of the department 'Solid State and Materials Chemistry' the work covers the route from design, preparation an characterisation to properties and applications of novel oxynitrides.

Oxynitrides show an extensive crystal chemistry: the substitution of oxygen on nitrogen sites either will lead to vacancies, or has to be compensated for by a heterova-

lent cation substitution. By variation of the O/N ratio (*i.e.* the covalency of the material) the properties can be manipulated. The objective is to understand the relationship between properties on the one side and composition and (micro)structure on the other hand, as controlled by processing.

The research takes place along three interconnected main lines, *viz.*

1. Crystal Chemistry
   Current topics: $BaAl_{11}O_{16}N$ with the β-alumina structure and related compounds, beside standard techniques, also more sophisticated techniques, like neutron diffraction and multiple quantum solid state NMR are applied.
2. Properties
   At present, mechanical, thermal and optical properties are included in this part of the program.
3. Processing
   At the moment the work is focused on the aqueous processing of Sialons and the conversion of the waste material fly ash into Sialons.

By strong interaction and mutual support a consistent program is running in which 4 graduate students, 5 under-graduate students and 1 technician participated. For this research co-operation takes place with several university groups (Nijmegen, Utrecht, Rennes, Bayreuth, Aveiro, Cornell USA, Rutgers USA), institutes (TNO, ISIS UK, Argonne National Laboratory USA) and industry (Philips, Xycarb).

8 *Alkaline-Earth Aluminium Oxynitrides with the β-Alumina or the Magnetoplumbite Type Structure: Preparation, Characterisation and Properties* (S. Jansen)

The primary objective of this research concerns the investigation of the compound

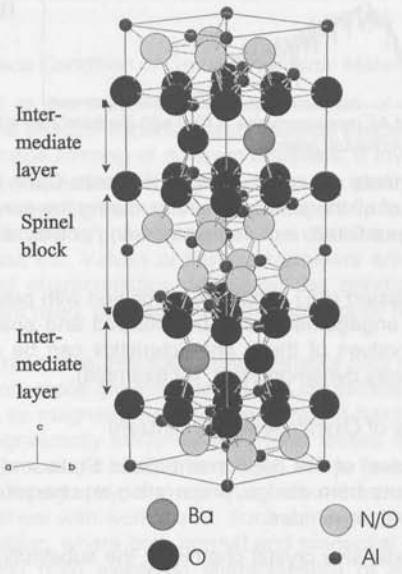


*Figure 9: The crystallographic structure of $BaAl_{11}O_{16}N$, showing the sites that are occupied by nitrogen*

$BaAl_{11}O_{16}N$, a novel material with the β-alumina type structure. The structural details of $BaAl_{11}O_{16}N$ are determined by Rietveld structure analysis which is applied on powder neutron diffraction data (recorded at the ISIS facility in the UK). In this way it is found that N incorporates on the two largest oxygen sites present in the so-called spinel block of the $BaAl_{11}O_{16}N$ structure (see Figure 9). These two oxygen sites are both co-ordinated to the Al site on which $Mg^{2+}$ is substituted in $BaMgAl_{10}O_{17}$ as was also shown with our neutron diffraction study. The $N^{3-}$ and $Mg^{2+}$ substitutions compensate for the difference in charge between the spinel block and the intermediate layer. Therefore no Reidinger defects are present in these two materials, in contrast to Ba aluminate phase I ($Ba_{0.83}Al_{11}O_{17.33}$) in which these defects are necessary to compensate for the charge difference. It is shown by neutron diffraction that in Eu-doped Ba β-alumina's (Ba aluminate phase I, $BaMgAl_{10}O_{17}$, and $BaAl_{11}O_{16}N$) one Eu-site is present near the so-called anti-Beevers-Ross site (0, 0, 1/4). This is in contrast to the commonly made assumption that $Eu^{2+}$ substitutes on the site that is normally occupied by $Ba^{2+}$ (2/3, 1/3, 1/4), the so-called Beevers-Ross site.

A relation is made between the luminescence properties of Eu-doped $BaAl_{11}O_{16}N$ and the crystallographic structure as mentioned above. The emission spectra of Eu-doped $BaAl_{11}O_{16}N$ show a green shoulder emission (next to the blue emission peak) which is also observed in Eu-doped Ba aluminate phase I but not in Eu-doped $BaMgAl_{10}O_{17}$. The presence of the green emission band was explained by the presence of Reidinger defects in the structure of Eu-doped $BaAl_{11}O_{16}N$ and Ba aluminate phase I. The possibility of energy transfer between the Eu ion giving blue emission band and the Eu ion giving green emission band is proven for $BaAl_{11}O_{16}N$:Eu.

The importance of $^{27}Al$ MAS NMR is discussed in detail for more profound investigations of $SrAl_{12}O_{19}$, a material with the magnetoplumbite type structure. In this material Al is present on five different sites. Besides tetrahedral and octahedral sites, one of these sites is fivefold co-ordinated by oxygen which is a quite rare co-ordination for Al ions. By using a new technique, Multiple Quantum MAS NMR, the complete NMR spectrum of this magnetoplumbite is resolved.

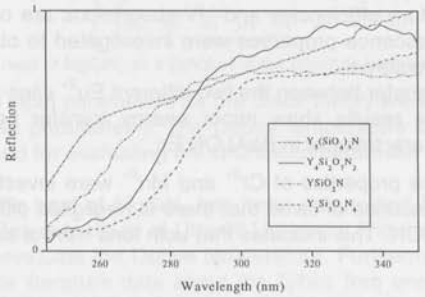


*Figure 10: Reflection spectra of the undoped Y-Si-O-N materials*

9 *Luminescence in Oxynitrides* (J.W.H. van Krevel)

The objective of this research is that oxynitride materials might be interesting phosphors when doped with rare-earth ions. This research is an exploratory research at the luminescence properties of rare-earth doped oxynitrides. The main results ob-

tained in 1997 are described in the following.

We have looked at the luminescence properties of undoped and rare-earth doped $Y_5(SiO_4)_3N$, $YSiO_2N$, $Y_4Si_2O_7N_2$ and $Y_2Si_3O_3N_4$. The rare-earth ions used are $Ce^{3+}$ and $Tb^{3+}$. The undoped materials show band gaps in the UV-part of the spectrum (Figure 10). For the Ce-doped materials low energy excitation and emission bands are observed with emission up to 504 nm for $Y_4Si_2O_7N_2$:Ce (Figure 11). To compare, emission in the blue or near UV part of the spectrum (350-450 nm) is found in most Ce doped systems. The Tb doped Y-Si-O-N compounds show high quantum efficiencies for 254 nm excitation. This radiation is also used in an mercury containing discharge lamp.

The efficiency drops when the Tb band is positioned in the 5d band, like in $Y_2Si_3O_3N_4$:Tb.

The $Y_2Si_3O_3N_4$:Tb systems were compared with other oxide containing systems like $Y_3Al_5O_{12}$:Tb. From this comparison it was shown that cross-relaxation effects obeys the behaviour as observed in other systems. The probability for non-radiative multiphonon $^5D_3$-$^5D_4$-transitions is slightly more as a result of lattice vibrations at higher energy.

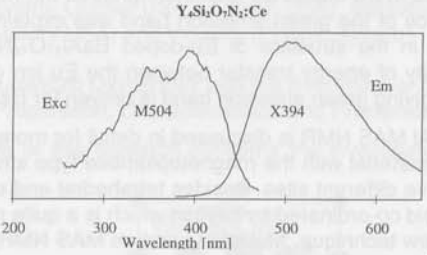


*Figure 11: Excitation and emission spectrum of $Y_4Si_2O_7N_2$ doped with 5% $Ce^{3+}$*

We examined $Eu^{2+}$ doped BaAlO, BaAlON and BAM with the β-alumina structure. Also here, high quantum efficiencies and UV-absorptions are observed for 254 nm excitation. The luminescence properties were investigated to obtain more insight in the different lattice structures.
Further, the energy transfer between the two different $Eu^{2+}$ sites present in BaAlO:Eu and BaAlON:Eu. The results show minor energy transfer between the sites in BaAlO:Eu and hardly any transfer in BaALON:Eu.

Also the luminescence properties of $Cr^{3+}$ and $Mn^{2+}$ were investigated. Research at $Cr^{3+}$ and $Mn^{2+}$ luminescence showed that there is negligible difference when doped in BaAlO versus BaAlON. This indicates that both ions have a similar environment in both systems.

10 *Thermal Conductivity/Diffusivity of $MgSiN_2$ Ceramics and Related Adamantine-Type Materials* (R. Bruls)

For a theoretical prediction of the maximum achievable thermal conductivity of a phonon conductor like $MgSiN_2$ (a potential interesting substrate material) several thermal properties as a function of the temperature have to be known. The most important properties for modelling are the thermal diffusivity, the specific heat and the

thermal expansion. The thermal diffusivity and specific heat data are needed for a semi-theoretical prediction method of the maximum achievable thermal conductivity whereas the specific heat and the thermal expansion are needed for theoretically calculating the maximum achievable thermal conductivity based on the theory of Slack.

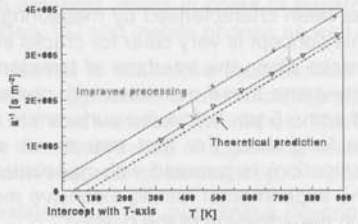


*Figure 12: Inverse thermal diffusivity versus the absolute temperature plot showing the intercept with the temperature axis*

The thermal diffusivity of $MgSiN_2$ as a function of the temperature was already measured in the past but the results were not fully understood. Last year we were able to obtain a better understanding of these results. If the inverse of the thermal diffusivity is plotted versus the absolute temperature a linear dependence is observed. For pure, defect free materials this line should intercept the *T*-axis and not as often stated in literature intercept at $T = 0$ K. For the highest conducting $MgSiN_2$ samples this negative intercept was indeed observed (Figure 12). Because the intercept with the temperature axis for a pure, defect free $MgSiN_2$ ceramics can be calculated the maximum achievable thermal conductivity can be evaluated.

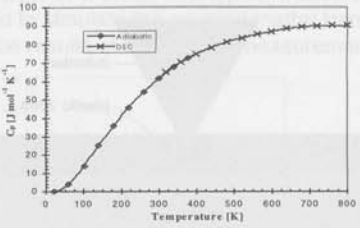


*Figure 13: The specific heat of $MgSiN_2$ as a function of the absolute temperature*

The most important input parameters for the Slack theory are the Debye temperature $\theta$ and the Grüneisen parameter $\gamma$. The Debye temperature can be evaluated from specific heat data and for evaluating the Grüneisen parameter the thermal expansion is needed.

Last year the specific heat of $MgSiN_2$ has been determined from 0 to 800 K in cooperation with the Debye Institute of Utrecht University (Figure 13). The specific heat data were used to evaluate the Debye temperature. Furthermore, using the specific heat data and some literature data about the Gibbs free energy of $MgSiN_2$ at high temperatures, the thermodynamic functions *S* (entropy), *H* (enthalpy) and *G* (Gibbs free energy) were calculated from 0 to 2000 K.

Contact with several institutes (Argonne National Laboratory (ANL) and TNO/TPD) have been made to measure the thermal expansion in the temperature range of 0 to 800 K. Some preliminary results are already available but further measurements and interpretation are needed.

11 *Failure* (P.G.Th. van der Varst)

The objectives are to model adhesion of thin, brittle coatings on metallic substrates. This research is an IOP-OT project in co-operation with Universities of Delft and Groningen, TNO-TPD and TNO Industries.

Traditionally, strength has been characterised by measuring critical values of stress intensity factors. While this concept is very clear for cracks in monoliths the matter is not straightforward for cracks along the interface of bimaterials. In addition, the experimental difficulties to measure these quantities with coated specimens where the interface crack is located some 5 μm below the surface are as yet unsolved and remain so for, probably, a long time. For that reason an energy based approach (energy release rate, dissipation) is pursued with nanoindentation as experimental technique. To interpret the experimental results extensive modelling is necessary so as to obtain information on the adhesion of the coating.

Since the thermal expansion coefficient of the coating and substrate material are generally different and production of the coatings occur at elevated temperatures residual stresses develop and the elastic energy associated with these stresses may act as an energy source for crack initiation or propagation. As elastic energy is a quadratic form of the stresses, the residual stresses interact at an energetical level with the stresses induced by an applied external load.
Although locally this interaction is surely present, it was found that globally the sources of elastic energy decouple. However, it was also found that the internal stresses interact with the loading mechanism. This interaction however is expected to be negligible in case the distance between crack tip and loading mechanism is sufficiently large.

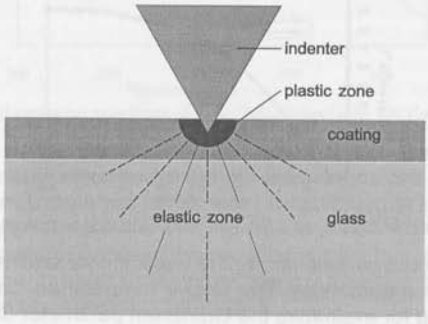


*Figure 14: The nanoindentation technique*

As loss of adhesion is essentially an irreversible process, a general thermodynamical framework for interface cracks of bimaterials has been developed. In this model a coating is viewed as an assembly of several system parts having different dimensionality (D) (substrate and coating 3D, interface 2D and crack front 1 D). These parts can exchange heat and mechanical energy. For each of the parts balance laws for the energy and a local version of thermodynamics' second law is derived. This enables one also to model processes (for example chemical attack of the crack front or viscous processes in the cohesive zone) local to the crack tip.
Plastic deformation of the substrate, damage in the coating and micro-delamination of the coating are considered as internal variables. It has been decided to model

evolution of these variables using the work potential theory of Schapery.

12 *Chemo-Mechanical Behaviour of Ferrites* (M.A.H. Donners)

Ferrites are oxide ceramic materials which are applied for their good magnetic properties. One can find them amongst others in cores of transformers, in filters of various equipment like TV, video, VC and mobile phones as well as in cars.

Mechanical behaviour of ferrites is influenced by subcritical crack growth. This implies that, in the presence of 'aggressive' compounds like water in the environment, the strengths and lifetime of these materials diminishes. This is caused by adsorption and/or chemical reactions directly at the tip of a growing crack, coupled with diffusion processes that furnishes new reagens tot he crack tip.

The objective of the investigation is the quantitative description of subcritical crack growth, revealing the mechanism involved and ultimately improvement of the material so that the sensitivity of the ferrite material for this effect is decreased.

To this purpose use is made of strength, life time and fracture toughness measurements under controlled pressure, chemical composition of the environment and temperature. Further experiments to measure directly the crack growth velocity in an electron microscope are being done. The adsorption and desorption of relevant gases is measured with TCD. The microstructure and chemical constitution of the ferrites is determined by SEM, TEM, XPS and LEIS (in co-operation with the group SKA and the faculty of Physics). Optical and electron microscopes are used to study fracture surfaces (fractography). An attempt will be made to measure diffusion and condensation of water vapour in a crack with typical thickness of 5 to 10 μm. A numerical model will be used to simulate the coupled matter transport and crack growth kinetics in order to describe results of the various measurements.

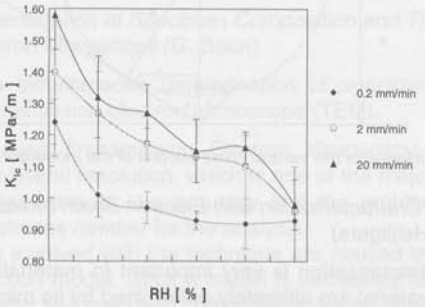


*Figure 15: Fracture toughness of MnZn ferrite versus relative humidity at three load rates (SENB measurements).*

These techniques are applied to ferrites of varying composition in order to be able to determine the influence of the chemical constitution and microstructure of the ferrite on its mechanical behaviour.

In this project there is a co-operation with TNO (within the Centre for Technical Ceramics, CTK), Philips Magnetic Products, Philips Research Laboratories Aachen, Philips WEB Hamburg and the faculties of Physics of the Groningen and Eindhoven Universities.

13 *Indentation* (V. Bondarenko)

In the last year attention was largely focused on indentation experiments. The ultimate goal of such experiments is not only the determination of the mechanical properties of various materials, like hardness and elastic modulus, but also the correlation with other properties.

The main goal was to determine in how far the mentioned mechanical properties can be measured with the "nano-indentor". We concluded that a number of characteristics (both of the hardware and software) are of crucial importance for proper measurement. These characteristics were determined. In particular the two most important characteristics, the "area function" and "compliance" were extensively studied and led to an improvement in accuracy and reliability of the data.

The reliability of the data of the nano-indentor was verified by independent measurements. The elastic modulus was determined by ultrasonic measurements. Both the "pulse-echo" and "transmission" method were used. For both methods conditions were found where the measurements can be considered as reliable.

The work done is a contribution towards the improvement of the measuring procedure for mechanical properties of solids.

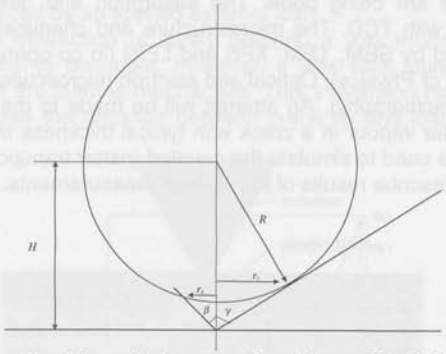


*Figure 16: Schematic drawing of the vertical cross-section of the modelled indenter*

14 *Microstructural Characterisation with Electron Beam based Instruments* (G.F. Bastin, H.J.M. Heijligers)

Microstructural characterisation is very important in materials science because the properties of any material are ultimately determined by its microstructure. Among the various techniques that are currently available for this purpose, those that are based on the use of (finely focused) beams of high-energy electrons, still appear to be the most popular and wide-spread. The equipment based on such techniques is well-represented in the Laboratory of Solid State and Materials Chemistry: Scanning Electron Microscopes (SEM's), Electron Probe Microanalysers (EPMA's, 2), and a Transmission Electron Microscope with Scanning Transmission unit (TEM-STEM).

Under the bombardment with high-energy electrons the atoms in the specimen start to emit their characteristic X-rays, which can be used for qualitative and quantitative analysis on the (required) μm-scale level. Unfortunately, the emitted X-ray signals are not proportional to the concentrations of the elements involved, and a lot of com-

plicated "matrix correction" procedures have to be applied in order to convert the measured X-ray signals into the correct concentration units.

One of our main research objects in the past decade has been to introduce and develop improved matrix correction procedures, not only for conventional bulk analysis in cross sectioned specimens in SEM and EPMA, but also for the analysis of thin films, either supported or unsupported. Invariably, our efforts in this respect have been based on attempts to use realistic descriptions of the X-ray ionisation function ($\varphi$) as a function of mass depth ($\rho z$), the so-called $\varphi(\rho z)$ curves. At the same time we have been very active in collecting (for the first time in literature) vast data bases of measurements for the ultra-light elements B, C, N, and O, which present enormous challenges for any matrix correction program. As a result of all these efforts we can say that, at the moment, we have one of the best matrix correction procedures ("PROZA96") for bulk applications, currently available.

In recent years the successful $\varphi(\rho z)$ approach has also been extended toward thin film applications (so far in SEM and EPMA, up to 40 kV), in which it is possible to determine simultaneously the thickness and the composition of a thin film (< 1 μm), either on a substrate or unsupported. In this field too we have been active in setting up vast data bases of thin film measurements (Al and Pd films, so far) (Bastin, Heijligers).

A very interesting possibility is to extend and test the existing thin film procedures for application in the TEM, up to 200 kV, where the specimen consists of a very thin (<< 1 μm) unsupported film. This idea is being pursued by our graduate student Gerben Boon, and the results obtained so far, are encouraging, in principle. Unfortunately, a number of hardware modifications to the TEM were found necessary, which proved very time consuming.

15 *Simultaneous Determination of Specimen Composition and Thickness using the Transmission Electron Microscope* (G. Boon)

The objectives is the simultaneous determination of specimen composition and thickness using the transmission electron microscope (TEM).

X-ray microanalysis using Transmission Electron Microscopy allows quantitative analysis with very high lateral resolution, which is one of the major advantages of the technique. Disadvantages are its low accuracy and the problems associated with preparing the thin specimens needed for the analysis.
Some of the problems involved with the technique are caused by the lack of an appropriate matrix correction model. Such a model is necessary to convert the measured X-ray intensities into the specimen composition, taking parameters like absorption and fluorescence into account.
We found the $\varphi(\rho z)$ matrix correction approach very useful for application in the analytical TEM. The model we used was based on the "Double Gaussian" $\varphi(\rho z)$ approach, which was originally developed for measurements on an Electron Probe Micro Analyser (up to 50 kV) and subsequently implemented into a computer program called 'PROZA' by G.F. Bastin in our group.

Using this model, we are able to calculate both composition and thickness from X-ray data measured with an EDX-detector at one single accelerating voltage. Both thin and thick specimens can be analysed, and light elements can also be studied, all

without major changes to the TEM set-up.

The beam current is a vital parameter in the collection of accurate X-ray data, since the ratio between the emitted intensities (in counts/sec/nA) from specimen and standard (the so-called *k*-ratio) is the crucial input parameter into the correction program. Therefore, we have designed and installed an accurate and highly sensitive probe current meter, which covers a large range in currents. The latter is necessary in order to deal with the huge differences in count rates between bulk standards and thin film specimens. This new device makes it possible to measure the electron beam current with the required high precision.
The validity of the $\varphi(\rho z)$ model under TEM conditions was checked (up to 200 kV) by performing measurements on bulk AlNi and AlTi samples and on an electropolished AlZr TEM specimen. For these measurements, the model was found to be correct. More testing has to be done to check the consistency of the model throughout the periodic table.

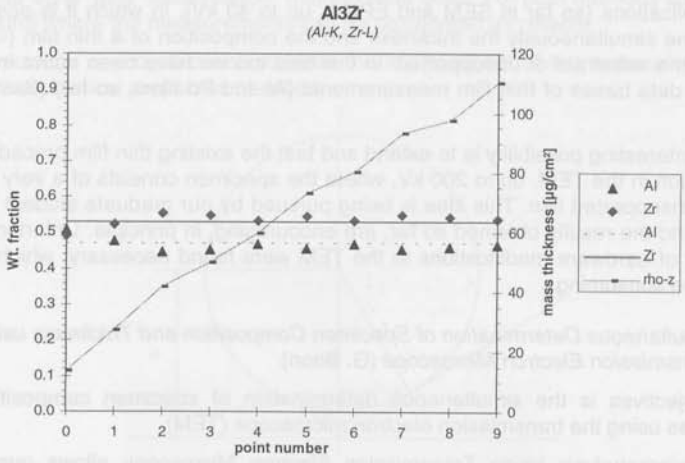


*Figure 17: Measured concentration and thickness profile of $Al_3Zr$ TEM specimen*

PUBLICATIONS

G.F. Bastin, J.H.M. Heijligers
*Quantitative EPMA of the ultra-light elements Boron through Oxygen*
Eur. J. Mineralogy 9 (1997) 2

E.G. Bennett, L.J.M.G. Dortmans, M. Hendrix, R. Morrell, G. de With
*CEN/VAMAS study of phase volume fraction measurement - A preliminary review of results*
In: J. Baxter, L. Cot, R. Fordham, V. Gabis, Y. Hellot, M. Lefebvre, H. Le Doussal, A. Le Sech, R. Naslain, A. Sevagen (eds.), Proceedings: 5th ECerS 22-26 June 1997, Euro Ceramics V Part 3, Trans Tech Publications, Switzerland, Key Engineering Materials 132-136 (1997) 2111-2114

S. van den Cruijsem, P.G.Th. van der Varst, G. de With

*Pressure-assisted sintering of high purity barium titanate*
In: P. Abelard, A. Autissier, A. Bouquillon, J.M. Haussonne, A. Mocellin, B. Raveau, F. Thevenot (eds.), Proceedings: 5th ECerS 22-26 June 1997, Euro Ceramics V Part 2, Trans Tech Publications, Switzerland, Key Engineering Materials 132-136 (1997) 1031-1034

M. Donners, L. Dortmans, G. de With, M. de Graaf
*Fracture behaviour and fractography of MnZn ferrites*
In: L. Parilak (ed.), Proceeding of International Conference FRACTOGRAPHY '97, Stará Lesná, High Tatras, October 26-29, 1997, IMR SAS Kosice, Slovakia

M. Donners, L. Dortmans, G. de With, M. de Graaf
*Modelling of Subcritical Crack Growth in MnZn Ferrites*
In: D. Bortzmeyer, M. Boussuge, Th. Chartier, G. Fantozzi, G. Lozes, A. Rousset (eds.), Proceedings: 5th ECerS 22-26 June 1997, Euro Ceramics V Part 1, Trans Tech Publications, Switzerland, Key Engineering Materials 132-136 (1997) 714-717

M. Donners, L. Dortmans, G. de With, M. de Graaf
*Subcritical crack growth in MnZn Ferrites with a Bimodal defect distribution*
J. Eur. Ceram. Soc. 17 (1997) 1591-1596

L.J.M.G. Dortmans, M. Donners, M. de Graaf, G. de With
*Reliability of ferrite cores in applications and quality control tests*
In: D. Bortzmeyer, M. Boussuge, Th. Chartier, G. Fantozzi, G. Lozes, A. Rousset (eds.), Proceedings: 5th ECerS 22-26 June 1997, Euro Ceramics V Part 1, Trans Tech Publications, Switzerland, Key Engineering Materials 132-136 (1997) 456-459

W.FJ. Fontijn, R.M. Wolf, R. Metselaar, P.J. van der Zaag
*Investigation of the stoichiometry of MBE-grown $Fe_3O_4$ layers by magneto-optical Kerr spectroscopy*
Thin Solid Films 292 (1997) 270-276

W.F.J. Fontijn, P.J. van der Zaag, M.A.C. Devillers, V.A.M. Brabers, R. Metselaar
*Optical and magneto-optical polar Kerr spectra of $Fe_3O_4$ and $Mg^{2+}$- or $Al^{3+}$-substituted $Fe_3O_4$*
Phys. Rev. B 56 (1997) 5432-5442

M.A.J. van Gils
*Quasi-Brittle Fracture of Ceramics*
Ph.D. thesis, Eindhoven University of Technology (1997)

M.A.J. van Gils, L.J.M.G. Dortmans, G. de With
*Thermal shock predictions for refractory ceramics*
In: Proceedings of the Second International Symposium on Thermal Stresses and Related Topics, June 8-11, 1997 Rochester Institute of Technology, 697-682

H.J. Glass, J.W.G.A. Vrolijk, M.J.M. de Graaf
Optimalisering van poeder compactie
Bulk 5 (1997) 66-69

Y.J. He, A.J.A. Winnubst, A.J. Burggraaf, H. Verweij, P.G.Th. Van der Varst, G. de With
*Influence of Porosity on Friction and Wear of Tetragonal Zirconia Polycrystal*
J. Am. Ceram. Soc. 80 (1997) 377-380

Y.J. He, A.J.A. Winnubst, A.J. Burggraaf, H. Verweij, P.G.Th. van der Varst, G. de With
*Sliding Wear of $ZrO_2$-$Al_2O_3$ Composite Ceramics*
J. Eur. Ceram. Soc. 17 (1997) 1371-1380

J.C.T. van der Heijde, R.A. Terpstra, J.W.T. van Rutten, R. Metselaar
*Total aqueous processing of carbothermally produced β-Sialon*
J. Eur. Ceram. Soc. 17 (1997) 319-326

E. Heikinheimo, I. Isomäki, A.A. Kodentsov, F.J.J. van Loo
*Chemical Interaction Between Fe and Silicon Nitride Ceramic*
J. Eur.Ceram.Soc. 17 (1997) 25-31

S.R. Jansen, J.W. de Haan, L.J.M. van de Ven, R. Hanssen, H.T. Hintzen, R. Metselaar
*Incorporation of nitrogen in alkaline-earth hexaaluminates with a β-alumina- or a magnetoplumbite-type structure*
Chem. Mater. (1997) 1516-1523

S.R. Jansen, H.T. Hintzen, R. Metselaar
*Phase Relations in the $BaO$-$Al_2O_3$-AlN System: Materials with the β-Alumina Structure*
J. Solid State Chem. 129 (1997) 66-73

S.R. Jansen, T. van Mol, H.T. Hintzen, R. Metselaar
*Properties of novel ceramic materials in the $BaO$-$Al_2O_2$-AlN-MgO system with a β-alumina type structure*
In: P. Abelard, A. Autissier, A. Bouquillon, J.M. Haussonne, A. Mocellin, B. Raveau, F. Thevenot (eds.), Proceedings: 5th ECerS 22-26 June 1997, Euro Ceramics V Part 2, , Trans Tech Publications, Switzerland, Key Engineering Materials 132-136 (1997) 783-786

A.A. Kodentsov, M.H.J. van Dal, Cs. Cserháti, J.K. Kivilahti, F.J.J. van Loo
*On Nitrigen Diffusion during the Internal Nitridation of Ni-Based Alloys*
In: H. Mehrer, Chr. Herzig, N.A. Stolwijk, H. Bracht (eds.), DIMAT 96, Proceedings of the International Conference on Diffusion in Materials, Nordkirchen, Germany, August 5th to 9th, 1996, Part 1, Defect and Diffusion Forum 143-147 (1997) 1619-1624

A.A. Kodentsov, F.J.J. van Loo
*Reactive Phase formation in inorganic materials*
In: E. Heikinheimo, L. Palmu (eds.), Proc. Of Postgraduate seminar Gas-Solid Reactions, Sjökulla, Finland, September 8-9, 1997, Helsinki University of Technology Publications in Materials Science and Metallurgy

A. Kudyba, M. Almeida, H.T. Hintzen, J.C.T. van der Heijde, J. Laven, R. Metselaar
*Aqueous processing of carbothermally prepared Ca-α-SiAlON and β-SiAlON powders: powder and suspension characterisation*
In: D. Bortzmeyer, M. Boussuge, Th. Chartier, G. Fantozzi, G. Lozes, A. Rousset (eds.), Proceedings: 5th ECerS 22-26 June 1997, Euro Ceramics V Part 1, Trans Tech Publications, Switzerland, Key Engineering Materials 132-136 (1997) 325-328

F.J.J. van Loo, A.A. Kodentsov
*Diffusion bonding of Si-containing ceramics to transition metals: Chemical aspects*

In: Proceedings of 5th International conference Joining, Jena Germany, May 12/14 1997, DVS-Berichte Band 184 (1997) 60-64

F.J.J. van Loo, M.R. Rijnders, K.J. Ronka, J.H. Gulpen, A.A. Kodentsov
*Solid state diffusion and reactive phase formation*
Solid State Ionics 95 (1997) 95-106

S.L. Markovski, J.A. van Beek, R.C.J. Schiepers, A.A. Kodentsov, F.J.J. van Loo
*Thermodynamic evaluation of Ga-X-Co (X=P, As,Sb) systems related to the metallization of III-V compound semiconductors*
J. Chim. Phys. 94 (1997) 992-997

R. Metselaar, A.A. Kodentsov, F.J.J. van Loo
*Microstructural evolution of SiC/metal interfaces at elevated temperatures*
In: J. Baxter, L. Cot, R. Fordham, V. Gabis, Y. Hellot, M. Lefebvre, H. Le Doussal, A. Le Sech, R. Naslain, A. Sevagen (eds.), Proceedings: 5th ECerS 22-26 June 1997, Euro Ceramics V Part 3, Trans Tech Publications, Switzerland, Key Engineering Materials 132-136 (1997) 1758-1761

A. Noordermeer
*Wet Chemical Processing of MnZn-Ferrites*
Ph.D. thesis, Eindhoven University of Technology (1997)

C. Qui and R. Metselaar
*Phase Relations in the Aluminum Carbide-Aluminum Nitride-Aluminum Oxide System*
J.Am.Ceram.Soc. 80/9 (1997) 2013-2020

M.R. Rijnders, A.A. Kodentsov, J.A. van Beek, J. van den Akker, F.J.J. van Loo
*Pattern formation in Pt-SiC diffusion couples*
Solid State Ionics 95 (1997) 51-59

K.J. Rönkä, A.A. Kodentsov, J.K. Kivilahti, F.J.J. van Loo
*Diffusion in a Ternary System Exhibiting a Miscibility Gap*
In: H. Mehrer, Chr. Herzig, N.A. Stolwijk, H. Bracht (eds.), DIMAT 96, Proceedings of the International Conference on Diffusion in Materials, Nordkirchen, Germany, August 5th to 9th, 1996, Part 1, Defect and Diffusion Forum 143-147 (1997) 541-556

K.J. Rönkä, F.J.J. van Loo, J.K. Kivilahti
*Thermodynamic and kinetic study of diffusion paths in the system Cu-Ag-Zn*
Z. Metallkd. 88 (1997) 9-13

K.J. Rönkä, F.J.J. van Loo, J.K. Kivilahti
*The local nominal composition-useful concept for microjoining and interconnection applications*
Scripta Materialia 37 (1997) 1575-1581

M. Sychev, V.H.J. de Beer, A.A. Kodentsov, E.M. van Oers, R.A. van Santen
*Chromia- and Chromium Sulfide-Pillared Clays: Preparation, Characterization, and Catalytic Activity for Thiophene Hydrodesulfurization*
J. Catalysis 168 (1997) 245-254

P.G.Th. van der Varst, G. de With
*The energy release rate of nonlinear double cantilever beam specimens*
Z. Metallkde. 88 (1997) 225-229

M.A. Verspui, G. de With
*Fracture characteristics of abrasive particles*
In: D. Bortzmeyer, M. Boussuge, Th. Chartier, G. Fantozzi, G. Lozes, A. Rousset (eds.), Proceedings: 5th ECerS 22-26 June 1997, Euro Ceramics V Part 1, Trans Tech Publications, Switzerland, Key Engineering Materials 132-136 (1997) 532-535

M.A. Verspui, G. de With
*Three-body abrasion: Influence of applied load on bed thickness and particle size distribution in abrasive processes*
J. Eur. Ceram. Soc. 17 (1997) 473-477

M.A. Verspui, G. de With, E.C.A. Dekkers
*A crusher for single particle testing*
Rev. Sci. Instrum. 68 (1997) 1553-1556

G. de With, H.J. Glass
*Reliability and Reproducibility of Mercury Intrusion Porosimetry*
J. Eur. Ceram. Soc. (1997) 753-757

X. Zhang, G.H.M. Gubbels, R.A. Terpstra, R. Metselaar
*Toughening of calcium hydroxyapatite with silver particles*
J. Mater. Sci., 32 (1997) 235-243

**TECHNICAL CERAMICS: THIN FILM AND POWDER TECHNOLOGY**

Delft University of Technology, Laboratory for Applied Inorganic Chemistry
Julianalaan 136, 2628 BL Delft
phone +31 (15) 2782647, fax +31 (15) 2788047, e-mail ...@stm.tudelft.nl

PERSONNEL

*Scientific staff*

| | |
|---|---|
| prof.dr. J. Schoonman | (2782647, J.Schoonman@...) |
| dr. A. Goossens (KNAW) | (2784919, A.Goossens@...) |
| dr. E.M. Kelder (STW) | (2783262, E.M.Kelder@...) |
| drs. P.J. van der Put | (2782634, P.vdPut@...) |

*Teaching staff*

| | |
|---|---|
| ir. J.G. van Berkum | (2782659, J.G.vanBerkum@...) |

*Post-doc's and International guests*

| | |
|---|---|
| prof.dr. L. Chen | |
| prof. M. Alavi | (27823891, A.Alavi@...) |
| dr. N.H.J. Stelzer | |
| dr.ir. A.A. van Zomeren | (2783262, A.A.vanZomeren@...) |

*Graduate students*

| | |
|---|---|
| ir. W.F.A. Besling | (2782637, Besling@...) |
| C.H. Chen, M.Sc. (SON/NWO) | (2782637, Chen@...) |
| ir. J. Driessen | (040-2656428) |
| drs. M.A. Hamstra | (2782676, M.Hamstra@...) |
| L. He, M.Sc. | (2783891, L.He@...) |
| drs. M.L.H. ter Heerdt | (2782637, M.L.H.terHeerdt@...) |
| H. Huang, M.Sc. | (2783891, H.Huang@...) |
| ir. M.J.G. Jak (SON/STW) | (2785536, M.Jak@...) |
| ir. M. Keijzer (Beek committee) | (2782637, M.Keijzer@...) |
| ir. R. van de Krol | (2782676, R.vanDeKrol@...) |
| ir. F.G.B. Ooms | |
| ir. L.N. van Rij | (2782676, L.N.vanRij@...) |
| drs. E.G.M. Veldman | (2784344, E.G.M.Veldman@...) |

*Materials designer*

| | |
|---|---|
| drs. M.H.J. Emond | (2782670, M.Emond@...) |

*Research students*

S.J. Everstein
J. Holtkamp
M. Maas
E.L. Maloney
B. Prihandoko
E. Serafini
A. Versleijen

*Technical staff*

ing. R. van Landschoot
N. van Landschoot

F. de Lange
W.J. Legerstee
B. Meester

## HIGHLIGHTS

Within the field of energy technology, a Delft Interfaculty Research Cluster program entitled: Decentralised Production and Storage of Electricity for Large-Scale Application of Renewable Energy has been granted. Prof. J. Schoonman is appointed as program leader. Participating research groups from the Faculties of Chemical Technology and Materials Science, Technical Physics, Electrical Engineering, Civil Engineering and the Interfaculty Research Institute (IRI) focus their expertise on the various projects to yield a multidisciplinary approach towards generation and storage of renewable energy. The Delft University of Technology has a long-term commitment towards this DIOC program extending for a minimum period of four years.

Related to our lithium battery investigations, the "Nederlandse Onderneming Voor Energie en Milieu" (NOVEM) has selected our laboratory as Dutch co-ordinator (Expert) within the International Energy Agency (IEA). The task as formulated by IEA is to keep track of Exploratory Research on Advanced Batteries and Capacitors for Electric Vehicles. The expansion of the existing technologies for electrochemical conversion systems for electrical vehicles is pursued. At least once a year, prior to the Electrochemical Society Meeting, the world-wide selected experts meet to discuss the observed progression in battery research and development.

## RESEARCH AREAS AND OBJECTIVES

In the Laboratory for Inorganic Chemistry, fundamental and applied studies of advanced inorganic materials are focused on functional ceramic for conversion and storage of renewable energy. Investigation of the relations between defects and microstructures, and the chemical and physical properties of these materials will contribute to new or optimised synthetic routes for custom-designed structural, functional, and active hybrid materials. The synthesis of properties is essential. Thin films, in particular, nanostructured films, as well as nano-sized ceramic particles are obtained using Chemical Vapour Deposition (CVD), Electrostatic Spray Deposition, and to minor-extend, sol-gel synthesis. The investigations aim at fundamental understanding of gas-phase synthesis of dense and nanostructured ceramic films with controlled porosity. In addition, gas-phase synthesis of nano-sized powders, particle surface modification, and dynamic compaction are studied in great detail. Our current research activities within this framework are the synthesis of new ceramic materials for rechargeable lithium batteries, photovoltaic solar cells and gas sensors.

With regard to densification of the electroceramic materials Cold and Hot Uniaxial Pressing (CUP, HUP), Hot-Isostatic Pressing (HIP), and explosive and magnetic pulse dynamic compaction are employed. The dynamic compaction techniques aim at preserving the nano- size powders in the compacts in order to take advantage of the improved properties of the nano-sized powders, or even of new introduced grain boundary interface effects. Furthermore, a new device-technology has developed for rechargeable ceramic batteries.
In our projects the generation of properties is essential. Hence relations between

structures, defect structures, microstructures and chemical or electrical properties are investigated in great detail in order to prepare new or improved materials for rechargeable lithium-ion batteries, novel photovoltaic cells, and structural and functional composites.

## FACILITIES

*CVD-reactors*

- Four hot-wall low-pressure CVD-reactors (LP-CVD)
- Industrial hot-wall, pilot LP-CVD reactor (Tempress)
- Cold-wall LP-CVD epi-reactor with inductive heating
- Atmospheric-Pressure hot-wall CVD-reactor (AP-CVD)
- Cold-wall AP-CVD-reactor for Light-CVD
- Single-wafer (8") cold-wall LP-CVD reactor (ASM)
- Two Hot-wall LP-CVD gravimetric reactors for kinetic studies
- Radio frequency Plasma-CVD reactor
- Micro-wave Plasma-CVD reactor
- Industrial $CO_2$ laser with AP-CVD reactor
- Tuneable $CO_2$ laser with LP-CVD reactor
- UV-excimer and dye laser with AP-CVD and gravimetric AP-CVD reactor
- Electrochemical Vapour Deposition (EVD) reactor for ionic solid electrolytes
- Up-scaled EVD reactor for mixed conductors
- LP-CVD fluid bed reactor
- Two custom-built desktop AP-CVD reactors for laboratory courses

*Other synthetic equipment*

- High-vacuum Physical Vapour Deposition (PVD) reactor
- DC sputter coater
- Four-target electron-beam evaporation system
- Two ESD set-ups
- Vertical tube furnace for sintering up to 1700 °C
- 12 kW rf-generator for inductive heating
- Furnaces for solid state synthesis
- Spin coating system
- Three glove-box units
- Screen Printer
- Coin cell press
- Wire bar coater

*Characterisation equipment*

- Three Frequency Response Analysers (FRA), Solartron 1250, 1255, and 1260
- Two Electrochemical interfaces Solartron 1286
- Potentiostats EG&G 273, EG&G PARC 253 VerSatat
- Gamry Potentiostat EIS900, FRA
- Kethley 575i Potentiostat
- Five high-temperature stainless-steel and nickel conductivity cells
- Maccor Battery Testing System (24 independent channels)
- Two cryostats (Cryoson) 4 - 300 K
- Low-temperature Thermally Stimulated Depolarisation Current (TSDC) equip-

ment
- Scanning Electron Microscope (JEOL, JSM 35) with EDX (Oxford)
- Two UV-VIS Photo-electrochemical spectrometers
- Nd-YAG Laser
- XRD, Philips (3)
- UV-VIS (3), UV-VIS-NIR (3)
- EPR, Varian EPR4 spectrometer
- Foil thickness meter

RESEARCH REPORT 1997

1 *Lithium Ion Batteries*

Large scale introduction of zero-emission Electric Vehicles and decentralised load levelling systems in society is obstructed by the availability of adequate rechargeable batteries. The Swing-type lithium-ion battery has been recognised to meet the required demands, and much effort has been devoted to the development of materials for large-scale lithium-ion batteries. The technology for the swing-type battery is based on the use of suitably chosen lithium intercalation compounds, i.e. carbons and $LiMn_2O_4$, for the electrodes and a polymeric electrolyte. Especially, the state-of-the-art carbon anodes are hampering the developments.

Lithium batteries are generally acknowledged for their superior energy density and it is anticipated that they will become one of the most important energy storage batteries within the next decade. In our laboratory, the study of the fundamentals of materials for lithium batteries is a major theme. Both the synthesis and characterisation of new, or improved materials and composites for transport and intercalation of lithium as well as the electrochemical properties of laboratory-scale batteries are being studied. A novel densification technique is being studied for the optimisation of electrode/electrolyte interfaces and assembling of all solid-state batteries.
In addition, a novel thin film technique, i.e. Electrostatic Spray Deposition (ESD), has been developed for the deposition of thin films of battery components with controlled morphology, and of thin film batteries.

1.1 *Solid State Lithium Ion Polymer Batteries* (E.M. Kelder, A.A. van Zomeren)

In collaboration with Danionics (Denmark), Saft (France), Sonnenschein Lithium GmbH (Germany), and the Universities of Southampton and St. Andrews (UK), Nantes/Armines (France), and Uppsala (Sweden), cathode materials are studied for solid state lithium ion batteries.

In this project $LiMn_2O_4$ has been synthesised with a new technique in order to improve the materials by addition of several dopants including extra lithium. Additional lithium is known to decrease the capacity of the material as the oxidation state of the manganese is influenced dramatically. Small amounts of additional lithium are used to stabilise the cathode material during operation of the cell. Furthermore, despite the change in oxidation state of the manganese, resulting in an expected loss in capacity, the excess lithium leads to a higher amount of lithium occupying the tetrahedral sites, i.e. the lithium ions attractive for the battery in question. In order to improve both the stability and the capacity, several dopant ions are proposed and studied with most of them part of the patent concerning the synthesis of the materi-

als. Materials containing a particular dopant concentration have been synthesised. The XRD spectra show pure spinel phases, with a hint of amorphous material. Because lithium diffusion in these samples is very low, structural and chemical characterisation is performed to determine the impurity levels.

1.2 *Preparation and Characterisation of Thin Film Components for Rechargeable Lithium Batteries* (C.H. Chen)

Thin-film lithium batteries are of potential importance for various applications. Two film fabrication techniques, i.e. electrostatic spray deposition (ESD) and plasma-enhanced chemical vapour deposition (PECVD), have been used to prepare battery materials, such as $LiCoO_2$, $Li_xMn_2O_4$,$LiPO_4$,$BPO_4$-$Li_2O$, and poly(methoxy-ethoxy-ethoxy)phosphazene (MEEP). Chemical Vapour Deposition of MEEP has not been reported in the literature. Optimisation of the ESD and PECVD deposition conditions and developing new synthetic routes for the preparation of submicron and nano-sized battery component materials have been the main focal points in this period. We found that besides dense and porous layers a unique reticular structure can be formed in the $LiCoO_2$, $LiMn_2O_4$ and $LiPO_4$ films made by ESD. The formation mechanism and pore-size scaling law have been investigated. This structure is expected to be beneficial for applications in rechargeable lithium-polymer batteries, in catalysis, for gas-sensors (viz. Section 2.3), and in gas/liquid separation and related devices. Complete solid-state thin-film batteries have been fabricated using $LiPO_4$ or $BPO_4 \equiv Li_2O$ as electrolyte, and $Li_x$ Mn $_2O_4$ as electrodes. The charge-discharge behaviour has been studied in detail and the concept of rocking-chair batteries has been confirmed. The chemical diffusion coefficient of lithium in the electrode materials has been studied using low-frequency impedance spectroscopy and Galvanostatic Intermittent Titration Technique (GITT). For $Li_xCoO_2$ films the lithium chemical diffusion coefficient increases with x and increasing porosity. In the reticular structures a diffusion enhancement of a factor of 100 has been measured. For the PECVD of MEEP films, polymer films containing different chlorine (Cl) contents depending on the plasma power and deposition temperature have been obtained and characterised by EDX and FT-IR.

In addition to lithium battery materials, yttria-stabilised zirconia (YSZ) films on gadolinia-doped ceria (GCO) substrate have also been synthesised by ESD in order to illustrate the potential of this novel method (viz. Section 2.1). The development of the ESD technique has strengthened and initiated collaboration with Imperial College, the University of Metz, Technion, ECN, The Illinois Institute of Technology, and Philips.

1.3 *All-Solid-State AA-Type Rechargeable Lithium Batteries with Swing Electrodes and a Ceramic Electrolyte Dispersed in Solufill™ for Consumer Electronics* (E.M. Kelder)

$Li_xMn_2O_4$ powders with optimised stability and capacity have been synthesised successfully. The electrolyte $BPO_4$-$Li_2O$ is synthesised with $H_3BO_3$ -$H_3PO_4$ -LiOH aqueous mixtures as well as $H_3BO_3$-$H_{3-x}(NH_4)_xPO_4$ aqueous mixtures. It appears that the ammonia containing mixtures give nano-sized powders arising from a foam. X-Ray diffraction together with gravimetry reveal a single-phase material of $Li_xB_{1-1/3x}$ $PO_4$ , with $x<0.3$. The maximal overall conductivity is observed for $x=0.035$. The as synthesised powders could be successfully dispersed in polymer foils such as PVC, Poly-Ethylene, Poly-Carbonate, etc. Conductivity measurements on these foils reveal per-

colation-type electrical conductivity. As an alternative of this electrolyte Li-beta-alumina has been synthesised. Conductivity measurements on this electrolyte are concordant with literature data, indicating the material to be suited for dispersion in a polymeric matrix. Symmetrical cells of $Li_{1+d}Mn_{2-d}O_4$ / $Li_xB_{1-1/3x}PO_4$ / $Li_{1+d}Mn_{2-d}O_4$ have been fabricated and their electrochemical behaviour has been characterised. These batteries are to be used as micro-batteries for animal implants and are now being tested at IMAG/DLO (Wageningen) for this purpose.

1.4 *Dynamic Compaction of Rocking Chair Type Rechargeable Lithium Batteries* (M.J.G. Jak)

The priority in this project is to study the relation between the structure of the dynamically compacted materials and the (electrical) properties. Different methods of compacting Li-ion battery components and complete battery systems have been investigated. These methods include explosive compaction (EXC), magnetic pulse compaction (MPC), hot isostatic pressing (HIP), and cold isostatic pressing (CIP). With these methods, a pressure range from 0.1 to 17 GPa is covered. Usually, rechargeable lithium-ion batteries comprise next to the electrodes a polymeric electrolyte. The advantage of the use of polymeric electrolytes is the intimate contact between the ceramic electrodes and the electrolyte. However, a major disadvantage of polymeric electrolytes is their inherent instability. Ceramic electrolytes lead to poor electrical contacts with ceramic electrodes. Dynamic compaction yields improved contacts between ceramic battery components.

Battery components have been compacted and investigated with SEM, EDX, XRD, AAS, AC-impedance spectroscopy, and DC measurements. The influence of the compaction method and related pressures on the micro-structure and on the electrical properties of the electrolyte material $BPO_4$-$Li_2O$ have been established in detail. For the cathode material $Li_xMn_2O_4$ the electronic conductivity increases as well as the lithium ion conductivity. The dc-resistance of a dynamically compacted ceramic battery is improved substantially as compared to a traditionally compacted ceramic battery.

Due to the attention this project has received world-wide, new collaborations with the Forschungszentrum Karlsruhe (Germany) concerning MPC, Institute for Chemical Physics, Russian Academy of Science (EXC, HIP, anode materials) (Russia), Russian Federal Nuclear Centre All Russian Research Institute of Experimental Physics (RFNC-VNIIEF)(Russia), and Norit (anode materials)(The Netherlands) have been established.

In close connection with the projects described in Sections 1.3 en 1.4 battery materials as well as batteries are studied for application in decolised energy storage systems, these includes electricity storage at hand, load levelling as well as for future Electrical Vehicles.

1.5 *Electrode and Electrolyte behaviour in polyethylene matrices* (F.G.B. Ooms)

Commercial polyethylene types filled with electrode or electrolyte materials will be tested on their suitability for Li-ion battery components. Cells will be constructed by dynamic compaction in order to gain intimate contact between the individual foils. The cells will be tested with a MACCOR battery tester.

1.6 *Advanced Anode Materials for Rechargeable Li-Ion Batteries* (H. Huang, L. Chen)

In this project, the fundamental relations between the structure, the defect and microstructure and the electrical and lithium intercalation properties of novel $BC_xN$-based matrices and of nanostructured $TiO_2$ and $SnO_2$ will be studied. These materials have only recently been recognised as potential anode for rechargeable Lithium-ion Batteries. Their behaviour in batteries using polymeric and ceramic electrolytes will be characterised in detail in order to select the most optimal anode material. Such a study has not yet been reported in the lithium battery literature.

1.7 *Advanced Cathode Materials for Rechargeable Li-Ion Batteries* (M. Alavi, L. He)

Fundamental relations between structure, the defect and microstructure and the Lithium intercalation properties of Novel $Li(Mn,Fe)PO_4$ compounds as well as $Li_xMn_4O_4$ materials will be studied. The aim of the research is to find optimised cathode-material with a high capacity and improved performance.

1.8 *Dynamic Compaction of Ceramics and Composites* (E.P. Carton)

In close connection with the research project described in Section 1.3, dynamic compaction is also studied for densification and sintering of ceramic monoliths and composites. This technique offers unique possibilities in the fabrication of new ceramic - metal composites (CERMETS), i.e. $B_4C$-Al, $B_4C$-Ti, $TiB_2$-Al and $B_4C$-Ta. In collaboration with TNO Rijswijk (Prins Maurits Laboratory) innovative applications for dynamic compaction of monolithic and compositic ceramics are investigated.

CERMETS, have been successfully prepared by dynamic compaction in conjunction with metal infiltration. For this purpose, the configuration of the explosive loads has been optimised. The fundamental studies involve the modelling of the shock-wave induced densification of the ceramic materials. Envelopes of different explosives are used in order to control the shock wave front in the ceramic to be densified aiming at improved densification processes. X-ray flash photography is employed to reveal the detonation shock fronts in various compaction configurations. Shock wave and particle velocities have been calculated in $B_4C$ ceramic powders using the shock detonation angles obtained from the X-ray photographs. A two-layer configuration is found to increase the pressure by a factor of 3.5 compared to the one-layer configuration, in agreement with the calculations. Also aspects of production, industrial design, and final machining have been investigated.

1.9 *Feasibility Study on the Formation of Prototype Li-ion Batteries Based on Ceramic Electrolytes* (W.J. Legerstee, E.L. Malony, A.A. van Zomeren)

A study will be undertaken to specify what should be done in order to fabricate several prototype batteries for down-hole operation, that can operate up to 220 °C without failure. The current commercial rechargeable batteries often operates with a wet or polymeric electrolyte. These are mostly of organic origin, which make them sensible for an irreversible reaction with the electrode materials of the battery, resulting in capacity fade during cycling, and finally to complete break-down of the battery. In addition, these electrolytes cannot operate above 100 °C (due to evaporation of the electrolyte solvent), that is absolutely required for down-hole operation, where temperatures up to 250 °C exists. Therefore a feasibility study is started in order to form a full ceramic battery with a ceramic electrolyte, that is supposed to be indispensable

to comply with the requirements for down-hole operation. The focus will be on what is important for the progress of the research in terms of man power, equipment etc. The final report will be the basis of a decision to come to an extended collaboration in order to fabricate prototype batteries as proposed in that report.

## 2 *Fuel Cells and Gas Sensors*

Fuel cells convert chemical energy into electrical energy with high efficiencies. Solid Oxide Fuel Cells (SOFCs) operate between 950 and 1000 °C, which demands compatibility between the various ceramic components. Molten Carbonate Fuel Cells (MCFCs) operate at a lower temperature, i.e. 650 °C but are severely affected by corrosion due to the extreme aggressive molten carbonate electrolyte. Our research focuses on and ceramic layers for corrosion protection in MCFCs.

### 2.1 *Corrosion Protection of MCFC Separator Plates with Ceramic Coatings* (M. Keijzer)

A collaborative program with the group of prof.dr. J.H.W. de Wit [MIDEG] is focused on the corrosion protection problems in Molten Carbonate Fuel Cells (MCFCs). One of the most severe technological problems in MCFC devices is the extremely aggressive molten carbonate electrolyte. Electrodes and especially the steel separator plates show fast degrading upon operation. In order to improve the MCFC lifetime, protective electrically conducting ceramic coatings are a necessity. The requirements for these electroceramics are i) excellent corrosion resistance and thermal stability, ii) high diffusion barrier for ions (such as $Li^+$), and iii) good electronic conductivity.

Phase diagrams of possible coating materials have been studied in order to predict the chemical reaction products in molten carbonate environment. Stability experiments of a number of materials has led to a few promising candidates, i.e. TiN, TiC and Ce-based ceramics. In order to determine the corrosion behaviour of stainless steel 304 in the MCFC environment, electrochemical measurements have been undertaken in collaboration with the University of Stockholm. With chronoamperometry and cyclic voltammetry the corrosion rates and the corrosion pattern as a function of exposure time were determined, respectively. The corrosion rate in anode gas was about eight times higher than in cathode gas. From the fits of the corrosion currents, obtained with chronoamperometry and the Avrami-equation, it was concluded that corrosion currents in cathode gas decreased almost parabolically, whereas it decreased in anode gas much slower than parabolically. Analysis of the corrosion layers with glow discharge optical emission spectrometry showed that iron can be oxidised in molten carbonates further than Fe(III), although valences above three have hardly been reported in the literature. A Microwave-Plasma enhanced CVD reactor has been constructed and tested. Dense TiN layers have been deposited on stainless steel 304 by Radio-frequent-Plasma enhanced CVD. Initial experiments have been performed to determine the detailed mechanism of the deposition.

In connection to project described in Section 2.2, ir. J. Driessen explores up-scaling of a plasma enhanced CVD process for titanium (carbo-) nitride ceramic coatings. This work is funded by the IOP-Surface Technology and by TNO. The experiments are performed at TPD-TNO (Centre for Technical Ceramics). A novel bi-polar radio-frequent pulse generator has been installed together with a newly developed Direct Liquid Injection (DLI) system. In situ mass spectrometry is used to monitor the CVD process. Computer control over the process has been installed. The results of this

new up-scaled reactor compares favourably to conventional thermal CVD. The produced coatings show similar microstructure and have comparable mechanical properties.

2.2 *Chemical Gas Sensors* (R. van Landschoot)

Mixed ionic-electronic conducting oxides have been studied as active components in gas-sensors. Taguchi-type sensors are based on the change in electronic conductivity upon adsorption of gases. The mechanism of this solid-gas interaction shows that this type of sensor is extremely sensitive, but not selective. In this research project, thin films of oxide semiconductors, which have been developed in this laboratory for the detection of sulphur oxides, nitrogen oxides, and carbon oxides, like the ceramic high $T_c$ superconductors as well as two- or three-phase mixtures of n-type and p-type semi-conducting oxides, have been studied for methane, ethane and propane detection. The objective is a chemical gas sensor capable of analysing natural gas for its hydrocarbon and carbon dioxide composition. As a result of this study, an asymmetrical Nernst-type gas sensor has been discovered, which comprises a proton conducting solid electrolyte and two catalytically different ceramic electrodes for the conversion of hydrocarbons to hydrogen. It is, therefore, a Nernst-type alternative to the Taguchi-type sensor with much improved selectivity. Because of patent application procedures no more details can be presented yet.

2.3 *Chemical Gas Sensor Arrays* (M.H.J. Emond, R. van Landschoot)

There has been an increasing interest in chemical gas sensors for on-line analysis of the composition of gases before and after burning processes. Conventional gas sensors, such as Taguchi- and Nernst type sensors, are not particularly selective or sensitive, respectively. By doping the Taguchi-sensor material or in particular, by making a sensor array this problem can be solved. The multi-phase mixtures of n- and p-type semi-conducting transition metal oxides, with an inert oxide like $Al_2O_3$ as the third component, show a response to nitrogen, sulphur and carbon oxides which is dependent on the ratio of the different semi-conducting transition metal oxides and the inert metal oxide. Hence an array of Taguchi-type gas sensors with as active sensing materials an array of multi-phase mixtures with specifically different compositions would yield an "electronic nose" which could map complex gas compositions in a single measurement. In relation to the work described in Section 2.3, this concept shall be extended to the asymmetrical Nernst-type gas sensor. In this Materials designer project a design of chemical gas sensor arrays is pursued.

3 *Photovoltaic Solar Cells*

Photovoltaic solar cells are anticipated to contribute substantially to our electrical energy demand in the 21$^{st}$ century. Already, Si-based photovoltaic devices are commercially available and compete with increasing effectiveness in the energy market. An important factor that prevents large-scale manufacturing and implementation of these devices is their cost. Therefore, materials research for cheap, efficient, and stable photovoltaic solar cells attract wide-spread attention.

3.1 *Photovoltaic Devices Based on Dye-Sensitised Smooth and Nanostructured Oxide Semiconductors* (A. Goossens, M.A. Hamstra, N. van Landschoot)

In order to investigate the feasibility of sensitising wide-band gap oxide semiconductors by organo-metal complexes as dyes in conjunction with an optical antenna sys-

tem, the "Nederlandse Onderneming voor Energie en Milieu, NOVEM" initiated and funded a national program. In this program the laboratory for Applied Inorganic Chemistry collaborates with the Departments of Molecular Physics and Organic Chemistry of the Agricultural University at Wageningen (LUW) and with the Department of Surface Physics of the Debye Institute at the Utrecht University (UU). In close connection with this network we also participate as sub-contractors in a Joule III, program on dye-sensitised solar cells and in an NWO priority program on surface modified Si solar cells.

Our research has been directed towards opto-electronic characterisation of dye-sensitised dense and porous nanocrystalline $TiO_2$ thin films. Photocurrent generation on dense CVD films of $TiO_2$ sensitised with zinc tetra phenyl porphyrins with a varying number of carboxyl groups (1 to 4) and octyl groups (none or 3) have been investigated.

3.2 *Opto-Electronic Properties of Oxide Semiconductors with Nanometer Scale Dimensions* (R. van de Krol, A. Goossens)

In close relationship with project described in Section 3.1 a fundamental study towards the elucidation of the chemical and physical properties of nanometer-scale oxide semiconductors has been undertaken. This program has been selected by the KNAW in 1993 and led to a 5-year appointment of Dr. A. Goossens as KNAW research fellow. Nanometer-scale thin films of $TiO_2$ are formed by either electrochemical anodic oxidation of Ti metal or by electron-beam (e-beam) evaporation of sub-stoichiometric $TiO_x$. With anodic oxidation, non-porous rutile $TiO_2$ films of 3-10 nm thickness can easily be obtained whereas e-beam evaporation produces $TiO_2$ films of 50-100 nm thickness onto ITO or $SnO_2$-coated glass substrates. The opto-electronic properties of these thin films are compared with the behaviour of nano-structured $TiO_2$ coatings as obtained in project C1. The main questions that are addressed are i) what is the exact potential distribution in these structures and how is this distribution related to the defect chemistry, ii) in what way do surface trapped electrons influence optical properties of $TiO_2$, iii) what is the influence of the reduced scale on the electronic properties of these materials.

A significant step towards objective i) has been made. Mott-Schottky analysis could be performed on nanometer thin films with a great accuracy and reproducibility. With this analysis, not only the stoichiometry has been defined, but also the dielectric constant of anatase $TiO_2$ could be determined to a high precision. It appeared that reported values are in many cases a factor of 2 too high. Photo-capacitance and photo-voltage studies have revealed the energy position of surface states. In order to define the chemical origin of these states additional experiments are in progress.

3.3 *Boron Phosphide* (E. Schroten, A. Goossens)

Boron phosphide (BP) is a refractory material with high mechanical strength and wear resistance. Moreover, it is a III-V semiconductor with a zinc-blende crystal structure and an indirect band gap of 2.0 eV. BP can be formed with radio-frequency activation in a cold-wall CVD reaction as polycrystalline or amorphous coating, as whiskers when a vapour-liquid-solid (VLS) growth technique is used, or as single crystalline epitaxial film onto silicon.

Single crystalline epitaxial BP films have been deposited onto Si (100). Both n-type and p-type BP could be synthesised, the latter Si as dopant. Current research fo-

cuses on the structural and electronic properties of the Si/BP epitaxial interface. The main questions here are i) how is the band line-up (the relative positions of the conduction and valence bands), and ii) what is the density of electronic interface states. The band line-up at Si/BP interfaces has been investigated by surface- photo-voltage spectroscopy. These measurements qualitatively show that although saturation cannot be reached with our monochromatic excitation source, distinct features appear. For n-Si/n-BP heterojunctions, the total band bending at the interface is small, i.e. 20-30 mV, indicating an almost ideal matching of the conduction bands of both materials. For p-Si/n-BP heterojunctions, a band bending of 425 ± 25 mV is present. Electrolyte electroreflection has been used to reveal the presence of an optical transition at 4.25 eV, which is probably the direct band gap of BP. To date, reported values have been much larger while theoretical values are widely distributed. Currently more experiments are in progress to validate our observations.

3.4 *Sensitisation of $TiO_2$ with pyrite* (B. Meester, A. Goossens)

Within the DIOC program "Decentralised Production and Storage of Electricity for Large-Scale Application of Renewable Energy" a research project is started aiming at sensitisation of $TiO_2$ with pyrite ($FeS_2$). Both $TiO_2$ and $FeS_2$ are synthesised with Ceramic Vapour Deposition. Smooth as well as nanostructured heterojunctions are investigated. Complete control over the stoichiometry and the phase purity of $FeS_2$ is the main challenge in this project.

4 *Electroceramic Composites*

In these projects ceramic composites and smart materials are synthesised. These investigations serve to strengthen the CVD infra-structure and know-how in the group and to test new ideas originating from previous investigations. All projects share the functional character of the materials which are formed.

4.1 *Silicon-Carbide-Nitride Composites* (W.F.A. Besling, P.J. van der Put, A. Goossens)

In this project, Si-C-N composites are synthesised by laser particle-precipitation aided CVD (L-PP-CVD), using a tuneable $CO_2$ laser to activate the CVD process. Depending on the process conditions, the composition of these films can be varied. For instance, semi-conducting cubic SiC particles in an insulating $Si_3N_4$ matrix can form. These nano-structured films then show unique photo- and electroluminescence phenomena and may find application in blue light-emitting-diodes and optical displays. In contrast, when nitrogen acts as dopant for cubic SiC, completely different kinds of optical phenomena are to be expected. Moreover, Si-C-N thin films may also find application as hard-coating because of the well-known mechanical characteristics of SiC and $Si_3N_4$.

In particular in situ characterisation of the CVD process by optical Raman spectroscopy has been elaborated on. In collaboration with the group of prof. B. Scarlett [Delft University of Technology], a laser Raman spectrometer set-up has been assembled and tested. With this technique intermediate radical gas phase species could be observed. Careful calibration and optimisation of the set-up has been worked out. Porous and dense silicon carbonitride films have been deposited. In L-PP-CVD experiments, particle sizes down to 20 nm are obtained and studied using TEM. In the Si-C-N system, a wide range of compositions can be obtained as is es-

tablished with XPS and EDX analysis. In addition to the Si-C-N system, preliminary experiments for the formation of nano-porous crystalline Si coatings have been made in order to explore alternative routes for thin-film silicon synthesis. At present, thin-film nanostructured silicon is investigated thoroughly for solar cell applications.

4.2 *Metallisation of Polymers* (M.L.H. ter Heerdt, A. Goossens)

In collaboration with the group of prof.dr. J.H.W. de Wit [MIDEG], TNO-TPD (Technische Fysische Dienst), TNO-KRI (Kunstoffen en Rubber Instituut), TNO-MI (Metaal Instituut) and ECN (Energie Centrum Nederland), a national research program for metallisation of polymers is under study. IOP-/Surface Technology provides additional funding.

Conventional polymer metallisation is based on initial seeding by sputtering Pd or Cu onto the polymer and subsequent electro-plating of a top layer of copper. Since these systems find application as printing screens in the electronic industry, the requirements for adhesion and electrical conductivity of the metal tracks are extremely demanding. Therefore, low-temperature CVD is explored in our group as alternative for selective metallisation of polymers.

A new photo-chemical vapour deposition reactor has been developed. In this reactor, metallic Cu has been deposited with thermal as well as photo-assisted CVD. Suitable substrates are $Al_2O_3$, and polyimide (PI), the latter being a high-temperature resistant polymer. It is found that UV-excitation enhances the CVD reaction rate when $Cu(hfac)_2$ is used as precursor and $H_2$ or ethanol as co-reactant. Currently, the process temperature for UV-enhanced CVD is 200 °C which is already 100 °C below the thermal CVD reaction temperature. UV-Vis absorption of gas phase $Cu(hfac)_2$ has been performed in order to determine its excitation spectrum which is of fundamental importance in the CVD process.

4.3 *Mechano-Electrical Transducers* (E.G.M. Veldman, P.J. van der Put, A. Goossens)

In collaboration with prof.dr.ir. J. van Turnhout [MIDEG], ceramic-polymer hybrid materials are explored for transducer applications. In these materials, a ferro-electric ceramic powder is dispersed in an elastomeric matrix. Upon applying mechanical stress, a piezoelectrical effect causes a potential. Vice versa, when external voltages are applied, mechanical movement is induced. It is our objective to synthesise this type of "smart hybrid material" with gas-phase deposition techniques preferably by a single CVD process.

Gas-phase experiments for synthesis of polydichloro-phosphazene have been carried out. This polymer is an intermediate for the ultimately desired polyphosphazene elastomeric matrix. As precursors $PCl_3$ and $NH_3$ have been used, but with these precursors only amorphous PN is obtained. To avoid this undesired product, $(NPCl_2)_3$ precursor has been selected since it is known from literature that its thermal decomposition can lead to polydichlorophosphazene. However, due to the low reaction rate and short residence time in the CVD reactor, it appeared that ring-opening polymerisation does not occur at a sufficient rate.

5 *Vapour-Phase Synthesis and Processing of Nano-Particle Materials (NANO)*

The ESF Programme on Vapour-Phase Synthesis and Processing of Nano-Particle

Materials (NANO) is funded by the EC. It aims to promote the synthesis of ceramic aerosols and films using gas phase techniques, with the aim of generating single-phase, or nano-dispersed structural ceramic materials and electroceramics with new or improved properties. The programme will run for five years, subject to a mid-term review, and is currently supported by research councils and academies of science in Belgium, Denmark, Finland, Germany, The Netherlands, Poland, Sweden, Switzerland, and the United Kingdom.

Interdisiplinary collaboration between aerosol community and the materials science community will be furthered within the NANO programme through the exchange of expertise and methods during workshops and task force meetings, and through the exchange of researchers. The NANO programme supports visits of up to one month for senior researchers and the exchange of Ph.D. students and post-doctoral researchers for up six months between aerosol and materials groups. Priority will be given to applications which focus on the interface between aerosol research and materials science, and to visits within the same country may also be funded.

## PUBLICATIONS

H. Berg, Ö. Bergström, T. Gustafsson, E.M. Kelder, J.O. Thomas
*Structural aspects of lithium insertion in transition metal oxide electrodes*
J. Power Sources 68 (1997) 24-29

T.N.M. Bernards
*Silicate sol-gel chemistry as studied by hydrolysis-gelation time curves*
Ph.D. thesis, Utrecht University (1997)

W.F.A. Besling, A. Goossens, J. Schoonman
*In-Situ Raman Spectroscopy During Laser-Induced Chemical Vapor Deposition of Silicon and Silicon Carbonitride Thin Films*
In: M.D. Allendorf, C. Bernard (eds.), Proceedings of the Fourteenth International Conference on Chemical Vapor Deposition and EUROCVD 11, Joint meeting of the Electrochemical Society, Paris, France, August 31-September 5, 1997, 97-25 (1997) 676-683

G.K. Boschloo, A. Goossens, J. Schoonman
*Investigation of the potential distribution in porous nanocrystalline $TiO_2$ electrodes by electrolyte electroreflection*
J. Electroanalytical Chem. 428 (1997) 25-32

G.K. Boschloo, A. Goossens, J. Schoonman
*Photoelectrochemical Study of Thin Anatase $TiO_2$ Films Prepared by Metallorganic Chemical Vapor Deposition*
J. Electrochem. Soc. 144 (1997) 1311-1317

E. Carton, H.J. Verbeek, M. Stuivinga, J. Schoonman
*Dynamic compaction of powers by an oblique detonation wave in the cylindrical configuration*
J. Appl. Physics 81 (1997) 3038-3045

C.H. Chen, H.J.M. Bouwmeester, R.H.E. van Doorn, H. Kruidhof, A.J. Burggraaf
*Oxygen permeation of $La_{0.3}Sr_{0.7}CoO_{3-\delta}$*
Solid State Ionics 98 (1997) 7-13

C.H. Chen, E.M. Kelder, J. Schoonman
*Effect of layer morphology on the lithium-ion diffusion in thin $Li_xCoO_2$ films*
J. Materials Science Letters 16 (1997) 1967-1969

C.H. Chen, E.M. Kelder, J. Schoonman
*Electrode and solid electrolyte thin films for secondary lithium-ion batteries*
J. Power Sources 68 (1997) 377-380

C.H. Chen, E.M. Kelder, J. Schoonman
*Functional Ceramic Films with Reticular Structures Prepared by Electrostatic Spray Deposition Technique*
J. Electrochem. Soc. 144 (1997) L289-L291

J.P. Dekker, P.J.J.M. van der Put, H.J. Veringa, J. Schoonman
*Particle-Precipitation-Aided Chemical Vapor Deposition of Titanium Nitride*
J. of the American Ceramic Society. 80/3 (1997) 629-636

A. Goossens
*Bandgap enlargement in anodic oxide films on titanium*
Surface Science 371 (1997) 390-398

A. Goossens, G.K. Boschloo, J. Schoonman
*Transient photocurrent response of dye-sensitized porous nanocrystalline $TiO_2$ electrodes*
In: Materials Research Society Symposium Proceedings 452 (1997) 607-612

A. Goossens, J. Schoonman
*Nieuwe generatie zonnecellen ziet het licht*
Chemisch Magazine mei 1997, 183-186

M.L.H. ter Heerdt, P.J.J.M. van der Put, A. Goossens, A.D. Kuijpers, J. Schoonman
*Cuprisation of Polyimide and Polyetherimide by Chemical Vapour Deposition*
In: M.D. Allendorf, C. Bernard (eds.), Electrochemical Society Proceedings 97-25 (1997) 1524

M. Keijzer, S.F. Au, K. Hemmes, J.H.W. de Wit, G. Lindbergh, D. Simonsson, J. Schoonman
*Corrosion of Stainless Steel 304 in Molten Carbonates*
In: J. R. Selman, I. Uchida, H. Wendt, D.A. Shores, T.F. Fuller, Proceedings of the fourth international symposium on Carbonate Fuel Cell Technology, Volume 97-4: High Temperature Materials, Battery, and Energy Technology Divisions, The Electrochemical Society, Inc., Pennington, USA (1997) 296-305

M. Keijzer, K. Hemmes, P.J.J.M. van der Put, J.H.W. de Wit, J. Schoonman
*A Search for Suitable Coating Materials on Separator Plates for Molten Carbonate Fuel Cells*
Corrosion Science 39 (1997) 483-494

E.M. Kelder, M.J.G. Jak, J. Schoonman, M.T. Hardgrave, S.Y. de-Andersen
*Quality control of $Li_{1+\delta}Mn_{2-\delta}O_4$ spinels with their impurity phases by Jaeger and Vetter titration*
J. Chem. Power Sources 68 (1997) 590-592

E.M. Kelder, P.J.J.M. van der Put, J. Schoonman
*Thermochemical Data of Boron Subphosphide*

Thermochimica Acta 3484 (1997) 1-4

M. Keijzer, P.J.J.M. van der Put, J. Schoonman, S.F. Au, K. Hemmes, J.H.W. de Wit
*Chemical Vapour Deposition of Titanium Nitride for Corrosion Protection in Molten Carbonates*
In: M.D. Allendorf, C. Bernard (eds.), Proceedings of the Fourteenth International Conference on Chemical Vapour Deposition and EUROCVD-11, Electrochemical Society Proceedings 97-25 (1997) 364-368

E.M. Kelder
*Kraan onder hoogspanning creeert 3-D doolhof voor gassen*
Klei, Glas en Keramiek 11 (1997) 13-17

E.M. Kelder, J. Schoonman
*Portable Hype Versnelt Komst Electrische Auto*
Chemisch Magazine, July/August (1997) 276-279

R. van de Krol, A. Goossens, J. Schoonman
*Mott-Schottky Analysis of Nanometer-Scale Thin-Film Anatase $TiO_2$*
J. Electrochem. Soc. 144 (1997) 1723-1727

R. van de Krol, A. Goossens, J. Schoonman
*Spectroscopic Investigation of Lithium Intercalation in Thin Smooth Films of Anatase Titanium Dioxide*
In: Materials Research Society Symposium Proceedings 448 (1997) 309-314

R. Moene, L.F. Kramer, J. Schoonman, M. Makkee, J.A. Moulijn
*Synthesis of high surface area silicon carbide by fluidized bed chemical vapour deposition*
Applied Catalysis A: General 162 (1997) 181-191

E. Moons, T.J. Savenije, A. Goossens
*Surface potential of porfyrin layers on ITO using the Kelvin probe technique*
J. Phys. Chem. B. 101 (1997) 8492-8498

E. Orij
*CVD of Molybdenum from Molybdenum. Hexafluoride: Kinetics and Reactor Modelling*
Ph.D. thesis, Eindhoven University of Technology (1997)

I. Riess, J. Schoonman
*Electrodics*
In: P.J. Gellings, H.J.M. Bouwmeester (eds.), The CRC Handbook of Solid State Electrochemistry, CRC Press Boca Raton, New York, London, Tokyo (1997) 269-294

T.J. Savenije, E. Moons, G.K. Boschloo, A. Goossens, T.J. Schaafsma
*Photogeneration and transport of charge carriers in a porphyrin p/n heterojunction*
Phys. Rev. B. 55 (1997) 9685-9692

J. Schoonman
*Defect Chemistry in Solid State Electrochemistry*
In: P.J. Gellings, H.J.M. Bouwmeester (eds.), The CRC Handbook of Solid State Electrochemistry, CRC Press Boca Raton, New York, London, Tokyo (1997) 161-193

J. Schoonman, E.M. Kelder

*Thin Film Solid Electrolytes and Electrodes for Rechargeable Lithium-ion Batteries*
J. Power Sources 68 (1997) 65-68

M. Schreiber
*Hydrogen Mixed Conductors Properties and Applications*
Ph.D. thesis, Delft University of Technology (1997)

E. Schroten, A. Goossens, J. Schoonman
*Electrolyte electro-reflectance of boron phosphide (BP)*
In: Materials Research Society Symposium Proceedings 451 (1997) 209-231

N.H.J. Stelzer, C.H. Chen, L.N. van Rij, J. Schoonman
*Electrostatic Spray Deposition of Doped YSZ Electrode Materials for a Monolithic Solid Oxide Fuel Cell Design*
In: Proceedings of 10th IEA SOFC Workshop, Annex VII, Les Diablerets, Switzerland, January 1997, 2 (1997) 236-247

N.H.J. Stelzer, A. Goossens, J. Schoonman
*Synthesis of terbia doped yttria stabilized zirconia thin films by using the electrostatic spray deposition (ESD) technique*
In: Materials Research Society Symposium Proceedings 453 (1997) 543-548

I.L. Tuinman
*The Production of $Si_3N_4$ Powders in a Laser-Driven Aerosol Reactor*
Ph.D. thesis, Delft University of Technology (1997)

I.L. Tuinman, M.A. van Drunen, J.C.M. Marijnissen, B. Scarlett, J.Schoonman
*Formation and Growth of Silicon Nitride Particles in a Laser-Driven Aerosol Reactor Investigated with Photon Correlation Spectroscopy and Electron Microscopy*
Aerosol Science and Technology 26 (1997) 55-73

**WELDING TECHNOLOGY & NON-DESTRUCTIVE TESTING**
Delft University of Technology, Laboratory of Materials Science
Rotterdamseweg 137, 2628 AL Delft
phone +31 (15) 2782235, fax +31 (15) 2786730, e-mail ...@stm.tudelft.nl

## PERSONNEL

*Scientific staff*

| | |
|---|---|
| prof.dr. G. den Ouden | (2782236, DenOuden@...) |
| dr.ir. M.J.M. Hermans | (2782286, Hermans@...) |
| ir. T. Luijendijk | (2782240, Luijendijk@...) |
| drs. W.J.P. Vink | (2784923, Vink@...) |

*Graduate students*

B. Hu, B.Sc.
T. Ma, M.Sc.
drs. W. Middel
D.N. Travessa, M.Sc.
ir. R.H. Vegter
ir. H.W. de Vries

*Research students*

G. van Gemert
C.H.J. Gerritsen
C. Goos
G.J. van Haasteren
A.T.J. van Helvoort
J.E. Janse
E.M. Jorritsma
M.W.H.M. Liebreks
Z.Z. Moeniralam
S.E. Offerman
P.R. Put

*Technical assistants*

F.J.A.M. Bosman
W.A.J. Brabander
E.R. Peekstok

## RESEARCH AREAS AND OBJECTIVES

Research is carried out in the area of joining of materials with emphasis on welding. Much attention is given to the behaviour of the welding process and to the influence of the process parameters on the properties of the materials to be joined. Work is also carried out aimed at evaluating the possibilities and limitations of mechanisation and automation of the welding process, with specific interest for sensors to be used in a welding robot. Furthermore, attention is given to the joining of ceramics to metals and ceramics to ceramics.

1 *Welding Processes*

Welding processes are used on a broad scale in the metals industry. The possibilities and limitations of these processes depend not only on the process parameters, but also on external factors and conditions.
The objective of this project is to obtain fundamental knowledge about existing and new welding processes with emphasis on the applicability of these processes in the metals industry.

2 *Sensing and Control of the Arc Welding Process*

Automation of the arc welding process is of considerable interest for the welding industry. This interest is based on the specific advantages offered by automation, such as increase of productivity and improvement of weld quality. Of specific importance is the development of sensors which can be used for obtaining real time information about the welding process. This information can be fed back to the control system and can - if required - be used to correct the relevant process parameters.
The objective of this project is to study new approaches to sensing during arc welding with emphasis on penetration sensing based on weld pool oscillation and position sensing based on tracer techniques.

3 *Structure and Properties of Welded Joints*

During welding part of the metal to be welded is subjected to a thermal cycle (heating, melting, solidification and cooling). This thermal cycle in most cases leads to significant changes in the structure and properties of the welded joint.
The objective of this project is to obtain detailed information about the structure of welds (weld metal and heat-affected zone) in relation to the welding conditions and to determine the relationship between the structure and the mechanical properties. Specific attention is given to aluminium alloys and to aluminium-matrix composites.

4 *Diffusion Welding of Ceramic Materials*

Due to their excellent high temperature properties, ceramic materials are being used increasingly in constructive applications. In most cases the ceramic materials are applied in combination with metals. To ensure good bonding between ceramic materials and metals, reliable joining techniques are required. A possible joining technique is diffusion welding. An important advantage of this technique is that joints can be produced which can withstand relatively high temperatures.
The objective of this project is to obtain fundamental knowledge in the field of diffusion welding of ceramics to metals. Attention is also given to diffusion welding of ceramics to ceramics.

FACILITIES

- Arc welding equipment for manual metal arc welding, GTA welding, GMA welding and pulsed current welding
- Diffusion welding equipment
- Thermal simulator
- Equipment for radiographic defect detection
- Equipment for ultrasonic defect detection
- Equipment for acoustic emission analysis
- Equipment for sensing and control of weld penetration (prototype)

## RESEARCH REPORT 1997

### 1 *Welding Processes* (F.J.A.M. Bosman, W.A.J. Brabander, G. van Gemert, M.J.M. Hermans, Z.Z. Moeniralam, T. Luijendijk, W.J.P. Vink, G. den Ouden)

In the framework of this theme attention was focused on two new welding processes: laser-assisted arc welding an friction-stir welding.

#### 1.1 *Laser-Assisted Arc Welding*

This project deals with the interaction between laser radiation and the welding arc with the aim to obtain fundamental insight in this interaction and to explore the possibilities of using it in specific applications. The laser-arc interaction is based on the fact that when a material is melted by laser radiation, a plasma plume is generated just above the molten metal. This plasma plume is characterised by a relatively high electrical conductivity and, hence, will attract the arc when the distance between laser plume and arc is sufficiently small (antenna function). Possible applications of the laser-arc interaction are stabilisation of the arc, manipulation of the arc (sensing), improvement of arc ignition (avoiding high-frequency ignition), improvement of heat transport and material transport during welding and increase of welding process efficiency. Of particular interest in this respect is the development of a new hybrid welding process (laser-aided arc welding), which is expected to be particularly suited for mechanised welding of thin plate material and also for mechanised welding of thin-thick and dissimilar material combinations.
As a first step, preliminary research in the field of laser-arc interaction was carried out in co-operation with Philips Centre of Fabrication Technology with the aim to examine the possibility of increasing the manipulability of the arc by means of a low-power laser (arc guiding). Tests were conducted under various process conditions to determine the largest distance over which the arc can be attracted by the plasma plume. It appears that this distance depends on a large number of process parameters, the most important being: arc current, arc voltage (arc length), laser intensity, material properties, workpiece geometry and arc atmosphere. At present preparations are made to continue this research in our laboratory as a project to be carried out under the auspices of the Netherlands Institute for Metals Research.

#### 1.2 *Friction-Stir Welding*

A start was made of a study aimed at assessing the possibilities and limitations of friction-stir welding. Friction-stir welding is a new solid-state welding process, which seems especially promising for welding of thin plate material. In this joining process use is made of the friction heat which is generated when a rapidly rotating non-consumable electrode is pressed onto (into) and moved along the seam of the workpiece to be welded. Due to the heat generation the temperature of the workpiece material is raised, which results in plastic deformation and local mixing and, consequently, to the formation of a weld. To test the feasibility of the friction-stir welding process for joining aluminium alloys, a large number of preliminary experiments was carried out under various experimental conditions. In this way the optimal process parameter settings were determined for joining of three aluminium alloys (AA 6060, 6082 and 7020). It was found that under optimal conditions acceptable welds can be produced. The welds obtained are all characterised by a flow pattern, which is z-shaped in transverse cross-section. The flow lines are marked by oxide particles, originating from the workpiece surface. It appears that the mechanical

properties of the welds produced, strongly depend on the distribution of these oxide particles: the more randomly the particles are distributed, the better the mechanical properties. A problem which is often encountered during friction-stir welding is pore formation in the weld zone. At present this phenomenon is further examined and attempts are made to determine the relation between the welding parameters and the mechanical properties of the weld.

2 *Sensing and control of the arc welding process* (F.J.A.M. Bosman, W.A.J. Brabander, G.J. van Haasteren, M.J.M. Hermans, B. Hu, J.E. Janse, W. Middel, S.E. Offerman, T. Luijendijk, W.J.P. Vink, G. den Ouden)

The research carried out in this area was focused on two new approaches to sensing during arc welding: penetration sensing based on weld pool oscillation and position sensing based on tracer techniques.

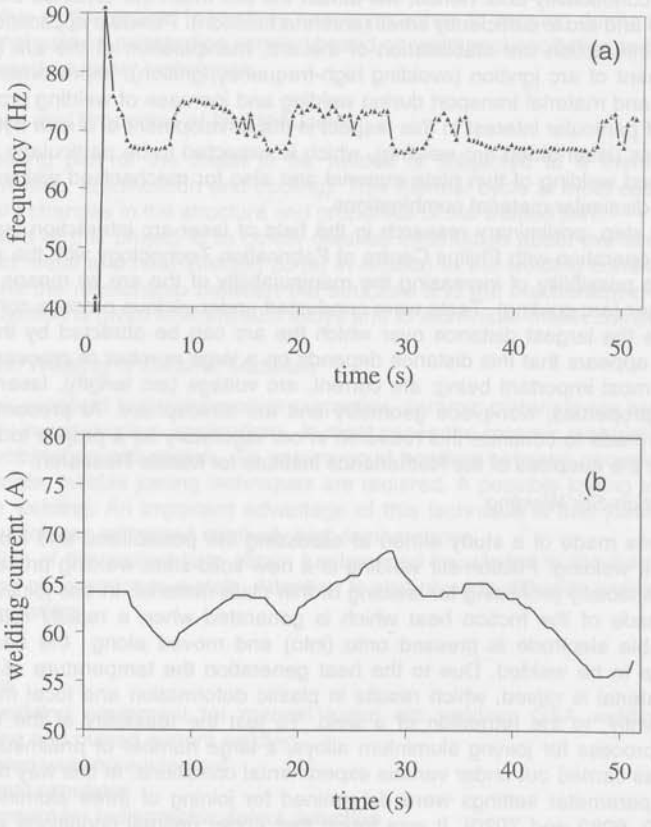


*Figure 1: Orbital tube welding with penetration control: oscillation frequency (a) and welding current response (b) as a function of time. (AISI 304 tube of diameter 48 mm and wall thickness 2.5 mm; travel speed 3 mm/s; control frequency 70 Hz)*

### 2.1 *Penetration Sensing Based on Weld Pool Oscillation*

The work dealing with weld penetration sensing and control based on weld pool oscillation was continued. In this approach, the weld pool is triggered into oscillation by means of short current pulses, superimposed on the welding current and the oscillation frequency is extracted from the arc voltage variation with the help of Fast Fourier Transform analysis. By monitoring the oscillation frequency during welding, direct information is obtained about the penetration of the weld pool. In the case of partial penetration the pool oscillates in a high frequency mode (double-ring mode) and in the case of full penetration the pool oscillates in a low frequency mode (up-and-down mode). The difference between the oscillation frequencies of both oscillation modes can easily be detected when monitoring the frequency spectrum and, hence, can be used as basis of weld penetration sensing.
However, it appears that this sensing approach is only successful in the case of stationary and low-speed welding. This is due to the fact that with increasing travel speed the shape of the weld pool gradually changes from a semi-sphere to a shape close to a semi-ellipsoid. As a consequence of this change in weld pool shape a switch in oscillation mode takes place in the case of partial penetration (the double-ring mode changes to the front-to-back mode) and the difference in frequency between the partially penetrated and the fully penetrated weld pool becomes too small to be used for sensing. In view of this, attempts were made to realise weld penetration sensing and control by following a different (single-frequency) approach. In this approach a specific (full penetration) control frequency is selected and the sensing and control system is designed in such a way that the control frequency is maintained during welding by adaptation of the welding current in small discrete steps. To test the feasibility of the single-frequency approach, welding experiments were carried out with different materials (mild steel and stainless steel plates of various thickness) under different conditions. The results clearly indicate that the single-frequency approach can be used successfully within a wide range of applications, including position welding and orbital tube welding (see Figure 1).

### 2.2 *Position Sensing Based on Tracer Techniques*

The principle of this sensing approach is based on the fact that the physical proper-

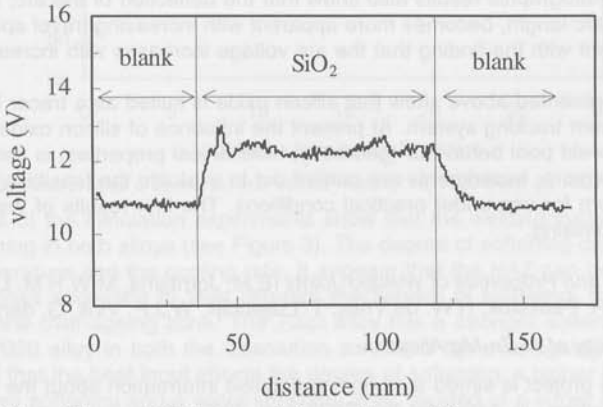


*Figure 2: Voltage-distance plot in the case of silicon oxide as additive*

ties of the welding arc, in particular the arc voltage and the current distribution, are influenced by the addition of small quantities of specific chemical compounds. By marking the seam with these compounds (tracers), the position of the torch can be sensed by simply monitoring the arc voltage during welding.
Previous work shows that especially oxides (like silicon oxide, titanium oxide and iron oxide) have a pronounced effect on arc voltage and, hence, are suitable as tracers in the envisaged position sensing system (see Figure 2).

To obtain more information about the influence of tracer addition on arc behaviour, experiments were carried out with emphasis on silicon oxide as tracer addition. In a first series of experiments arc voltage was measured as a function of arc length. When the measured voltage values are plotted as a function of the arc length a straight line should be obtained. The slope of this line gives information about the electric field strength in the column of the arc, whereas extrapolation to zero arc length yields the sum of the anodic fall voltage and the cathodic fall voltage. It appears that silicon oxide addition gives rise to both an increase of the field strength in the arc column and to an increase of the sum of the fall voltages. These effects can be explained in terms of constriction of the arc due to the formation of negative ions in the outer regions of the arc. Furthermore, it was found that with increasing welding current the effect of silicon oxide on arc voltage decreases and eventually disappears. This can be explained by the fact that with increasing current the gas vortex increases rapidly, causing the removal of the additive from the arc zone.
Additional information about the effect of silicon oxide on arc behaviour was obtained by taking photographs of the arc in various directions under different conditions. These photographs show that, in addition to arc constriction, the presence of silicon oxide leads to arc trailing: the arc remains behind with respect to the electrode resulting in a longer effective arc length, which in turn leads to a larger voltage drop over the arc column. When the welding current is increased, not only the gas vortex will be more violent (causing the removal of additives from the arc zone), but also the arc pressure will increase, resulting in a stiffer arc. This effect will lead to a reduction of the arc deflection and, hence, to a smaller contribution of the arc column to the change in arc voltage. It appears that with increasing current the change in electric field strength decreases more rapidly than the change in the voltage drop in the fall areas. The photographic results also show that the deflection of the arc, and hence the effective arc length, becomes more apparent with increasing travel speed, which is in agreement with the finding that the arc voltage increases with increasing travel speed.
The results presented above show that silicon oxide is suited as a tracer in an additive based seam tracking system. At present the influence of silicon oxide and other additives on weld pool behaviour (geometry, mechanical properties) is being investigated. Furthermore, experiments are carried out to evaluate the feasibility of the envisaged system for use under practical conditions. The first results of these experiments are promising.

## 3 *Structure and Properties of Welded Joints* (E.M. Jorritsma, M.W.H.M. Liebreks, T. Ma, E.R. Peekstok, H.W. de Vries, T. Luijendijk, W.J.P. Vink, G. den Ouden)

### 3.1 *Weldability of Al-Zn-Mg Alloys*

This research project is aimed at obtaining detailed information about the weldability of Al-Zn-Mg alloys, in particular the 7020 and 7022 alloys, by means of thermal

simulation. Simulation experiments require precise knowledge about the thermal cycle experienced by the HAZ during welding. Of particular interest in this respect are the peak temperature and the cooling rate. In a first approach, the thermal cycle was calculated under the assumption of infinite plate width. However, the results obtained in this way appear to deviate from the results obtained experimentally. Improvement is achieved when the finite width of the plate is taken into account in the calculation. This leads to results which are sufficiently accurate to be used as input for the simulation experiments.

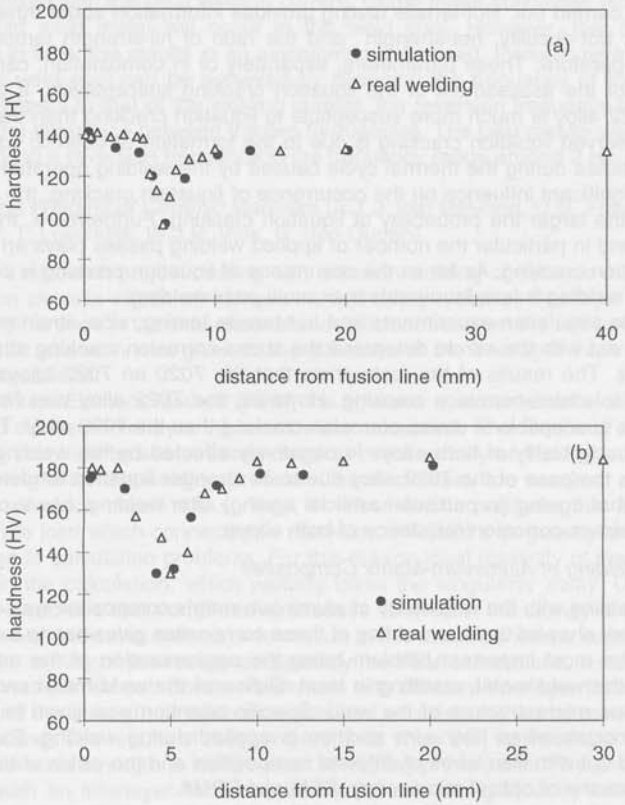


*Figure 3: Hardness profiles of simulated and welded material: (a) 7020 alloy, (b) 7022 alloy*

The results of the simulation experiments show that the welding cycle leads to severe softening in both alloys (see Figure 3). The degree of softening depends on the peak temperature and the cooling rate. It appears that the HAZ can be divided into two sub-zones according to their different mechanism of softening: the dissolution zone and the over-ageing zone. The 7022 alloy has a stronger softening tendency than the 7020 alloy in both the dissolution zone and the over-ageing zone. It was also found that the heat input affects the degree of softening: a higher input leads to more severe softening and a wider softening area, located at a larger distance from

the fusion line. The softening in the HAZ can be partly recovered by post-weld heat treatment. As far as recovery is concerned artificial ageing is more effective than natural ageing.

On the basis of the results obtained, a model for HAZ softening was developed. The model is conservative, but can be used to predict the softening behaviour in practical situations both in the case of single-pass welding and in the case of multi-pass welding.
In order to assess the susceptibility to liquation cracking of the two alloys, hot-tensile testing was carried out. Hot-tensile testing provides information about three decisive parameters: hot-ductility, hot-strength and the ratio of nil-strength temperature to melting temperature. These parameters, separately or in combination, can be used as criteria for the assessment of the liquation cracking susceptibility. It was found that the 7022 alloy is much more susceptible to liquation cracking than the 7072 alloy. The observed liquation cracking is due to the formation of eutectic liquid at the grain boundaries during the thermal cycle caused by the welding operation. Heat input has a significant influence on the occurrence of liquation cracking: the larger the heat input, the larger the probability of liquation cracking. Furthermore, the welding procedure and in particular the number of applied welding passes plays an important role in liquation cracking. As far as the occurrence of liquation cracking is concerned, single-pass welding is less favourable than multi-pass welding.
In addition to simulation experiments and hot-tensile testing, slow strain rate testing was carried out with the aim to determine the stress-corrosion cracking susceptibility of the alloys. The results of the tests show that the 7020 an 7022 alloys are both susceptible to stress-corrosion cracking. However, the 7022 alloy was found to be slightly more susceptible to stress-corrosion cracking than the 7020 alloy. The stress-corrosion susceptibility of both alloys is negatively affected by the welding process, especially in the case of the 7022 alloy due to its stronger liquation tendency. It was also found that ageing (in particular artificial ageing) after welding, has a positive effect on the stress-corrosion resistance of both alloys.

### 3.2 *Arc Welding of Aluminium-Matrix Composites*

The work dealing with the weldability of aluminium-matrix composites was continued. Previous work showed that arc welding of these composites gives rise to a number of problems, the most important problem being the agglomeration of the non-metallic particles in the weld metal, resulting in local dilution of the weld metal and in an in-homogeneous microstructure of the weld. Specific attention was given to the situation which occurs when filler wire addition is applied during welding. Experiments were carried out with filler wires of different composition and the welds obtained were studied by means of optical microscopy, SEM and EPMA.
It appears that welding with filler wire addition leads to an in-homogeneous weld, characterised by a large particle-denuded zone, which is due to poor mixing between the filler wire material and the composite material. The degree of mixing between the filler wire material and the composite material was quantified in terms of a mixing parameter and this mixing parameter was measured as a function of welding conditions (travel speed, wire feed rate). It was found that mixing between the filler wire material and the composite material improves with increasing travel speed and is virtually independent of wire feed rate. Furthermore, it appears that welding under droplet transfer conditions results in improved mixing between the filler wire material and the composite material. It is evident that the observed poor mixing between the filler wire

material and the composite material has a detrimental influence on the mechanical properties of the weld. Considerable improvement of the particle distribution in the weld can be obtained by electro-magnetic stirring of the weld pool during welding. Electro-magnetic stirring is based on the interaction between an externally applied magnetic field and the welding current, resulting in a Lorentz force on both the arc plasma and the liquid metal in the weld pool. In order to make electro-magnetic stirring possible for arc welding of aluminium alloys and aluminium based composites a new approach was followed. In this approach an axial magnetic field is applied which is synchronised with the (AC) welding current. Under these conditions rotational flow of the liquid weld metal will occur in the weld pool. However, this flow is unidirectional in time and results in an asymmetric weld bead. Periodic reversion of the flow in the weld pool can be achieved by changing the frequency of the magnetic field with respect to that of the welding current, the reversion frequency being determined by the difference between the two frequencies. The best results were obtained when applying a reversion frequency in the frequency range around 2 Hz.

4 *Diffusion Welding of Ceramic Materials* (A.T.J. van Helvoort, D.N. Travessa, R.H. Vegter, T. Luijendijk, W.J.P. Vink, G. den Ouden)

As part of a research project dealing with diffusion welding of ceramic materials, the combination zirconia-silicon nitride was studied using nickel as interlayer material to bridge the difference in thermal expansion coefficient between the two ceramic materials. Specific attention was given to the influence of the interlayer thickness on the residual stress level.
Using the Finite Element Method (FEM) the stresses in zirconia-nickel-silicon nitride bonds with different interlayer thickness were calculated. The results of the calculations show that high tensile stresses develop in the vicinity of the $Si_3N_4$-Ni interface during cooling after the welding process. These stresses are maximal at the point where the interface meets the surface. In linear elastic analysis, this node at the surface of the joint which connects two materials, will yield a singularity and therefore will give rise to calculation problems. For this reason ideal plasticity of the nickel was assumed in the calculation, which partially takes the singularity away. Under these conditions it appears that compressive stresses develop in the vicinity of the $ZrO_2$-Ni interface, which indicates that crack formation at this interface will be suppressed.
To verify the validity of the results obtained by the FEM calculations, a number of experiments was carried out. Bonds were made with different interlayer thickness (0.1 - 0.8 mm) and the strength of the bonds obtained was determined by means of shear strength testing. The results of these experiments show that for interlayer thickness > 0.1 mm, the bond strength is independent of interlayer thickness. The shear strength of bonds with an interlayer thickness below 0.1 mm is significantly lower than the strength obtained for larger values of the layer thickness. The majority of the fractures takes place at the $Si_3N_4$-Ni interface or close to this interface. Microstructural examination shows that at this interface a reaction layer is formed during the welding process. This layer is due to dissociation of the $Si_3N_4$, which leads to the formation of free silicon and free nitrogen. The silicon dissolves in the Ni, whereas the nitrogen recombines to $N_2$. Part of this nitrogen results in the formation of pores. As expected, the dissociation reaction does not depend on the interlayer thickness. Under the present experimental conditions (gas pressure $4 \cdot 10^{-4}$ Pa, temperature 1050 °C) the reaction layer was found to be about 5 µm thick and irregular in appearance.
The results of the mechanical tests show that the bond strength is virtually not af-

fected by the interlayer thickness. This can be understood by considering the fracture mechanism in more detail. It appears that the bond fails in most cases at the $Si_3N_4$-Ni interface or partly in this interface and partly in the bulk of the $Si_3N_4$. This behaviour is due to the fact that the difference in thermal expansion between $Si_3N_4$ and Ni is relatively large, whereas the difference between zirconia and nickel is much smaller. The highest residual stresses therefore are present in the vicinity of the $Si_3N_4$-Ni interface, which is confirmed by the FEM calculations. An additional factor affecting fracture is the formation of reaction products at this interface (mainly in the form of pores), which also weakens the bond. A crack normally starts at the surface between the silicon nitride and the nickel and then propagates along the interface. During crack propagation some nickel of the reaction zone remains attached to the silicon nitride. It should be noted that the stresses which are present in the reaction layer are actually not properly dealt with in the FEM calculations, as the specific properties of this layer are not taken into account. However, it is plausible that these stresses are relatively large because of the irregular shape of this layer. Especially around inclusions and pores in the nickel, the curved interfaces are expected to yield high stress concentrations. Thus, the reaction layer - nickel interface will probably be a weak link in the $Si_3N_4$-Ni-$ZrO_2$ combination.
Both failure promoting conditions, the stress concentration at the $Si_3N_4$-Ni interface and the presence of a reaction zone along the interface between the $Si_3N_4$ and the Ni, are independent of interlayer thickness, which implies that the strength of the bond is also independent of interlayer thickness. Only at small interlayer thickness the zirconia starts to play a role in the stress distribution at the nickel-silicon nitride interface. This is probably the reason for the low strength obtained in bonds with an interlayer thickness smaller than about 0.1 mm.

PUBLICATIONS

A.J.R. Aendenroomer, G. den Ouden
*A new approach to penetration sensing and control during orbital tube welding*
In: Proceedings of the International Conference on Advances in Mechanical and Industrial Engineering, Roorkee, India, 6-8 February 1997, 1091-1097

A.J.R. Aendenroomer, G. den Ouden
*Een doorlassingssensor voor orbitaal pijplassen gebaseerd op lasbadoscillaties*
Lastechniek 63 (1997) 7-10

A.J.R. Aendenroomer, G. den Ouden
*Oscillation monitoring provides data on weld penetration*
Welding Review International 16 (1997) 34-37

M.J.M. Hermans
*A study of short circuiting arc welding*
Ph.D. thesis, Delft University of Technology, Delft (1997) 165

M.J.M. Hermans, T. Luijendijk
*Spatter behaviour and weld pool oscillations during dip transfer of GMA-welding*
In: Proceedings of the International Conference on Advances in Mechanical and Industrial Engineering, Roorkee, India, 6-8 February 1997, 35-43

M.J.M. Hermans, G. den Ouden
*A stability criterion for short circuiting gas metal arc welding*

In: Proceedings of the International Conference on the Joining of Materials (JOM-8), Helsingor, Denmark, 12-14 May 1997, 112-119

J.W. Hooijmans, G. den Ouden
*A model of hydrogen absorption during GTA welding*
Welding Journal 76 (1997) 264s-268s

J.W. Hooijmans, G. den Ouden
*$H_2$ influence on the arc and weld pool geometry during GTA welding of austenitic stainless steel*
Welding Review International 16 (1997) 154-156

T. Luijendijk
*Het lassen van aluminiumlegeringen van ongelijke samenstelling*
Lastechniek 63 (1997) 5-10

T. Ma
*Weldability of Al-Zn-Mg alloys*
Ph.D. thesis, Delft University of Technology, Delft (1997)

T. Ma, T. Luijendijk, G. den Ouden
*Hardheidsafname in de WBZ van AlZnMg-legeringen*
Lastechniek 63 (1997) 3-7

T. Ma, G. den Ouden
*HAZ liquation cracking susceptibility of Al-Zn-Mg alloys*
In: Proceedings 7th International Symposium on Physical Simulation of Casting, Hot Rolling and Welding, Tsukuba, Japan, 21-23 January 1997, 461-467

A. Maloletkov, E. Gladkov, T. Luijendijk, G. den Ouden
*Influence of pulsed TIG welding parameters on welding quality*
In: Proceedings of the Conference on Modern Problems of Welding Science and Technology (Welding 97), Voroneg, Russia, 5-9 September 1997, 1-6

R.H. Vegter, G. den Ouden
*Diffusion bonding of zirconia to silicon nitride*
In: Proceedings of the 5th European Conference on Advanced Materials and Processes and Applications, EUROMAT 97, Maastricht, The Netherlands, 21-23 April 1997, 2 (1997) 371-374

H.W. de Vries, G. den Ouden
*Particle mixing in GTA welding of an aluminium matrix composite*
In: Proceedings of the 5th European Conference on Advanced Materials and Processes and Applications, EUROMAT 97, Maastricht, The Netherlands, 21-23 April 1997, 1 (1997) 463-466

Y.H. Xiao, G. den Ouden
*Measurement of surface tension of liquid metals and alloys under arc welding conditions*
Materials Science and Technology 13 (1997) 791-794

## PERSONNEL INDEX

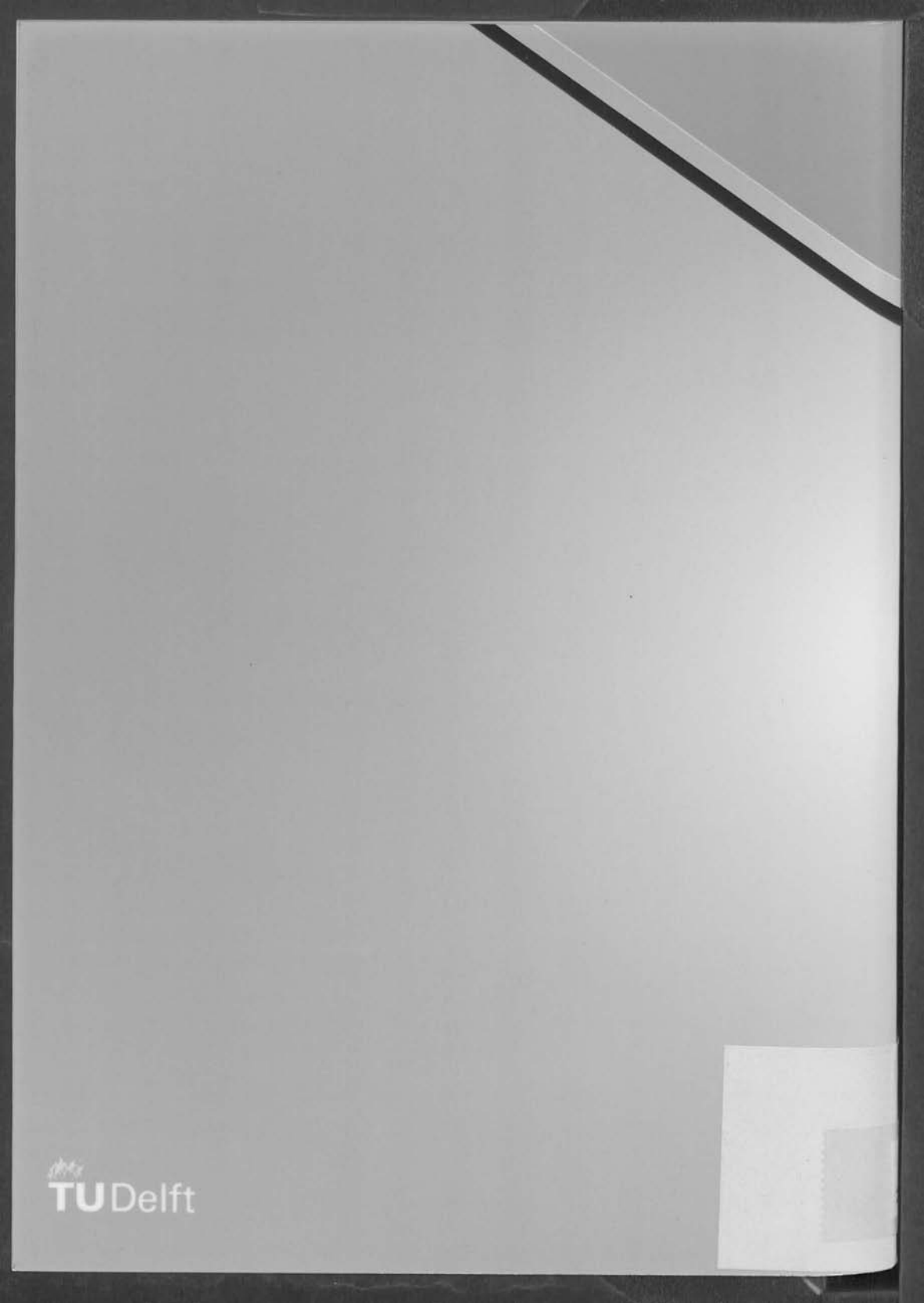
TU Delft